

**Characterisation of
Anthocyanin Transport and
Storage in *Vitis vinifera* L.
cv. Gamay Fréaux Cell
Suspension Cultures**

Simon James Conn

B.Biotech (Hons.)

**Submitted for the degree of Doctor of Philosophy
Flinders University, Adelaide, Australia**

I certify that this thesis does not contain material which has been accepted for the award of any degree or diploma; and to the best of my knowledge and belief it does not contain any material previously published or written by another person except where due reference is made in the text of this thesis or in the notes.

Simon James Conn

ACKNOWLEDGMENTS.....	VIII
ABBREVIATIONS	XI
THESIS SUMMARY	XIII
CHAPTER 1 - LITERATURE REVIEW	1
1.1 PLANT SECONDARY METABOLITES	2
1.2 FLAVONOIDS	2
1.2.1 ANTHOCYANINS	3
1.2.1.1 Biological role of anthocyanins in the plant.....	3
1.2.1.2 Anthocyanin biosynthesis.....	5
1.3 ANTHOCYANINS AS BIOPRODUCTS	9
1.3.1 COMMERCIAL USES	9
1.3.2 CHOICE OF PRODUCTION SYSTEM.....	11
1.3.2.1 Plant cell and tissue cultures for bioproducts.....	12
1.3.2.2 Anthocyanin production in plants	13
1.3.2.3 Anthocyanin production in suspension culture	14
1.3.2.4 Anthocyanin stability and accumulation in suspension culture	15
1.3.3 METHODS OF ENHANCING ANTHOCYANIN PRODUCTION.....	17
1.3.3.1 Empirical approaches	17
1.3.3.2 Semi-rational approaches	17
1.3.3.3 Rational/Integrated approaches	18
1.4 ANTHOCYANIN BIOSYNTHETIC EVENTS	19
1.4.1 SUBCELLULAR LOCALISATION OF ANTHOCYANIN BIOSYNTHESIS	20
1.4.2 REGULATION OF ANTHOCYANIN PRODUCTION	21
1.4.2.1 Biosynthetic enzymes.....	21
1.4.2.2 Transcription factors.....	22
1.4.2.3 Post-transcriptional and post-translational regulation.....	26
1.5 ANTHOCYANIN POST-BIOSYNTHETIC EVENTS.....	27
1.5.1 ANTHOCYANIN TRANSPORT	28
1.5.1.1 ER-derived vesicular model	28
1.5.1.2 GSTs as escort proteins	29
1.5.1.2.1 Maize	32
1.5.1.2.2 Petunia	33
1.5.1.2.3 Arabidopsis.....	34
1.5.1.2.4 Carnation	34
1.5.2 TRANSPORTERS/MEMBRANE PUMPS.....	35
1.5.3 ANTHOCYANIN STORAGE	38
1.5.3.1 Anthocyanic Vacuolar Inclusions	39
1.5.3.1.1 Lisianthus	41
1.5.3.1.2 Sweet potato	41
1.5.3.1.3 Rose	43
1.5.3.1.4 Radish.....	44
1.5.3.1.5 Maize	45
1.5.3.1.6 Grape	45
1.5.4 ANTHOCYANIN DEGRADATION.....	46
1.6 SUMMARY	48
1.7 BROAD RESEARCH OBJECTIVES.....	49

CHAPTER 2 - MATERIALS AND METHODS.....	50
2.1 CHEMICALS	51
2.2 PLANT CELL CULTURE	51
2.2.1 CELL LINE DETAILS.....	51
2.2.2 GROWTH MEDIUM.....	51
2.2.3 SELECTION AND SUBCULTURE OF CELL LINES	52
2.2.3.1 Callus cultures	52
2.2.3.1.1 Subculture.....	52
2.2.3.1.2 Clonal selection and micro-calli selection.....	52
2.2.3.2 Suspension cultures	53
2.2.3.2.1 Subculture.....	53
2.2.3.2.2 Selected cell lines utilised in experiments.....	54
2.3 ELICITATION EXPERIMENTS.....	54
2.3.1 PREPARATION OF CHEMICALS FOR ADDITION TO CULTURES.....	54
2.3.1.1 Jasmonic acid (JA)	54
2.3.1.2 Sucrose	54
2.3.2 ADDITION OF CHEMICALS TO CULTURES AND LIGHT IRRADIATION.....	55
2.4 KINETIC ANALYSIS	55
2.4.1 CULTURE GROWTH	55
2.4.2 METABOLITE ANALYSIS.....	56
2.4.2.1 Extraction of anthocyanins.....	56
2.4.2.2 Spectrophotometric assay for anthocyanin content.....	56
2.4.2.3 HPLC analysis of anthocyanin composition	57
2.4.2.3.1 Solvent preparation and gradient program	57
2.4.2.3.2 Sample preparation.....	58
2.4.2.3.3 Identification of peaks	58
2.4.2.4 Estimation of pigmented cell ratio	60
2.4.2.4.1 Protoplasting of suspension culture cells	60
2.4.2.4.2 Vacuole purification	60
2.4.2.4.3 Microscopy and cell counting using a haemocytometer	61
2.4.2.5 Cellular staining	61
2.4.3 PROTEIN EXTRACTION AND PRECIPITATION	62
2.4.3.1 Total protein extraction	62
2.4.3.2 Whole-cell protein extraction.....	62
2.4.3.3 Protein precipitation and desalting.....	63
2.4.3.3.1 Acetone precipitation	63
2.4.3.3.2 Ammonium sulphate precipitation	63
2.4.3.3.3 HiTrap desalting.....	63
2.4.3.4 Protein quantification	64
2.4.3.4.1 Bicinchoninic acid protein assay kit.....	64
2.4.3.4.2 EZQ protein quantification kit	64
2.4.4 PURIFICATION OF GLUTATHIONE S-TRANSFERASES (GSTs).....	64
2.4.4.1 Glutathione-affinity chromatography.....	64
2.4.4.2 GST assay.....	65
2.5 GEL ELECTROPHORESIS	65
2.5.1 SDS POLYACRYLAMIDE GEL ELECTROPHORESIS (SDS-PAGE)	65
2.5.2 TWO-DIMENSIONAL GEL ELECTROPHORESIS (2D-GE)	66
2.5.2.1 Sample preparation.....	66
2.5.2.2 Strip rehydration.....	66
2.5.2.3 Isoelectric focussing.....	67

2.5.2.4 Strip equilibration.....	67
2.5.3 GEL STAINING TECHNIQUES	68
2.5.3.1 Silver staining.....	68
2.5.3.2 Sypro Ruby staining.....	68
2.5.3.3 Coomassie Blue staining	69
2.5.4 COMPARATIVE GEL IMAGING	69
2.5.5 GEL DRYING	69
2.6 PROTEOMIC ANALYSES	69
2.6.1 MASS SPECTROMETRY	69
2.6.2 EDMAN (N-TERMINAL) PROTEIN SEQUENCING.....	70
2.6.3 SAMPLE PREPARATION FOR REVERSE-PHASE HPLC	71
2.7 POLYMERASE CHAIN REACTION (PCR).....	71
2.7.1 GENOMIC DNA ISOLATION	71
2.7.2 TOTAL RNA ISOLATION	71
2.7.2.1 Concert™ RNA extraction.....	71
2.7.2.2 Hot borate method.....	71
2.7.2.3 RNA quantification	72
2.7.2.4 Removal of contaminating DNA by DNase 1 treatment.....	72
2.7.2.5 Efficacy of DNase treatment	72
2.7.2.6 Electrophoretic verification of RNA integrity.....	74
2.7.2.7 Reverse transcription of total RNA to cDNA	74
2.7.3 CLONING GST SEQUENCES	74
2.7.3.1 Primer design.....	74
2.7.3.2 Amplification from cDNA	76
2.7.3.3 Amplification from genomic DNA	76
2.7.4 GST SEQUENCE CLONING PROCEDURES.....	77
2.7.4.1 Purification of PCR products	77
2.7.4.1.1 Gel purification.....	77
2.7.4.1.2 PCR column purification.....	77
2.7.4.2 T·A cloning.....	77
2.7.4.3 Directional cloning.....	78
2.7.4.4 Screening colonies for positive insert	78
2.7.4.5 DNA sequencing	79
2.7.5 CODING SEQUENCE ANALYSES.....	80
2.8 6-HIS FUSION PROTEIN PURIFICATION AND ANALYSIS	80
2.8.1 GENERATION OF COMPETENT <i>E. COLI</i>	80
2.8.2 <i>E. COLI</i> EXPRESSION OF 6-HIS FUSION PROTEIN.....	81
2.8.3 IMMOBILIZED NICKEL AFFINITY CHROMATOGRAPHY	81
2.8.4 WESTERN BLOTTING USING UNIVERSAL HIS-TAG DETECTION KIT	82
2.9 QUANTITATIVE REVERSE TRANSCRIPTASE PCR (QPCR).....	83
2.9.1 PRIMER DESIGN	83
2.9.2 PCR RUNNING CONDITIONS	84
2.9.3 CONFIRMATION OF CORRECT PRODUCT FORMATION	85
2.9.4 ANALYSIS AND QUANTIFICATION.....	86
2.9.5 GENERATION OF STANDARDS FOR METHOD VALIDATION AND QUANTIFICATION	86
2.9.6 MATHEMATICAL MODEL FOR QUANTIFYING GENE EXPRESSION	87
2.9.7 VALIDATION OF QPCR ASSAYS.....	88
2.10 MAIZE KERNEL BOMBARDMENT	88
2.10.1 PREPARATION OF GOLD PARTICLES	88

2.10.2 COATING OF GOLD PARTICLES.....	89
2.10.3 PREPARATION OF <i>Bz2</i> -DEFICIENT CORN SEEDS.....	90
2.10.4 BOMBARDMENT.....	90
2.11 MICROSCOPY.....	91
2.11.1 CONFOCAL MICROSCOPY.....	91
2.11.2 CRYOGENIC-SCANNING ELECTRON MICROSCOPY (CRYOSEM).....	91
2.12 GRAPE CELL TRANSFECTION.....	92
2.12.1 PREPARATION OF CELLS.....	92
2.12.2 PREPARATION AND COATING OF GOLD PARTICLES.....	92
2.12.3 BOMBARDMENT.....	93
2.13 PURIFICATION AND ANALYSIS OF AVIS.....	93
2.13.1 AVI ISOLATION.....	93
2.13.2 LIPID ANALYSIS.....	94
2.13.3 HPLC ANALYSIS AND QUANTIFICATION OF TANNINS.....	94
2.13.3.1 Solvent preparation and gradient program.....	94
2.13.3.2 Sample preparation.....	95
2.13.3.3 Identification and quantification of peaks.....	96
2.13.4 STARCH QUANTIFICATION.....	96
2.13.5 ANALYSIS OF TOTAL SOLUBLE SOLIDS.....	96
CHAPTER 3 - CELL LINE KINETICS AND CHARACTERISATION	97
3.1 INTRODUCTION.....	98
3.2 CHARACTERISATION OF <i>VITIS VINIFERA</i> L. CELL LINES.....	99
3.2.1 FU-01 (INTERMEDIATE-PIGMENTED).....	99
3.2.2 FU-03 (NON-PIGMENTED).....	103
3.2.3 FU-02 (HIGH-PIGMENTED).....	105
3.3 TWO-DIMENSIONAL GEL ELECTROPHORESIS.....	106
3.4 DISCUSSION.....	107
CHAPTER 4 - GLUTATHIONE S-TRANSFERASES AND THEIR INVOLVEMENT IN ANTHOCYANIN TRANSPORT IN <i>VITIS VINIFERA</i> L. CELL-SUSPENSION CULTURE	110
4.1 INTRODUCTION.....	111
4.2 GST CLONING STRATEGIES.....	113
4.2.1 DEGENERATE PCR TO CLONE GST SEQUENCES.....	113
4.2.2 PROTEIN PURIFICATION TO CLONE GST SEQUENCES.....	114
4.2.2.1 Selection of time-point for purification.....	114
4.2.2.2 Glutathione (GSH) affinity chromatography.....	116
4.2.2.3 Two-dimensional gel electrophoresis of purified GSTs.....	119
4.2.2.4 Edman sequencing.....	122
4.2.3 SELECTION OF GST EXPRESSED SEQUENCE TAGS.....	123
4.2.3.1 Cloning of GST ESTs.....	124
4.2.3.2 Cloning of GST genomic sequences.....	125
4.2.3.3 Analysis of non-coding sequences.....	132
4.2.3.4 Categorisation of <i>V. vinifera</i> GST protein sequences.....	134
4.2.4 RECOMBINANT PROTEIN EXPRESSION.....	136
4.2.4.1 Confirming size of protein.....	136
4.2.4.2 GST activity of crude <i>E. coli</i> extracts.....	137
4.2.4.3 GST activity of purified protein.....	137

4.3 CORRELATION OF GST EXPRESSION WITH ANTHOCYANIN ACCUMULATION	139
4.3.1 TRANSLATIONAL LEVEL	139
4.3.1.1 FU-03 (anthocyanin-deficient cell line)	139
4.3.1.2 FU-01 treated with sucrose, jasmonic acid and light	140
4.3.2 TRANSCRIPTIONAL LEVEL (QPCR).....	141
4.3.3 EFFECT OF INDIVIDUAL ELICITORS ON GST1 EXPRESSION	143
4.3.4 GST PROFILING IN GRAPE BERRY SKINS AT VERÁISON	144
4.4 ANTHOCYANIN TRANSPORT COMPLEMENTATION ASSAY	146
4.4.1 BOMBARDMENT	146
4.4.2 GST SEQUENCE ALIGNMENTS	149
4.5 DISCUSSION	153
4.5.1 VITIS VINIFERA GSTs	153
4.5.2 GST SEQUENCES	153
4.5.3 PROFILE OF GSTs FOLLOWING ELICITATION.....	155
4.5.4 ANTHOCYANIN TRANSPORT COMPLEMENTATION ASSAY	161
4.6 CONCLUSIONS	164
CHAPTER 5 - CHARACTERISATION OF ANTHOCYANIC VACUOLAR INCLUSIONS (AVIS) AND THEIR ROLE AS ANTHOCYANIN STORAGE SITES IN VITIS VINIFERA L. CELL-SUSPENSION CULTURES	166
5.1 INTRODUCTION	167
5.2. LOCALISATION OF AVIS IN <i>V. VINIFERA</i> CELL CULTURES	169
5.2.1 LIGHT MICROSCOPY	169
5.2.2 CONFOCAL MICROSCOPY	170
5.3 FORMATION OF AVIS	174
5.3.1 BOMBARDMENT OF NON-PIGMENTED <i>V. VINIFERA</i> CELLS WITH ANTHOCYANIN TRANSCRIPTION FACTORS	174
5.3.2 CONFOCAL MICROSCOPY ON AVI-CONTAINING <i>V. VINIFERA</i> CELLS EXPRESSING ANTHOCYANIN TRANSCRIPTION FACTORS.....	175
5.3.3 INTRAVACUOLAR DYNAMICS OF AVIS.....	177
5.3.4 CRYOGENIC SCANNING ELECTRON MICROSCOPY OF AVIS.....	179
5.4 CORRELATION OF AVI ABUNDANCE AND ANTHOCYANIN CONTENT IN <i>V. VINIFERA</i>	182
5.4.1 PREVALENCE OF AVIS IN <i>V. VINIFERA</i> SUSPENSION CELL LINES AND CALLUS CULTURES	182
5.4.2 CORRELATION OF AVI ABUNDANCE AND ANTHOCYANIN CONTENT IN FU-01 SUSPENSION CELLS WITH AND WITHOUT ELICITATION.....	183
5.5 COMPOSITIONAL ANALYSIS.....	186
5.5.1 PROTEIN	186
5.5.2 DRY MASS	189
5.5.3 ANTHOCYANIN PROFILES OF AVIS, VACUOLES AND WHOLE CELLS.....	189
5.5.4 KINETIC STUDY OF ANTHOCYANIN PROFILE IN FU-01 CELLS AND AVIS	193
5.5.5 CELLULAR STAINING	195
5.5.6 TANNIN (PROANTHOCYANIDINS)	196
5.6 DISCUSSION	199
5.6.1 AVI LOCALISATION AND FORMATION.....	202
5.6.2 AVI COMPOSITION	205
CHAPTER 6 - MAJOR PROJECT FINDINGS	209

APPENDIX 1 - B5 MEDIUM COMPOSITION	213
APPENDIX 2 – PROTEIN STANDARD CURVES	214
2.1 BICINCHONINIC ACID PROTEIN QUANTIFICATION ASSAY KIT	214
2.2 EZQ PROTEIN QUANTIFICATION KIT	214
2.3 GLUTATHIONE S-TRANSFERASE ASSAY	215
APPENDIX 3 – QPCR PRIMER DATA	216
APPENDIX 4 – MASS SPECTROSCOPY ANALYSIS OF GSTS.....	218
4.1 GROUP 1	218
4.1.1 MASCOT REPORT	218
4.1.2 BLASTp ALIGNMENT.....	219
4.2 GROUP 2	220
4.2.1 MASCOT REPORT	220
4.2.2 BLASTp ALIGNMENT.....	221
4.3 GROUP 3	222
4.3.1 MASCOT REPORT	222
4.3.2 BLASTp ALIGNMENT.....	223
4.4 GROUP 4	225
4.4.1 MASCOT REPORT	225
4.4.2 BLASTp ALIGNMENT.....	226
4.5 GROUP 5	227
4.5.1 MASCOT REPORT	227
4.5.2 BLASTp ALIGNMENT.....	228
4.6 NEGATIVE CONTROL SPOT	230
4.6.1 MASCOT REPORT:	230
4.6.2 BLASTp ALIGNMENT:	231
APPENDIX 5 – V. VINIFERA CV. GAMAY FRÉAUX GLUTATHIONE S- TRANSFERASES SUMMARY TABLE.....	232
APPENDIX 6 –	233
6.1 – ANTHOCYANIN HPLC OF <i>V. VINIFERA</i> L. CV. SHIRAZ GRAPE BERRIES.....	233
6.2 - IMAGE HISTOGRAM OF AUTOFLUORESCENT CONFOCAL MICROSCOPY ON <i>V. VINIFERA</i> L. SUSPENSION CELLS	234
6.3 - UNCLEAVED TANNIN CHROMATOGRAM HIGHLIGHTING UNIDENTIFIED COMPUNDS.....	235
APPENDIX 7 – LIPID GAS CHROMATOGRAMS.....	236
APPENDIX 8 - ANALYSIS OF PROTEIN FROM AVI PELLET.....	237
8.1 2-D GEL SEPARATION OF PROTEIN EXTRACTED FROM AVIS	237
8.2 MASS SPECTROMETRY ANALYSIS OF AVI PROTEIN	238
REFERENCES	239

Acknowledgments

First and foremost I wish to thank my wife, Vanessa (or Dr. Conn as she likes to be called). It is no understatement that without your support and constant encouragement, this would never have been completed. If for only that I would be eternally grateful, but that is only one of the things I wish to acknowledge you for. Your love, patience, and good humour has made me a happier person than I ever thought possible and I am so lucky that you came into my life. My second thanks go to my, as yet, unborn child – I promise if you have trouble sleeping that I will be only too happy to read you some of this and it will solve your problems. Despite the effort I put into this thesis, I know you are my greatest work and I am so happy you have chosen us as your parents. For that we could not be more proud.

I would like to thank my family, especially Dad, Mum, Sarah, Emily, and Grandma Daphne. Your interest in my study has made it all the easier to feel excited about science even when you know you have 300 PCR reactions to set up. I would also like to thank my newer family – Marg, Mike, El, John, Michelle, Andrew, Tayla, Hayley, Tyson and Connor – for believing that I was a nice enough guy to not throw food at (apart from you Tayla!!!).

A sincere thankyou to my supervisors – Prof. Chris Franco and Dr. Wei Zhang – for their wisdom and attention during my studies. I have learnt a lot during my time at Flinders and it has made me a better scientist. I would like to thank Chris Curtin for his assistance and for his friendship. I also wish to thank all the members of the Department of Medical Biotechnology. While there is not nearly enough room to mention you all, I trust you know that you all contributed to my completion and I hope I helped you in some small way also.

Enormous thanks go to my colleagues at the CSIRO Plant Industry, Adelaide for their constant support and guidance. In particular I would like to thank Dr. Mandy Walker , Dr. Simon Robinson, Nicole Cordon, Dr. Jochen Bogs, and Debra McDavid for their help and analysis of samples for tannin and with grape cell bombardment assays. I also appreciate the discussions had with Assoc. Prof. Graham Jones (School of Agriculture and Wine, Adelaide University, Adelaide) in interpreting some of my results.

I would like to thank Miss Kathryn Boyd and Dr. Karen Murphy (School of Medicine, Paediatrics and Child Health, FMC, Adelaide) for their lipid analysis expertise. Great amounts of help were afforded me by Dr. Meredith Wallwork with confocal and all matters microscopy and Lyn Waterhouse (Adelaide Microscopy, Adelaide) for her assistance with cryoSEM. Dr. Chris Winefield (Cell Biology Group, Lincoln Univeristy, New Zealand) was kind enough to run extracts from my cells on his fluorescence HPLC. I would also like to thank Dr. Kevin Gould and Dr. Ken Markham for letting me ask all of the specific details that one cannot fit into a great paper.

My proteomics work could not have been completed without the help of numerous people. My primary thanks go to Dr. Tim Chataway (Dept. of Human Physiology, FMC, Adelaide) for his help with 2D-gels and for introducing me to Mark Raftery (Bioanalytical Mass Spectrometry Facility, University of NSW) who ran all my Mass Spectrometry samples free of charge. Further support was given to me with Edman sequencing and reverse-phase HPLC of my GST proteins by Dr. Antony Bacic and Dr. Shaio-Lim Mau (Dept. of Botany, University of Melbourne, Victoria, Australia).

Dr. Fabienne Bailleul (Laboratoire de Stress, Défenses et Reproduction des Plantes, Reims, France) provided great assistance in obtaining the 5' region of GST3 by RACE-PCR. For this collaboration I am particularly grateful. I wish to acknowledge Prof. Rossitza Atanassova (Bâtiment Botanique, Université de Poitiers, France) who was kind enough to send me the Q84N22 sequence for comparison. I look forward to the opportunity to collaborate with both of these individuals in the future to repay their generosity and kindness. My final thanks are to the individuals who assisted with maize kernel bombardment. In particular Prof. Virginia Walbot and Dr. Guo-Ling Nan (Biological Sciences, Stanford University, USA) for sending me the kernels and the maize expression vector which started me on the road to completing my PhD. I would also like to thank Dr. Mark Alfenito and Dr. C. Dean Goodman (Dept. of Botany, University of Melbourne, Victoria, Australia) for their interpretation of my results. It is always a strange scenario when people you have referenced are discussing your results with so much interest and for that I will be ever grateful to these gentlemen.

Abbreviations

µl; ml; l: microlitre; millilitre; litre
pM; µM; mM; M: picomolar; micromolar; millimolar; molar
AVI: anthocyanic vacuolar inclusion
BMS: black Mexican sweetcorn
bp: base pairs
C3G: cyanidin 3-glucoside
C3pCG: cyanidin 3-p-coumaroylglucoside
cDNA: complementary DNA
CDNB: 1-chloro-2,4-dinitrobenzene
CHAPS: 3-cholamido propyl dimethyl ammonio-1- propane sulfate
DNA: deoxyribonucleic acid
dNTPs: dinucleotide triphosphates
DTT: dithiothreitol
EDTA: ethylenediamine tetraacetic acid
eGFP: enhanced green fluorescent protein
EST: expressed sequence tag
GSH: glutathione
GST: glutathione *S*-transferase
H₂O: water
HPLC: high pressure liquid chromatography
hr: hour(s)
IPTG: isopropyl β-D-thiogalactoside
JA: jasmonic acid
kDa: kilodaltons
LB: Luria broth
M3G: malvidin 3-glucoside
M3pCG: malvidin 3-p-coumaroylglucoside
MeJa: methyl jasmonate
min: minute(s)
MS: mass spectroscopy
mW: molecular weight

nos: Nopaline synthase
NCBI: National Centre for Biotechnology Information
ng; µg; mg; kg: nanograms; micrograms; milligrams; kilograms
P3G: peonidin 3-glucoside
P3pCG: peonidin 3-p-coumaroylglucoside
PBS: phosphate buffered saline
PCR: polymerase chain reaction
PEG: polyethylene glycol
aPMSF: a-phenylmethanolsulfonylfluoride
QPCR: quantitative PCR
RACE: rapid amplification of cDNA ends
rER: rough endoplasmic reticulum
RNA: ribonucleic acid
rRNA: ribosomal ribonucleic acid
RT: room temperature
SDS: sodium dodecyl sulphate
sER: smooth endoplasmic reticulum
sp.: species (singular)
spp.: species (plural)
Std. Dev.: standard deviation
TBE: tris-borate EDTA
TIGR: The Institute for Genomic Research
UV: ultraviolet
W: watts
X-gal: 5-bromo-4-chloro-3-indolyl-β-D-galactopyranoside

Thesis Summary

Anthocyanins are ubiquitous plant pigments with strong antioxidant activity, stimulating interest in the development of a plant cell-based bioprocess for their production to replace toxic synthetic food dyes and for application as pharmaceuticals, or nutraceuticals. Anthocyanin-producing plant cell suspension cultures are the currently favoured model production system facilitating rapid scale-up of production and circumventing the seasonal growth of crop plants. However, the level of anthocyanin production in these cells is commonly less than that seen in the intact plant, requiring anthocyanin enhancement strategies to improve the commercial feasibility of this approach. Attempts to enhance anthocyanin production by augmenting anthocyanin biosynthesis alone, without considering the post-biosynthetic limitations (transport and storage) have been largely unsuccessful in the development of a commercial bioprocess. The aims of this study were to characterise the anthocyanin transport pathway and storage sites in *Vitis vinifera* L. suspension cells towards significantly improving anthocyanin production by rational enhancement strategies at the molecular level. Anthocyanins are thought to be transported from their site of biosynthesis in the cytosol via the non-covalent (ligandin) activity of glutathione *S*-transferases (GSTs) to the vacuole where they are concentrated in insoluble bodies, called anthocyanic vacuolar inclusions (AVIs).

Five GSTs were affinity purified from pigmented grape suspension cells, characterised by nano-LC MS/MS and Edman sequencing, with the coding sequences identified and cloned. Bombardment of anthocyanin transport-deficient maize kernels with *V. vinifera* L. GST sequences indicated the potential involvement of two GSTs, GST1 and GST4, in anthocyanin transport. Gene expression analyses by QPCR indicated a strong correlation of these two GSTs

with anthocyanin accumulation. GST4 was enhanced 60-fold with veraison in Shiraz berry skins, while GST1 and to a lesser extent GST4, was induced in *V. vinifera* L. cv. Gamay Fréaux suspension cells under elicitation with sucrose, jasmonic acid and light irradiation (S/JA/L) to enhance anthocyanin synthesis. Purified GSTs quantified by reverse-phase HPLC from control and S/JA/L-treated suspension cells supported the gene expression data. Sequence alignments of these genes with known anthocyanin-transporting GSTs have shown conserved putative anthocyanin-binding regions. Furthermore, analysis of short upstream regions identified anthocyanin transcription factor- (R/C1) binding regions in the promoter of GST1. Increasing the expression of these GSTs provides an avenue to enhance anthocyanin production by more rapid removal of anthocyanins from biosynthetic complexes, potentially increasing biosynthetic flux.

AVIs have been documented in 45 of the highest anthocyanin-accumulating suspension cell cultures, with few detailed studies on their composition, or anthocyanin profile. AVIs in grape cell cultures were found to be highly dense, membrane-delimited bodies containing a complex mix of anthocyanins, long-chain tannins and other unidentified organic compounds. Furthermore, while the proportion of individual anthocyanin species were maintained between whole-cell and AVI extracts, the AVIs were found to selectively bind a subset of highly stable acylated (*p*-coumaroylated) anthocyanins. Strategies to enhance anthocyanin accumulation in grape suspension cultures lead to a proportionate increase in the abundance of AVIs. Unlike AVIs in sweet potato and, to a lesser extent lisianthus, protein was not a major component of AVIs in *V. vinifera* L. It is likely from this evidence that AVIs represent a by-product of ER-derived vesicular transport of anthocyanins, and therefore not a target for rational enhancement of anthocyanin production.

CHAPTER 1

LITERATURE REVIEW

1.1 Plant Secondary Metabolites

Plants have long been exploited, not only as a staple food, but also a source of valuable and therapeutic chemicals, accounting for over 80% of all known natural products (Zhang and Furusaki, 1999; Rao and Ravishankar, 2002). Over 100,000 plant metabolites have been identified, representing only 20% of the total estimated number in the plant kingdom (Hadacek, 2002). These include primary metabolites vital for plant survival, such as essential amino acids and vitamins; and secondary metabolites, such as pigments, flavours and fragrances. Furthermore, plant extracts range from crude herbal forms to highly purified preparations for human therapeutics, including the arrhythmia medication Digoxin from *Digitalis lanata* (US\$3,000 kg⁻¹) and the anti-cancer drug Taxol from *Taxus* spp. (US\$600,000 kg⁻¹) (Srinivasan *et al.*, 1996). These secondary metabolites are of greatest commercial interest due to their medium-to-high unit value, with complex structures that are unable, or uneconomical, to be chemically synthesised.

Nutraceuticals are natural, bioactive compounds possessing health-promoting and/or disease-preventing properties, including antioxidant, antiallergic, antiviral, anticancer and antiinflammatory activities (Nair *et al.*, 2004). These compounds can be added into foodstuffs (functional foods), taken as supplements, or both (Lachance, 2004). A major class of low-molecular weight, secondary metabolites with a range of these effects are the plant flavonoids.

1.2 Flavonoids

Flavonoids are a relatively diverse family of plant secondary metabolites biosynthesised from phenylpropanoid (phenylalanine) and acetate-derived

(malonyl-CoA from fatty acid pathway) precursors that perform a variety of essential functions in angiosperm growth, signalling, reproduction and survival (Moller and Chua, 1999). Flavonoids are divided into 7 major subgroups: chalcones, flavanols, flavanones, flavones, flavan-3-ols (catechins), anthocyanins, and isoflavones (Manach *et al.*, 2004; Taylor and Grotewald, 2005). One class of flavonoids, common to most flowers, fruits and vegetables, are the water-soluble anthocyanins which provide the variety of attractive red to deep-purple and blue colours.

1.2.1 Anthocyanins

1.2.1.1 Biological role of anthocyanins in the plant

Beyond the role of anthocyanins as attractants for pollinators (McClure *et al.*, 1975), the unique chemical structure and response to environmental cues suggest additional roles (Bridle and Timberlake, 1997). Anthocyanins have long been known to be antioxidants, due to their free radical scavenging capacity, possessing between 2 and 6-times the activity of common antioxidants, including ascorbate, and glutathione (Wang *et al.*, 1997). Several mechanisms may explain this including hydrogen donation, metal chelation, and protein binding (Sarma *et al.*, 1997; Satue-Gracia *et al.*, 1997; Wang *et al.*, 1997; Espin *et al.*, 2000; Wang *et al.*, 2000; Wang and Lin, 2000). For this reason, anthocyanins are believed to provide endogenous protection from various environmental stresses – including nutrient deprivation (Dedaldechamp *et al.*, 1995).

Anthocyanins are rapidly induced upon wounding and attack by pathogens, presumably to counteract the damaging effects of the oxidative burst in the plant defence response (Suzuki, 1995; Fang *et al.*, 1999; Davies and Robinson,

2000). Anthocyanins are induced in response to ultraviolet light (blue-spectral, 260-400nm; (Wellmann et al., 1976) and are therefore presumed to play a role in defence against its damaging effects, including mutagenesis, photobleaching or molecular cross-linking (Gould *et al.*, 2000). This is in spite of only minor absorptive properties with respect to the blue-region, with a maximum absorption of around 560nm for the predominant anthocyanic species (Blank, 1946). Acylated anthocyanins have a higher absorbance in the UV region, thought to be due to the intramolecular copigment stacking phenomenon where the acyl group interacts with the flavylum nucleus (Dangles *et al.*, 1993).

In flowers, fruits and vegetables the epidermis and sub-epidermis accumulate anthocyanins, thereby protecting the internal layers (Stafford, 1994). However, it has been suggested that photoprotection is not always a key function of anthocyanins, as evident in the leaves of *Quintinia serrata* L. In this plant, anthocyanins are predominantly located in the palisade and spongy mesophyll layers where damaging UV-B light cannot penetrate, rather than the upper epidermis where many other UV-absorbing pigments are present (Gould *et al.*, 2000). Furthermore, they predominate in chlorophyllous cells and, in leaves grown under only partially covered canopies, anthocyanin levels increase with diminishing annual exposure to irradiation (Gould *et al.*, 2000). This implies a role in protecting shade-adapted chloroplasts from brief exposure to high-intensity sunflecks (Gould *et al.*, 2000). The appearance of anthocyanins as Dogwood (*Cornus stolonifera* L.) leaves senesce has also been partially explained by reducing the photo-oxidative damage to chlorophyll in these leaves to optimise nutrient retrieval by the plant (Feild *et al.*, 2001). A unique role of anthocyanins was demonstrated by their ability to sequester molybdenum in *Brassica juncea* L.

seedlings, thus increasing tolerance of the seedlings to this abiotic stress (Hale *et al.*, 2001).

1.2.1.2 Anthocyanin biosynthesis

Anthocyanins are synthesised via a branch of the 3-hydroxy flavonoid biosynthetic pathway (Fig. 1.1) at the cytosolic face of the endoplasmic reticulum in plant cells and accumulate in the vacuole (Hrazdina *et al.*, 1978; Zobel and Hrazdina, 1995; Winkel-Shirley, 1999; Saslowsky and Winkel-Shirley, 2001). Figure 1.2 depicts the general flavan skeleton of anthocyanins, consisting of two aromatic hydroxylated (phenolic) rings, bridged by a planar pyrylium core (Figueiredo *et al.*, 1996). Various combinations of hydroxylation and methylation at positions R₁ and R₂ yield the different aglycone anthocyanidin varieties which exhibit different hues (red-purple), with the common forms shown in the adjacent table (Fig. 1.2; Figueiredo *et al.*, 1996).

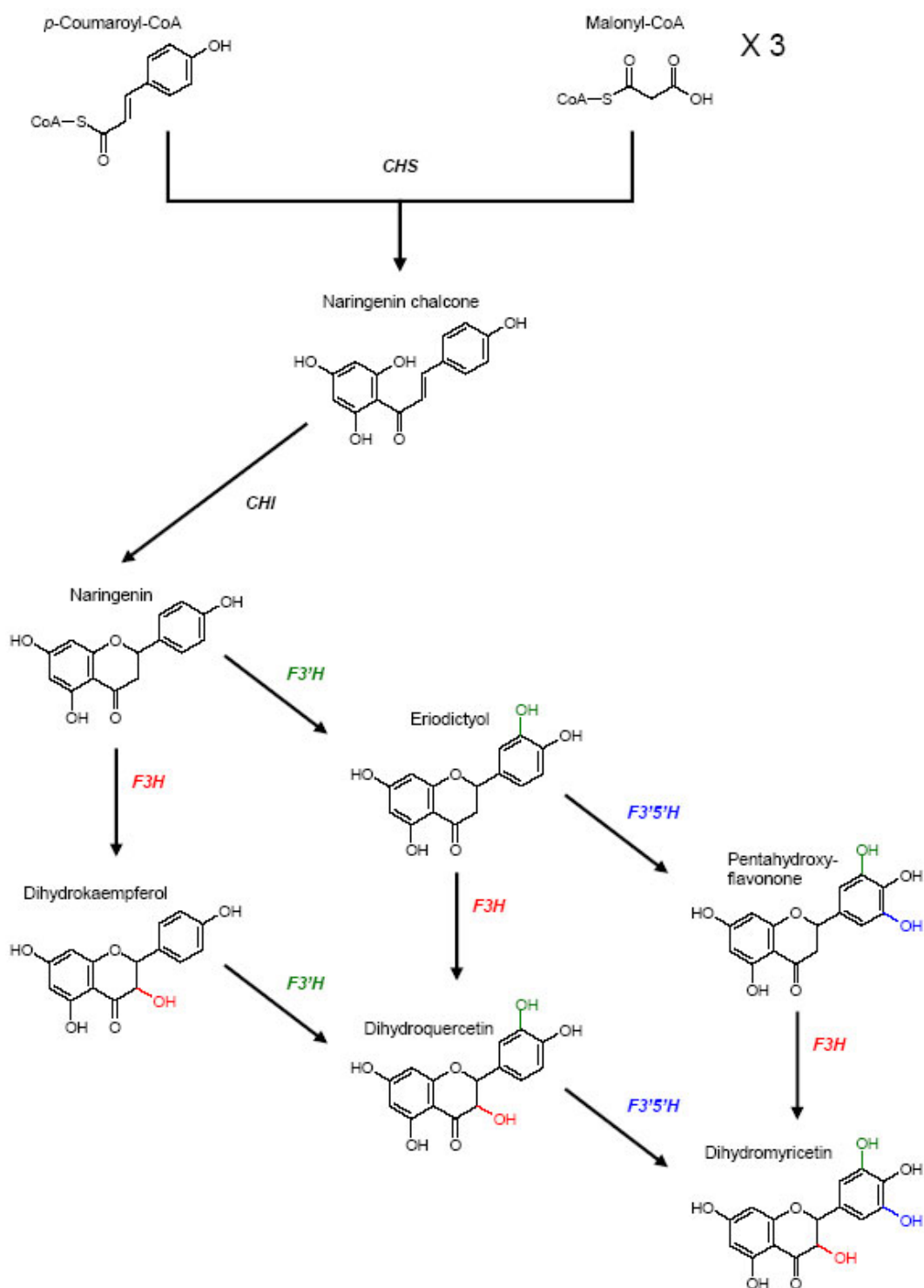
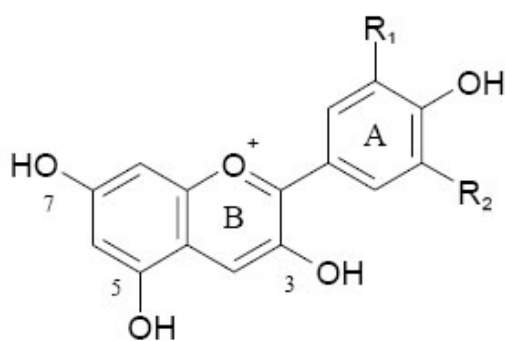


Figure 1.1: Central flavonoid metabolism, enzymes responsible for hydroxylation at particular positions indicated by colour. Enzyme abbreviations: *CHS* – chalcone synthase, *CHI* – chalcone isomerase, *F3'H* – flavonoid 3'-hydroxylase, *F3'5'H* – flavonoid 3'5'-hydroxylase, *F3H* – flavonoid 3-hydroxylase. Adapted from Winkel-Shirley (1999); Glassgen *et al.* (1998); Boss *et al.* (1996b).



Compound	R ₁	R ₂
Pelargonidin	H	H
Cyanidin	OH	H
Delphinidin	OH	OH
Peonidin	OCH ₃	H
Petunidin	OCH ₃	OH
Malvidin	OCH ₃	OCH ₃

Figure 1.2: Common anthocyanidin structure with variations at R₁ and R₂. Ring structures labelled as A and B, while possible glycosylation sites are numbered.

The term ‘anthocyanin’ refers to the coloured product accumulating in the vacuole, whereas ‘anthocyanidin’ refers to the non-pigmented aglycone (Zhang and Furusaki, 1999). The predominant anthocyanidins in *Vitis* sp. are cyanidin, peonidin and malvidin that are then stabilised by 3-glucosylation (Mazza, 1995). Monoglycosidic anthocyanins are the most common, with the sugar moiety attached at the 3, 5, or 7 hydroxyl residues of the phenolic groups (Figs. 1.2 and 1.3; Miller *et al.*, (2002). However, the sugar can be a monosaccharide, disaccharide, or trisaccharide and can be attached at any, or all of the hydroxyl residues (Yamazaki *et al.*, 1999; 2002). The currently accepted anthocyanin biosynthetic pathway is shown in Figure 1.3.

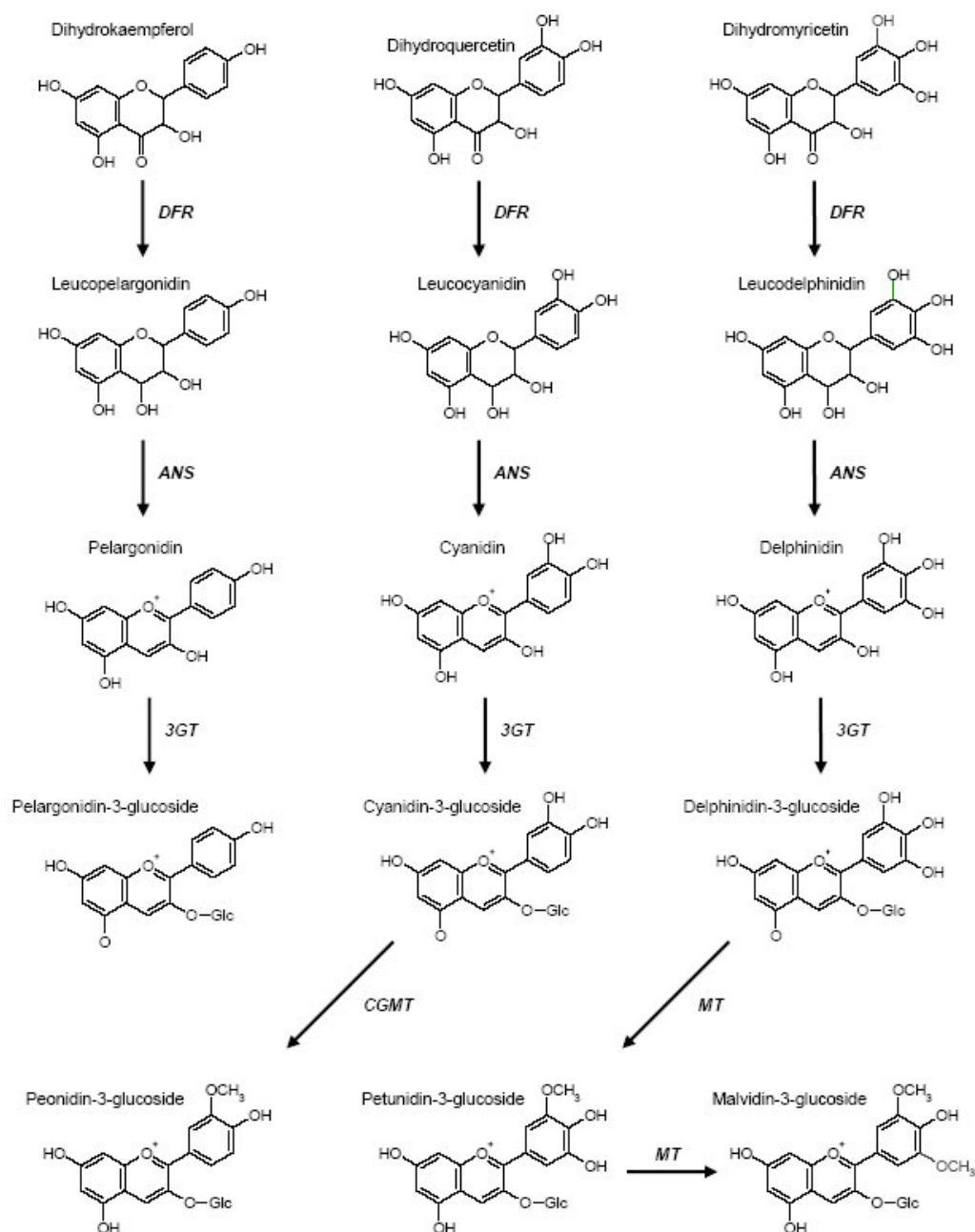


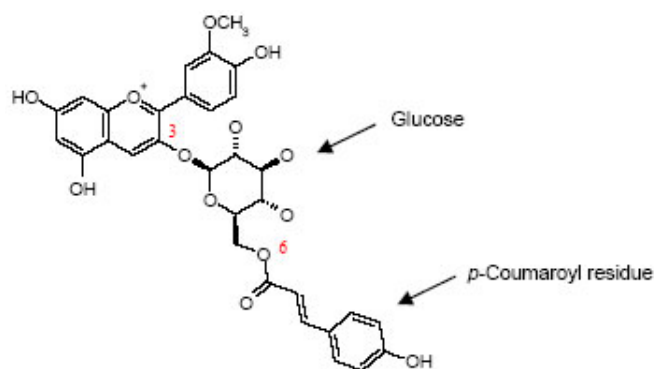
Figure 1.3: Anthocyanin-specific biosynthetic pathway reactions. Enzyme abbreviations: DFR – dihydroflavonol 4-reductase, ANS – anthocyanidin synthase, 3GT – anthocyanidin 3-O-glycosyltransferase, CGMT - S-adenosyl-L-methionine:cyranidin 3-glucoside 3'-O-methyltransferase, MT – methyltransferase. Glucose abbreviated to Glc. Adapted from Boss *et al.* (1996); Glassgen *et al.* (1998), and Winkel-Shirley (1999).

This potential for exponential variation in glucoside residues is rarely observed in any one plant. The most prevalent structures are 3-, or 5-monosaccharide moieties, supplied by uridine diphosphate (UDP) conjugates of glucose, galactose, xylose, rhamnose and arabinose (Francis, 1989). Furthermore, some sugars may be acylated with aliphatic (acetic acid) or aromatic (commonly one of the four cinnamic acids - *p*-coumaric, caffeic, sinapic or ferrulic) acyl moieties (Gross, 1987; Fujiwara *et al.*, 1997).

Aromatic acylation stabilises the colour of anthocyanins by intramolecular copigmentation, where the acyl moiety folds over and interacts with the pyryllium core, protecting it against nucleophilic water attack (Glassgen and Seitz, 1992; Figueiredo *et al.*, 1996). Acylated anthocyanins accumulated by *V. vinifera* are the acetylated and *p*-coumaroylated forms of the 3-glucosides already described (Fig. 1.4; Curtin *et al.* (2003).

Figure 1.4: Peonidin-3-*p*-coumaroylglucoside.

An example of an acylated anthocyanin accumulating in *Vitis vinifera* L.



1.3 Anthocyanins as Bioproducts

1.3.1 Commercial Uses

The main commercial interest in anthocyanins is their use as a food and beverage colorant, an application that has an estimated 4-6% annual growth rate

due to consumer concern over synthetic red food colourants (Zhang and Furusaki, 1999). This niche was created by the toxicity and immunogenicity of RED C No. 2 and 4 and an increased risk of asthma associated with their excess consumption (Bridle and Timberlake, 1997; Fu, 1998). Whereas, common natural colorants do not, in most cases, induce these responses in human studies (Kuhnau, 1976; JECFA, 2000). Natural colourants can be divided into anthocyanins, betalains, chlorophylls, carotenoids, flavonoids, polyphenols, Monascus, hemes, quinones, biliproteins, safflower, turmeric, and miscellaneous (Francis, 1989; Hanssen and Marsden, 1989; Bridle and Timberlake, 1997; Espin *et al.*, 2000). Currently, the predominant use for anthocyanins is in acidic beverages such as blackcurrant drinks and soft drinks, along with sugar confectioneries and fruit preparations such as jams (Bridle and Timberlake, 1997).

There is also growing interest in the health-promoting effects that are being attributed to anthocyanin dietary intake with evidence for antimutagenic effects (Yoshimoto *et al.*, 1999b), antioxidant properties (Sarma *et al.*, 1997; Degenhardt *et al.*, 2000) and reduced risk of coronary heart disease (Waterhouse, 1995). Intake of anthocyanins is correlated with the so-called 'French Paradox' where, despite the high fat content in foods, the consumption of anthocyanins (and other flavonoids) in red, but not white wine reduces the prevalence and mortality from coronary heart disease in France (Yarnell and Evans, 2000). While recent studies focussing on different phenolics in red wine have suggested that these can interfere with atherogenesis, anthocyanins in general have higher bioavailability and possess stronger *in vitro* activity (Donovan *et al.*, 1999; Bell *et al.*, 2000; Bub *et al.*, 2001; Ignatowicz and Baer-Dubowska, 2001).

Anthocyanins have also been beneficial in treating other circulatory disorders and certain inflammatory and ophthalmological conditions (Bridle and Timberlake, 1997). On this basis, anthocyanin-containing products, such as the variety of sweet-potato derived products sold in Japan, are being marketed for their health benefits. There are potentially numerous applications for anthocyanins; therefore, there is a requirement for a consistent, scalable means of production.

1.3.2 Choice of Production System

The best method of production of plant chemicals has long been debated. Field crop production is advantageous due to the relative ease of cultivation, yet has the disadvantages of variations in availability due to seasonal growth, heterogeneity of cell types reducing the purity and increasing purification costs, and yield losses from disease and predation (Dornenburg and Knorr, 1996). Furthermore, the level of production cannot be augmented in the crop without large-scale, costly and wasteful plantation treatments. Use of transgenic plants ectopically producing the chemicals may overcome this, but face the same environmental limitations, in addition to public scepticism surrounding genetically modified products. Finally, microbial transformation or an adapted chemical synthesis utilising intermediate metabolites from plants may be disadvantageous due to concerns regarding stereoisomerism and incomplete stoichiometric conversion (Fischer *et al.*, 1999). These considerations have restimulated the interest in anthocyanin-producing *in vitro* plant cell/tissue culture-based approaches (Zhang and Furusaki, 1999; Choi *et al.*, 2001).

1.3.2.1 Plant cell and tissue cultures for bioproducts

The distinction between plant cell and tissue cultures is that cell cultures are made up of mostly non-differentiated growth, while tissue cultures consist of differentiated or semi-differentiated cells. The intended purpose dictates what type of culture is initiated, as the level of differentiation effects the growth characteristics and metabolic profile. While the level of metabolite production may be lower than for tissue (ie. shoot, flower) cultures, cell cultures are the ideal starting plant material for a production process as their high growth rate enables rapid scaling-up of the culture (Verpoorte *et al.*, 1999).

The controllability of the microenvironment in plant cell culture is commercially advantageous by permitting a year-round, uniform supply of the chemicals and the ability to induce higher levels of production in the homogeneous cell population, including a precise control of the concentration of elicitors by their direct addition into the media. This enables a more simplified approach to quantitative kinetic analysis, as opposed to the use of whole plants or tissue culture, critical for assessing process enhancement strategies (Dornenburg and Knorr, 1996; Yeoman and Yeoman, 1996; Verpoorte *et al.*, 1999).

Bioprocessing in plant cell culture is attracting much interest because products can still be considered natural, and production quantity and quality is afforded through a continuous, controlled production process. Due to the costs involved in establishing plant cell culture bioprocesses, high value pharmaceuticals are the most likely targets for development. This is especially the case for drugs such as paclitaxel¹, where production from the natural resource is limited due to its slow growth in narrow geographical regions, resulting in supply-

¹ Paclitaxel is the generic name of Taxol[®], which is a trademark of Bristol-Myers Squibb

demand inequities (Ketchum *et al.*, 1999). Examples of bioproducts obtainable from plant cell cultures are given in Table 1.1.

Table 1.1: Examples of secondary metabolites produced by plant cell suspension cultures.

Chemical (class)	Application	Plant Species	Production capability	References
Paclitaxel (diterpenoid)	Anti-cancer drug	<i>Taxus brevifolia</i> L.	295 mg.l ⁻¹ 10-20× that of normal cell culture when elicited.	(Tabata, 2004)
Camptothecin (alkaloid)	Anti-tumour drug	<i>Camptotheca accuminata</i> L.	1/20th level of production in intact plants.	(DiCosmo and Misawa, 1995; Kim <i>et al.</i> , 1999)
Berberine (isoquinoline alkaloid)	Anti-microbial	<i>Papaver somniferum</i> L.	15% increase compared to intact plant material	(Bock <i>et al.</i> , 2002; Kirakosyan <i>et al.</i> , 2004)
Caffeine (purine alkaloid)	Flavour	<i>Coffea arabica</i> L.	13-fold improvement by immobilization and 10-fold by light irradiation over standard cell cultures	(Dornenburg and Knorr, 1996; Kurata <i>et al.</i> , 1998)
Hyperforin	Anti-depressant	<i>Hypericum perforatum</i> L.	6-fold improvement over intact plant production	(Kirakosyan <i>et al.</i> , 2004)
Shikonin (naphthaquinone)	Pigment	<i>Lithospermum erythrorhizon</i> L.	Production at commercial levels.	(Dornenburg and Knorr, 1996)

1.3.2.2 Anthocyanin production in plants

Table 1.2 shows the level of anthocyanin content of some common fruits and vegetables, with certain grape varieties topping the list on a per weight basis. Anthocyanins for commercial use have been prepared by extraction from grape pomace (a by-product of winemaking) in Italy since 1879 and marketed under the name “Encocyanin” (Bridle and Timberlake, 1997; FDA, 2003). While grape

extracts such as this are the main commercial source of anthocyanin for use as food colourants, other plant materials used include red cabbage, elderberries, blood oranges, black chokeberries and sweet potatoes (Bridle and Timberlake, 1997).

Table 1.2: Anthocyanin content of some common fruits and vegetables (reproduced from Clifford (2000); Manach *et al.* (2004)).

Source	Pigment Content (mg.100g-FCW ⁻¹)	Reference(s)
Apples (Scucog)	10	(Mazza and Maniati, 1993)
Bilberries	300-320	(Mazza and Maniati, 1993)
Blackberries	83-326	(Mazza and Maniati, 1993)
Black currants	130-400	(Bridle and Timberlake, 1997)
Black raspberries	300-400	(Bridle and Timberlake, 1997)
Blubberies	25-495	(Mazza and Maniati, 1993)
Black chokeberries	560	(Kraemer-Schafhalter <i>et al.</i> , 1996)
Cherries	4-450	(Kraemer-Schafhalter <i>et al.</i> , 1996)
Cranberries	60-200	(Bridle and Timberlake, 1997)
Elderberry	450	(Kraemer-Schafhalter <i>et al.</i> , 1996)
Grapes	6-750	(Mazza and Maniati, 1993; Clifford, 2000)
Kiwi	100	(Kraemer-Schafhalter <i>et al.</i> , 1996)
Plum	2-25	(Timberlake, 1988)
Red cabbage	25	(Bridle and Timberlake, 1997)
Red onions	7-21	(Mazza and Miniati, 1993)
Red radishes	11-60	(Giusti <i>et al.</i> , 1998)
Red raspberries	20-60	(Mazza and Miniati, 1993)
Rhubarb	200	(Manach <i>et al.</i> , 2004)
Strawberries	15-35	(Bridle and Timberlake, 1997)

1.3.2.3 Anthocyanin production in suspension culture

Choice of initial explant for generation of suspension culture is important to obtain a stable, high expressing line responsive to various elicitation strategies. Seitz and Hinderer (1988) documented 27 families producing anthocyanins in *in vitro* suspension culture. In the following decade, this number had increased only

to 29 different plant species (Bridle and Timberlake, 1997), yet increased focus on anthocyanin production in the past decade has placed a more recent estimation at 45 plant families (Rao and Ravishankar, 2002). Some of the more intensively studied varieties include snapdragon (*Anthirrinum majus* L.); maize (*Zea mays* L.); petunia (*Petunia hybrida* L.) and more recently sweet potato (*Ipomoea batatas* L.); strawberry (*Fragaria* spp.); carrot (*Daucus carota* L.) and grape (Winkel-Shirley, 2001a).

There are currently no plant cell culture systems for commercial anthocyanin production, although preliminary economic evaluations for a *V. vinifera* L. cell suspension suggest the development of an industrial process is feasible (Cormier *et al.*, 1996). The authors estimated the costs of production at US\$931 kg⁻¹ for 100% pure anthocyanins, while market price at the time for a 3.35 g.l⁻¹ anthocyanin solution was \$7US.kg⁻¹. Thus, pure anthocyanin preparations could be sold for US\$2038 kg⁻¹.

Advantages of using plant cell culture for anthocyanin production include those mentioned in section 1.3.2.1 and the ability to engineer cultures to produce a specific profile of anthocyanins including the more stable, acylated anthocyanins, permitting a wider range of applications (Baker *et al.*, 1994; Dougall *et al.*, 1998).

1.3.2.4 Anthocyanin stability and accumulation in suspension culture

Cell and tissue cultures of plants retaining anthocyanin-productivity generally display similar expression profiles to the intact plant. In fact, in order to gain governmental recognition in Japan as a natural product, the *in vitro* profile must match the *in vivo* profile. However, in a seemingly tissue-specific manner, some reports have demonstrated differences in the proportion and identity of

anthocyanins present in *Vitis* spp. (Yamakawa *et al.*, 1983b; Tamura *et al.*, 1989), sweet potato (Yoshinaga *et al.*, 1999) , *Carthamus tinctorius* (Hanagata *et al.*, 1992) and strawberry calli (Mori *et al.*, 1993). While other species have demonstrated the appearance of new pigments (Hanagata *et al.*, 1992), *Vitis* spp. exhibit only varied ratios of the predominant pigmented species, from pelargonidin to peonidin in cell cultures compared to the whole plant. The overactivity of both 3'MT and F3'H in culture was proposed to explain this phenomenon. Over-expression of proteins is often noted in cells cultured from callus, due to their dedifferentiation, various stresses, or even selective pressures favouring the survival of cell types with atypical anthocyanin expression patterns (Frank *et al.*, 2000; Che *et al.*, 2002).

Reports on the stability of anthocyanin production have demonstrated varied responses within cell lines and between different cell lines. *Ajuga reptans* cell suspension and callus lines possessed high stability in terms of anthocyanin quantity and type over 5 years of subculturing (Callebaut *et al.*, 1990). Curtin (2005) showed that a high anthocyanin-expressing *V. vinifera* L. cv. Gamay Fréaux suspension cell culture (FU-02) with predominating malvidin species tended toward the more stable acylated, cyanidin and peonidin-enriched suspension line (FU-01) after long-term, non-selective subculturing. This anthocyanin instability was also observed by Deus-Neumann and Zenk (1984) in *Catharanthus roseus*. However, as this FU-01 line is highly stable for biomass yield and anthocyanin production over continuous subculturing, *V. vinifera* L. cell cultures offer distinct advantages in the production of medium unit value secondary metabolites, such as anthocyanins.

However, despite the interest in this field, there has been no patenting of commercial processes for *in vitro* production of anthocyanins due to an insufficient yield (Zhang and Furusaki, 1999). For example, while Cormier *et al.*, (1994) achieved *V. vinifera* suspension cell cultures accumulating between 44-102 mg.100g-FCW⁻¹ anthocyanins after active clonal selection this is still 7.5-fold less anthocyanin than in the intact berry (Mazza and Miniati, 1993). Therefore, improved strategies are required to augment production of anthocyanins in suspension cell culture to a commercial level.

1.3.3 Methods of Enhancing Anthocyanin Production

1.3.3.1 Empirical approaches

Many groups have utilised seemingly random approaches for enhancing production of specific products. These approaches are used initially in situations where little is known about the production/regulation of a particular compound. As much is known regarding the biosynthesis of anthocyanins, contemporary reports of purely empirical approaches for enhanced production are rare. However, Yamamoto *et al.* (1996) co-cultivated *Sophora flavescens* and *Glycyrrhiza glabra* cultured cells with cork tissue, with a resultant increase in a variety of secondary metabolites, including anthocyanins. This approach rarely leads to an effective strategy for improving anthocyanin production to commercial levels; however, can provide a starting point for rational elicitation.

1.3.3.2 Semi-rational approaches

Anthocyanins, as with other secondary metabolites, are general indicators of stress in plants. The biological role of anthocyanins referred to in Section

1.2.1.1 are relevant to anthocyanin production in plant cell culture as the majority of enhancement strategies that have been developed have exploited their response to environmental stimulation, including mimicking the pathogen defense response. This has been attributed to the induction of multiple enzymes in the flavonoid biosynthetic pathway, including PAL, CHS and CHI (Seitz and Hinderer, 1988; Gleitz and Seitz, 1989). Thus, strategies for enhancing productivity have exploited their *in vivo* response to environmental cues – UV light (Gleitz and Seitz, 1989; (Noh and Spalding, 1998), fungal elicitors in *Daucus carota* (Rajendran *et al.*, 1994), yeast cell wall (Yamamoto *et al.*, 2001), nitrate (Do and Cormier, 1991) and phosphate deprivation (Dedaldechamp *et al.*, 1995), low pH and high osmotic stress (Suzuki, 1995) and increased sucrose concentration (Roubelakis-Angelakis and Kliewer, 1986). These approaches are commonly utilised when little is known of the biosynthetic steps, but often leads to a loss in cell viability (Zhang and Furusaki, 1999; Zhang *et al.*, 2004). However, as more is learnt about the system, it is possible to further rationalise the metabolic engineering, enhancing the likelihood of a successful approach.

1.3.3.3 Rational/Integrated approaches

Metabolic engineering of biosynthetic pathways in order to augment production of specific compounds is a rarely taken approach in the past due to the need for complete understanding of the pathway and its regulation. Strategies may require supplementation of key precursors, or intermediates and eliminating feedback inhibition/degradation by product sequestration at various times during the culture. The characterisation of the anthocyanin biosynthetic pathway and, to a lesser extent, its regulation in grape, facilitates a rational enhancement strategy.

Zhang *et al.* (2002a) noted a 14-fold induction of anthocyanin accumulation in *V. vinifera* L. suspension cells by integrating jasmonic acid treatment and light irradiation. This integrated approach yielded a synergistic increase in anthocyanins, greater than the sum of the effects of the individual treatments and was explained by the effects on specific anthocyanin biosynthetic genes (Curtin, 2005). The majority of these rational approaches to increase anthocyanin production target the biosynthetic pathway, without any focus on post-biosynthetic events – transport, storage, degradation (Zhang *et al.*, 2002b). Despite these enhancement strategies to increase the biosynthetic pathway, the level of production of anthocyanins in suspension culture is often less than that of the intact plant (Clifford, 2000; Rao and Ravishankar, 2002; Manach *et al.*, 2004). Therefore, post-biosynthetic events may limit anthocyanin accumulation and need to be considered in order to achieve maximum anthocyanin production.

1.4 Anthocyanin Biosynthetic Events

The availability of a myriad of anthocyaninless-mutants and recovery of non-functional alleles from commercial varieties of maize, snapdragon and petunia have not only led to the elucidation of the general biosynthetic pathway (Fig. 1.2), but also has permitted the study of pathway regulation (Grotewold *et al.*, 1998; Mol *et al.*, 1998; Winkel-Shirley, 2001a). This is of primary importance to a rationalised method for maximising productivity in plant cell culture (Zhang and Furusaki, 1999). The pivotal, or control point is the link between primary and secondary metabolism and has, therefore, attracted extensive research efforts. It appears that pathway induction, in particular secondary metabolic pathways, is initiated by genome-wide regulation by specific transcription factors, but

controlled by the transcriptional and translational repression and feedback inhibition of individual biosynthetic enzymes (Holton and Cornish, 1995; Glassgen *et al.*, 1998; Terrier *et al.*, 2005). These shall be addressed in the following sections.

1.4.1 Subcellular Localisation of Anthocyanin Biosynthesis

Much debate existed about the site of anthocyanin biosynthesis and so numerous microscopic studies were undertaken to localise biosynthetic enzymes. CHS was shown to be associated with the rough endoplasmic reticulum (rER) in buckwheat hypocotyls (Hrazdina *et al.*, 1987) and Arabidopsis (Saslowky and Winkel-Shirley, 2001). The co-localisation of this enzyme with CHI, both 'soluble cytosolic' enzymes, implies another enzyme acting as the rER anchor (Burbulis and Winkel-Shirley, 1999). Using immunoprecipitation and yeast two-hybrid assays, Burbulis and Winkel-Shirley (1999) demonstrated that the successive anthocyanin biosynthetic enzymes CHS, CHI, F3'H and DFR interact in an orientation-specific manner in Arabidopsis. F3'H was proposed as this putative anchor as a mutation that deleted the cytoplasmic domain resulted in altered localisation of both CHS and CHI, but not F3'H (Saslowky and Winkel-Shirley, 2001). This supports the hypothesis of enzymes possessing both structural and catalytic roles, thereby constraining the independent evolution of protein structure.

The final enzymes in the biosynthetic pathway – glycosyltransferases (Hrazdina *et al.*, 1978; Do *et al.*, 1995; Rose *et al.*, 1996), acyltransferases (Suzuki *et al.*, 2003a) and methyltransferases (Jonsson *et al.*, 1983), respectively - have not been studied to the same depth. All glycosyltransferases to date have

been localised to the cytosolic fraction, with the only vacuolar activity attributed to non-specific absorption in the purification protocol (Do *et al.*, 1995; Rose *et al.*, 1996; (Ford *et al.*, 1998). A number of glycosyltransferases have been characterised, with a distinct enzyme presumed to attach each distinct sugar moiety to the anthocyanidins.

Glycosylation may be considered both a biosynthetic and a post-biosynthetic event (Zhang *et al.*, 2002b). Only glycosylated anthocyanins accumulate in the vacuole with, at least, a monosaccharide at the 3'-position, catalysed by UFGT. Any further glycosylation at other residues, in addition to acylation and methylation, may therefore be considered post-biosynthetic modifications. A methyltransferase from petunia, and acyltransferases from *Gentiana triflora* and *P. frutescens* performing the final biosynthetic modifications of anthocyanins, have also been located in the cytosol (Jonsson *et al.*, 1983, (1984); Fujiwara *et al.*, 1998; Yonekura *et al.*, 2000). Anthocyanins are subsequently transported to the central vacuole for storage and accumulation, which shall be discussed in more detail in the following sections.

1.4.2 Regulation of Anthocyanin Production

1.4.2.1 Biosynthetic enzymes

Regulation of the anthocyanin biosynthetic pathway in *V. vinifera* has been investigated in ripening berries (Boss *et al.*, 1996a) and UV-irradiated berries (Sparvoli *et al.*, 1994). Evidence from these and other studies (Boss *et al.*, 1996b) point towards UFGT gene expression being the critical determinant in anthocyanin biosynthetic control in both *V. vinifera* berry skins and cell culture. There is, however, limited knowledge of anthocyanin pathway regulation in cell

culture, with the focus on early pathway genes PAL and CHS (Kakegawa *et al.*, 1995). In addition to UFGT, Curtin (2005) also demonstrated that F3'5'H was a critical determinant for anthocyanin yield in cell culture. Furthermore, a reduced inducibility of these transcripts in cells with constitutively high transcription levels indicates a possible upper limit to this expression (Curtin, 2005).

Regarding biosynthetic control, UFGT and CHS are both likely candidates as both have non-toxic substrates with moderate stability able to accumulate and possibly drive gene induction (Ahmed *et al.*, 1994; Baker *et al.*, 1994; Piffaut *et al.*, 1994). However, other candidates cannot be readily discounted on the basis of this property alone due to the possibility that they complex with other pathway proteins and sequester the reactive or toxic intermediates. It is widely believed that few, if any, proteins involved in cytosolic metabolic pathways act alone, but rather as part of a macromolecular enzymatic complex, as mentioned in Section 1.4.1 (Winkel-Shirley, 2001b). Therefore, it would seem that induction of a single enzyme could not lead to an increase in anthocyanin accumulation without the concomitant increase in other biosynthetic enzymes.

1.4.2.2 Transcription factors

Anthocyanins are synthesised from a branched pathway responsible for producing other secondary metabolites (Fig. 1.2), with pathway-wide regulation achievable by the involvement of transcription factors (Grotewold *et al.*, 1998). Kobayashi *et al.* (2002) identified three consecutive Myb factors in the grape genome as transactivators of the anthocyanin pathway. However, UFGT may still be the control enzyme for the anthocyanin biosynthetic pathway possibly

requiring activation by all upstream enzymes, or in combination with other conditions, including build up of metabolites.

Primary transcriptional control of anthocyanin metabolism revolves around interaction of *trans*-acting transcriptional activators with specific *cis*-acting regions in the promoters of anthocyanin structural genes. The model system of anthocyanin biosynthesis in maize seeds facilitated isolation of the first plant transcription factor, C1, which was found to encode a protein with a conserved DNA-binding domain also found in the *c-myb* proto-oncogene (Paz-Ares *et al.*, 1987). A second myb-factor of the C1 family, P1, was found to activate a subset of the flavonoid genes that C1 could activate, leading to biosynthesis of another class of pigments – the phlobaphenes (Grotewold *et al.*, 1994). However, in order to functionally activate pigmentation, C1/P1 require expression of a second class of transcription factor from the R family – those that contain a bHLH (basic helix-loop-helix) motif also classified as myc proto-oncogene-like. This was demonstrated by Sainz *et al.* (1997), where C1 was able to physically bind the DFR promoter but without co-expression of bHLH-factor B (part of the R gene family) the promoter was not activated.

Another model system in which transcriptional regulation of anthocyanin biosynthesis has been studied is that of *Petunia hybrida*. Myb- and bHLH-factors have been characterised from petunia, along with another class of regulator– the WD40 repeat protein (de Vetten *et al.*, 1997). The AN11 WD-repeat protein was localised to the cytoplasm and given the protein-protein interactions promoted by the WD-repeat it is thought to modulate the activity/localisation of the Myb/bHLH factors (de Vetten *et al.*, 1997). Functional homology of maize and petunia transcription factors was demonstrated by Quattrocchio *et al.* (1993),

where maize Lc (of R family) and C1 were able to induce transcription of anthocyanin structural genes in petunia. Furthermore, two petunia *CHS* copies were differentially activated in the same manner by the maize transcription factors as by native petunia factors, suggesting the regulatory proteins were functionally similar and their choice of target genes was determined by promoter sequences. Functional equivalence of *JAF13* from petunia with *R* of maize, and *AN2* from petunia with *C1* of maize further extended the idea that regulatory genes are interchangeable between species while specific responses to regulatory genes are determined by the cis-acting promoter elements (Quattrocchio *et al.*, 1998).

Transcription factors regulating anthocyanin biosynthesis have also been characterised from other species; for example *Arabidopsis thaliana*, *Perilla frutescens* and *Gerbera hybrida*. Table 1.3 summarises the homologues of known petunia transcription factors that have been characterised from these systems, while Figure 1.5 illustrates the generic model of transcriptional control of anthocyanin structural gene expression.

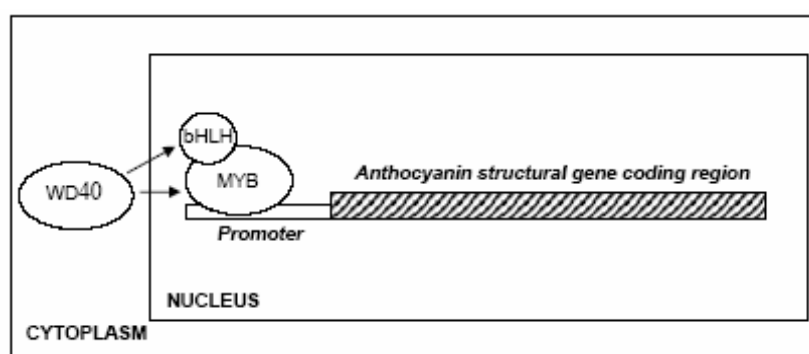


Figure 1.5: Generic scheme for transcriptional control of anthocyanin biosynthetic genes, based on model systems in maize and petunia. Adapted from Walker *et al.* (1999a).

Table 1.3: Transcription factors homologous to those of maize and/or petunia.

Species	Locus	Type of Factor	Homologue	Reference
<i>A. thaliana</i>	PAP1 TTG1	Myb WD40	AN2 AN11	(Borevitz <i>et al.</i> , 2000); (Walker <i>et al.</i> , 1999a)
<i>P. frutescens</i>	Myc-rp/gp Myc-F3G1 Myb-P1 PFWD	bHLH bHLH Myb WD40	JAF13 AN1 Myb305* AN11	(Saito and Yamazaki, 2002)
<i>G. hybrida</i>	GMyb10 GMyc1	Myb bHLH	AN2 JAF13	(Elomaa <i>et al.</i> , 1998; 2003)

* Myb305 is a MYB-factor from *Antirrhinum majus* (snapdragon) that does not have a known homolog in maize or petunia.

While transcription factors have specific effects on anthocyanin biosynthesis, it is both interesting and important to note that in addition they control other cellular processes. Bruce *et al.* (2000) noted a much wider influence on gene expression than expected, where *CI* and *R* altered expression levels of hundreds of genes in maize suspension cultures. Spelt *et al.* (2000) found that *ANI* of petunia had roles in control of vacuolar pH and seed coat development, along with the better known regulation of anthocyanin synthesis. Going a step higher in the regulatory cascade, *VP1* – a known regulator of *CI* – globally alters gene expression relating to seed development (Suzuki *et al.*, 2003b).

Using degenerate PCR, Kobayashi *et al.*, (2002) cloned 37 Myb-related clones from Kyoho grape (*V. labruscana*), categorised into 8 groups (MybA-H) based on sequence similarity. The MybA group were closely linked to colour development and full-length cDNAs were obtained, being further characterised into MybA1, MybA2 possessing a single and double acidic (X-Y) region, respectively. Bombardment of the MybA, but not the MybB sequences into non-

pigmented embryos saw the development of colour and UFGT expression (Kobayashi *et al.*, 2002). Kobayashi *et al.* (2002) favoured *VlmybA1* as the key transcription factor due to its expression profile, while Walker *et al.* (unpublished results) demonstrated an alternate sequence, *VvmybA2*, was influential in a range of grape species.

Transcriptional control alone is thought to be insufficient to regulate activities within a complex, branched metabolic system such as the phenylpropanoid and flavonoid pathways (Winkel-Shirley, 1999). Other mechanisms such as altered rates of mRNA degradation (Metzlaff *et al.*, 1997) or covalent modification of enzymes to alter their specific activity are possibly involved to allow fine-tuning of the pathway.

1.4.2.3 Post-transcriptional and post-translational regulation

Most evidence for the involvement of post-transcriptional and post-translational regulation in anthocyanin biosynthesis is from studies where the pattern of structural gene expression does not correlate with the level of anthocyanin accumulation or enzyme activities (Kakegawa *et al.*, 1995; Shvarts *et al.*, 1997; Noh and Spalding, 1998). Similarly, PAL and CHS enzyme activities were more efficiently induced at high elicitor concentrations, even though the rate of *de-novo* enzyme synthesis did not change (Lawton *et al.*, 1983). Evidence for post-transcriptional regulation was found for cytokinin regulated anthocyanin biosynthesis in *Arabidopsis*, where CHS and DFR were found to be under transcriptional control while PAL and CHI were not (Deikman and Hammer, 1995).

Strong evidence for post-transcriptional control over PAL (and STS) was evident for *Vitis* cell cultures when elicited with fungal cell walls (Melchior and Kindl, 1991). Despite identical transcription patterns, the enzyme activities reached maxima at different times. Further evidence for non-transcriptional regulation of PAL was evident in the study of Blount *et al.* (2000), where flux through the subsequent enzymatic step (C4H) increased the level of cinnamate, which in turn slowed the rate of flux through PAL. Earlier, pharmacological work had inferred this relationship but due to criticism of the chemical inhibitors used, Blount *et al.* (2000) utilised a genetic approach which demonstrated more definitively the feedback loop.

There is evidence for regulation of anthocyanin production at the biosynthetic level, transcription factor level and by post-transcriptional and post-translational modification in whole plants. However, the level of anthocyanin accumulation in certain cell suspension cells cultured to upregulate biosynthetic genes is lower than that in the intact plant, suggesting other possible limiting factors (Mazza and Miniati, 1993).

1.5 Anthocyanin Post-Biosynthetic Events

As mentioned, immunohistochemistry and cell-fractionation experiments performed to determine the subcellular localisation of the biosynthetic enzymes have shown association with the ER and cytosolic fractions (Hrazdina *et al.*, 1978; 1987). In *lisianthus* some petal flavonoids are deposited in the cell wall (eg. piceid), or compartmentalised within the cytoplasm, while anthocyanins are stored in the vacuole (Markham *et al.*, 2000; 2001). Furthermore, in sorghum, cytoplasmic vesicles accumulate pigmented 3-deoxyanthocyanidin flavonoids in

response to specific fungal infection (Snyder and Nicholson, 1990). This raises the question of how the anthocyanins are specifically targeted to the vacuole during normal growth. Characterisation of the mode of transport is of great importance in the current study towards determining the rate limiting steps in anthocyanin accumulation to enhance production.

1.5.1 Anthocyanin Transport

Mueller and Walbot (2001) proposed three models for anthocyanin sequestration in vacuoles: (1) direct transport of unmodified anthocyanins; (2) transport after their modification; and (3) transport mediated by a carrier protein. These models are difficult to reconcile due to the range of anthocyanins in each plant species, therefore they hypothesised that different plant species utilise different sequestration strategies. In light of available evidence, it is more likely that a combination of these transport mechanisms exists in plant cells, with a specific glutathione *S*-transferase protein as the carrier protein interacting with ER-derived vesicles with integral membrane transport pumps able to deliver both unmodified and modified anthocyanins. These shall be discussed in the following sections.

1.5.1.1 ER-derived vesicular model

Electron microscopy studies indicated that multiple ER-derived vesicles bud off and fuse with the central vacuole, facilitating transport of various polyphenolics in red cabbage (Deus-Neumann, 1983), Douglas-fir (Parham and Kaustinen, 1977) and mung bean (Duke and Vaughn, 1982). Furthermore, black Mexican sweetcorn (BMS) cells expressing *P*, a regulator of 3-deoxy flavonoid

biosynthesis, accumulate yellow and green autofluorescent bodies (of unknown composition) that are targeted to the central vacuole and cell wall, respectively (Grotewold *et al.*, 1998; Lin *et al.*, 2000). The *trans*-Golgi network (TGN), a conduit for numerous secretory vesicles, was not shown to be involved in the transfer of these autofluorescent compounds by incubation with the specific inhibitor, brefeldin A (Grotewold *et al.*, 1998). Despite this, the involvement of the TGN has been implicated in anthocyanin transport as auxin-deprivation, which induces anthocyanin accumulation (Ozeki and Komamine, 1981) also causes an increase in the secretory activity of the Golgi apparatus in tobacco suspension cells (Winicur *et al.*, 1998).

This transport model may apply to anthocyanins as biosynthetic enzyme complexes are associated with the rER in buckwheat hypocotyls (Hrazdina *et al.*, 1987) and the rER and the tonoplast in *Arabidopsis* (Saslowsky and Winkel-Shirley, 2001). Vacuolar deposition of anthocyanins was observed in grape cell suspension cultures in a focal – both unifocal and bifocal - fashion (Garcia-Florenciano *et al.*, 1992). In support of this, anthocyanin containing bodies (anthocyanoplasts) were observed in the cytosol of suspension-cultured grape cells after initial transfer from callus, by vacuolar purification (Calderon *et al.*, 1993).

1.5.1.2 GSTs as escort proteins

While strong evidence exists for anthocyanin vacuolar deposition via vesicular fusion, it is clear from other reports that glutathione S-transferases (GSTs) are critical in anthocyanin transport. GSTs are enzymes originally identified by their capacity to detoxify chemically diverse xenobiotics,

particularly herbicides. However, it is apparent that they also play a critical role in the shuttling and accumulation of endogenous, electrophilic compounds in specific cellular compartments, eg. the vacuole (Marrs *et al.*, 1995; Marrs, 1996; Alfenito *et al.*, 1998; Wang and Ballatori, 1998; Edwards *et al.*, 2000; Mueller *et al.*, 2000). GSTs are a large, highly divergent family of ubiquitous proteins that constitute around 1-3% of cellular protein (Marrs, 1996). While mammalian GSTs have been divided into at least 7 groups (α , β , χ , ρ , μ , π , σ , and θ) based primarily on substrate specificity and sequence similarities, the majority of plant GSTs are purported to fall into the theta (θ) class (Marrs, 1996). These plant GSTs are further categorised into three subdivisions – type I, II and III – based on the above parameters, but also exon/intron structure (Droog *et al.*, 1995; Droog, 1997). Further complexity is added by the fact that GSTs in all systems function as homo- and hetero-dimers. It is believed that this complexity contributes to the capacity of plants to detoxify unique and chemically diverse compounds (Prade *et al.*, 1998).

Barley has been used as a model system to study the function of GSTs on xenobiotics. Each GST monomer has a GSH-binding site (G-site) and an adjacent electrophilic substrate binding site (H-site; (Mannervik and Danielson, 1988). GSTs covalently link the glutathione tripeptide (γ -Glu-Cys-Gly; GSH) to the substrate(s) via the reactive sulphhydryl moiety, forming a glutathione S-conjugate (Pickett and Lu, 1989; Ishikawa, 1992). This conjugate is actively sequestered into the vacuole via an integral, Mg-ATP-dependent tonoplast-membrane pump (Martinoia *et al.*, 1993). Furthermore, the activity of these pumps can be upregulated by co-incubation with chemical safeners (Gaillard *et al.*, 1994). The

hostile environment inside the vacuole then degrades the conjugates, either enzymatically or chemically (Matile, 1978; Marty, 1999).

In addition to their catalytic function, GSTs act as nonenzymatic carrier proteins (ligandins) enabling intracellular shuttling of steroids, bilirubin, heme, and bile salts in mammalian cells (Litwack *et al.*, 1971; Ketley *et al.*, 1975; Listowski *et al.*, 1988) and other compounds in plant cells, most notably indole acetic acid (Jones, 1994; Bilanz and Sturm, 1995). Binding of non-substrate ligands (and the GST inhibitor, cibacron blue) to the human π -class GST P1-1 was shown to occur at a site overlapping the H-site by X-ray crystallography (Oakley *et al.*, 1999). Few non-inhibitory compounds were shown to bind a surface pocket of the enzyme, deemed the ligandin-site, or L-site (Oakley *et al.*, 1999). This is in support of findings in *Schistosoma japonica* (McTigue *et al.*, 1995) and squid (Ji *et al.*, 1996). This interaction may facilitate the trafficking of compounds to receptors/pumps for transport and has been suggested to modulate the activity and reduce feedback inhibition and cytotoxicity during high production rate of the compounds (Wolkoff *et al.*, 1979; Listowski *et al.*, 1988).

Many endogenous secondary metabolites are sequestered into the vacuole for storage without their apparent subsequent degradation, including anthocyanins (Marty, 1999). While GSTs have primarily been implicated in anthocyanin shuttling, their involvement in flavonoid production has been categorised into two groups – firstly, in parsley where it is involved in the early steps of a UV light-dependent signal transduction pathway leading to CHS expression (Loyall *et al.*, 2000) and secondly, where it is involved in transport of anthocyanins (and potentially proanthocyanidins in *Arabidopsis*) to the vacuole as for maize, petunia and *Arabidopsis* (Mueller *et al.*, 2000; Mueller and Walbot, 2001). In contrast to

the former phenomenon, the latter mode of action has been correlated with direct binding of anthocyanins and shall be discussed in the following sections.

1.5.1.2.1 *Maize*

Maize mutants exhibiting modified anthocyanin accumulation have been produced using the Mutator (Mu) transposable element, with functions subsequently attributed for most genes (Robertson, 1978; Chandler *et al.*, 1988). Bronze-2 (Bz2) performs the last genetically defined step in anthocyanin biosynthesis (Reddy and Coe Jr, 1962), with the sequence cloned and mapped by transposon tagging and differential hybridisation (McLaughlin and Walbot, 1987). Bz2 mutants accumulate cyanidin-3-glucoside in the cytoplasm of the aleurone, whereupon it is oxidised imparting a bronze colour (Marrs *et al.*, 1995). Bz2 (type III GST) demonstrated GST activity when expressed as a recombinant protein in an *in vitro* assay and after transformation of *Arabidopsis*, *bz2* (Bronze-2 deficient) *Zea mays* protoplasts, and *Escherichia coli* (Marrs *et al.*, 1995). Thin-layer chromatography (TLC) of metabolites revealed that ³⁵S-GSH taken up by protoplasts co-localised with anthocyanins extracted from Bz2, but not from untransformed *bz2* maize protoplasts (Marrs *et al.*, 1995). However, other experiments have detected many unconjugated components co-migrating with anthocyanins via TLC (Grotewold, 2001). As these products were not analysed further, it is not clear whether this result confirms glutathionation of the anthocyanins. Furthermore, subsequent analyses in other plants demonstrate a differential mode of action for GSTs with anthocyanins (Mueller *et al.*, 2000).

While the majority of plant GSTs have been identified as soluble enzymes, *Bronze-2* (when transiently expressed in black Mexican sweetcorn (BMS) suspension cells) associates with the insoluble membrane fraction (Dixon *et al.*,

2002; Pairoba and Walbot, 2003). This finding supports the combinatorial theory of anthocyanin transport, requiring a close proximity between anthocyanin biosynthesis at the ER membrane and the transport mechanisms.

1.5.1.2.2 *Petunia*

A type I plant GST from petunia, called An9, with limited sequence homology to Bz2 was found to complement the loss-of-function phenotype in *Bz2* knockout corn kernels (Alfenito *et al.*, 1998). Mueller *et al.* (2000) demonstrated the interaction of recombinant An9 with anthocyanins in *P. hybrida*, though its activity was shown to be as an escort protein ('ligandin'), not via GSH conjugation. No ^{35}S -GSH anthocyanin conjugates were detected by HPLC in either *in vitro* GST assays or *in vivo* feeding experiments, while herbicide-GSH conjugates were readily detected. Furthermore, determination of *in vivo* free thiol concentration confirmed that GSH was not conjugated to anthocyanin, rather than an inability to detect labile conjugates via HPLC (Mueller *et al.*, 2000).

An9 was shown to bind anthocyanins and other flavonoids in three assays including inhibition of GST activity against the control substrate 1-chloro-2,4-dinitrobenzene (CDNB), equilibrium dialysis and tryptophan quenching (Mueller *et al.*, 2000). Equilibrium dialysis on recombinant An9 indicated that eight isoquercetin molecules bound the GST dimer, while co-incubation with GSH reduced the number of binding isoquercetin molecules to four. Finally, the intrinsic autofluorescence of the 3 tryptophan residues within the C-terminus of An9 were quenched by luteolin, cyanidin and to a lesser extent isoquercetin and cyanidin-3-glucoside without major detectable conformational changes by spectral analysis using circular dichroism (Mueller *et al.*, 2000). While there was

a change in mobility of An9 following incubation with various flavonoids through native polyacrylamide gels, inference of major conformational changes upon binding ligands would require x-ray crystallography. Together, this indicated that An9 is able to bind flavonoids at distinct regions of the protein, dependent upon the structure of the ligand.

1.5.1.2.3 Arabidopsis

Another GST-like sequence implicated in anthocyanin vacuolar transport is the TRANSPARENT TESTA 19 (*tt19*) gene in *arabidopsis* (Kitamura *et al.*, 2004). The orthologous An9 protein was found to complement for the loss of anthocyanin accumulation in *tt19*-deficient mutants. However, An9 did not complement for the altered deposition of proanthocyanidin precursors, indicating an additional function for *tt19*. This sequence is yet to be expressed recombinantly, preventing further analysis of the interaction with anthocyanins and proanthocyanidins.

1.5.1.2.4 Carnation

A carnation mutant (*Flavonoid3*) was shown to have similar phenotypes to *An9*-, *tt19*- and *Bz2*-deficient mutants. As with *tt19*, this mutant was complemented by known anthocyanin-transporting GSTs, in this case both *An9* and *Bz2* (Larsen *et al.*, 2003).

As mentioned, GSTs are critical for transporting anthocyanins with the loss of the gene yielding cells unable to accumulate anthocyanins in the vacuole in a number of plant cells despite the expression of putative functional pumps (Goodman *et al.*, 2004). As the anthocyanins are now considered to not be

covalently modified by these GSTs, proposed models for their involvement are based around the GST covalently modifying or directly binding a motif on the transporter (possibly a GSH-like tripeptide microsequence) to induce a conformational change, facilitating anthocyanin transport. In either situation, GSTs cannot deliver the anthocyanins to the vacuole without an integral membrane transport pump (Mueller and Walbot, 2001).

1.5.2 Transporters/Membrane Pumps

Due, in part, to their structure flavonoids require the activity of integral membrane transport pumps for translocation to their final destination (Kutchan, 2005; Yazaki, 2005; Yoshida *et al.*, 2005). Various groups of pumps have been implicated in the transport of a number of flavonoids, including ATP-binding cassette (ABC) transporters, multidrug resistance-associated proteins (MRPs), multidrug and toxic compound extrusion (MATE) transporters and multidrug resistance (MDR) proteins (Yazaki, 2005).

Anthocyanins, being positively charged at physiological pH, are unable to passively diffuse into the vacuole. Furthermore, this charge contributes to the pH-sensitivity of the chromophore, with low-pH imparting a more reddish tinge (Dangles *et al.*, 1993). The concentration of anthocyanins in the vacuole far exceeds the detectable level in the cytoplasm implicating some active transport mechanism to facilitate this uptake against the concentration gradient (Anderson and Orci, 1988). Using isolated vacuoles from *Daucus carota* and other species, Hopp and Seitz (1987) investigated the uptake of a spectrum of radiolabelled anthocyanins. Acylated anthocyanins isolated from *Daucus carota* were taken up by intact vacuoles extracted from the same species (Model II, Section 1.5.1).

However, experiments utilising non-acylated anthocyanins; vacuoles isolated from other plant species, or no Mg-ATP saw their exclusion from the vacuole (Hopp and Seitz, 1987). This suggests the influence of an integral membrane pump in the vacuolar sequestration of acylated anthocyanins (Rea *et al.*, 1998). In support of this, Klein *et al.* (1996) observed the ATP-dependent uptake of unmodified flavonoid-glucosides into isolated barley vacuoles (Model I, Section 1.5.1). The author suggested the exact methods by which glycosylated, non-acylated anthocyanins breach the tonoplast membrane in *Daucus carota* is still unknown. However, GSTs, or ER-derived vesicles (not incorporated in this experiment) may facilitate this uptake.

Marrs *et al.* (1995) tested the effects of pump inhibitors on anthocyanin accumulation. Protoplasts treated with vanadate, a specific inhibitor of ABC (ATP-binding cassette) transporters, accumulated one-third of the level of cyanidin-3-glucoside of bafilomycin- (H⁺-ATPase pump inhibitor) treated cells and control cells. The authors concluded that as vanadate-sensitivity is a feature of the glutathione (GS-X) pump this must be the method by which anthocyanins are transferred to the vacuole. Such pumps belong to the family of the ATP-binding cassette (ABC) transporters (Rea *et al.*, 1998) and transport glutathione conjugates, with candidates identified in barley (Martinoia *et al.*, 1993), mung bean (Li *et al.*, 1995) and two distinct genes cloned from *A. thaliana* (Lu *et al.*, 1997; 1998). These pumps, called AtMRP1 and AtMRP2, have been shown to be capable of transporting cyanidin-3-glucoside into yeast vacuoles, only when conjugated to glutathione (Lu *et al.*, 1998).

Goodman *et al.* (2004) identified an integral tonoplast membrane pump, belonging to the multidrug resistance-associated protein (MRP) family, deemed

ZmMRP3, which plays a role in anthocyanin transport in *Z. mays* L. Antisense mutants all displayed markedly reduced anthocyanin accumulation and, in some cases, complete absence of pigment in anthocyanin-accumulating tissues. This effect on pigmentation was demonstrated to be effected by the inability of the anthocyanins to be localised to the vacuole, not a deficiency in any biosynthetic enzymes as the anthocyanin profile of the mutants was identical to that of the wild type. The expression of this protein is under the control of the anthocyanin regulators *R/CI*, but appears to be redundant in the aleurone tissue as the accumulation of anthocyanin in the antisense transgenic plants was unaffected by the antisense construct (Goodman *et al.*, 2004). The expression of another *R/CI*-regulated MRP, deemed ZmMRP4, is unaffected by the antisense ZmMRP3 construct and may complement for the loss of ZmMRP3 in the aleurone (Goodman *et al.*, 2004).

An H⁺-gradient dependent transporter has been shown to have a role in anthocyanin accumulation in Arabidopsis and tomato. The *TT12*-deficient Arabidopsis mutant shows greatly reduced proanthocyanidin pigment accumulation in vacuoles of endothelial cells (Debeaujon *et al.*, 2001). The *tt12* product encodes a secondary metabolite transporter like protein belonging to the MATE family. A similar MATE-type permease has been identified as being upregulated in tomato (*Lycopersicon esculentum*) plants with high anthocyanin content resulting from overexpressing the myb-type transcription factor, *Ant1* (Mathews *et al.*, 2003), suggesting that this transport mechanism is conserved in many plant species. The level of anthocyanin accumulation in the body of *tt12* mutants is unaffected, implicating another transporter, possibly an MRP as argued by Mathews *et al.* (2003) in anthocyanin sequestration in these tissues. This may

indicate a role for the MATE protein in channelling excess anthocyanin precursors into proanthocyanidin that utilise MATEs for their localisation. Alternatively, this may indicate the redundancy of this protein, or the combined effects of MATE-MRP-GST systems for efficient transport of anthocyanins. Certainly interplay is inferred between the GST (tt19) and the MATE (tt12) by both deficient mutants exhibiting a reduced proanthocyanidin phenotype in *Arabidopsis* (Debeaujon *et al.*, 2001; Kitamura *et al.*, 2004).

The presence of these pumps is widely accepted and as their influence is rapid and displays redundancy in the maize model, it is considered not to be a rational target for enhancing anthocyanin accumulation.

1.5.3 Anthocyanin Storage

Once localised to the vacuole, further modification of anthocyanins is believed to occur to maximise their retention, enhance their stability and limit feedback inhibition of specific vacuolar enzymes (Calderon *et al.*, 1992). Due to the pH gradient across the tonoplast membrane, there is thought to be a spontaneous ionisation of anthocyanins upon entry, preventing loss due to passive diffusion. In differently coloured genotypes of *Matthiola incana* anthocyanins are stored as soluble compounds, or in an “insoluble state” as either rhombic crystals or pigmented balls called anthocyanoplasts (Hemleben, 1981). The appearance of either storage structures is dependent on the presence of specific anthocyanin types, specifically acylated 3-biglycosides (Hemleben, 1981). While, the appearance of the crystalline storage structures as opposed to the spherical bodies coincides with the presence of cyanidin-, rather than pelargonidin-based anthocyanins. This dependency upon anthocyanin species suggests these bodies

arise from interactions between their chemical constituents and the cellular environment, also seen by Asen *et al.* (1975).

Many more cell types possess anthocyanins associated with insoluble globular vesicles, forming intensely pigmented structures in the vacuole, deemed cyanoplasts (Politis, 1911), anthocyanophores (Lipmaa, 1926) anthocyanoplasts (Pecket and Small, 1980) or anthocyanic vacuolar inclusions (Markham *et al.*, 2000). The term AVI was coined by Markham *et al.* (2000) and for concision, all bodies accumulating anthocyanins shall be referred to as AVIs.

1.5.3.1 Anthocyanic Vacuolar Inclusions

Initially, it was thought that these intravacuolar structures were organelles capable of anthocyanin synthesis. This proposition was based on membrane-bound, non-coloured globules being transported from the cytosol to the vacuole where the development of colour was seen (Politis, 1911, 1914, 1959); (Guillermond, 1931, 1932). Kubo *et al.* (1995) witnessed unpigmented spherical bodies in the vacuole of epidermal cells of dark-grown seedlings of *Polygonum cuspidatum* not accumulating anthocyanin. These bodies developed colour, becoming anthocyanoplasts, when seedlings were irradiated with white light to induce anthocyanin synthesis. Furthermore, AVIs were not seen in betacyanin accumulating species (Nozzolillo, 1972), or non-anthocyanin producing lines (Jasik and Vancova, 1992). However, cells lacking these vesicles are still capable of synthesising anthocyanins (Pecket and Small, 1980; Markham *et al.*, 2000; (Conn *et al.*, 2003). The pool of evidence demonstrating cytoplasmic localisation of the biosynthetic and post-biosynthetic enzymes and their neutral-to-alkaline pH optimum makes them unsuited to the acidic environment of the vacuole and AVIs

(Marty, 1999). Finally, no internal structure was visualised in any of these globules, which is unexpected if these structures are synthesising secondary metabolites (Small and Pecket, 1982; Nozzolillo, 1994).

Pecket and Small (1980) and Small and Pecket (1982) observed the encasement of AVIs within a membrane by electron microscopy in red-cabbage seedlings. Yasuda and Kumagai (1984) also noted that the AVIs in radish seedling hypocotyls had a “membranous structure”. This phenomenon is seen for a number of lytic organelles immediately following vacuolar invagination, but the membrane is often destroyed and the contents released (Robinson *et al.*, 1998; Di Sansebastiano *et al.*, 2001; Jiang *et al.*, 2001; Yamamoto *et al.*, 2003; Jurgens, 2004; Ovecka *et al.*, 2005; Ruthardt *et al.*, 2005).

The permanent membrane encasement of AVIs inside vacuole argues against the fundamental theory of organelle compartmentalisation (Fineran, 1971). In agreement with this, Deus-Neumann (1983) failed to find a membrane-boundary for the AVIs in red-cabbage seedlings, concluding the AVIs were large hydrophobic droplets. This observation is in direct disagreement with those of Small and Pecket (1982) in the same species and could only be explained by differences in sample preparation. However, the lack of a visible membrane has been noted in lisianthus (Markham *et al.*, 2000), sweet potato (Nozue and Yasuda, 1985; Nozue *et al.*, 1993) and *Polygonum cuspidatum* (Kubo *et al.*, 1995). These contradictory reports regarding the presence of a delimiting membrane infer additional species-specific differences in AVI composition. These differences shall be highlighted in the following sections for the most intensively studied varieties.

1.5.3.1.1 *Lisianthus*

Anthocyanin pigment/copigment composition largely accounts for the colour differences (eg. white, orange, purple, and pink) between lisianthus petals (Markham and Ofman, 1993). However, each petal has an intensification of pigment in the inner region, due to the higher prevalence of AVIs compared to the outer petal (Fig. 1.6; Markham *et al.*, 2000). Preliminary results from lisianthus show three major protein species comprising the AVI, all with isoelectric points in the range of 4-5 (Markham *et al.*, 2000). Furthermore, these AVIs preferentially bind di-glucosidic anthocyanins, rather than the more prevalent tri-glucosides by large-scale AVI purification (Markham *et al.*, 2000).



Figure 1.6: Various coloured lisianthus flowers, showing the colour intensification of the inner petal due to the higher AVI prevalence (http://www.american-farms.com/text_plant_pages/lisianthus.htm).

1.5.3.1.2 *Sweet potato*

Prevalence of AVIs has been correlated with anthocyanin accumulation in *Ipomoea batatas* (sweet potato) suspension cultures. It was found that spherical, pigmented bodies increased in size and proportion in cultures grown only under light conditions (Nozue and Yasuda, 1985). Furthermore, treatment of the cultures

with the auxin, and 2,4-dichlorophenoxyacetic acid (2,4-D), known to reduce anthocyanin accumulation in higher concentrations (Takeda *et al.*, 1993; Ko *et al.*, 1994; Meyer and Van Staden, 1995), saw a reduction in both anthocyanin content and prevalence of these AVIs (Nozue and Yasuda, 1985; Nozue *et al.*, 1995; 1997).

This structure has been shown to comprise a hydrophobic proteinaceous matrix, capable of the non-covalent binding of anthocyanins. A component of the AVIs was determined to be a 24 kDa protein (VP24), which has been purified (Nozue *et al.*, 1995; 1997) and the gene cloned (Xu *et al.*, 2001). The expression profile of VP24 (transcript and protein) strongly correlated with the accumulation of anthocyanins and AVIs (Nozue *et al.*, 1997).

VP24 cDNA was cloned and shown to encode a 96.3 kDa proprotein containing a highly hydrophobic C-terminal region with eight putative transmembrane domains (Xu *et al.*, 2000). Investigation of the C-terminal region was attempted to resolve the possibility of a functional transmembrane protein (Xu *et al.*, 2000). While Xu *et al.* (2000) were unable to express the transmembrane region as a fusion protein in *E. coli*, a smaller 37.6 kDa fusion peptide at the C-terminus was purified and polyclonal antibodies raised. A 36 kDa protein (VP36) isolated from vacuoles of sweet potato suspension cells with an expression pattern similar to that of VP24 was shown to cross-react with the antiserum. This suggested that VP36 may be derived from the VP24 proprotein (Xu *et al.*, 2000).

While much is known regarding the transport of soluble storage proteins to the vacuole, the transport of insoluble proteins, like VP24, has not been investigated in the same depth (Nakamura and Matsuoka, 1993; Neuhaus and

Rogers, 1998). As both VP24 and VP36 are localised to the vacuole, it may be that the proprotein is transported to the vacuole by vesicular shuttling where vacuolar processing enzymes release the individual peptides (Hara-Nishimura *et al.*, 1998). Alternatively, peptides may be liberated prior to vacuolar sequestration performing their functions, ie. binding anthocyanins, before being transported to the vacuole. Either way, this implies the involvement of vesicular transport in exploiting the putative transmembrane domains observed in the VP24 proprotein to facilitate vacuolar sequestration.

1.5.3.1.3 *Rose*

Much work has also been carried out in black roses (*'Charles Mallerin'*), where massive, rod-like pigmented structures were observed with the blackening of the petals (Yasuda, 1974a). Treatment of AVI-containing cells with acid or alkali solution saw characteristic colour changes associated with anthocyanins and were thus concluded to comprise the insoluble state of anthocyanins, or AVIs (Yasuda, 1970). This body was seen to stain negative for chromic acid and partially blue for ferric chloride, indicating the presence of a tannic component within the structures (Yasuda, 1974b, 1976). Based on staining results, predominant components were identified as protopectin, anthocyanin, tannin (Yasuda, 1974b, 1976) and iron (Yasuda, 1973). This was supported by Guillermond (1931; 1932) who saw that the AVIs were comprised of tannin, mucous substances and pectin.

Yasuda (1979) observed the formation of these bodies during opening of the rosebuds and recorded that they arose from the inside of the cell wall, or cytosol, rapidly and within 16 hours was enveloped in the tonoplast. In a different

rose species, cl-Crimson Glory, cells exhibit a “bluing” effect associated with a pigmented body that appears to radiate from fused cytoplasmic strands (Yasuda, 1974b). This body was shown to comprise a central tannic substance due to a positive stain with toluidine blue, with a membrane-like encasement which is also sensitive to toluidine blue (Yasuda, 1974b). Occasionally, sap within this structure was seen and comprised a cytoplasmic component from staining with fuchsin and fast green. An histochemical survey on various ‘bluing’ roses, showed that these bodies were compositionally identical to the structure observed in the cl-Crimson Glory black rose (Yasuda and Kikuchi, 1978).

More recently, the colour shift from red-purple to blue shades as rose petals age was noted by Gonnet (2003) to be correlated with the intensification of cyanidin-3,5-O-diglucoside within AVIs in the vacuoles. Development of these bodies follows anthocyanin accumulation, reaching their maximum size in the darkest petal stage (Yasuda and Kikuchi, 1978).

1.5.3.1.4 Radish

AVIs were visualised in radish seedling hypocotyls in contact with the cytoplasmic layer and, as with roses, a characteristic anthocyanic colour change was seen when exposed to acid and alkali solution. Reaction with a panel of stains implied that the structure possessed some cytoplasmic nature, but stained negative for tannin, pectin, polysaccharide, reducing sugars and starch (Yasuda and Shinoda, 1985). While this may reflect a compositional difference in AVIs in this species to all others tested, it is likely that the staining strategies employed may have been flawed as no positive control (ie. rose AVIs) was incorporated (Yasuda and Shinoda, 1985). Light was shown to be critical for the development of

pigment in these bodies (Yasuda and Tsujino, 1988). When cultured in dark conditions, unpigmented bodies were seen and when hypocotyls were cultured in the dark after pre-treatment with light, the bodies lost visible pigmentation. Finally, an inverse relationship was noted between the number of AVIs and their diameter, shown to arise from fusion of the bodies (Yasuda *et al.*, 1989). Coalescence of radish AVIs resulted in a spherical body having the combined calculated volume of the fusing AVIs (Yasuda *et al.*, 1989).

1.5.3.1.5 Maize

Electron dense material, suggested to be AVIs, was demonstrated to accumulate only in C1/R-expressing maize cell smooth endoplasmic reticulum that accumulates and coalesces in the central vacuole (Grotewold *et al.*, 1998). These observations were supported by light microscopic imaging of coalescing AVIs in the vacuole (Grotewold *et al.*, 1998; Grotewold, 2001; Irani and Grotewold, 2005).

1.5.3.1.6 Grape

AVIs have been noted in grape varieties for a long time, but analysis of their structure has not extended beyond microscopic observations. Furthermore, Calderon *et al.* (1993) could only find AVIs in the cytoplasm of grapevine cell-suspension culture as did Nozzolillo and Ishikura (1988) in radish. However, these are the only two reports of this observation with pigmented osmiophilic globuli varying in size and number generally placed within the central vacuole.

They have been noted in ‘Kyoho’ and ‘Beniizu’ grape berry skin, with the post-veraison colour intensification associated with their appearance (Nakamura,

1989). Nakamura (1993) observed the AVIs ability to coalesce within the vacuole and observed a membrane boundary as with radish AVIs (Yasuda *et al.*, 1989). Conversely, Jasik and Vancova (1992) demonstrated no apparent membrane in grape callus, but retained the capacity to fuse.

These bodies respond to a number of environmental cues, including nutrient levels and light. AVIs in skin of 'Pione' grapes reduced in number, size and ability to coalesce with increasing fertiliser levels (Okamoto *et al.*, 2003). This may be due to the nitrogen concentration as AVIs in red cabbage increased in numbers when grown hydroponically under nitrogen starvation (Hodges and Nozzolillo, 1996).

Clearly, there exists a strong relationship between the abundance of AVIs and the level of anthocyanin accumulation in all species examined. Despite this, there are a number of differences in published reports on AVIs between and within species (Sections 1.5.3.1.1-6). Where mentioned these were attributed to variations in methodology, but is suggestive of species-specific composition. Determining the composition of the AVIs is important as an approach to the rational enhancement of AVI abundance as a target for increasing anthocyanin accumulation. Furthermore, anthocyanins sequestered into these bodies are theorised to be less susceptible to degradative processes (Marty, 1999).

1.5.4 Anthocyanin Degradation

Due to the instability of the aglyconated form, any modification that exposes this nucleus would contribute to the degradation. Therefore, potential degradation mechanisms include alkaline pH, thermal treatment and enzymes including glycosidases, oxidases and hydroxylases (Piffaut *et al.*, 1994; Romero

and Bakker, 2000). Phenol oxidases have been shown to be capable of degrading anthocyanins (Gouka *et al.*, 2001) and one polyphenol oxidase (PPO) has been isolated from blueberry (Kader *et al.*, 1998). This enzyme is responsible for the intense browning of blueberries after crushing and the exact method and stoichiometry of the degradation has been determined (Kader *et al.*, 1998; 1999). It appears that, while anthocyanins are poor substrates for PPO, the presence of chlorogenic acid in the plant accelerates the degradation (Kader *et al.*, 1998). These enzymes are all cytosolic and are therefore thought to have no effect on anthocyanin accumulation in viable cells with intact vacuoles.

It is well-known that flowers, foliage and fruit change colour during development and in response to changes in the environmental conditions. Some of these changes involve decrease in anthocyanin concentrations. Examples for this are changes in flower colour after pollination (Weiss, 1995), change of foliage colour from red to green during development, loss of red pigmentation in flowers, foliage and fruit due to increased temperatures or due to decrease in light intensity (Oren-Shamir and Levi-Nissim, 1997a, 1997b; Oren-Shamir *et al.*, 1999; Shaked-Sachray *et al.*, 2002; Nissim-Levi *et al.*, 2003). One recent study looking at the petals of *Brunfelsia calycina* (yesterday-today-tomorrow) flowers showed active *in planta* anthocyanin degradation (Vaknin *et al.*, 2005). This is a unique model system as colour loss (from dark purple to white) occurs rapidly and is spatiotemporally consistent. It was shown that the loss of pigmentation was dependent on early mRNA and protein synthesis (prior to day 2 following flower opening), and was independent of the senescence process of flower petals (Vaknin *et al.*, 2005).

Active anthocyanin degradation has not been demonstrated to occur in grape cells and as a result, will not be investigated in this study.

1.6 Summary

A strong demand exists for the industrial production of anthocyanins for use in functional foods and as pharmaceuticals, with *V. vinifera* suspension cultures providing an excellent candidate production system. Strategies to improve anthocyanin production by augmenting biosynthetic pathways have not yielded a quantum increase. Post-biosynthetic pathways - transport, pumping, storage, and degradation - that have been largely overlooked previously may be limiting this accumulation. As both transport mediated by GSTs and storage in AVIs have not been fully investigated and are the rate-limiting candidates in anthocyanin post-biosynthesis in *V. vinifera*, they were the focus of this study.

GSTs have been shown to be critical for anthocyanin accumulation in a number of species. We propose they will be involved in transport of anthocyanins in *V. vinifera* and their expression and activity will be correlated with anthocyanin accumulation. It is hypothesised that AVIs are the result of ER-derived vesicular transport of anthocyanins and their subsequent fusion with the vacuole. This would explain the variations in basal composition in various species identified in previous studies. Furthermore, the composition of AVIs in *V. vinifera* L. may give rise to altered profiles of bound flavonoids, in particular anthocyanins over the course of flavonoid accumulation.

1.7 Broad Research Objectives

- Develop a panel of *Vitis vinifera* L. Gamay Fréaux suspension cell lines and elicitation strategies for enhancing anthocyanin accumulation
- Purify glutathione *S*-transferase proteins from pigmented *V. vinifera* L. cell suspension cultures
 - Clone the corresponding GST sequences
 - Determine the anthocyanin transport capacity of heterologously expressed GSTs
 - Determine the expression profile of candidate GSTs under anthocyanin enhancement strategies.
- To determine the relationship between anthocyanin accumulation and AVI abundance in *V. vinifera* suspension cells
 - Localise AVIs intracellularly
 - Optimise an AVI purification strategy for undertaking compositional analyses
 - Correlate the anthocyanin profile in AVIs with whole cell anthocyanins in various cell suspension cultures and under alternate elicitation strategies

CHAPTER 2

MATERIALS AND METHODS

2.1 Chemicals

All chemicals used were obtained from Sigma-Aldrich (Sydney, Australia) unless otherwise specified, and were of the highest available purity. Water used was of milliQ grade, prepared using a Modulab™ PureOne + Type 1 analytical grade water purification system (Continental Water systems, Australia), unless otherwise specified.

2.2 Plant cell culture

2.2.1 Cell line details

The cell line used predominantly throughout this work was developed by Cormier *et al.* (1994), originating from callus established in 1978 from *Vitis vinifera* L. cv. Gamay Fréaux var. Teinturier berry pulp. Designated FU-01, it has been maintained in our laboratory since July 2000. This cell line, capable of anthocyanin accumulation in the dark, was a gift from Dr. Francois Cormier's group (Quebec, Canada).

Other cell lines utilised in this project were derived from FU-01 by selection protocols detailed in Section 2.2.3.1.2, and were characterised by either a high anthocyanin level (FU-02) or very low anthocyanin level (FU-03) during incubation in the dark. FU-02 was established in December 2001, FU-03 in November 2002 and FU-02 in May 2003.

2.2.2 Growth medium

All suspension cell lines were grown in GC-2 medium, which consists of B5 macronutrients and micronutrients (Gamborg *et al.*, 1968) supplemented with 30 g.l⁻¹ sucrose, 250 mg.l⁻¹ casein enzymatic hydrolysate, 0.1 mg.l⁻¹ α -

naphthaleneacetic acid (NAA) and 0.2 mg.l⁻¹ kinetin. For callus culture the medium was additionally supplemented with 8 g.l⁻¹ type-1 agar.

The initial pH was adjusted using 0.1 M KOH to 5.7 - 5.8, medium was dispensed into Erlenmeyer flasks (liquid) or Schott bottles (solid) and autoclaved at 121 °C for 20 mins.

2.2.3 Selection and subculture of cell lines

2.2.3.1 Callus cultures

2.2.3.1.1 *Subculture*

All callus material was subcultured fortnightly using a sterile scalpel onto fresh agar supplemented GC-2 medium, poured into 100 mm Petri dishes. Callus was approximately 5mm in diameter after transfer, with 4-5 calli per plate. All plates were sealed with parafilm and incubated in the dark at 27±1 °C.

2.2.3.1.2 *Clonal selection and micro-calli selection*

Regions of intensely pigmented callus were selectively transferred from plates during the subculture process, in order to develop stable high-pigmented callus. After 39 transfers this material was designated FU-02.

Micro-callus selection was applied in order to generate non-pigmented callus from the FU-01 material, according the method of Wysokinska and Nguyen (1990). Small aggregates were harvested from 50 ml of a 7-day old FU-01 suspension flask by filtration through 60 µm nylon mesh (Millipore). The resultant suspension was mixed with an equal volume of molten GC-2 (supplemented with 12 g.l⁻¹ type-A agar) at 40 °C, and poured into petri dishes which were sealed with parafilm and incubated in the dark at 27±1 °C. After two

weeks non-pigmented micro-calli with a diameter of 2 mm were isolated with sterile forceps and transferred to solid GC-2 plates, and subcultured as detailed in the previous section. Material obtained by this method remained non-pigmented for over 50 transfers, and was designated FU-03.

2.2.3.2 Suspension cultures

2.2.3.2.1 *Subculture*

Suspension cultures were maintained in 50 ml of GC-2 medium, in 250 ml Erlenmeyer flasks enclosed with aluminium foil, with a minimum of 5 flasks at all stages. Prior to subculturing, 3-5 ml samples were collected from 3 randomly selected flasks and analysed for growth and anthocyanin content, with extracts stored at -20°C for HPLC analysis. Three of the five flasks were visually selected for subculture on the basis of healthy appearance, while the remaining flasks were returned to the culture room and kept for a further 7 days as backup cultures.

Cells from the three flasks were mixed together and filtered through sterile stainless steel 1 μm pore size mesh filters (Biomedical Engineering Department, FMC), in order to remove large aggregates. The filtrate was collected in custom-made sieves lined with 60 μm nylon mesh. The cells were washed once with fresh sterile GC-2 medium and left until all medium was drained from the sieve. A measure of 2.5 ± 0.1 g-wet cells were transferred to sterile GC-2 medium in 250 ml Erlenmeyer flasks, closed with aluminium foil and incubated at $27\pm 1^{\circ}\text{C}$ in a temperature-controlled room at 100 rpm on a reciprocating shaker (Ratek, Australia).

2.2.3.2.2 Selected cell lines utilised in experiments

Callus material selected for either high or low pigmentation was initiated into suspension by transfer of 2.5 ± 0.1 g-wet cell weight into 50 ml fresh sterile GC-2 medium, in 250 ml Erlenmeyer flasks. The first few subcultures were carried out essentially as detailed in the previous section, although the initial filtration step to remove large aggregates was not done. Once the cell lines were growing at a comparable rate to that of FU-01 the subculturing was then performed as per Section 2.2.3.2.1.

2.3 Elicitation Experiments

2.3.1 Preparation of Chemicals for Addition to Cultures

2.3.1.1 Jasmonic acid (JA)

JA was prepared by mixing 250 mg of the chemical into a final volume of 5 ml ethanol:water (12:13) to give a stock concentration of 100 mM. This stock was then filter sterilised through 0.22 μm filter unit (Millipore) and stored at -20°C until required. A further 1:10 dilution in pre-sterilised ethanol:water (12:13) was carried out at time of experiments to give a 1000 \times concentrated stock (10 mM).

2.3.1.2 Sucrose

A concentrated stock of plant cell culture-grade sucrose was prepared by dissolving 80 g in water with heating to a final volume of 100 ml. This stock was then autoclaved in a 250 ml Schott bottle at 121°C for 20 mins and stored at 4°C until required.

2.3.2 Addition of chemicals to cultures and light irradiation

Jasmonic acid was prepared at 1000× the required final concentration, thus for a 100 ml culture, 100 µl of chemical stock was added. In this way, the amount of vehicle solvent added to cultures was less than or equal to 0.1% of the total volume. Control flasks received an equal volume of vehicle solvent, ethanol:water (12:13).

Sucrose was added at the rate of 2.5 ml concentrated 80% (w/v) stock to 100 ml of culture, giving a final concentration in the culture of 20 g.l⁻¹ sucrose. A 2.5% dilution for all other medium components resulted; 2.5 ml of sterile water per 100 ml of culture was added to control flasks to compensate for this and ensure validity of results.

Where cultures were required to be grown under continuous light irradiation, they were moved to reciprocating shakers that were set up under 36W fluorescent light banks (Osram Dulux, Italy) controlled by a standard light dimmer. Light intensity was measured by placing a Lux meter (MC-88, TPS Pty. Ltd.) in multiple positions on the shaker, and the dimmer was adjusted until light intensity was 8200±200 lux.

2.4 Kinetic analysis

2.4.1 Culture growth

Samples of approximately 3 ml were taken from cultures using sterile wide-mouth glass pipettes into 15 ml centrifuge tubes (Corning, USA). The sample was vacuum-filtered on Whatman #1 filter paper (Whatman International Ltd., England) and rinsed with water. Cells were transferred onto preweighed aluminium foil and 40-60 mg fresh cell weight (FCW) was removed into 1.5 ml

ependorf tubes (Sarstedt, Germany) for anthocyanin extractions (see Section 2.4.2.1). The foil was sealed and the remainder of the cells were dried in an oven at 80-90°C for at least 48 hours for dry cell weight (DCW) determination.

2.4.2 Metabolite analysis

2.4.2.1 Extraction of anthocyanins

Anthocyanins were extracted from the FCW samples with a 20× volume of 50% (v/v) glacial acetic acid (BDH, England) in water, or 0.1% HCl in methanol for 1 hour at room temperature after brief vortexing. Use of 50% acetic acid in water as the extractant was found to liberate >97% of total anthocyanins from *V. vinifera* cell samples (Jayram and Konczak-Islam, 2000). Extracts were centrifuged at 10,000g for 5 mins in a microcentrifuge (Hettich, Germany), with supernatants stored at -20°C prior to analysis.

2.4.2.2 Spectrophotometric assay for anthocyanin content

Anthocyanin extracts were diluted 1 in 4 with McIlvaine's buffer (40 mM Na₂HPO₄/80 mM citrate buffer, pH 3.0), and the absorbance read at 535nm against a blank of 50% acetic acid diluted 1 in 4 with McIlvaine's buffer, in a Shimadzu UV mini 1240 UV-Vis spectrophotometer (Japan). Under these conditions, anthocyanin content can be calculated using an industrial measurement of pigment called Colour Value (CV). Colour value can be calculated against FCW, DCW or on a per-litre basis according to the equations 2.1 to 2.3.

Equation 2.1: Calculation of anthocyanin content as CV.g-FCW⁻¹

$$\text{CV.g} - \text{FCW}^{-1} = 0.1 \times \text{Abs}_{535} \times \text{Dilution factor}$$

- Dilution factor is 80 (1/20 during extraction, 1/4 in McIlvaine's buffer).

Equation 2.2: Calculation of anthocyanin content as CV.g-DCW⁻¹

$$\text{CV.g} - \text{DCW}^{-1} = \text{CV.g} - \text{FCW}^{-1} \times \text{FCW} : \text{DCW ratio}$$

Equation 2.3: Calculation of anthocyanin production as CV.l⁻¹

$$\text{CV.l}^{-1} = \text{CV.g} - \text{FCW}^{-1} \times \text{g} - \text{FCW.l}^{-1}$$

2.4.2.3 HPLC analysis of anthocyanin composition

2.4.2.3.1 Solvent preparation and gradient program

High performance liquid chromatography (HPLC) was undertaken to examine anthocyanin composition, using the Shimadzu Class-VP10A system and Class-VP software V5.3.2 (Shimadzu Biotech, Japan). Ten microlitres of each sample was injected onto a Luna 3 µm C18(2), 10 cm × 0.46 cm internal diameter column (Phenomenex, Australia) and eluted as detailed below. Detection was at 520 nm and spectral data from 190-600 nm was collected using a photo-diode array detector.

Anthocyanins were eluted according to the method of Yoshinaga *et al.* (1999), utilising Buffer A (H₃PO₄:H₂O, 1.5:98.5) and Solvent B (orthophosphoric acid:acetic acid:acetonitrile:H₂O, 1.5:20:25:53.5). Buffer A was filtered through 0.22 µm nitrocellulose membranes (Millipore, Australia), while Solvent B was filtered through 0.45 µm HVHP membranes (Millipore, Australia) and degassed for 5 mins by helium sparging, or sonicated for 80 mins in an ultrasonic water bath (Soniclean, Australia).

A linear gradient of 25 to 85% Solvent B in Buffer A was run for 40 mins at 1 ml.min⁻¹, followed by an equilibration period of 10 mins at 25% Solvent B in Buffer A.

2.4.2.3.2 Sample preparation

Samples were centrifuged at 10,000g for 10 mins, and the supernatant transferred into glass HPLC vials with low volume inserts (Alltech, Australia).

2.4.2.3.3 Identification of peaks

As described in Chapter 1, *V. vinifera* accumulates a mixture of anthocyanins, for which the order of elution in reverse-phase HPLC has been established (Wulf and Nagel, 1978). Authentic standards of cyanidin 3-glucoside and malvidin 3-glucoside (Polyphenols, Norway) were used to confirm this order under our elution system.

In addition, two peaks that partially co-eluted were distinguished by comparison of UV-visible spectra obtained by the photo-diode array detector, according to Hong and Wrolstad (1990). Here the order of elution deviated from those published, where we observed delphinidin 3-*p*-coumaroylglucoside eluting before malvidin 3-acetylglucoside. Figure 2.1 and Table 2.1 detail the anthocyanins present in *V. vinifera* cell cultures.

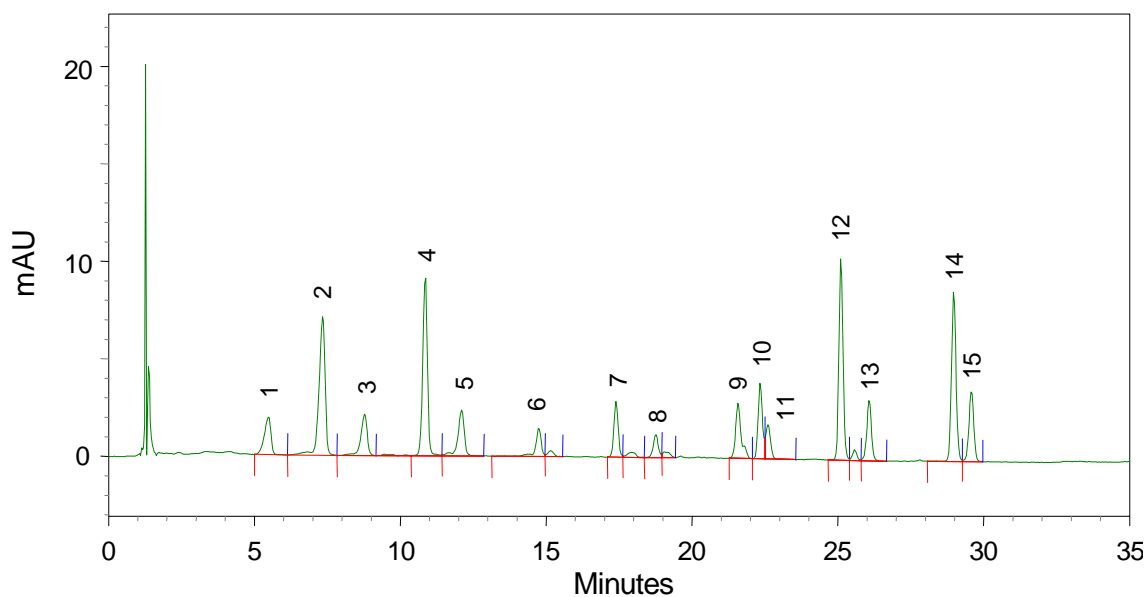


Figure 2.1: HPLC chromatogram (520 nm) of anthocyanins from *V. vinifera* L. cell culture as per running conditions in Section 2.4.2.3.1.

Table 2.1: Peak identification in anthocyanin chromatogram.

	Anthocyanin	Retention Time (Minutes)
1	Delphinidin 3-glucoside	5.5
2	Cyanidin 3-glucoside	7.8
3	Petunidin 3-glucoside	8.9
4	Peonidin 3-glucoside	11.2
5	Malvidin 3-glucoside	12.1
6	Delphinidin 3-acetylglucoside	14.8
7	Cyanidin 3-acetylglucoside	17.5
8	Petunidin 3-acetylglucoside	18.8
9	Peonidin 3-acetylglucoside	21.5
10	Delphinidin 3-p-coumaroylglucoside	23
11	Malvidin 3-acetylglucoside	23.5
12	Cyanidin 3-p-coumaroylglucoside	25
13	Petunidin 3-p-coumaroylglucoside	26.8
14	Peonidin 3-p-coumaroylglucoside	29
15	Malvidin 3-p-coumaroylglucoside	30

2.4.2.4 Estimation of pigmented cell ratio

2.4.2.4.1 *Protoplasting of suspension culture cells*

Protoplasts were prepared according to the method of Conn *et al.* (2003) from 1.5 g-FCW *V. vinifera* L. suspension cultured cells in a final volume of 5 mls containing 0.4% (w/v) PEG-8000, 0.5% (w/v) Driselase, 1% (w/v) Macerozyme and 2% (w/v) Cellulase in mannitol buffer (0.7 M *D*-Mannitol, 5 mM KCl, 2 mM CaCl₂·2H₂O, 25 mM K-MES, pH 5.0±0.1). Enzymes were obtained from Yakult Pharmaceuticals Inc., Tokyo, Japan.

Suspensions were incubated at 30°C on rotary shaker at 50 rpm for 6 hrs, then gravity filtered through Miracloth (Calbiochem, San Diego, USA) into a beaker by gentle agitation, after which all steps were done at 4°C. Protoplast samples were transferred to a 35 ml Oakridge tube (Nalgene, Rochester, USA) and centrifuged at 250g for 5 mins in an IEC-Centra CLD centrifuge (International Equipment Company, Japan). The pellet was washed twice and resuspended in fresh Mannitol buffer. An equal volume of 60% (v/v) Percoll™ (Amersham Biosciences, Uppsala, Sweden) in Mannitol buffer was mixed with the protoplast solution (30% (v/v) final concentration) and this was overlaid with a 10% (v/v) Percoll™ solution. After centrifugation at 250g for 5 mins in an eppendorf bench top centrifuge, protoplasts were collected from the 10/30% interface and washed twice in Mannitol buffer.

2.4.2.4.2 *Vacuole purification*

Vacuoles were purified from protoplasted cells by phosphate buffer lysis as per Wagner and Seigelman (1975).

2.4.2.4.3 *Microscopy and cell counting using a haemocytometer*

Ten microlitres of protoplast samples were loaded into a haemocytometer (Weber Scientific Int. Ltd., Teddington, England), and visualised using an Olympus BX50 light microscope (Olympus America, New York, USA). Cell concentration was calculated according to Equation 2.4:

Equation 2.4: Calculation of cell concentration in cell.ml⁻¹

$$\text{Cell concentration} = \text{Average count per large square} \times 10^6$$

Pigmented cells, cells with anthocyanic vacuolar inclusions (AVIs) and total cell numbers were counted from 3 large squares each containing 100-120 cells, from 3 replicate slides. Microscopy photographs were taken in the Image Analysis Suite at Flinders Medical Centre, using an Olympus BX50 light microscope equipped with a Canon EOS digital camera. Measurements were made with the use of an Olympus eyepiece micrometer (35040: 10 mm/100 ticks) Statistical correlations were made using Wilson's coefficient of correlation, or student's t-test (where noted) with significance given when $P < 0.05$.

2.4.2.5 Cellular staining

Staining was performed on unfixed, hand sections of *V. vinifera* L. callus or suspension cells. Staining strategies used were as published for toluidine blue (O'Brien *et al.*, 1964), ruthenium red (Pearse, 1985), Sudan III and iodine-potassium iodide (Ruzin, 1999).

2.4.3 Protein extraction and precipitation

2.4.3.1 Total protein extraction

A 250 mg-FCW aliquot of suspension cells was ground on liquid nitrogen and placed into 1 ml 10% (w/v) trichloroacetic acid (TCA), 0.07% (v/v) β -mercaptoethanol in acetone and incubated at -20°C for 4 hrs. This was centrifuged at 10,000g, the supernatant was removed and the pellet resuspended in 1 ml ice-cold acetone. This washing was repeated 5 times to remove residual TCA. The pellet was divided into two, with one resuspended in $1\times$ SDS load (Sambrook and Maniatis, 1989) and the other in 2D solubilisation solution (7 M Urea, 2 M thiourea, 0.5% (v/v) carrier ampholytes, 0.4% (w/v) DTT) with 4% (v/v) 3-[3-(cholamidopropyl)-dimethylammonio]-1-propanesulphonate (CHAPS).

2.4.3.2 Whole-cell protein extraction

Cells were vacuum dried, washed, frozen on liquid nitrogen and stored in 2-2.5 g-FCW aliquots in aluminium foil at -80°C until use. Cells were ground using a pre-chilled mortar and pestle and placed in cooled 35ml Oakridge tubes containing 400 mg polyvinyl polypyrrolidone (PVPP). Ten millilitres of RT extraction buffer (100 mM Tris-HCl pH 7.8, 0.25% Triton X-100, 3 mM β -mercaptoethanol, 1 mM EDTA, 1 μM aPMSF, 1 μM leupeptin, 1 μM pepstatin) was added and this slurry was sonicated on ice at 50W for three 10 sec bursts (Sonifier B-12, Branson Sonic Power Company, USA). The solution was centrifuged at 10,000g at 4°C for 15 mins (Beckman Coulter J2MC). The supernatant was filtered through 6 layers of Miracloth, generating the crude protein extract.

2.4.3.3 Protein precipitation and desalting

2.4.3.3.1 *Acetone precipitation*

A 10-fold excess of ice-cold acetone was added to the protein solution to be separated and inverted to mix. This was incubated at -20°C for at least 2 hrs and centrifuged at 13,000g for 10 mins. The supernatant was discarded and the pellet air-dried and resuspended in the appropriate solution.

2.4.3.3.2 *Ammonium sulphate precipitation*

Ammonium sulphate was added to the crude protein extract to a final concentration of 60% (w/v) and shaken on ice for 20 mins to partially remove contaminating anthocyanins and for buffer exchange. The solution was centrifuged at 15,000g at 4°C for 15 mins and the supernatant discarded. The pellet was dissolved in PBS (140 mM NaCl, 2.7 mM KCl, 10 mM Na_2HPO_4 , 1.8 mM KH_2PO_4 , pH 7.3) with 3 mM β -mercaptoethanol, 1 mM EDTA, 1 μM aPMSF, 1 μM leupeptin and 1 μM pepstatin on ice for 10 mins. This was centrifuged at 15,000g for 5 mins and the supernatant filtered through a 0.22 μm filter (Minisart, Sartorius AG, Göttingen, Germany).

2.4.3.3.3 *HiTrap desalting*

Crude protein was desalted using Hi-trap columns (Amersham Biosciences, Uppsala Sweden) according to manufacturers instructions, into an exchange buffer that was identical to protein extraction buffer, without the addition of protease inhibitors.

2.4.3.4 Protein quantification

2.4.3.4.1 *Bicinchoninic acid protein assay kit*

Whole-cell protein was quantified using the TCA precipitation modification of the colorimetric bicinchoninic acid assay according to manufacturer's protocols (Sigma-Aldrich, Sydney, Australia). Standard curves generated using bovine serum albumin (BSA), with a representative graph shown in Appendix 2.1.

2.4.3.4.2 *EZQ protein quantification kit*

Prior to 2D-gel electrophoresis, protein samples were quantified using the fluorescent EZQ quantification kit according to manufacturer's protocols (Molecular Probes, Eugene, USA) and imaged using the Typhoon 9400 Multi-format Imager (Amersham Biosciences, Uppsala, Sweden). Standard curves were generated using ovalbumin (Molecular Probes, Eugene, USA), with a representative graph shown in Appendix 2.2.

2.4.4 Purification of glutathione S-transferases (GSTs)

2.4.4.1 Glutathione-affinity chromatography

Whole-cell protein was extracted (section 2.4.3.2), ammonium sulphate precipitated (Section 2.4.3.3.2) and recirculated through a 1 ml GSTrap FF affinity column (Amersham Biosciences, Australia) via a P1 peristaltic pump (Amersham Biosciences, Uppsala, Sweden) at a flow rate of 15 ml.hr⁻¹ at 4°C for 16-18 hrs. The column was attached to a spectrophotometer/chart recorder (Amersham Biosciences, Uppsala, Sweden) and the OD₂₈₀ was plotted as the column was washed with PBS at a flow rate of 60 ml.hr⁻¹ until a steady baseline

was achieved. Bound proteins were eluted with elution buffer (10 mM reduced glutathione, 50 mM Tris-HCl, pH 8.0). Fractions (0.5 ml) were collected and protein precipitated by acetone precipitation (Section 2.4.3.3.1).

2.4.4.2 GST assay

GST assay was performed as per Habig *et al.* (1974a), with the following modifications. The spectrophotometric assay was performed in a 1 ml volume in quartz cuvettes (path length = 1 cm) with a final concentration of 3 mM glutathione (GSH) and 1 mM 1-chloro-2,4-dinitrobenzene (CDNB, $\epsilon=0.0096\mu\text{M}^{-1}\cdot\text{cm}^{-1}$) in 100 mM phosphate buffer, pH 7.4. Assay was run for 2 mins according to standard curves for whole cell extracts (Appendix 2.3). Activity was calculated according to Equation 2.5, by measuring formation of GS-DNP at 340nm.

Equation 2.5: GST activity calculation for Units of activity.

$$\text{GST Activity } (\mu\text{mol}/\text{min}/\mu\text{g}) = \Delta/\epsilon.t.m$$

Where Δ = Change in OD_{340} compared with no protein control
 ϵ = Extinction coefficient for CDNB ($0.0096\mu\text{M}^{-1}\cdot\text{cm}^{-1}$)
 t = Assay time (2 mins)
 m = Mass of protein added (μg)

2.5 Gel electrophoresis

2.5.1 SDS polyacrylamide gel electrophoresis (SDS-PAGE)

SDS-PAGE was performed as per Laemmli (1970). The separating gel (375mM Tris-Cl, pH 8.8; 0.1% SDS; 6-15% Bis/Acrylamide (1:37.5); 0.05% Ammonium Persulphate; 0.2% TEMED) was poured and overlaid with water for 15-30 mins. The stacking gel (125mM Tris-Cl, pH. 6.8; 0.1% SDS; 4%

Bis/Acrylamide; 0.05% Ammonium Persulphate; 0.2% TEMED) was poured on top of the separating gel and the comb inserted. Gels were used immediately or stored in running buffer overnight in sealed bags at 4 °C. The protein was mixed with 5× SDS loading dye, heated at 95 °C for 4 mins prior to loading (Sambrook and Maniatis, 1989). Protein samples (20 µl) were loaded into each well and the gel run at 200V until the dye front reached the bottom of the gel.

2.5.2 Two-dimensional gel electrophoresis (2D-GE)

2.5.2.1 Sample preparation

Protein samples were purified with 2-D Plus One cleanup kit (Amersham Biosciences, Uppsala, Sweden) and the pellet solubilised with the appropriate detergent in 7 M Urea, 2 M Thiourea, 0.5% IPG buffer (Amersham Biosciences, Uppsala, Sweden), 0.4% DTT. This was performed at RT with gentle shaking overnight to maximise solubilisation.

2.5.2.2 Strip rehydration

The protein solution was lightly stained by touching the solution with a yellow tip containing a saturated solution of bromophenol blue. This was centrifuged at 13,000g for 5 mins and the supernatant added into the strip holder between the electrodes. The IPG drystrip (Amersham Biosciences, Uppsala, Sweden) was placed into the holder with the acrylamide touching the solution and electrodes. This was overlaid with dry strip cover fluid (Amersham Biosciences, Uppsala, Sweden) and the lid placed on the holder. The protein was focussed at 50V for 16-20 hrs at 20 °C. Complete rehydration was marked by the absorption and slow migration of the bromophenol blue towards the anode.

2.5.2.3 Isoelectric focussing

The gel was removed and the strip holder cleaned with cleaning solution and dried with tissues. Small wicks made of filter paper (Whatman) were moistened with water and placed over each electrode to absorb any precipitating salts. The rehydrated strip was inserted into the holder placed with the acrylamide lying on the wicks and overlaid with cover fluid. The strip was focussed as per Table 2.2.

Table 2.2: Voltage settings for first dimension isoelectric focussing on 13cm strips.

Voltage Setting (Ramp Program)	Time
100V (Step-n-Hold)	30 mins
1000V (Step-n-Hold)	30 mins
Gradient to 8000V	1 hr
8000V (Step-n-Hold)	6-8 hrs
Gradient to 100V	30 mins
100V (Step-n-Hold)	20 hrs

2.5.2.4 Strip equilibration

The strip was immersed in 3 mls equilibration buffer (50 mM Tris-HCl, pH 8.8, 6 M urea, 30% (v/v) glycerol, 2% (w/v) SDS) with 1% (w/v) DTT and gently mixed for 15 mins. The strip was removed and excess equilibration buffer removed with tissues. The strip was placed in 3 mls equilibration buffer with 4% (w/v) iodoacetamide and 0.5% (v/v) saturated bromophenol blue for 15 mins with shaking. Excess buffer was again removed and the strip placed horizontally on top

of a pre-poured polyacrylamide gel consisting of separating gel, with 2 cms of space at the top of the gel. A plastic comb with a single well was placed in the glass and the space was filled with molten 1% low melting point agarose and set rapidly in a 4°C room for 30 secs. The comb was carefully removed and filled with running buffer and the molecular marker was added to the well. The proteins were separated by standard SDS-PAGE running conditions and subsequently stained.

2.5.3 Gel staining techniques

2.5.3.1 Silver staining

Polyacrylamide gels were fixed in 7% acetic acid, 30% ethanol for 30 mins with gentle shaking. The gel was then transferred to sensitizing solution (30% ethanol, 0.2% (w/v) sodium thiosulphate, 0.125% (w/v) glutaraldehyde, 6.8% (w/v) sodium acetate) for 40 mins, followed by three 10 min washes in water. The gel was placed in 0.25% (w/v) silver nitrate solution with 0.015% (w/v) formaldehyde for 25 mins, followed by two 1 min washes in water. The gel was placed into developing solution (2.5% (w/v) sodium carbonate, 0.0075% (w/v) formaldehyde) for 1-5 mins to develop the protein bands.

2.5.3.2 Sypro Ruby staining

After fixing, the gel was placed in 1× Sypro Ruby stain (BioRad Laboratories) for 16-24 hrs, in the dark at room temperature with shaking. The gel was destained in destain/fixative solution for 45 mins, then photographed under UV light.

2.5.3.3 Coomassie Blue staining

Gels were fixed and stained as per Sambrook and Maniatis (1989). The gel was stored in reswell (10% ethanol, 5% acetic acid, 4% glycerol in H₂O) at 4 °C.

2.5.4 Comparative gel imaging

Sypro Ruby-stained gels were imaged at 100 µm resolution using a Typhoon 9400 Multi-format Imager (Amersham Biosciences, Uppsala, Sweden) and spots were counted using the ImageMaster 2D Platinum version 5.0 software (Amersham Biosciences, Uppsala, Sweden).

2.5.5 Gel drying

Gels equilibrated in reswell were placed on a sheet of cellophane, prewetted with water. This was overlaid with another sheet of prewetted cellophane, excluding all air bubbles. This sandwich was crimped in the drying cassette and placed into a fan blowing heated air for 3-4 hrs until the sandwich was visibly dry.

2.6 Proteomic analyses

2.6.1 Mass spectrometry

Protein spots were excised from Sypro Ruby-stained gels with a sterile scalpel and placed into separate eppendorf tubes. Samples were sent to the Bioanalytical Mass Spectrometry Facility, University of New South Wales, Sydney, Australia, for in-gel trypsin digestion and nano-LC MS/MS analysis (Zhao *et al.*, 2004).

2.6.2 Edman (N-terminal) protein sequencing

Four pieces of blotting paper (Whatman) and one piece of nitrocellulose membrane (0.45 μm pore size) were cut to the same size of the gel. Prior to loading protein, the gel was pre-run with 1 mM thioglycolic acid in running buffer. The gel was run and then equilibrated in CAPS buffer (10 mM 3-[cyclohexylamino]-1-propanesulfonic acid, pH 11, 10% (v/v) methanol in H_2O) for 30 mins with the nitrocellulose membrane. Two pieces of blotting paper were wetted in CAPS buffer and laid flat on a glass sheet. The membrane was placed on top of this, ensuring no bubbles were present between layers. The gel was carefully placed on top of the membrane and finally the sandwich was completed by placing two more sheets of blotting paper on the top. This sandwich was placed in a semi-phor, semi-dry transfer apparatus, with the membrane on the cathode side of the gel. The transfer was carried out at 1.8 mA/cm^2 of gel for ~2 hrs. The membrane was removed from the sandwich and stained with 0.25% (w/v) G-250 Brilliant Blue in 50% (v/v) methanol for 30 mins, or until the bands develop. The membrane was destained with 50% (v/v) methanol until the background was free of blue colour. The membrane was then air dried at RT on paper tissues for ~10 hrs. Bands were excised with a scalpel, placed in an eppendorf tube and sent for sequencing. This work was kindly performed by Dr. Shaio-Lim Mau in the laboratory of Prof. Antony Bacic at the School of Botany, University of Melbourne, and was supported by funds from a Commonwealth Government grant to the CRC for Bioproducts.

2.6.3 Sample Preparation for Reverse-phase HPLC

The protein solution was frozen on liquid nitrogen in a 10 ml polypropylene tube (Sarstedt, Numbrecht, Germany) and two holes were made in the cap with a large gauge needle. This was placed inside a lyophilisation chamber, or glass bulb and lyophilised overnight. Once dried, the tube was removed and covered with parafilm and the lid returned, storing at room temperature until required. Samples were submitted to the University of Melbourne for HPLC separation as per 2.6.2.

2.7 Polymerase Chain Reaction (PCR)

2.7.1 Genomic DNA Isolation

Genomic DNA was extracted from 5 day-old *V. vinifera*, pigmented suspension cultured cells with the Nucleospin[®] Plant kit, according to manufacturer's instructions (BD Biosciences, Australia).

2.7.2 Total RNA Isolation

2.7.2.1 Concert[™] RNA extraction

One hundred mg FCW of snap-frozen suspension cells were ground under liquid nitrogen in a pre-chilled mortar and pestle. Total RNA was then extracted using Concert[™] RNA Reagent (Invitrogen, Australia) according to the manufacturer's instructions, with the pellet resuspended in 30 µl sterile H₂O.

2.7.2.2 Hot borate method

Skins were removed from *Vitis vinifera* cv. Shiraz berries, frozen rapidly on liquid nitrogen and stored at -80°C until use. Total RNA was extracted from

600 mg-FCW of bery skins using the hot borate method as per Downey *et al.* (2003b).

2.7.2.3 RNA quantification

One microlitre of RNA samples were diluted 1/80 in sterile TE buffer (10 mM Tris-Cl, 1 mM EDTA, pH 7.4) and quantified using Genequant Pro (Amersham Biosciences, Uppsala, Sweden), in triplicate. The remainder of the samples with A_{260}/A_{280} ratios of >1.95 were diluted to $250 \text{ ng}\cdot\mu\text{l}^{-1}$ in sterile H_2O and stored at -80°C for further processing.

2.7.2.4 Removal of contaminating DNA by DNase 1 treatment

Contaminating DNA was removed as per Creelman and Mullet (1997). Ten micrograms of each RNA sample by treatment with 1U RQ1 RNase-free DNase I (Promega) in 50 μl total volume with RQ1 buffer. RNA was then re-extracted using Trizol reagent (Gibco BRL) and chloroform to remove salts and degraded DNA. RNA was precipitated using an equal volume of isopropanol, and washed 3 times with 75% (v/v), ice-cold ethanol. The pellet was air dried and then resuspended in 10 μl sterile H_2O . RNA was quantified as per Section 2.7.2.3.

2.7.2.5 Efficacy of DNase treatment

Total RNA and DNase-treated RNA were run on an agarose gel (Figure 2.3) and after DNase treatment, disappearance of the genomic DNA (gDNA) band was observed. PCR results confirmed the treatment was effective at removing DNA contaminants without degradation of RNA. Selected total RNA samples and their accompanying DNase-treated portions were subjected to PCR with primers for GAPDH (Accession No.: BE846404; Curtin, 2005) as they were capable of

detecting genomic DNA (Curtin, 2005). Reactions were set up as in the previous section, and analysed on a 2% agarose TBE gel (Figure 2.4).

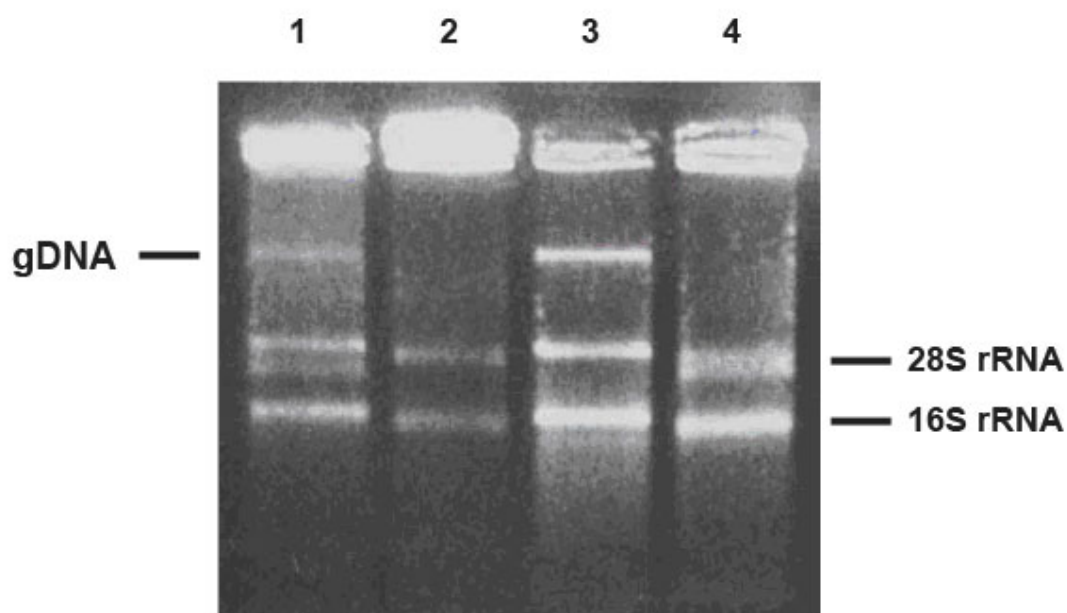


Figure 2.3: Agarose gel of total RNA (lanes 1 and 3) and DNase-treated RNA (lanes 2 and 4) showing loss of prominent genomic DNA (gDNA) band following the treatment.

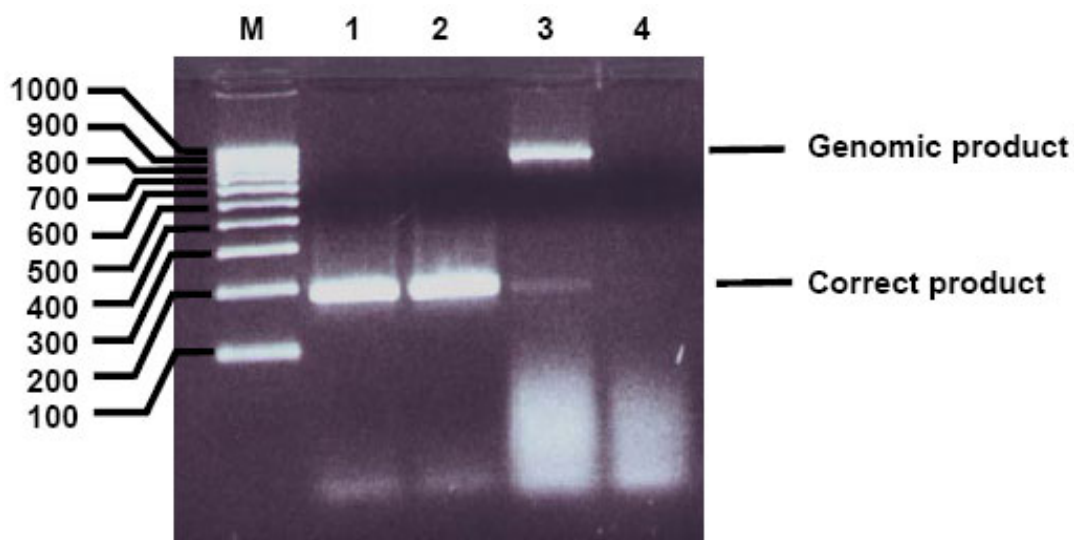


Figure 2.4: Analysis of GAPDH PCR for detection of genomic DNA contamination. Templates used for PCRs were cDNA from (1) total RNA and (2) DNase-treated RNA, (3) Total RNA, (4) DNase-treated RNA.

2.7.2.6 Electrophoretic verification of RNA integrity

Integrity of RNA extracts was evaluated before and after DNase treatment by agarose gel electrophoresis. Five hundred nanograms of RNA was denatured for 2 mins at 65°C with 1× DEPC-treated loading dye, and then placed on ice for at least 10 mins. Samples were run for 30 mins at 100V on a 1.5% (w/v) agarose gel in 0.5× TBE (5.4 g.l⁻¹ Tris-Base, 2.75 g.l⁻¹ Boric Acid, 1mM EDTA, pH 8.0) containing 10 µg.ml⁻¹ ethidium bromide. Gels were photographed on a UV-transilluminator, with a Tracktel documentation system (Department of Haematology, Flinders Medical Centre), and RNA bands were visualised.

2.7.2.7 Reverse transcription of total RNA to cDNA

Reverse transcription was carried out with 500 ng DNase I-treated RNA using 100U Superscript III RNase H-reverse transcriptase and 5 µM oligo-dT₂₀ primers in a final volume of 10 µl in Superscript III cDNA synthesis buffer (Stratagene, USA). cDNA was diluted 1/5 in sterile water and stored at -20°C in 2 µl aliquots in 0.1 ml PCR tubes (Corbett Research, USA).

2.7.3 Cloning GST Sequences

2.7.3.1 Primer design

All primers were manufactured by Geneworks (Adelaide, Australia), suspended in sterile water at 1 µg.ml⁻¹, and stored at -80°C until required. Working primer solutions were prepared (200 ng.ml⁻¹) and stored at -20°C.

Primers for directional cloning of GSTs were designed from published EST sequences (www.tigr.org/indices.grape.html) using the web-based tool Primer 3 (www-genome.wi.mit.edu/cgi-bin/primer/primer3_www.cgi). Forward

primers were designed with the putative initiation codon (ATG) at the start of the annealing portion of the primer with restriction sites immediately upstream to facilitate in-frame expression (Table 2.3). Reverse primers also possessed a unique restriction site enabling the directional cloning of the full-length EST, and genomic sequence.

Table 2.3: Primers for amplifying GST sequences (underlined sequence corresponds to addition of restriction enzyme site onto sequence). Annealing temperature for all pairs was 55°C, while for degenerate primers was set at 40°C.

Primer Name	Sequence (5' → 3')	cDNA Size (bp)
GSTIII Sense	TGGCCN(A/T)(G/C)NCCNTT(T/C)G	268
GSTIII Anti	TCNGCCCA(A/G)AANC(G/T)NGC	
GST1fBamHI	ATGGATCCATGGCAAACAGTGACCACATAG	767
GST1rPstI	AACTGCAGTCAAACAACCGCAATAATATCC	
GST2fBamHI	TAGGATCCATGGCGGTCTTGAAAGTCCAC	709
GST2rSalI	AAGTCGACAGGGCAAAGCCACACAAC	
GST3fSalI	TAGTCGACATGGTGGTGAAGGTGTATGG	682
GST3rPstI	ATCTGCAGTCACTCCAAGAGGGGCCATC	
GST4fBamHI	AAGGATCCATGGTGATGAAGGTGTATGGC	750
GST4rPstI	AACTGCAGAAGCCAACCAACCAACAAAC	
Q84N22fBamHI	AAGGATCCATGGCAGACGAGATTATCTTG	934
Q84N22rPstI	ATCTCGAGGAACACGTCTCTAGTCCAAAACA	

2.7.3.2 Amplification from cDNA

Reactions consisted of 1× PCR buffer including 2 mM MgCl₂, 200 μM mixed dNTPs (Biotech Australia), 2.3 μM each primer (see Tables 2.3-2.4), 1 U HotStar Taq DNA Polymerase (Qiagen) and 2 μl cDNA from DNase-treated RNA in a 50 μl reaction. This was placed into a thermal cycler according to the following cycles: 95°C for 15 mins; 35 cycles (94°C for 30 secs, 40/55°C for 30 secs, 72°C for 30-60 secs); hold at 25°C.

PCR products were gel purified and cloned into a T·A vector for sequencing (Section 2.7.4.5). The plasmid was digested with restriction enzymes to liberate the insert, which was gel purified and ligated into both the HIS-fusion (pQE9) and maize expression (pJD288) vectors.

2.7.3.3 Amplification from genomic DNA

Reactions consisted of 1× PCR buffer including 2 mM MgCl₂, 200 μM mixed dNTPs (Biotech Australia), 2.3 μM each primer (see Tables 2.3-2.4), 1 U HotStar Taq DNA Polymerase (Qiagen) and 4 μl gDNA (Section 2.7.1) in a 50 μl reaction. This was placed into a thermal cycler according to the following cycles: 95°C for 15 mins; 35 cycles (94°C for 30 secs, 55°C for 30 secs, 72°C for 2-3 mins); hold at 25°C. PCR products were gel purified and cloned into a T·A vector for sequencing (Section 2.7.4.5).

2.7.4 GST sequence cloning procedures

2.7.4.1 Purification of PCR products

2.7.4.1.1 *Gel purification*

PCR bands were separated in an ethidium bromide-stained, TBE agarose gel and visualised briefly using low UV light. Bands were cut from the gel using a sterile blade and placed into pre-weighed eppendorf tubes. The DNA was eluted with the MoBio Ultraclean 15™ Gel Purification system, according to manufacturer's instructions (MoBio, Carlsbad, USA) and resuspended in sterile H₂O.

2.7.4.1.2 *PCR column purification*

Each 50 µl PCR reaction mixture was purified using a MoBio PCR purification column kit according to manufacturers instructions (Mobio, Carlsbad, USA) to remove primers, salts and Taq polymerase and resuspended in 30 µl sterile H₂O.

2.7.4.2 T·A cloning

Gel purified PCR products (3 µl) were ligated into pGEM T-Easy vector (50ng; Promega, Australia) using 1U T4 DNA ligase in 1× Rapid ligation buffer (Promega, Australia). This was incubated at 4°C for a minimum of 24 hrs.

High competency JM109 (>10⁸ CFU.µg⁻¹ DNA; Promega, Australia) *E. coli* cells were transformed using the heat shock method as per manufacturer's standard transformation protocol.

They were plated on Luria Broth (LB; 10 g.l⁻¹ tryptone, 5 g.l⁻¹ yeast extract 5 g.l⁻¹ sodium chloride) with 1.5% (w/v) Type A Agar. The media was

autoclaved, cooled and ampicillin was added to $100 \mu\text{g.ml}^{-1}$ before pouring plates. For blue/white screening, $100 \mu\text{l}$ of 0.1 M IPTG and $20 \mu\text{l}$ of 50 mg.ml^{-1} X-Gal (Promega, Australia) were spread onto solid plates and incubated at 37°C for 30 mins prior to plating transformed cells at various dilutions. Transformed cells were plated onto solid media and grown overnight at 37°C .

2.7.4.3 Directional cloning

DNA was digested with a 5-fold excess of restriction enzyme(s) in $1\times$ enzyme buffer (New England Biolabs, Australia) with $10 \mu\text{g.ml}^{-1}$ BSA. Cloning vectors (pJD288, pQE9) were sequentially digested with the restriction enzymes with a gel purification step (section 2.7.4.1.1) in between. Inserts were digested with enzymes simultaneously and gel purified.

DNA was quantified by estimation from the agarose gel and the ligation set up with a 5-fold molar excess of insert to vector (50 ng) in $1\times$ ligation buffer and 5U T4 DNA ligase (New England Biolabs) in a $10\text{-}20 \mu\text{l}$ reaction volume at 4°C for a minimum of 16 hrs.

pJD288 ligation mixtures were transformed into JM109 *E. coli* as per Section 2.7.4.2. pQE9 ligation mixtures were transformed into M15:pREP4 *E. coli* as per Section 2.7.4.2. These were plated on LB with 1.5% (w/v) Type A Agar. The media was autoclaved, cooled and ampicillin ($100 \mu\text{g.ml}^{-1}$) and kanamycin ($25 \mu\text{g.ml}^{-1}$) were added before pouring plates.

2.7.4.4 Screening colonies for positive insert

Minipreps were performed according to the standard alkaline lysis method (Sambrook and Maniatis, 1989). Minipreps were screened for correct in-frame

inserts by sequencing using vector-specific primers (Table 2.4) and PCR using insert-specific primers (Table 2.3). PCR reactions consisted of 1× Thermo Pol PCR buffer including 1.5 mM MgCl₂, 200 μM mixed dNTPs (Biotech Australia), 2.3 μM each primer, 1U Vent (-exo) DNA polymerase (New England Biolabs) and 0.2 μl miniprep plasmid in a 20 μl reaction. This was placed into a thermal cycler according to the following cycles: 95°C for 5 mins; 35 cycles (94°C for 30 secs, 37-55°C for 30 secs, 72°C for 30-60 secs); hold at 25°C.

Table 2.4: Primers specific for cloning vectors

Vector	Primer name-Sequence (5' → 3')	Annealing Temp (°C)
pGEM-T	T7 – TAATACGACTCACTATAGGG SP6 – TATTTAGGTGACACTATA	39°C
pJD288	F – CCTTCGCAAGACCCTTCCTC R – AAGACCGGCAACAGGATTC	50°C
pQE9	F – CGGATAACAATTTTCACACAG R – GTTCTGAGGTCATTACTGG	47°C

2.7.4.5 DNA sequencing

Purified PCR products, or plasmid preparations were again verified on an agarose gel and then submitted to be sequenced (DNA Sequencing Facility, Department of Haematology, Flinders Medical Centre, Adelaide) using forward and/or reverse primers. Sequencing reaction was performed with BigDye Terminator version 3.1 and products analysed on an Applied Biosystems ABI 3100 Genetic Analyzer (Foster City, USA).

2.7.5 Coding Sequence Analyses

ESTs were selected from the TIGR grape database (www.tigr.org/tigr-scripts/tgi/T_index.cgi?species=grape) by performing BLASTp alignments with predicted mass spectroscopy fingerprints according to default settings (Altschul *et al.*, 1990; 1997). Once obtained, coding sequences were translated using the ExPaSy interface (<http://au.expasy.org/tools/dna.html>) and protein descriptives obtained with the PeptideMass tool, enabling prediction of mW and pI of unmodified proteins (Wilkins *et al.*, 1997; Gasteiger *et al.*, 2005).

Multiple sequence alignments for phylogenetic studies were performed using the BioEdit program (Isis Pharmaceuticals Inc., USA; Hall, 1999), creating a ClustalW file (Thompson *et al.*, 1994) and trees generated using the Treeview program² ver. 1.6.6. Multiple sequence alignments for observation of protein similarity and identification of conserved residues were performed using the WebANGIS BioManager interface (<http://www.angis.org.au>) and creating a ClustalW file analysed by BestFit (GCG) version 4.0 (Accelrys Inc., Wisconsin, USA) and BoxShade (Hofmann K. and Baron M.D.), respectively.

2.8 6-HIS Fusion Protein Purification and Analysis

2.8.1 Generation of Competent *E. coli*

A glycerol stock of M15:pREP4 *E. coli* was streaked onto LB solid media with 25 µg.ml⁻¹ kanamycin and grown with shaking at 37°C overnight. A single colony was used to inoculate a 10 ml LB liquid media + 25 µg.ml⁻¹ kanamycin and grown at 37°C overnight with shaking at 100 rpm. This inoculum was transferred into fresh LB + kanamycin and grown with shaking until the OD₆₀₀

² Copyright Roderic. D.M. Page, 2001

was 0.5-0.6. The flask was placed on ice, then centrifuged at 5,000g for 5 mins at 4°C. The supernatant was discarded and the pellet gently resuspended in cold, sterile 0.1 M MgCl₂ (1/3 vol. of original culture). The centrifugation was repeated and the pellet was resuspended in cold, sterile 0.1 M CaCl₂ (1/3 vol. of original culture). This was incubated on ice for 20 mins and the centrifugation repeated resuspending in cold, sterile 0.1 M CaCl₂ + 15% (v/v) glycerol (1/15 vol. of original culture). Aliquots (200 µl) were stored at -80°C.

2.8.2 *E. coli* Expression of 6-HIS Fusion Protein

M15:pREP4 *E. coli* possessing the fusion construct was grown in 10ml LB + 25 µg.ml⁻¹ kanamycin + 100 µg.ml⁻¹ ampicillin and grown at 37°C with shaking at 100 rpm overnight. Induction of the HIS-fusion protein by IPTG was confirmed on Coomassie Blue-stained polyacrylamide gels of whole cell protein extract and by Western blotting using an anti-HIS antibody. Western blotting was necessary to ensure presence of the N-terminal HIS residues for purification due to the alternate start codon within the GST sequence.

These minicultures were used to inoculate 500 mls of prewarmed LB and cultured until the OD₆₀₀ was 0.5-0.7. The culture was inoculated with 1 mM IPTG and cultured for a further 4-24 hrs at 37°C with shaking.

2.8.3 Immobilized Nickel Affinity Chromatography

Protein was extracted from IPTG-induced *E. coli* under native conditions according to standard protocols (Sambrook and Maniatis, 1989). The 1 ml HISTrap column (Amersham Biosciences, Uppsala, Sweden) using Ni²⁺ sepharose high performance affinity resin was equilibrated with 5ml distilled

H₂O, 10ml wash buffer (0.5 M NaCl, 20 mM sodium phosphate buffer, pH 7.4) and then the native protein extract was loaded at 1 ml.min⁻¹ with recirculation of the total sample volume 3 times. Unbound proteins were eluted with wash buffer until a stable baseline was reached on a chart recorder connected to a UV monitor (280 nm). Protein was eluted with stepwise gradients of increasing imidazole (20-500 mM) in wash buffer.

2.8.4 Western Blotting Using Universal HIS-Tag Detection Kit

E. coli cultures (1.5ml) were pelleted at 10,000g for 1 min and the supernatant was discarded. Eighty microlitres of 1× SDS loading dye was added to the pellet and this was heated for 10 mins at 95°C. The mixture was centrifuged at 10,000g for 10 mins and the supernatant transferred to a fresh eppendorf tube for SDS-PAGE.

SDS minigels were run as per 2.5.1 then equilibrated in transfer buffer (25mM Tris, 190mM Glycine, 0.025% (w/v) SDS) for 30 mins. The PVDF membrane was prewetted in 100% methanol and then immersed in transfer buffer for 5 mins. The Western transfer was performed as per manufacturer's instructions (BioRad mini-blot) at 350 mA for 55 mins at 4°C. Probing conditions were performed according to manufacturer's instructions (BD Biosciences, USA). Chemiluminescence was detected using the Imagemaster VDS-CL system (Amersham Biosciences, Uppsala, Sweden) and photographed using a thermal imager.

2.9 Quantitative Reverse Transcriptase PCR (QPCR)

2.9.1 Primer Design

Primers for QPCR are required to conform to generic primer design ‘rules’ such as random distribution of bases within the primer, 50-60% G/C content, balanced melting temperatures (T_m) for the primer pair, non-complementary bases at 3’ end of primers (Kohler, 1995). Primers were designed according to these guidelines, to amplify products 120-200 base pairs in length.

Primers for GST1, GST2, GST3, GST4, and Q84N22 were designed using the web-based tool Primer 3 to cross an intron (excluding the intronless GST4). Potential primer pairs were evaluated using the Netprimer analysis tool (www.premierbiosoft.com/netprimer/netprlaunch/netprlaunch.html), and selected on the basis of low self- and cross-complementarity, balanced T_m , and the software ranking. *β -Tubulin* (BE846404) and *Vvubiquitin1* (BN000705) primer sequences as per Curtin (2005) and Bogs *et al.* (2006), respectively. Details of each QPCR primer set used in this project are shown in Table 2.5, with products shown in Fig. 2.5 with no visible primer dimer formation.

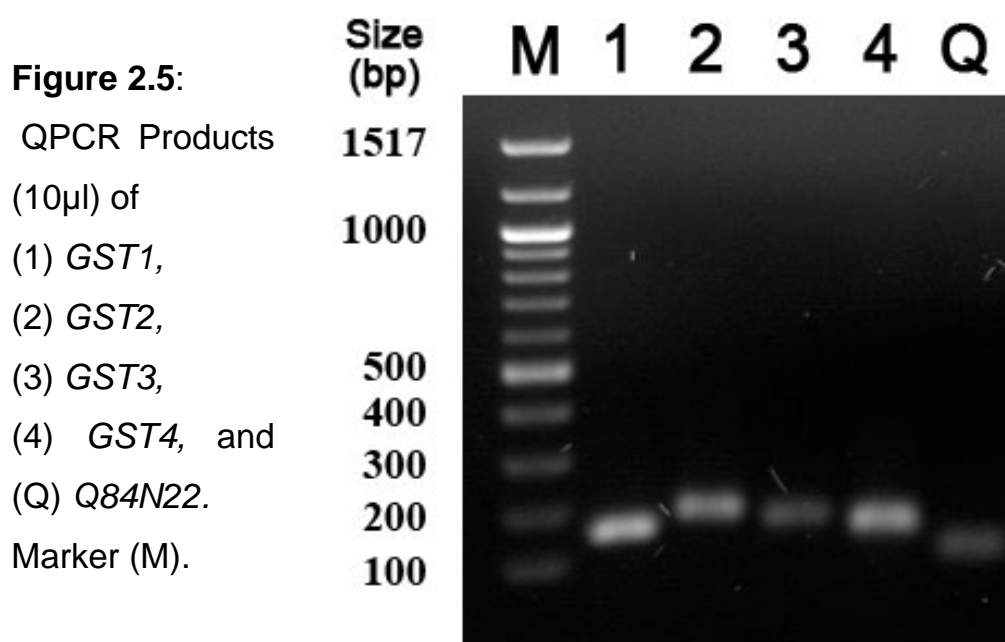


Table 2.5: Primers for QPCR analysis of GST sequences. Annealing temperature for all GST pairs was 50°C. Targeted region based on genomic sequence numbering.

Gene	Accession Number	Primer Sequence (5'→3')	Targeted Region
GST1	AY156048	F – CCA AAG AGC AAA AGC CAA GT R – TGT CCA GAA AAC CCA AAG TC	279-472
GST2	TC44916	F – TTT CCT TGC TCT CAA TCC AT R – CCT CCA CCT CTA TCC ACA CT	135-313
GST3	AY156052 ¹	F – TCC TGT CAT TCA AGA TGG AG R – GGG TGG TAA CTT TGT GCT TC	159-323
GST4	AY971515	F – CGA GGG CGA TTG TGA GGT A R – TTC CAC TTC CAG CCA TTG AT	200-309
Q84N22	AF501625	F – TAT TGA TGG GGT TTG GTG R – GTT TCC TGC TCT TCT CCT TT	219-368

¹ Partial sequence, full sequence obtained by RACE-PCR not published.

2.9.2 PCR Running Conditions

Templates used in QPCR were diluted PCR products for standards cleaned as per Section 2.7.4.1.2, or cDNA made as per Section 2.7.2.7. Each template was aliquotted in 2 µl volumes in 100 µl PCR tubes (Corbett Research, USA) and stored at -20°C.

Due to the significant cost of SYBR-green PCR kits it was necessary to develop an 'in-house' protocol that would give similar results, as has been achieved previously (Karsai *et al.*, 2002). For all samples, duplicate reactions with a final volume of 10 µl consisted of Qiagen PCR buffer (Qiagen, Venlo, Netherlands) with 2.5 mM magnesium, 2.3 µM forward and reverse primers, 200 µM dNTPs (Roche, Basel, Switzerland), 0.25 units Hotstar Taq (Qiagen, Venlo,

Netherlands), 0.2 x SYBR-green 1 DNA dye (Molecular Probes, Eugene, USA), and Qiagen pH balanced H₂O. Amplification was carried out on the Rotorgene 2000 (Corbett Research, USA) by the following protocol: enzyme activation (15 mins, 95°C), then 35 cycles of denaturation (20 sec, 94°C), primer annealing (20 sec, GSTs – 50°C, β -Tubulin – 55°C), and extension/fluorescence acquisition (20 sec, 72°C). Following amplification, products were melted from 65°C to 92°C over 5 mins for detection of primer-dimer or other incorrect amplification products.

Data was acquired on the SYBR-green channel with gain set at 9.33, and for both quantitation and melt analysis a ‘light’ digital filter was utilised to smooth raw fluorescence readings. Melt-curve analysis was carried out with the dF/dT threshold set above the fluorescence background at a value of 1 for detection of single melt-products. Example melt-curve analyses for each gene assayed are shown in Appendix 3.1, where it can be seen that in each case there was a single melt-product – confirming the specificity of the PCR reactions.

2.9.3 Confirmation of Correct Product Formation

Each product was amplified in 5 identical reactions from 100 ng cDNA prepared from FU-01 cells, harvested after 7 days of culture. Products were verified by size on a 1.8% (w/v) agarose gel, pooled and purified with the Ultraclean PCR clean-up kit. (MoBio, Carlsbad, USA). Purified products were again verified on an agarose gel, and submitted for sequencing with the reverse primer. PCR product sequences were aligned with target gene sequences using BLAST bl2seq alignment program (www.ncbi.nlm.nih.gov/blast/blast2.cgi; Altschul *et al*, 1990; (Gish and States, 1993). The sequences aligned with high

levels of homology to their target sequences, confirming correct amplification of desired genes.

2.9.4 Analysis and quantification

Cycle threshold (Ct) values, were obtained from raw fluorescence data using quantitation analysis options in Rotorgene 2000 software (Corbett Research, USA). The fluorescence threshold was set at 0.2752, while dynamic tube normalisation was applied to correct for background fluorescence in raw data, ignoring the first three cycles. Ct values were calculated in software as the fractional cycle number at which the pre-set fluorescence threshold was reached for that sample. Data was exported to Excel (Microsoft Office XP) for further analysis using custom-designed spreadsheets to calculate relative expression.

2.9.5 Generation of standards for method validation and quantification

The purified products generated in Section 2.9.2 were serially diluted in duplicate over 6 orders of magnitude (10^{-3} to 10^{-8}) and included in 3 separate experiments, in order to establish test linearity, coefficients of variation and amplification efficiencies.

During validation experiments, the dilution series of purified PCR products were assigned arbitrary copy number, or concentration values (Rajeevan *et al.*, 2001) in the Rotorgene 2000 software, reflecting the 10-fold dilutions. The software automatically calculates a standard curve based on the least-squares linear regression method for the dilution series, with Ct values plotted against \log_{10} (concentration) as shown in Appendix 3.1. The slope of this standard curve

was then used to derive amplification efficiency (E) based on equation 2.6, with efficiencies shown in Appendix 3.2.

Equation 2.6: QPCR amplification efficiency based on calibration curve

$$E = 10^{(-1/\text{slope})}$$

2.9.6 Mathematical model for quantifying gene expression

The formula used to calculate expression levels of genes utilised the Delta-Delta Ct model, accounting for the varied amplification efficiencies of target and housekeeping genes as per Pfaffl (2001). Curtin (2005) demonstrated this method of calculation, given by equation 2.7, to be the most accurate means of quantification for our cell lines.

Equation 2.7: Delta-Delta Ct modified to take into account different amplification efficiencies for target and housekeeping genes.

$$R = \frac{E_T^{\Delta Ct_T[C-U]}}{E_H^{\Delta Ct_H[C-U]}}$$

Where E_T and E_H are the amplification efficiencies for target and housekeeping genes respectively, $\Delta Ct_T[C-U]$ is the difference in cycle threshold value for the target gene between the calibrator cDNA (from 7-day old control FU-01 suspension cells) and the unknown sample, while $\Delta Ct_H[C-U]$ describes the same value for the housekeeping gene.

As all QPCR reactions performed utilized the same set of template cDNA that was made in a single batch, it was unnecessary to highlight a reference cDNA

in order to obtain relative expression levels, as advocated by Curtin (2005). Fold-induction was calculated by comparing Delta-Delta Ct values obtained for each condition, with the Delta-Delta Ct value for the corresponding control sample at the same timepoint.

2.9.7 Validation of QPCR assays

The reproducibility of RNA extraction and cDNA transcription from a single RNA sample has been performed by Curtin (2005). Validation of the reproducibility and reliability of the PCR reactions was performed here by comparison of intra- and inter-assay coefficients of variation (CV). CV is calculated as the fractional percentage of standard deviation divided by the mean. The dilution series of each purified PCR product were run in duplicate to generate intra-assay CV, which was averaged over three separate runs. Inter-assay CV was calculated by running the dilution series in duplicate on at least 3 separate occasions and including all data in the CV calculations. The results of these analyses are shown in Appendix 3.2.

2.10 Maize kernel bombardment

2.10.1 Preparation of Gold particles

Gold was prepared as per Sanford *et al.* (1993) and bombardment as per Alfenito *et al.* (1998), with the following modifications. Twenty milligrams of 1 μm diameter gold particles (BioRad) was weighed into an eppendorf tube and 500 μl of ice-cold 100% ethanol was added to each tube, then sonicated in an ultrasonic water bath for 15 sec. The tube was tapped on the bench to gather all droplets to the tube bottom and gold particles allowed to settle for 30 mins. The

gold was pelleted by centrifugation for 60 secs at 800g and the supernatant was discarded. One millilitre of ice-cold, sterile milliQ H₂O was slowly added to the microcentrifuge tube, with the pellet slightly disturbed by finger vortexing and again allowed to settle.

The gold was pelleted by centrifugation for 60 secs at 800g. The water rinse step was repeated two more times, the third time centrifuging for 15 sec. at 2,300g. The pellet was resuspended in 250 µl sterile water and sonicated in an ultrasonic water bath for 15 sec. The tube was immediately transferred to a vortex on high speed and 25 µl single-use aliquots (2 mg gold) were transferred to sterile eppendorf tubes and stored at -20°C until use.

2.10.2 Coating of Gold particles

GST sequences in maize expression plasmids for bombardment were purified using the Wizard MaxiPrep Column Kit (Promega, Australia) and phenol:chloroform treated. Plasmids were ethanol precipitated and resuspended at a concentration of 1 µg.µl⁻¹ by spectrophotometric quantification.

A 1× aliquot (2 mg) of gold was briefly defrosted on ice and 25 µl of plasmid solution was quickly added and gently agitated. This was put onto a vortex at high speed and the following solutions added in order: 220 µl sterile H₂O, 250 µl 2.5M CaCl₂·2H₂O and 50 µl spermidine and continued to vortex for 2 mins. This was left to settle for 1min. and pelleted at 5,000 g for 1 min. The supernatant was removed and 500 µl of 100% ethanol added and finger mixed to disturb pellet. This was allowed to settle for 1 min then pelleted at 5,000g for 1 min. The supernatant was removed and 36 µl of 100% ethanol was added and mixed by pipetting. This was used immediately for bombardment.

2.10.3 Preparation of *Bz2*-Deficient Corn Seeds

Maize seeds with a complete deletion of the *Bz2* gene (from atomic bomb-irradiation) have been used to confirm the anthocyanin-transporting role of An9, a GST purified from *Petunia* (Alfenito *et al.*, 1998). As mentioned previously in Section 1.5.1.2.1, the aleurone in these seeds is capable of producing anthocyanins, however, it remains in the cytosol, unable to be transported to the vacuole, giving it the bronze-coloured phenotype. Bombarding a GST that is able to transport anthocyanins into these seeds, leads to the phenotype being rescued and complementation zones of red/purple spots appear (Alfenito *et al.*, 1998).

Corn seeds were sourced from Virginia Walbot's laboratory, Stanford University, USA and stored in a dessicator at RT. Seeds were allowed to rehydrate overnight under a moist tissue and immediately prior to bombardment, the pericarp from the upper abaxial face (near the crown) was removed with tweezers to expose the aleurone layer. The corn seeds were positioned in clay for bombardment

2.10.4 Bombardment

The macrocarriers were rinsed in isopropanol and fully dried in the laminar flow. The coated gold particles were then aspirated with a pipette and 10 μ l transferred to the macrocarrier by slow pipetting from the centre outwards. This was allowed to air dry and loaded into the Helios Genegun (BioRad) 1cm below an 1100 psi rupture disc. A stopping screen was positioned 5.9 cm above the surface of the corn seeds. The corn seeds were bombarded twice using 27 mm Hg vacuum and covered between shots to keep moist. The seeds were incubated at 26°C for 24-72 hrs and then scored for revertant sectors (per mm²) by microscopy.

2.11 Microscopy

2.11.1 Confocal microscopy

Suspension cultured cells, or thinly hand-sectioned callus were mounted on microscope slides in GC-2 medium, or a solution of 4% (w/v) sucrose in PBS, pH 5.2. Observations were made using a Bio-Rad MRC-1000UV Confocal Scanning Laser Microscope System, attached to a Nikon Diaphot 300 inverted microscope. Specimens were excited using a Krypton/Argon laser at wavelengths referred to in Table 2.6.

Table 2.6: Fluorescence settings for BioRad MRC 1000-UV confocal microscope.

Fluorescence	Excitation Wavelength (nm)	Emission Wavelength (nm)
GFP	488	522\35
Red	568	585LP
Far Red	647	680\32

Z-series of images of the specimen were collected at 0.25 μ m intervals in the z-axis and 3-dimensional reconstruction performed using 3-dimensional reconstruction software, AMIRA 3.1 (Template Graphics Software, Houston, Texas). Eight slides, containing 23 AVI-containing cells were analysed from FU-01, FU-03 and FC-01 samples, with representative images shown.

2.11.2 Cryogenic-scanning electron microscopy (cryoSEM)

Suspension cells were dried on filter paper and callus samples were hand-sectioned (2 mm x 2 mm x 3 mm) and mounted onto the preparation stage in

carbon dag. This was rapidly frozen by immersing into nitrogen slurry and placed into the pre-chilled fracturing compartment under vacuum. The sample was fractured using a sterile scalpel blade, sublimated and the sample coated in platinum. The stage was transferred into the Philips XL30 Field Emission Scanning Electron Microscope equipped with an EDAX DX4 integrated energy dispersive X-ray analyser for analysis. X-ray counts were taken at 5kV for 60 secs.

2.12 Grape cell transfection

2.12.1 Preparation of Cells

All techniques were performed under aseptic conditions. *V. vinifera* L. cv. Chardonnay cells were grown in the dark in GC-2 media for 4-5 days following subculture. The equivalent of 1ml packed cell volume (PCV) of cells was vacuum dried onto filter paper, which was transferred to solid GC-2 media at room temperature for 2 hrs.

2.12.2 Preparation and Coating of Gold Particles

Preparation of gold was performed as per Sanford *et al.* (1993). The microcarriers in 50% glycerol at 60 mg.ml⁻¹ were vortexed on a platform vortexer for 5 mins to disperse. Fifty microlitres was transferred to a fresh eppendorf tube to which was added 5 µg DNA (in 5 µl), 50 µl of 2.5 M CaCl₂•2H₂O and 20 µl of 0.1 M spermidine, while vortexing. This was vortexed for a further 3 mins and the carriers allowed to settle for 1 min. This was pelleted for 2 secs at 14,000g in a microcentrifuge and the supernatant discarded. The pellet was washed without disturbing by adding 140 µl 70% ethanol and then carefully removing the

supernatant. The pellet was washed in 140 μ l 100% ethanol and repeated twice. The pellet was then resuspended in 48 μ l 100% ethanol by vortexing and pipetting.

2.12.3 Bombardment

Six microlitres of the coated gold slurry was pipetted on the macrocarriers. A vacuum of 75kPa was applied to the chamber and a 350kPa jet of N₂ gas was applied to bombard the cells with the DNA. The plates were then sealed with parafilm and incubated at 25°C in the dark for 1-4 days. Cells were visualised by fluorescence microscopy.

Pigmented cells were picked from 2 transfected plates using a scalpel blade at 24, 48, 72, 96 hrs post-transfection and transferred to GC-2 medium. Cells were pelleted by centrifugation at 6,000g for 5 mins and the supernatant discarded. Fifty microlitres of 50% acetic acid in water was added and the cells briefly vortexed and incubated at room temperature for 1 hr, or overnight at 4°C. The supernatant was collected after centrifugation and subjected to HPLC as per Section 2.4.2.3 to confirm the presence of anthocyanins (data not shown).

2.13 Purification and analysis of AVIs

2.13.1 AVI isolation

Protoplasted cells were frozen at -20°C overnight at a concentration of $1 \times 10^6 \text{.ml}^{-1}$ in 300 μ l aliquots, with all mannitol buffer removed. Samples were defrosted, 200 μ l of fresh, cold mannitol buffer was added and sonicated on ice at 50W for 2 x 15 sec bursts (Sonifier B-12, Branson Sonic Power Company, USA). Samples were loaded onto a 10%/30%/50%/80% (v/v) Percoll gradient and

centrifuged at 250g for 5 mins. The supernatant was discarded and the pellet was washed 3 times in mannitol buffer. The Percoll gradient centrifugation and washing wash repeated. The pellet was then allowed to settle by gravity through a 95% Percoll solution, with subsequent washing, to remove all traces of starch granules.

2.13.2 Lipid analysis

AVIs and vacuum-dried grape cells were weighed and frozen in liquid nitrogen. Total fatty acids were extracted according to Blank *et al.* (2002), without thin layer chromatographic separation of phospholipids. Fatty acid methylester (FAME) analysis was performed on a Hewlett Packard 6890 Gas Chromatograph fitted with a Flame Ionisation Detector (FID), using a SGE BPX70 column (SGE International, Victoria, Australia) as per Blank *et al.* (2002). Lipid was quantified by interpolation of peak heights from chromatograms to standard curves of pure compounds.

2.13.3 HPLC analysis and quantification of tannins

2.13.3.1 Solvent preparation and gradient program

HPLC was undertaken to examine tannin composition, using the Hewlett Packard HP 1100 high performance liquid chromatograph with Chemstations software. Ten microlitres of each sample was injected onto a Wakosil C18 RS 3 μm , 15 cm x 0.46 cm internal diameter column (Wako Pure Chemicals, Osaka, Japan) and eluted as per Table 2.2. Detection was at 520, 353, 320, 280 nm and spectral data from 190-600 nm was collected using a photo-diode array detector.

Samples were run according to the method of Downey and Kristic (In press), utilising Buffer A (10% formic acid in water) and Solvent B (100% methanol). Buffer A was filtered through 0.22 μm nitrocellulose membranes (Millipore), while Solvent B was filtered through 0.45 μm HVHP membranes (Millipore) and degassed for 5 mins by helium sparging, or sonicated for 80 mins in an ultrasonic water bath.

Table 2.2: HPLC elution method for uncleaved samples

Time (minutes)	Solvent B (%)
0	17
1	17
15	35
40	37
42	100
48	100
50	17
52	17

2.13.3.2 Sample preparation

Cell suspensions were vacuum dried and ground to a fine powder under liquid nitrogen using a mortar and pestle. Protoplasts and AVIs were pelleted, the supernatant removed and samples frozen on liquid nitrogen. These samples (5-100 mg) were extracted in 10 volumes of 70% Acetone with 0.1% (w/v) ascorbic acid overnight and tannin analysis was performed by acid-catalysed cleavage and phloroglucinol adduct formation as per Kennedy and Jones (2001) with modifications as per Downey *et al.* (2003a).

2.13.3.3 Identification and quantification of peaks

Peaks were identified by comparison with known standards and Mass Spectrometry analysis of peaks. Quantification was done using a standard curve for each peak as run by Nicole Cordon, CSIRO Plant Industry, Waite Campus, Adelaide.

2.13.4 Starch Quantification

Starch composition of AVI preparations was quantified with the Megazyme total starch and resistant starch quantification kits, according to manufacturer's instructions (Megazyme International, Ireland).

2.13.5 Analysis of Total Soluble Solids

V. vinifera cv. Shiraz berries from the Coombe vineyard, Waite campus, Adelaide University were analysed by a hand refractometer (Rochert, Buffalo, NY) by crushing individual berries onto the optical path. For each condition, 6 berries were quantified (°Brix) and results presented as mean \pm standard deviation.. The accuracy of this measurement strategy was confirmed by measuring the crushed berries retained after removal of skins for RNA extraction (Section 2.7.2.2).

CHAPTER 3

CELL LINE KINETICS AND CHARACTERISATION

3.1 Introduction

Anthocyanins accumulate in defined tissues and at a specific stage of differentiation, eg. in grape berry skins, and only during veráison (Zhang and Furusaki, 1999). It was this ideal genetic adherence that enabled Gregor Mendel to use seed coat colour and flower colouration in peas (*Pisum sativum*), both due to anthocyanin pigmentation, to study inheritance (Mendel, 1865). Furthermore, anthocyanins are of chemotaxonomic interest as most plant species exhibit a unique profile of these compounds.

As anthocyanin production occurs only in grape berry skins after veráison, callus was initially generated from anthocyanic berry skins. These cells when grown as callus on solid medium or introduced into suspension culture containing appropriate combinations of plant hormones, retain their totipotency and their ability to produce anthocyanins (Hawker *et al.*, 1973).

The *Vitis vinifera* L. cv. Gamay Fréaux cell line has been previously characterised for its ability to produce anthocyanins, under dark and light conditions (Cormier *et al.*, 1990; Calderon *et al.*, 1993; Bailly *et al.*, 1997). The intermediate-pigmented *V. vinifera* cell culture (FU-01) does not produce substantial amounts of anthocyanin, therefore elicitation strategies to yield ectopic levels of anthocyanin were developed to probe steps in the anthocyanin post-biosynthetic pathway. Furthermore, generation of anthocyanin-deficient (FU-03) and high-anthocyanin accumulating (FU-02) cells was achieved by growing FU-01 suspension cells as microcallus and selecting for these phenotypes (Fig. 3.1). The purpose of this chapter is to present the kinetics of the various *V. vinifera* suspension lines used in this study and the effects of various elicitation strategies.

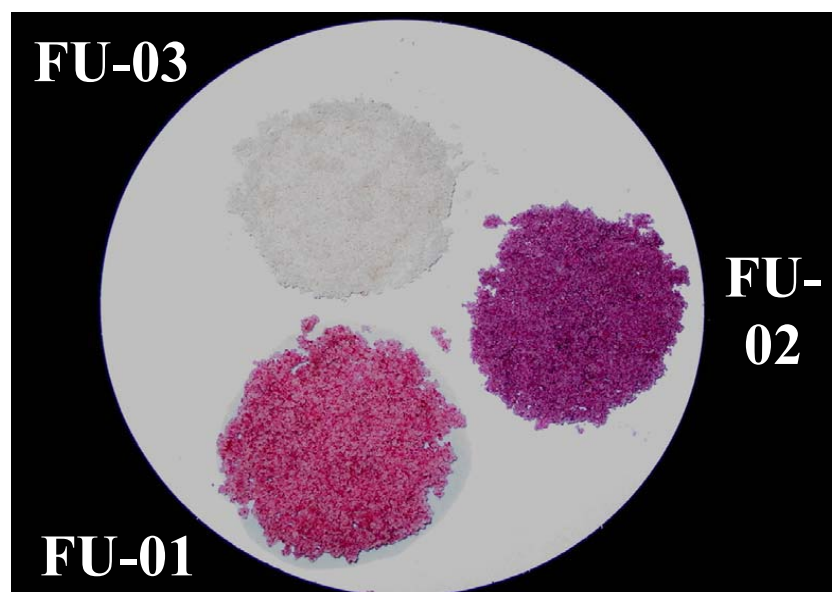


Figure 3.1: Seven day-old, vacuum dried *V. vinifera* L. suspension cell lines used in this study.

3.2 Characterisation of *Vitis vinifera* L. Cell Lines

3.2.1 FU-01 (intermediate-pigmented)

The FU-01 cell line was analysed over a 9-day culture period, with and without jasmonic acid (JA) elicitation, which is known to increase anthocyanin accumulation (Curtin *et al.*, 2003). Results shown in Fig. 3.2 were taken from a single representative experiment, while tabulated (Table 3.1) data combines results from all relevant kinetic studies. Similar results were obtained in repeat experiments regarding growth for all lines, although anthocyanin production in high anthocyanin-expressing lines was variable.

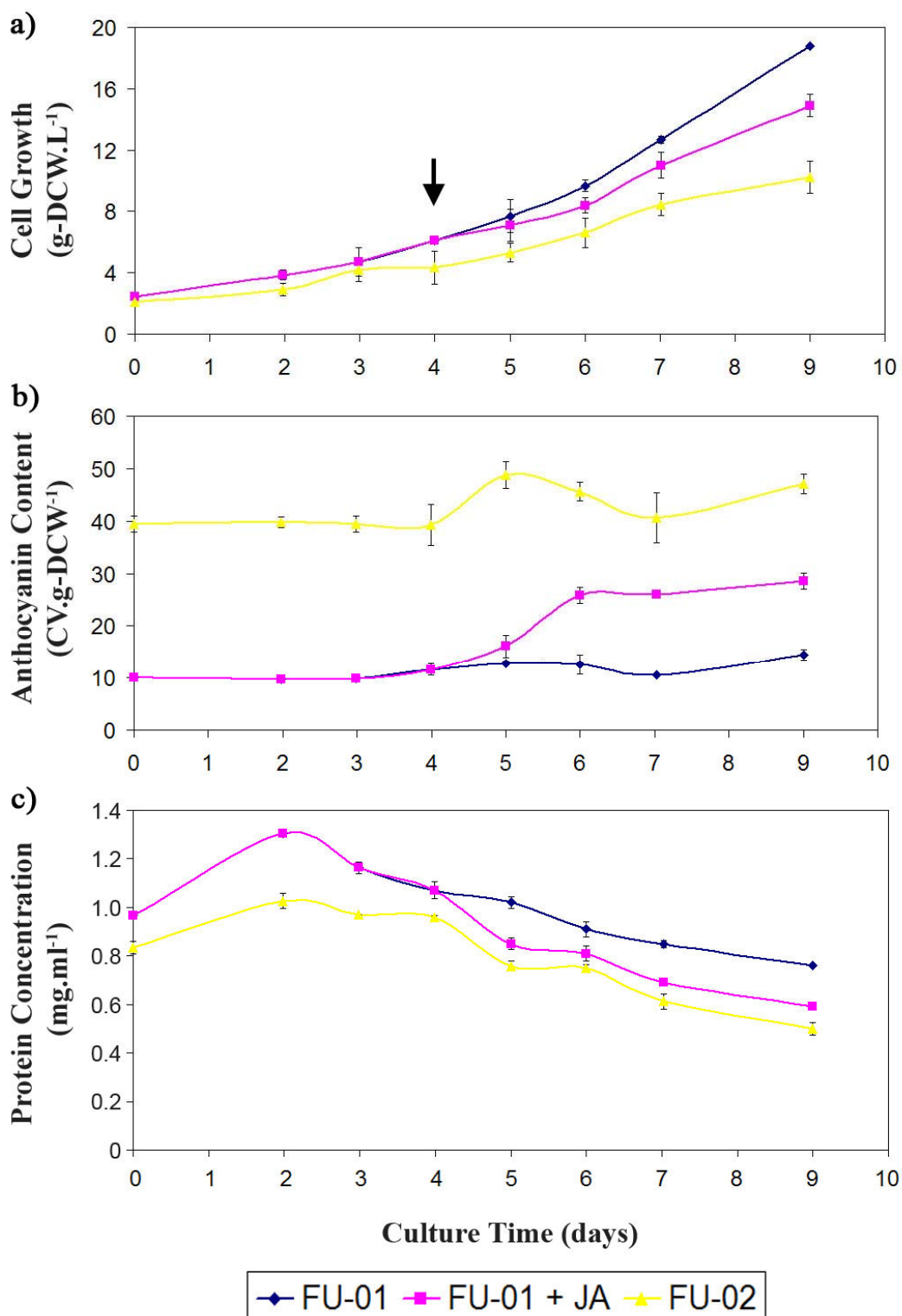


Figure 3.2: Kinetic measurements (a) Cell growth, b) anthocyanin content and c) protein concentration) on *V. vinifera* L. suspension cells with and without elicitation with 10 μM jasmonic acid (JA) at day 4 (arrow). Mean of triplicate values at each time point \pm Std. Dev.

The anthocyanin content (CV.g-DCW^{-1}) of FU-01 (intermediate-pigmented) cells does not significantly change over a 9-day culture period, while when elicited at day 4 with $10 \mu\text{M}$ JA, a 2-fold increase was observed from day 6 (Fig. 3.2b, FU-01 + JA). Concomitantly, a reduction in biomass yield was observed under jasmonic acid treatment (Fig. 3.2a). Secondary metabolite production in plant cell culture is often inversely proportional to cell growth (Sakuta *et al.*, 1994). Anthocyanin production (CV.l^{-1}) gives an estimate of total anthocyanin accumulation, uncompromised by growth rate of various cell lines. By day 7, the level of anthocyanin production was 145, and 299 CV.l^{-1} for FU-01, and FU-01 + JA, respectively.

Treatment of cells with 50 g.l^{-1} sucrose (S) and white light (L) irradiation increased anthocyanin production, with light causing a significant reduction in biomass (Table 3.1). When elicitors were combined, the increases in anthocyanin content were seemingly additive, rather than synergistic. Furthermore, all elicitation strategies utilising JA (JA, JA+L and S+JA+L) increased the proportion of malvidin-based anthocyanins. Treatment of *V. vinifera* suspension cultures with S+JA+L was the best strategy for enhancing anthocyanin accumulation, with fold-increases similar to those observed in our laboratory previously (Curtin, 2005).

Various protein extraction methods and buffers were attempted; with grinding cells on liquid nitrogen and suspending cells in a Tris-EDTA buffer being the best strategy. The yield of whole-cell protein from all cell samples reduced as cells aged in culture. Elicitation with JA (Fig. 3.1c) alone and in combination with light (data not shown) reduced cellular protein concentration, reflecting the acquisition of slower growing cells committed to enhanced secondary metabolite – particularly anthocyanin – synthesis.

Table 3.1: Profile of suspension cell lines after 7 days growth in GC-2 medium (n: number of independent measurements). ND: not determined.

CELL LINE	Growth (g-DCW.l ⁻¹)	Anthocyanin Production (CV.l ⁻¹)	Anthocyanin Content (CV.g-DCW ⁻¹)	Fold-Induction	Malvidin (% of total)	Pigmented Cell Count
FU-01 (n=120)	12.6 ± 0.35	145 ± 21	11.5	1.0	3.1 ± 0.4%	39.6 ± 6.1%
FU-01 + S (n=6)	12.1 ± 0.2	196 ± 9	16.2	1.3	2.8 ± 0.1%	ND
FU-01 + JA (n=15)	11.5 ± 0.31	299 ± 16	26.0	2.5	22.8 ± 2.1%	ND
FU-01 + L (n=6)	11.0 ± 0.12	253 ± 5	23.0	2.2	3.1 ± 0.1%	ND
FU-01 + JA/L (n=36)	10.5 ± 0.42	451 ± 35	43.0	4.1	5.2 ± 0.4%	45.1 ± 3.5%
FU-01 + S/JA/L (n=12)	10.4 ± 0.12	691.6 ± 65	66.5	6.0	12.2 ± 1.4%	47.1 ± 2.3%

Counts of protoplast preparations revealed that only 40% of the population of FU-01 cells were visibly pigmented, despite the callus used for generation of this suspension line being absent of visibly non-pigmented regions. This suggests either these cells lost the capacity for anthocyanin synthesis, or there was rapid somaclonal expansion of a small population of non-pigmented cells. Elicitation strategies did not significantly alter the proportion of pigmented cells, signifying an increase in the quantity of anthocyanin per cell by these strategies (Table 3.1).

3.2.2 FU-03 (non-pigmented)

Based on the difference in anthocyanin content between FU-01 and FU-03, it would be assumed that ~3-4% of FU-03 cells were pigmented. However, as no pigmented cells were discernible by microscopic count for FU-03 suspension cultures, this suggests that numerous cells must accumulate small amounts of anthocyanin, indistinguishable from the haemocytometer background. This observation is corroborated by the infrequent appearance of lightly pigmented regions in FC-02 callus cultures. The growth rate for control cultures from inoculation to day 7 was $1.6 \text{ g-DCW.l}^{-1}\text{day}^{-1}$ for FU-01, and $0.6 \text{ g-DCW.l}^{-1}\text{day}^{-1}$ for FU-03. This 2.5-fold slower growth rate is despite a reduction in total anthocyanin (Table 3.2) and phenolic accumulation (Curtin, 2005). FU-03 cultures accumulate no malvidin, but are predominated by peonidin (66%) and cyanidin (34%).

Table 3.2: Profile of the FU-03 suspension cell after 7 days growth in GC-2 medium (n: number of independent measurements). ND: not determined.

CELL LINE	Growth (g-DCW.l ⁻¹)	Anthocyanin Production (CV.l ⁻¹)	Anthocyanin Content (CV.g-DCW ⁻¹)	Fold-Induction	Malvidin (% of total)	Pigmented Cell Count
FU-03 (n=16)	7.1 ± 0.6	7.1 ± 0.6	1.0	1.0	0%	0%
FU-03 + S/JA/L (n=8)	5.7 ± 0.3	23.4 ± 1.1	4.1	4.1	0%	10.3 ± 0.2%

Table 3.3: Profile of the FU-02 suspension cell lines after 7 days growth in GC-2 medium (n: number of independent measurements). Range shown for malvidin composition in parentheses.

CELL LINE	Growth (g-DCW.l ⁻¹)	Anthocyanin Production (CV.l ⁻¹)	Anthocyanin Content (CV.g-DCW ⁻¹)	Fold-Induction	Malvidin (% of total)	Pigmented Cell Count
FU-02 (n=54)	9.0 ± 3.2	346 ± 148	40.6	1.0	19.2 ± 17.4% (3.1-39.6%)	52.1 ± 2.5%
FU-02 + S/JA/L (n=3)	8.4 ± 0.2	560 ± 113	125.1	3.1	21.2 ± 3.4%	55.7 ± 2.3%

Induction with sucrose, jasmonic acid and light lead to a 4-fold increase in anthocyanin accumulation in FU-03. This was defined by a 6.6-fold increase in peonidin-3-glucoside and 1.7-fold increase in cyanidin-3-glucoside levels as seen by Curtin (2005). The proportion of visible pigmented cells was 3.9-fold less in FU-03 +S/JA/L compared with FU-01 cells, yet FU-03 cells were lightly coloured. As the anthocyanin content of FU-01 cells was approximately 3-fold that of the elicited FU-03 cells (Table 3.1 and 3.2), this indicates more lightly pigmented cells, invisible to the naked eye, may be present in FU-03 to contribute to the anthocyanin content.

3.2.3 FU-02 (high-pigmented)

As with the elicited FU-01 lines, the increase in anthocyanin in FU-02 is associated with a concomitant reduction in growth rate – $1.6 \text{ g-DCW.l}^{-1}.\text{day}^{-1}$ for FU-01, twice that for FU-02 ($0.8 \text{ g-DCW.l}^{-1}.\text{day}^{-1}$). FU-02 cells had a 13% increase in the proportion of pigmented cells compared to FU-01. The difference in anthocyanin content between these cell lines was around 4-fold, implying that as well as a difference in number of pigmented cells FU-02 contains more anthocyanin per pigmented cell. This phenomenon may explain the reduced inducibility of FU-02 compared with FU-01 when treated with S/JA/L - 3.1 and 6-fold, respectively.

The high anthocyanin production of the FU-02 cell line is an unstable phenotype, as seen by the coefficients of variation for FU-02 and FU-01 being 0.43 and 0.14, respectively (Table 3.3). The FU-02 line lost this high production capacity under conditions where no selective pressure was placed on the high-expressing cells, also seen by Hirasuna *et al.* (1991) for a similar line. This was

seen actively by culturing from flasks that did not possess the greatest anthocyanin production, or by a passive washout effect with the faster growing cells (a phenotype of the cells accumulating less anthocyanin, Table 3.1) out-competing those with greater energy commitment towards secondary metabolism (somaclonal variation). The resultant cellular kinetics (anthocyanin production, proportion of pigmented cells and cell growth) closely matched that of the FU-01 line in less than 10 subcultures, as documented previously in our laboratory (Curtin, 2005). The anthocyanin profile of the FU-02 line was dominated by malvidin-based anthocyanins (3-glucoside and 3-*p*-coumaroylglucoside), imparting a more purple colour to the culture (Fig. 3.1). However, as anthocyanin production waned it became a cyanidin and peonidin-dominant profile akin to FU-01 as documented here and by Curtin (2005). In comparison to other similar cell lines, FU-01 accumulates a metabolically advanced mixture of anthocyanins, with high proportions of methylated (peonidin and to a lesser extent malvidin) and coumaroylated derivatives. These characteristics are desirable due to the chemical stability they confer (Sections 1.3.2.1-4). All these observations lead this research towards the use of the more stable FU-01 line for the majority of analyses.

3.3 Two-dimensional gel electrophoresis

Whole-cell protein was extracted from seven day-old FU-01 cells with and without jasmonic acid and light treatment at day 4. These were quantified and the same mass of protein was separated by 2-D gel electrophoresis. Following Sypro Ruby-staining, these gels were imaged (Fig. 3.3) and analysed by 2D image analysis software (Amersham Biosciences, Uppsala, Sweden). In this representative experiment, 1434 spots were identified in the FU-01 sample, with

1289 (90%) being altered by less than 1.5% of its intensity by the elicitation. The remaining affected proteins were both upregulated (135) and downregulated (10), with 39 spots found to be expressed only in elicited cells. Of the detectable proteins in the FU-01 sample, the most strongly upregulated spot was increased 15.3-fold. While this is a single protein separation from a representative experiment, this demonstrates the specific molecular influence of these elicitation strategies on cells within 3 days of treatment.

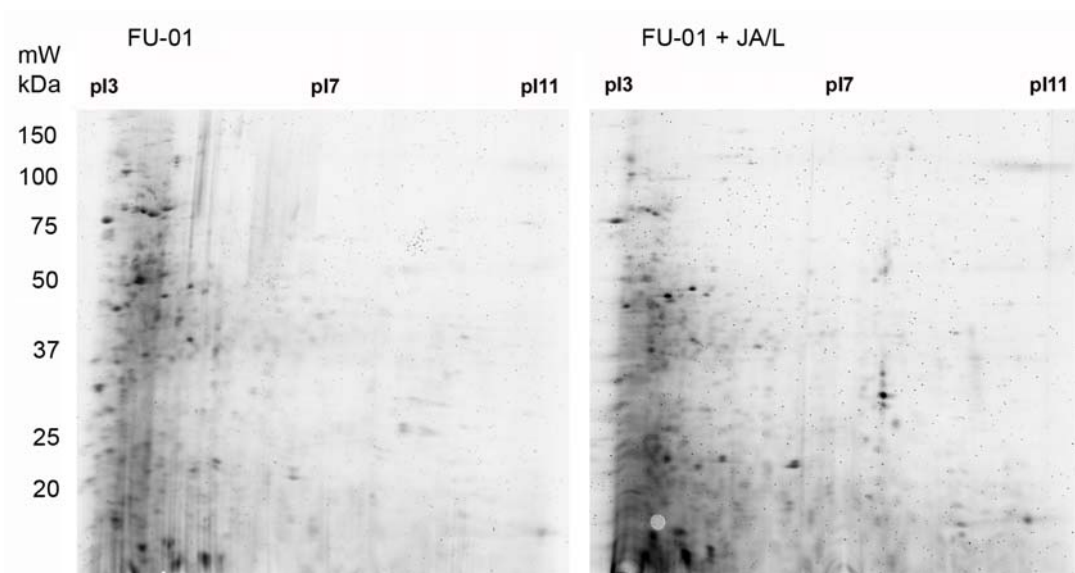


Figure 3.3: Sypro Ruby-stained 2-dimensional gels of whole cell protein from FU-01 and FU-01 under jasmonic acid and light elicitation (FU-01 + JA/L).

3.4 Discussion

Three cell types – intermediate-pigmented (FU-01), non-pigmented (FU-03) and high-pigmented (FU-02) – were utilised in this study. *V. vinifera* L. cv. Gamay Fréaux var. Teinturier cell cultures have been reported to synthesize predominantly peonidin- and cyanidin-based anthocyanins (Do and Cormier,

1991b; Cormier *et al.*, 1994; Krisa *et al.*, 1999b). This was seen for the FU-01 line used here, while the darker pigmented, FU-02 line had a predominance of malvidin-based anthocyanins. The proportion of malvidin for both lines increased when cells were treated with jasmonic acid, suggesting an increase in activity of methyltransferases; able to convert cyanidin and peonidin to malvidin.

Increases in the production of anthocyanins were achieved by various combinations of sucrose, jasmonic acid and white light on pigmented *V. vinifera* L. suspension cells. JA (and its methyl ester) is a known elicitor of secondary metabolism in many plant species (Gundlach *et al.*, 1992), and has previously been shown to elicit increased anthocyanin production in *V. vinifera* cell cultures (Curtin *et al.*, 2001).

In order to achieve quantum increases in anthocyanin accumulation and to probe the anthocyanin post-biosynthetic pathway, JA was combined with other effective metabolic stimulators. The importance of common cell culture parameters such as light (Zhong *et al.*, 1991) and carbohydrate concentration (Larronde *et al.*, 1998) in achieving high anthocyanin yields has been shown previously. These conditions were selected on the basis they were likely to stimulate anthocyanin production via different mechanisms, although cross-talk in transduction of stress signals has been noted to occur (Knight and Knight, 2001). The increase compares in magnitude to those observed in studies with a *V. vinifera* cell line related to FU-01 by Do and Cormier (1990; 1991a; 1991b) and with previous observations in our laboratory (Curtin, 2005).

Molecular evidence was presented in the form of 2D gel analysis of FU-01 suspension cells with and without elicitation with JA and light. The increase in anthocyanin synthesis was shown to be accompanied with an increase in the

expression of approximately 9% of discernible proteins and a decrease in 1% of spots. The spots that increase in relative intensity may comprise anthocyanin biosynthetic proteins in support of the increase in expression of these genes noted by qPCR for JA and light elicitation in our laboratory (Curtin, 2005).

Previous strategies to increase anthocyanin accumulation in grape suspension cell cultures by targeting the biosynthetic pathway have still not lead to the level of accumulation in intact berry skins, or grape callus. Thus, factors must be limiting this accumulation and post-biosynthetic modifications – transport and storage – are thought to be contributing factors. This chapter provided a panel of elicitation strategies/probes with which to characterise anthocyanin transport and storage sites, in the following chapters.

CHAPTER 4

GLUTATHIONE S-TRANSFERASES AND THEIR INVOLVEMENT IN ANTHOCYANIN TRANSPORT IN *VITIS VINIFERA* L. CELL-SUSPENSION CULTURE

4.1 Introduction

GSTs are a family of dimeric proteins able to transport a variety of compounds (xenobiotics and allelopathics) intracellularly by both covalent modifications and non-covalent interactions (Marrs, 1996). Single GSTs have been cloned that demonstrate a non-redundant role in the transport of anthocyanins from the cytosol to the vacuole in maize (Marrs *et al.*, 1995), petunia (*An9*; Alfenito *et al.*, 1998) and *A. thaliana* (*TT19*; Kitamura *et al.*, 2004). They were all cloned via a knockout approach yielding a phenotype of anthocyanin mislocalisation that could be reciprocally complemented by expressing any of the other anthocyanin transporting GSTs. In addition, *An9* was shown to interact with anthocyanins in a non-covalent manner using various binding assays mentioned in Section 1.5.1.2.2, inferring its functional role as a ligandin, or escort protein (Mueller *et al.*, 2000).

Each plant species possess numerous GST species, presumably to act on a wide range of substrates. GSTs have been purified to homogeneity by multi-step chromatographic procedures from a variety of plant sources, including *Sorghum bicolor* L. (Gronwald and Plaisance, 1998), *Oryza sativa* L. (Deng and Hatzios, 2002a), *Brassica oleracea* L. (Lopez *et al.*, 1994), *Glycine max* L. (Andrews *et al.*, 1997), *Triticum aestivum* L. (Mauch and Dudler, 1993), *Dianthus caryophyllus* L. (Itzhaki and Maxon, 1994), *Zea mays* L. (Mozer *et al.*, 1983), and *Avena sativa* L. (Zachariah *et al.*, 2000). However, none of these studies proceeded to clone the gene sequences, only characterising the activity of the protein(s) with various substrates.

The majority of plant GST gene sequences and all of those with a known function have been cloned by genome sequencing or as a result of large-scale

screening of transposable element-mediated, mutagenesis projects (Marrs, 1996). These are costly processes, requiring a high level of automation, handling and/or containment, therefore an alternative cloning strategy was required. As each of these proteins retains the capacity to bind glutathione (GSH), GSH-affinity chromatography represents the optimum initial purification strategy from plant cells where knockout phenotypes are not available. The following approach sought to clone functional *V. vinifera* L. GSTs by a fully rational combination of protein purification, proteomic analysis, amplification of corresponding expressed sequence tags (ESTs) and complementation analysis for anthocyanin transport. Particular attention was placed on identifying candidate anthocyanin transporting GSTs by comparing cell lines with varying levels of anthocyanin accumulation. Identification of the anthocyanin-transporting GST was desirable in order to determine if it is limiting the rate of anthocyanin accumulation. Therefore, a rational enhancement strategy targeting transport may lead to an increase in the amount of anthocyanin accumulated in suspension culture.

4.2 GST Cloning Strategies

4.2.1 Degenerate PCR to clone GST sequences

Attempts were made to clone GSTs utilising degenerate PCR primers, targeting conserved regions. However, as GSTs contain limited homology across GST types as well as within and between species, no degenerate PCR approach to date has yielded numerous GST clones from within a single species. Specific residues within the N-terminal region (~77aa) have been demonstrated to be critical in protein folding and GSH-binding (G-sites), as they are also present in other GSH-dependent proteins. Residues conserved across the largest class of plant GSTs (τ class, Type I GST), and other GSTs, include Ser13, Lys40, Ile54, Pro55, Glu66, Ser67, using *PtGSTU1* numbering. These are critical G-sites and, in addition, Ile54 was shown to be critical for protein folding processes (Zeng and Wang, 2005). Fewer conserved residues are seen in the C-terminus of the proteins, presumed to interact with the substrates (H-sites), in these and other GSTs (Marrs, 1996).

The conservation of the WSPPF[V/G] and ARFWAD motifs in the N-terminus have been exploited in a degenerate cloning procedure of a single Type III GST in opium poppy suspension cells (Yu and Facchini, 2000). The highly conserved WSPPF[V/G] motif of type III GSTs motif was used in this study to generate a sense primer, but were highly degenerate (n=128 alternate primers) and yielded numerous products with the oligo dT₂₀ reverse primer. The predominant product was sequenced and identified as highly homologous to an unrelated (β -coatamer) protein from Arabidopsis and other plants. A single 268bp product was produced using the degenerate reverse primer designed in this study based on the ARFWAD motif (data not shown) and identified as having a GST-like sequence,

with 99% identical to a *V. vinifera* EST, Q84N22, except for forward primer-specific sequence differences (Fig. 4.1). As this approach yielded only a single partial product, a proteomics method was chosen as the preferred method for identifying multiple GSTs in pigmented *V. vinifera* suspension cells.

```

D:  1 tggcctagcccgtttggtatgaggggcagacttgcctggcagagaagggtctcaagtat
   |||||||  |||||||  |||||||  |||||||  |||||||  |||||||  |||||||  |||||||
Q: 31 tggcctagcatgtttgggtatgaggggcagacttgcctggcagagaagggtctcaagtat

D: 61 gaatatagagaggaggacctgtggaacaagagccctttgcttcttgagatgaaccagtt
   |||||||  |||||||  |||||||  |||||||  |||||||  |||||||  |||||||  |||||||
Q: 91 gaatatagagaggaggacctgtggaacaagagccctttgcttcttgagatgaaccagtt

D:121 cataagaaaatcccagttctgatccacaatggaaagcccatttgtgagtctctgataata
   |||||||  |||||||  |||||||  |||||||  |||||||  |||||||  |||||||  |||||||
Q:151 cataagaaaatcccagttctgatccacaatggaaagcccatttgtgagtctctgataata

D:181 gttcagtatattgatgaggtttggtgcgataaatctccgcttttgcttagtgaccatac
   |||||||  |||||||  |||||||  |||||||  |||||||  |||||||  |||||||  |||||||
Q:211 gttcagtatattgatgaggtttggtgcgataaatctccgcttttgcttagtgaccatac

D:241 cagagagctcaggccaggttctgggcgga 268
   |||||||  |||||||  |||||||  |||||||  |||||||
Q:271 cagagagctcaggccaggttctgggcgga 300

```

Figure 4.1: BLAST2 alignment of degenerate PCR product (D) and Q84N22 sequence (Q; numbering as per accession number AF501625).

4.2.2 Protein Purification to Clone GST Sequences

4.2.2.1 Selection of time-point for purification

Analysis of total GST activity was performed on whole-cell, desalted protein from *V. vinifera* L. suspension cells grown under various conditions across a 9-day time course. This assay exploited a spectrophotometric measure of GSH conjugation to a model substrate 1-chloro 2,4-dinitrobenzene (CDNB) and was used to monitor purification and determine the optimum sampling time for protein extraction. CDNB is only one of numerous model substrates utilisable in the GST

assay. While there are certain GSTs that are unable to conjugate GSH to CDNB, it is the most widely used model substrate (Marrs, 1996). Therefore, it was utilized as the model substrate for the total GST activity assay.

The wave-like pattern of GST activity over the kinetic time-course (Fig. 4.2) represents the combined activity of a number of uniquely regulated GSTs.

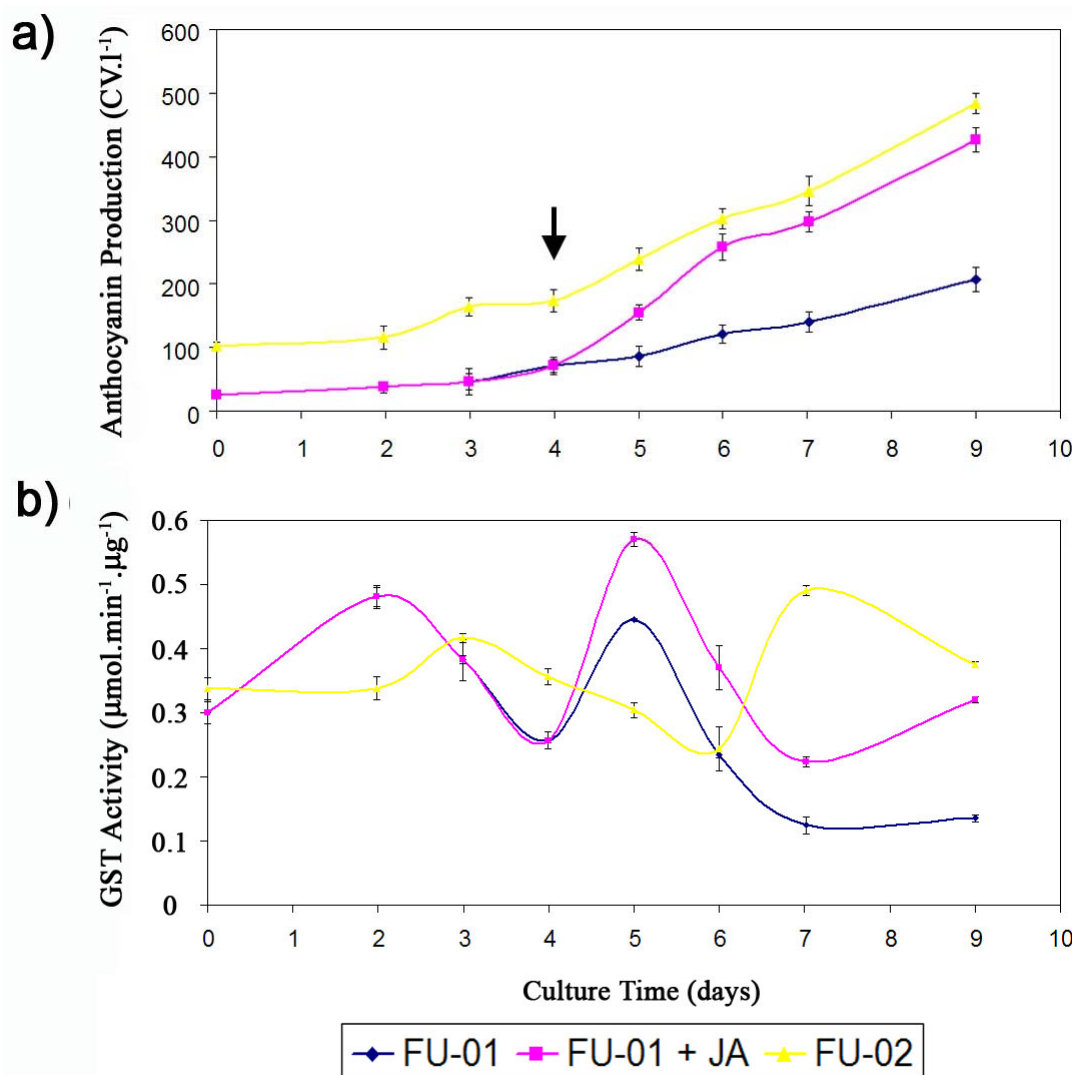


Figure 4.2: a) Anthocyanin production and b) specific GST activity detected in protein extracts from *V. vinifera* suspension cells FU-01, FU-01 with 10 μM JA treatment on day 4 (black arrow) and FU-02 during the 9-day culture period. $n=3$. Mean \pm Std Dev.

The cell line chosen for GST purification was FU-01 due to its anthocyanin production and biomass yield stability in culture, with day 5.5 chosen as the sampling point. This time-period from day 5 to 6 saw the highest rate of anthocyanin accumulation ($35.8 \text{ CV.l}^{-1}.\text{day}^{-1}$; Figure 4.2a) and GST activity was greater than half its maximum (Figure 4.2b). Treatment of FU-01 with jasmonic acid saw a 2-fold increase in anthocyanin production of cells (Fig. 4.2a) and a 1.5-fold increase in GST activity by day 5.5 (Fig. 4.2b). This co-responsiveness indicates a potential role for GSTs in anthocyanin accumulation.

4.2.2.2 Glutathione (GSH) affinity chromatography

Whole-cell protein was extracted from FU-01 cells at day 5.5; buffer-exchanged into phosphate buffered saline (PBS) by ammonium sulphate precipitation and underwent GSH-affinity chromatography to identify GSH-binding proteins as per Mozer *et al.* (1983) and Deng and Hatzios (2002b). Plants contain various categories of glutathione-binding proteins, including glutathione lyases, peroxidases, reductases and transferases (Marrs *et al.*, 1995). The GSTs are unique in this group as they are all soluble or loosely membrane-associated dimers with a monomeric size of 15-28 kDa and together comprise 1-3.5% of total cellular protein (Droog *et al.*, 1995; Pairoba and Walbot, 2003). The GST assay was used to monitor purification as it is a specific measure of the activity of GSTs, that is unaffected by the other proteins (Marrs, 1996). Table 4.1 outlines the purification process quantified by GST activity.

Table 4.1: Purification table for GSTs from *V. vinifera* FU-01 suspension cells. GST Activity in Units: $\mu\text{mol}\cdot\text{min}^{-1}\cdot\mu\text{g}^{-1}$ protein.

Sample	Protein Mass (mg)	GST Activity (Units)	Purification (-fold)	Total GST Activity ($\mu\text{mol}\cdot\text{min}^{-1}$)
Crude Extract	40.2	0.083	1	3,350
Ammonium Sulphate Precipitation				
Pellet	32.2	0.101	1.22	3,250
Supernatant	7.8	0.006	0.072	46
Glutathione Affinity Column Purification				
Bound Fractions	0.978	3.713	44.7	3,631
Flow-through	30.9	0.0004	0.005	12

Ammonium sulphate precipitation enabled protein concentration and buffer exchange to remove contaminating buffers and salts (including intracellular glutathione), capable of interfering with the binding to the column. While a 20% reduction in total protein mass was seen, there was <1.5% loss of total GST activity (Table 4.1; Crude extract vs. Pellet). This is in agreement with protocols for GST purification from corn (Mozer *et al.*, 1983), and rice (Deng and Hatzios, 2002a). Furthermore, total activity was consistently higher in the bound fractions (5-13.5%), suggesting some interfering or inhibitory substance effecting the GSTs in the crude and ammonium sulphate extracts (Table 4.1).

Recirculating the crude protein extract through the column overnight at 4°C removed >99% of GST activity (bound fractions vs. flowthrough) and, compared with a single chromatographic pass, greatly improved GST protein binding to the column (data not shown). The column was washed with binding

buffer to remove non-specifically bound proteins and then eluted with a 10-fold excess (10mM) of GSH. When separated by SDS-PAGE, the predominant eluates contained proteins that ranged between 21-26 kDa (Fig. 4.3a), with minor bands seen at 47 kDa and 60 kDa. The presence of these smaller proteins corresponded with the profile of GST activity (Fig. 4.3b).

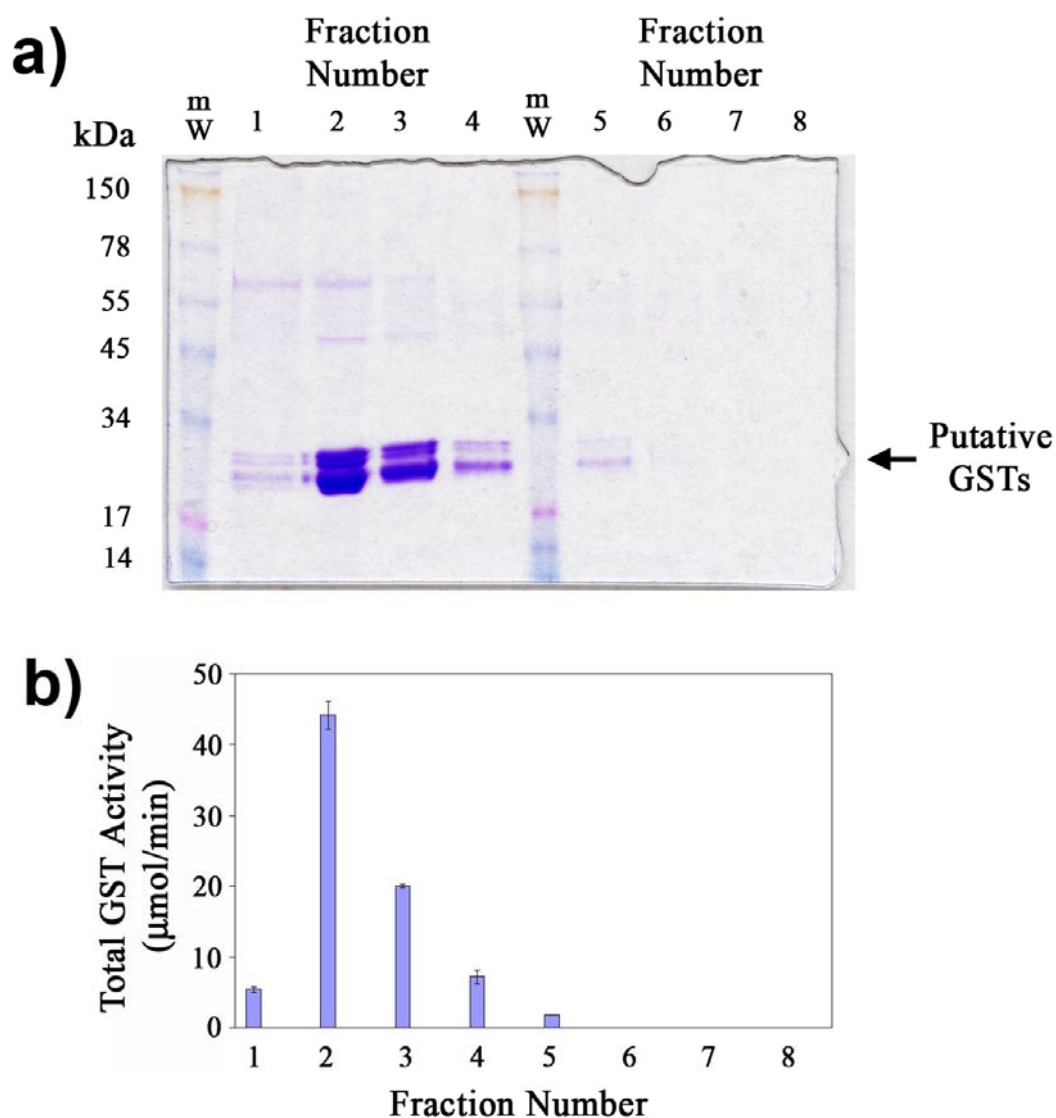


Figure 4.3: GST purification from *V. vinifera* FU-01 suspension cells. (a) Coomassie-stained, 10% SDS-PAGE of fractions collected from GSH-affinity column and (b) their corresponding total GST activity from 2.5% of total elution volume (n=3).

GSTs were estimated to comprise >95% of protein in the bound fractions from the 1D-gel, indicating the proportion of GSTs in the protein extract from *V. vinifera* cell cultures to be 2.3%, similar to previous observations (Droog *et al.*, 1997; Pairoba and Walbot, 2003). Increasing the concentration of Triton X-100 (0.25-2.0% (v/v) in the extraction buffer did not alter GST activity or yield any additional GSTs on 1D or 2D-SDS PAGE indicating 0.25% is sufficient to sequester any GSTs that may be loosely membrane-associated (data not shown).

4.2.2.3 Two-dimensional gel electrophoresis of purified GSTs

Large-format (18 cm x 20 cm gel), two-dimensional SDS-PAGE was used to separate the protein species with near-identical molecular weight. Column fractions possessing GST activity (Fig. 4.3, Fractions 1-5) were pooled and separated by 2D SDS-PAGE (Fig. 4.4). Protein spots were excised from a Sypro Ruby-stained 2D-gel and underwent trypsin digestion and nanoLC-MS/MS analysis of peptide fragments. The predicted amino acid composition of these fragments was determined and these sequences were aligned with SWISSProt/EMBL protein databases (Appendix 4).

This analysis initially enabled categorisation of spots into protein groups, based on their identical fingerprints. The large change in pI (~0.5 pI unit per modification) and minimal alteration in mass between spots within the same group indicates chemical modification. As no GST has been reported to be phosphorylated, this may represent carbamylation of lysine residues, a common artefact in 2-D separation procedures (McCarthy *et al.*, 2003).

Each protein possessed 3 or more peptide fragments with identity to known and predicted GSTs from various plant species (Appendix 4). This

approach was validated by one of the purified GSTs having high identity with Q84N22 an expressed sequence tag (EST) from grape, predicted as a GST. This EST was isolated from *Botrytis cinerea*-infected grapevines by differential display and in the degenerate cloning procedure in this study (Section 4.2.1), with no identification of the protein (Atanassova, Pers. Comm.).

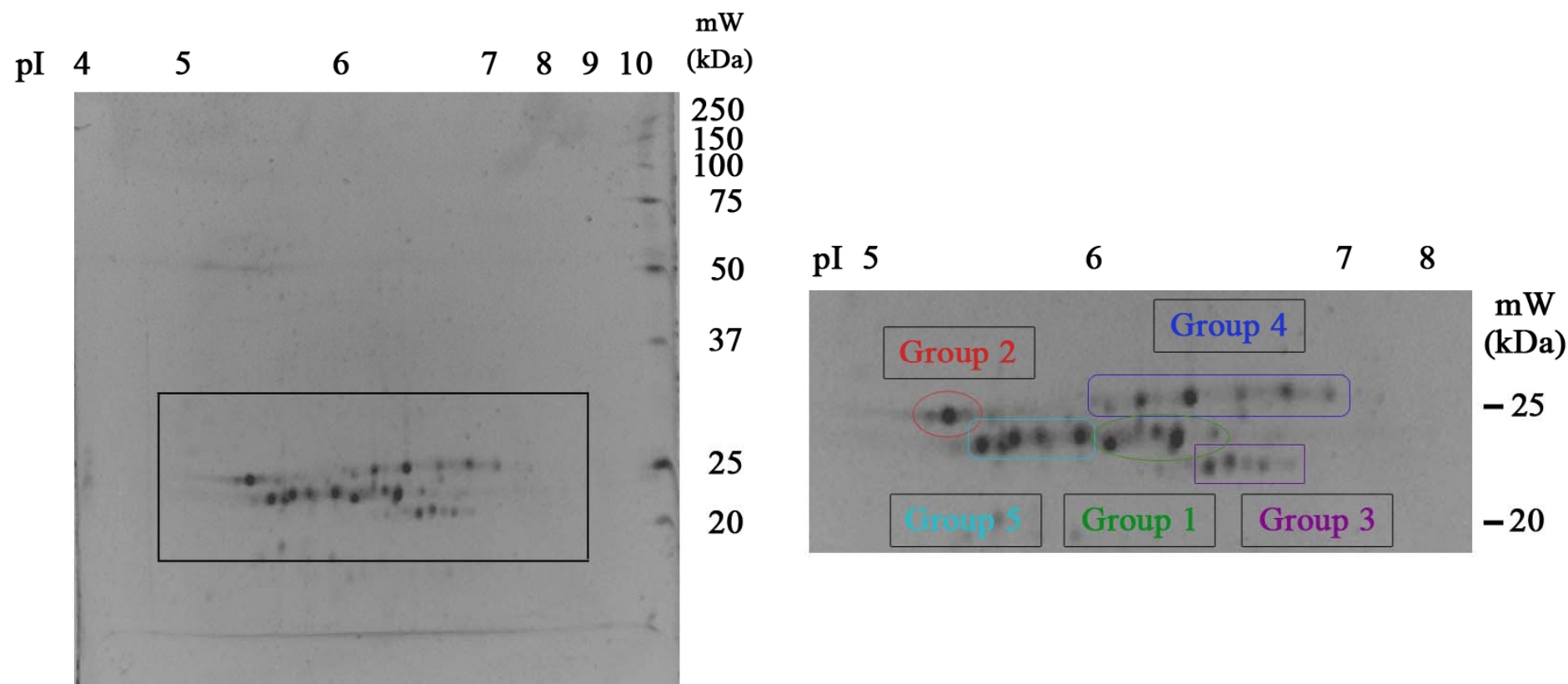


Figure 4.4: Two-dimensional gel electropherogram of solubilised fractions from GSH-affinity chromatography possessing GST activity. Enlarged image showing grouping based on MS fingerprints.

Numerous grapevine ESTs with similarity to plant GSTs are available on the TIGR website (www.tigr.org). Therefore, isolation of the appropriate sequences required some additional protein sequence information to support the predicted peptide sequences from the mass spectroscopy data.

4.2.2.4 Edman sequencing

Edman (N-terminal) protein sequencing was undertaken on proteins separated by both large format, gradient 1D and 2D SDS-PAGE (4-20% Acrylamide). While bands were not sufficiently discriminated under 1D-GE, 2D-GE separation yielded two proteins corresponding to groups 1 (Spot #2) and 5 (Spot #1) from Fig. 4.4 that were not N-terminally blocked (Fig. 4.5; despite the precautionary use of thioglycolic acid throughout the procedure). These two sequences are shown below, where X is an indiscernible residue:

Spot #1: X-X-M-K-V-Y-G-X

Spot #2: X-X-L-V-X-G-P-D-F-A-G-X-X-X-E-L-X

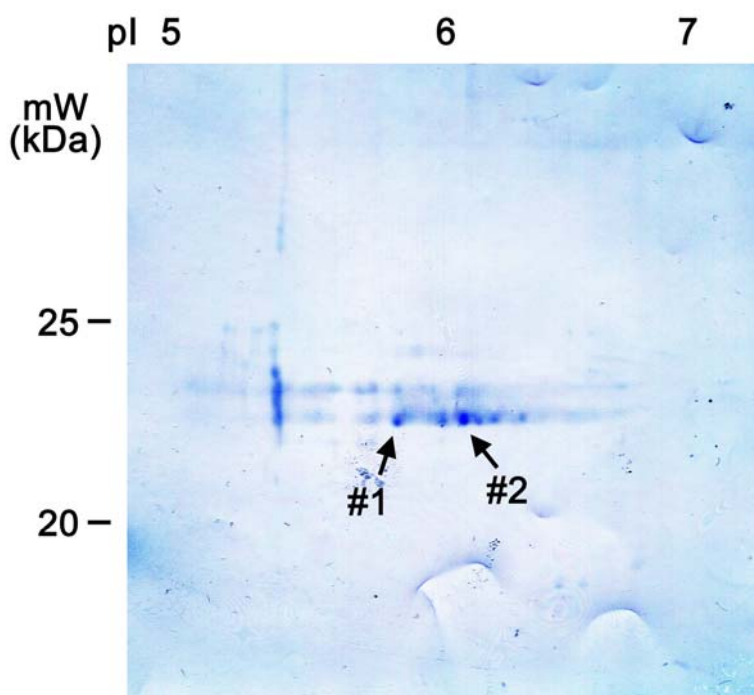


Figure 4.5: Coomassie-stained, nitrocellulose membrane. Western transfer of GSTs separated by 2D-gel electrophoresis. Spots picked for Edman sequencing indicated with arrows.

4.2.3 Selection of GST expressed sequence tags

The N-terminal sequences did not enable robust degenerate PCR primer design, yet was crucial in the cloning process. Alignment of the mass spectroscopy peptide fingerprints not only inferred these proteins as GSTs, but the use of those predicted peptide sequences assisted in the identification of possible coding ESTs. The predicted peptide fingerprint sequences from the mass spectroscopy analysis were aligned with published sequences in SWISS/PROT, not the *V. vinifera* EST database, thereby complicating the identification of the correct coding sequence. As a result, a combined visual search and BLASTp alignment targeting short highly conserved regions was performed. A few fragments were found in the ESTs from *V. vinifera*, often with rearrangements of the amino acid order (Table 4.2). This enabled the identification of 3 putative ESTs, each containing at least 2 matching mini-sequences. The sequences obtained from Edman analysis further confirmed the identity of the ESTs with only a single matching peptide (Table 4.2).

Table 4.2: Summary of predicted peptide fingerprint sequences with known ESTs from databases (see Fig.4.4 for grouping).

Contig Name	Accession Number(s)	Corresponding Group	Matching Peptides
GST1	AY156048	Group 4	LLPADPYER, VFEEIGER
GST2	TC44916, TC14045, TC25424 AY156049	Group 3	VLDVYEAR, AITAYIAEK, RLALYEK
GST3	¹ NP864089 AY156050	Group 1	*VXGPDFA
GST4	TC39256 AY971515	Group 5	*MKVYG
Q84N22	AF501625	Group 2	LYELGR, SPLLEMNPVHK, LGEZPYFGGEK

¹ Full-length sequence obtained by RACE-PCR from this partial sequence

* Sequences obtained from Edman sequencing

From the Edman sequence for spot #2 there were residues that did not match the translated EST sequence. These residue differences can be explained by the mis-identification of chemically similar amino acids by the approach utilised. The underlined lysine (L) and glycine (G) residues from Edman sequencing were represented by leucine (K) and serine (S) residues in the translated EST. These residues differ by only a single amine and hydroxymethyl moiety, respectively, confounding their discrimination.

4.2.3.1 Cloning of GST ESTs

Once contigs were generated, primers were designed to clone the full-length ESTs with unique restriction site overhangs (*Bam*HI, *Sal*I, or *Pst*I) to enable in-frame insertion into both the HIS-fusion vector for recombinant expression (pQE9) and the maize expression vector (pJD288, Figure 4.6). The GSTs were amplified from FU-01 *V. vinifera* suspension cell cDNA. GST1, GST2, GST3 and GST4 all produced single PCR products of the predicted size, while Q84N22 yielded two PCR products (data not shown). The shorter PCR product possessed 99% identity with the published Q84N22 sequence, with the sequence differences summarised in Appendix 5. Of note is a frameshift mutation common in all three sequenced clones (AAA, instead of AAAA), altering the predicted protein size for the Q84N22 EST of 15.7 kDa, to a predicted mW of 25.5kDa. The second (80bp larger product) was shown to have regions of high similarity to Q84N22, but possessed numerous stop codons in all 6 frames throughout the sequence.

GSTs were gel purified and cloned into pGEM-T, with at least two vectors sequenced in the forward and reverse directions. All inserts were shown to be functional coding sequences, proving the validity of the contig generation. Base

pair differences were witnessed when compared with the published sequence for all GSTs (Appendix 5). In these cases an additional positive colony was chosen and sequenced to resolve the difference. Purified vectors were digested with appropriate restriction endonucleases to liberate the insert, gel purified and cloned into pJD288 and pQE9.

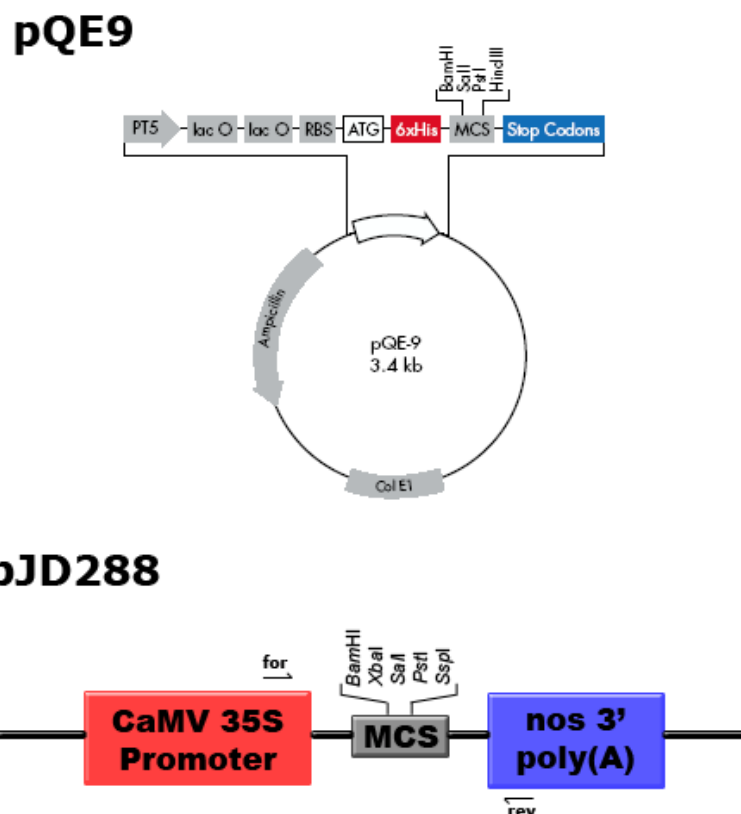


Figure 4.6: Vectors used in this study: pQE9 (HIS-fusion vector) and pJD288 (maize expression vector, in pUC18 backbone). Forward and reverse sequencing primers shown for pJD288 vector. pQE9 map reproduced from Qiagen Expressionist™ booklet.

4.2.3.2 Cloning of GST genomic sequences

As mentioned in Section 1.5.1.2, obtaining the genomic sequence of GSTs is useful for their categorisation and to further infer their functionality within the

plant (Dixon *et al.*, 2002). Genomic DNA was purified from FU-01 cells and GST sequences amplified using the same primers used for EST cloning. Multiple products were produced for each primer pair, with all products cloned and sequenced. Both *GST1* and *Q84N22* possessed a single intron; *GST2* and *GST3* possessed 2 introns with the classical intron/exon junctions, while *GST4* did not possess any introns. The exon sequences were identical to the mature ESTs cloned in this study by PCR (Figs. 4.7-11).

```

1 ATGGCAAACAGTGACCACATAGTTCTTTTAGATTACTCCGCAAGCCCTTTTGCATGAGG
  M A N S D H I V L L D Y S A S P F A M R
61 GTGCGACTGGCTTTGGCAGCCAAGGGGATCGAGTATCTGATTAAGGAAGAAGACTTGACC
  V R L A L A A K G I E Y L I K E E D L T
121 CAAAGTAAAAGCTCTCTACTCTTGAAAGTGAATCCAGTTCATCAGAAAATTCCAGTTCTA
  Q S K S S L L L K V N P V H Q K I P V L
181 ATTCACAATGGGAAGCCCGTATGCGAGTCCTTGATAATAGTGAATACATTGATGAGGTT
  I H N G K P V C E S L I I V E Y I D E V
241 TGGAAGGATAGATGTCGTCTTCTGCCGGCTGACCCTTACCAAAGAGCAAAAGCCAAGTTC
  W K D R C R L L P A D P Y Q R A K A K F
301 TGGGCCGACTTCATTGACAAAATGgtgcttagttaattaactcatttctccttttctccc
  W A D F I D K M
361 cccttcatttttcttaatttccatcagactacttgtttcttgaactactttggatgtgt
421 aattacattaattttttattgtgattcagGTATACCCATCCTGTTATAACGTGTGGGCAG
  V Y P S C Y N V W A A
481 CAAACGGAGAAGTGCAAGAGGCTGGCAAGAAGGAATTCATAGACAGGATTAAGATGTTAG
  N G E V Q E A G K K E F I D R I K M L E
541 AAGGAGAGCTTAAGTCGAACCCTTACTTTGGGGGTGAGACTTTGGGTTTTCTGGACATTG
  G E L K S N P Y F G G E T L G F L D I V
601 TTTTCTCCCATCGTACTACTGGTTCATACATTTCGAACTTTTGGGAAGTTCAGCATAG
  F L P S Y Y W F H T F E T F G K F S I E
661 AAGCGGAGTGTCCAAAGCTGGTGGCATGGGGTAAGAGGTGCATGGAGGAGGAGTTCGTGT
  A E C P K L V A W G K R C M E E E F V Y
721 ACACCTCTCTCCCTCACCCACATAAGGTCTATGACTTGGTGGTGGATTACAGGAAGAAAA
  T S L P H P H K V Y D L V V D Y R K K M
781 TGGGGATATAGCCTTGTTGTGATGTAATTGGACACCTTTGAAGATTTGTCTTCTGTTTT
  G I *
841 GTTTAATTAATAAGGGATATTATTGCGGTTGTTTGAAGTACTTGTGTCAAGAATCAATAA
901 TAAATTACAGTACTTTTTGATGGGACTAAAAAAA

```

Figure 4.7: GST1 sequence. Translation shown below coding sequence, with numbering representing genomic sequence. Intron sequence written in lowercase, polyA tail written in blue. Real-time PCR primer-binding sites are underlined. Stop codon indicated by asterisk.

1 ATGGCGGTCTTGAAAGTCCACGGTAGCCCGATCTCCACGGCAGTGATGCGAGTTGTCGCT
 M A V L K V H G S P I S T A V M R V V A
 61 GCGCTCTACGAGAAGGGGCTTGAGTTCGAGTTCGTTACGATTGACATGAAGCCGGCCAG
 A L Y E K G L E F E F V T I D M K A G Q
 121 CACAAATCGGAGGCTTTTCCTTGCTCTCAATgtaagttgaatcgattctcccgtgatcgg
 H K S E A F L A L N
 181 gggaaactttttgctaagtgtttgttgaaggtttttttgtgaatggtgtgtggccagag
 241 cgaattcttcgcttttcgttgaccgatgagtgagtgggtttgtgagatagagtcttcca
 301 tgtgatggtttgagatctgattagtaggaagcgacgagtcacagttcgtacagttgccc
 361 tgagttcatttatcattgattaatttgtttaactgttgctttttaatccgaaaggcccaa
 421 attgccctctccatatggctaacgaacatcttttcaacatggctagtaatgacttttgtt
 481 cacgattaaaaccctcaactaaattctttttcattaagacgtgaatgatgtcaatgataa
 541 aattcgatttgcggaatgatgcagCCATTTGGTCAAGTTCAGCCTTTGAAGACGGAGAC
 P F G Q V P A F E D G D
 601 CTGAAGCTCTTCGgtaaagtctcctcaccaattaccattcttgttttctgaaaaagaaaa
 L K L F E
 661 ttgtaatcgaagcaaaatagtaaaataaagaaaaacgaaatattccaacggtttgacttt
 721 tggagtatgcagAATCAAGGGCCATCACACAATACATCGCCACGAGTACGCGTCAAACG
 S R A I T Q Y I A H E Y A S N G
 781 GGA^{CTCAACTGATATGCCAGATTCAAAGAAAATGGCTATCATGT}CAGTGTGGATAGAGG
 T Q L I C P D S K K M A I M S V W I E V
 841 TGGAGGCCACCAGTACGACCCCATGCCGGCAAGCTCGGTTACGAGCTATTTTACAAGC
 E A H Q Y D P H A G K L G Y E L F Y K P
 901 CAATGTTTCGGCCAGACCACTGACCCAGCTGCAGTGGAGGACCTAGAGGCCAAACTCGGCA
 M F G Q T T D P A A V E D L E A K L G K
 961 AGGTTTGGATGTGTACGAGGCTCGGTTGACTCAGTCCAAGTACTTGGGCGGAGACTGCT
 V L D V Y E A R L T Q S K Y L G G D C F
 1021 TTGGGCTGGCCGACCTTCACCACCTCCCCACCCTACACTACTTGTGGGCAGTTCAGCCA
 G L A D L H H L P T L H Y L L G S S A K
 1081 AGAAGCTCTTTGACTCGCGTCCACACGTGTCCGCTTGGGTCGCTGATATCACTGCCAGGC
 K L F D S R P H V S A W V A D I T A R P
 1141 CTGCTTGGGCCAAGGTGATTGCCATGCAGAAGAGTTAAGAGAAAAAAAAAAGTTGTGTGGC
 A W A K V I A M Q K S *
 1201 TTTGCCCTTGAGTTTCTATGTGGGTGTATGTTTCTAAAATCACTATCAAATATTAGAATG
 1261 TATTTTCAGAGTGATATAGTGTAGTTCATAATGATAATATAAAGCGTTTCTACCAAAAAA

Figure 4.8: GST2 sequence. Translation shown below coding sequence, with numbering representing genomic sequence. Intron sequence written in lowercase, polyA tail written in blue. Real-time PCR primer-binding sites are underlined. Stop codon indicated by asterisk.

1 ATGGTGGTGAAGGTGTATGGCCCAGATTTTGCTTCTGCAAAGCGCGTGCTTGTTTTGCCTC
 M V V K V Y G P D F A S A K R V L V C L
 61 ATTGAGAAGGAGGTCTGAATTCGAGACTCTCCCCATTGATATCATCAAAGGACAGAATAAG
 I E K E V E F E T L P I D I I K G Q N K
 121 GATCCAGAATTCCTGAAGTTGCAGgttctaatttcttcttctgtcgtttaagctttgtttt
 D P E F L K L Q
 181 gagctcaggaacaacataagaaacgagacgatttctgatttggtggttagtgaaaaagct
 241 gatgatttcgaaaagcttttaagtagaaataagatcaacagagaaggaattgatggagtt
 301 caaactcgaacttcattaaatttctttcatttttttttttttgcagcagttggtgagagc
 361 cgaacaaaaggcttaatgattgaagtatcacaatttcttgatttggtgtacatattggtga
 421 taatttatgcttctttctctcatcaaatgcagCCTTTTGGAGTTGTTCTGTCATTCAAG
 P F G V V P V I Q D
 481 ATGGAGACTATACCTTATTTGgtaattatcagtgatctcacttctaataaatttctatca
 G D Y T L F E
 541 cagaatttctatagtagtgttccatatacagaaatgcctttcttataaagacaacatttc
 601 cacttaaggaatagaatgctctttttcactctttaagtgatttatgatgtggttagtctca
 661 aagttgatcttttcagtaaagcttagaaccatgaattgctgaaaacaatttatttgtt
 721 ttaccaaacaggccctttgggttcttgatgaatgagtatgatttggatttcagAATCTCG
 S R
 781 TGCAATCATGAGGTACTATGCTGAGAAGTACAAGTCTCAAGGAAGTACTGAGGGGAA
 A I M R Y Y A E K Y K S Q G T D L L G K
 841 GACAATAGAGGAGAGGGGAGTGGTGGAAACAATGGCTGGAGGTTGAAGCACAAAGTTACCA
 T I E E R G V V E Q W L E V E A Q S Y H
 901 CCCAGCAATTGACAATTTAGTCATTGAAATTCTGTTTGGCCGCAAACGGGGTATTCCCCC
 P A I D N L V I E I L F G R K R G I P P
 961 AGATGCGAAAAGTGATCGAAGAGAGTGAAAAGAAGCTTGCAAAGGTGTTGGACATCTATGA
 D A K V I E E S E K K L A K V L D I Y E
 1021 AGAGAGGCTGTCCAAGAGCAAGTACCTGGCTGGGGATTTCTTTAGCCTTGCTGATCTTAG
 E R L S K S K Y L A G D F F S L A D L S
 1081 CCACCTTCCATTACAAAAGTACTTGGCTGATATGGGGAAGATGTATTTGATTGAGGAGAG
 H L P F T K Y L A D M G K M Y L I E E R
 1141 GAAACACGTGAAGGCATGGTGGGATGATATCAGTAATAGACCATCCTGGAAGAAGGTCTT
 K H V K A W W D D I S N R P S W K K V F
 1201 CAGCTCTAGATGGCCCTCTTGAGTGATTCAATTCCTTGTAGATTAGGAAAATCATGG
 S S R W P L L E *
 1261 ATTAATAATATCCTTCACTGGATTAGGCAATGTCCTACATGTTTTGGCTGATGTAATTTCT
 1321 CTGTCTTGGTTATGTATCTTAGAATAATGTCCTGTGTGTTCTGACCGATGTATTTTCTGT
 1381 TCTGTCTTAGTGTATAATTATCTTTATGATCGGCCAAGTTCTACAATAAAATTGATTTAA
 1441 ATGCCAAAAAAAAA

Figure 4.9: GST3 sequence. Translation shown below coding sequence, with numbering representing genomic sequence. Intron sequence written in lowercase, polyA tail written in blue. Real-time PCR primer-binding sites are underlined. Stop codon indicated by asterisk.


```

1 ATGGTGATGAAGGTGTATGGCCCAGTGAGGGCTGCATGCCACAGAGGGTGTGGCTTGC
  M V M K V Y G P V R A A C P Q R V L A C
61 CTTGTAGAGAAGGGCGTGGAGTTTGGAGTTGTCCATGTGACCTCGACTCTGGCGAGCAA
  L V E K G V E F E V V H V D L D S G E Q
121 AAACGGCCTGATTTCCCTTCGACAGCCTTTTGGGCAAGTCCAGTGGTAGAAGATGGC
  K R P D F L L R Q P F G Q V P V V E D G
181 GATTTCAGGCTGTTTGTGATCGAGGGCGATTGTGAGGTACATCGCGCCAAGTACGCGGAG
  D F R L F E S R A I V R Y I A A K Y A E
241 CAAGGGCCTGACCTCTTGGGAAAAAGCTTGGAGGAGAAAGCGGTAGTTGATCAATGGCTG
  Q G P D L L G K S L E E K A V V D Q W L
301 GAAGTGGAAGCTCACAACTTCAACGAGTTGGTGTACACACTGGTCATGCAGCTAGTGATC
  E V E A H N F N E L V Y T L V M Q L V I
361 CTACCTCGAATGGGTGAGCGGGGGGACTTGGCTTTAGCCACACTTGTGAGCAGAAGCTG
  L P R M G E R G D L A L A H T C E Q K L
421 GAAAAGGTGTTTGTATGTATGAGCAGAGGCTGTCTGAAGAGCCGGTACCTTGCAGGAGAT
  E K V F D V Y E Q R L S K S R Y L A G D
481 TCATTCACTCTCGCTGATCTGAGTCATCTTCCGGCCATCAGATACTTGGTGAAGGAAGCT
  S F T L A D L S H L P A I R Y L V K E A
541 GGAATGGCGCACTTGGTTACTGAGAGGAAGAGTGTGAGTGCATGGTGGGAGGACATTTCC
  G M A H L V T E R K S V S A W W E D I S
601 AACAGGGCTGCTTGGAAAAAAGTCATGGAGCTCGCTGCTTGATATATGTTGTTAATTTCC
  N R A A W K K V M E L A A *
661 CTACGTGGCCATGTATGCACCTTTCCAATTATCTTCTGCTGTACTCGTTGGTTTGT
721 TGGTTGGTTGGCTTGTGGCTTGTGGTATGTTATTAACCTTATTAAGGAAAAATCATC
781 TACCCTTGATAATATTTTCCATGAC

```

Figure 4.10: GST4 sequence. Translation shown below coding sequence, with numbering representing genomic sequence. polyA tail written in blue. Real-time PCR primer-binding sites are underlined. Stop codon indicated by asterisk.

```

1  ATGGCAGACGAGATTATCTTGTGGATTTCTGGCCTAGCATGTTTGGTATGAGGGTCAGA
   M A D E I I L L D F W P S M F G M R V R
61  CTTGCCCTGGCAGAGAAGGGTCTCAAGTATGAATATAGAGAGGAGGACCTGTGGAACAAG
   L A L A E K G L K Y E Y R E E D L W N K
121 AGCCCTTTGCTTCTTGAGATGAACCCAGTTCATAAGAAAATCCCAGTTCGATCCACAAT
   S P L L L E M N P V H K K I P V L I H N
181 GGAAAGCCCATTTGTGAGTCTCTGATAATAGTTCAGTATATTGATGAGGTTTGGTGCAT
   G K P I C E S L I I V Q Y I D E V W C D
241 AAATCTCCGCTTTTGCCTAGTGACCCATACCAGAGAGCTCAGGCCAGGTTCTGGGCGGAC
   K S P L L P S D P Y Q R A Q A R F W A D
301 TACATAGACAAGAAGgtatgcctttgctggtgatttaagcattctttccatttattca
   Y I D K K
361 tggcgattgactcagatthtgattatggtgagggagttgtccaaaatgctgggtttcttc
421 acacgttcccttctgctattgagthtggtgggctttggggttccaaactagaacttttac
481 tgattctccttctgctthgttcaacaggactctactctgcatttctgatatgggtttaa
541 tttctttgttatgthgaatacgaattctgttcgthccatcaggaaaaacagatctcaaga
601 ataccttttttccccaagcaaggcgaatacataaatttctttgactttattgthttccac
661 agCTCTATGAACTTGAAGGAAGATATGGTCAACCAAAGGAGAAGAGCAGGAAACAGCCA
   L Y E L G R K I W S T K G E E Q E T A K
721 AGAAGGAATTCATAGAGTGCCTTAAGCTTTTGAAGGAGAGCTTGGAGAGAAGCCTTACT
   K E F I E C L K L L E G E L G E K P Y F
781 TCGGTGGTGAAAAAATGGGTTTGTAGATGTGGCTCTGGTGACCTTCTCTTGCTGGTTTT
   G G E K I G F V D V A L V T F S C W F Y
841 ATGCATACGAGACCTTTGGCAACTTCAGCATAGAGGCGGAGTGCCCCAAGTTGATCGCTT
   A Y E T F G N F S I E A E C P K L I A W
901 GGACCAAGAGGTGCATGGAAAAGGAGAGCGTGTCTGCTCTCTGGAAGACCCACACAAGG
   T K R C M E K E S V S S S L E D P H K V
961 TCCATGGCTTTATCATGGGGATGAGAAAGAGTTTGGTATAGAGTAGAAGGGGAACATCA
   H G F I M G M R K R F G I E *
1021 TGTGTGGGGTCTTCCCATCGAAGACCCACAGAAGGTCCATGGCTTTGTCTTGTGGATCA
1081 GAAAGAAGTTTCGTGTAGAATAAAAGGGCTTTTGAATCGTGTTCATTGGTAATATGAGA
1141 GGAGTGTGTGCTTTAAGTATGCTTTGAAAATGTATCGTTAATATTTCCGTTTTAAATCCC
1201 TTCCTGAGGGCTGGAAAGACATGTTTCCAATTTGTTTTCTTTTGTGTTTGGACTAGAGACG
1261 TGTTTC

```

Figure 4.11: Q84N22 sequence. Translation shown below coding sequence, with numbering representing genomic sequence. Intron sequence written in lowercase, polyA tail written in blue. Real-time PCR primer-binding sites are underlined. Stop codon indicated by asterisk.

These sequences were inputted into the ExPASy protein analysis tools, with results summarised in Table 4.3. The frameshift mutation for Q84N22 was seen in both the EST and genomic sequences and altered the predicted protein size from 15.7 kDa to 25.5 kDa, matching the 2D SDS-PAGE results. While the predicted molecular weights of the proteins matched the observed pattern on the 2D-gel – decreasing size: GST1, Q84N22, GST3, GST4, GST2 - discrepancies were noted with regards to predicted pI. The more acidic Q84N22 (group 2) protein on the 2D-gel had a higher predicted pI than GST4 (group 5; Fig. 4.4; Table 4.3). This may be a possible result of differences in isoelectric weighting of residues by the program.

Table 4.3: Summary table for cloned GSTs and corresponding protein descriptives

Sequence	Intron # and Length (bp)	GST Type	Protein Length (aa)	Predicted Size (kDa)	Predicted pI
GST1	1: 125	III	221	25.6	6.32
GST2	2: 414, 119	I	214	23.7	6.13
GST3	2: 308, 272	I	215	25.0	5.79
GST4	0	I	212	24.2	5.62
Q84N22	1: 347	III	219	25.5	5.73

4.2.3.3 Analysis of non-coding sequences

Varying lengths of the 5' untranslated region of these *V. vinifera* GSTs were available on the TIGR database. These short regions were inputted into promoter analysis software to search for known motifs (Table 4.4). GST1 was the only sequence to possess the Myb and Myc consensus binding regions, present in

all maize anthocyanin biosynthetic genes and the Bz2 promoter region (Paz-Ares *et al.*, 1986; 1987; Ludwig *et al.*, 1989; Bodeau and Walbot, 1992, 1996). Furthermore, each GST possessed a putative 3' polyA tail, with numerous in-frame stop codons a 10-26% enrichment in A/T content compared with the coding region (Figs. 4.7-4.11).

Table 4.4: Summary table for upstream region of cloned GSTs with listing of detectable promoter motifs/elements from PLACE program (<http://www.dna.affrc.go.jp/PLACE/signalscan.html>; Prestridge, 1991; Higo *et al.*, 1999). Numbering from ATG start codon, +/- sense/antisense orientation. IUB mixed base codes R = AG, Y = CT N = AGCT. bHLH: basic helix-loop-helix.

Sequence	Length of 5' Region (bp)	Motifs
GST1	86	CAATBOX1 -5 (-) CAAT MybCORE/C1-bHLH -36 (-) CNGTTR -57 (+) Myc/R -36 (+) CANNTG -36 (-) Myb2 -36 (+) YAACKG MybPZM -56 (-) CCWACC
GST2	45	ARR1AT -11 (-) NGATT -39 (-) CAATBOX1 -12 (+) CAAT GATABOX -23 (-) GATA
GST3	0	
GST4	46	NODCON2GM -11 (-) CTCTT OSE2ROOTNODULE -11 (-) CTCTT CAATBOX1 -24 (-) CAAT TATABOX4 -30 (-) TATATAA ARR1AT -33 (+) NGATT
Q84N22	69	ARR1AT -15 (-) NGATT -24 (-) -30 (+) CAATBOX1 -16 (+) CAAT -28 (-) -43 (+) GATABOX -19 (-) GATA NODCON2GM -33 (-) CTCTT OSE2ROOTNODULE -33 (-) CTCTT

4.2.3.4 Categorisation of *V. vinifera* GST protein sequences

Alignment of these sequences with known Type I, II and III GSTs confirmed the correct categorisation of the *V. vinifera* GSTs based on genomic structure alone (Figure 4.12). Furthermore, the intronless GST4 was shown to align most strongly with type I GSTs. It is interesting that the Type I GST4 genomic sequence was intronless, but this has been seen before for numerous functional proteins, including GSTs (Lougarre *et al.*, 1999; Singh *et al.*, 2000; Akgul and Tu, 2004) and anthocyanin-related proteins (Chang *et al.*, 2005). As the genomic sequence was the same as the EST, it is unlikely to be due to an inability to clone the intron-containing sequence of a second copy of the gene elsewhere in the genome.

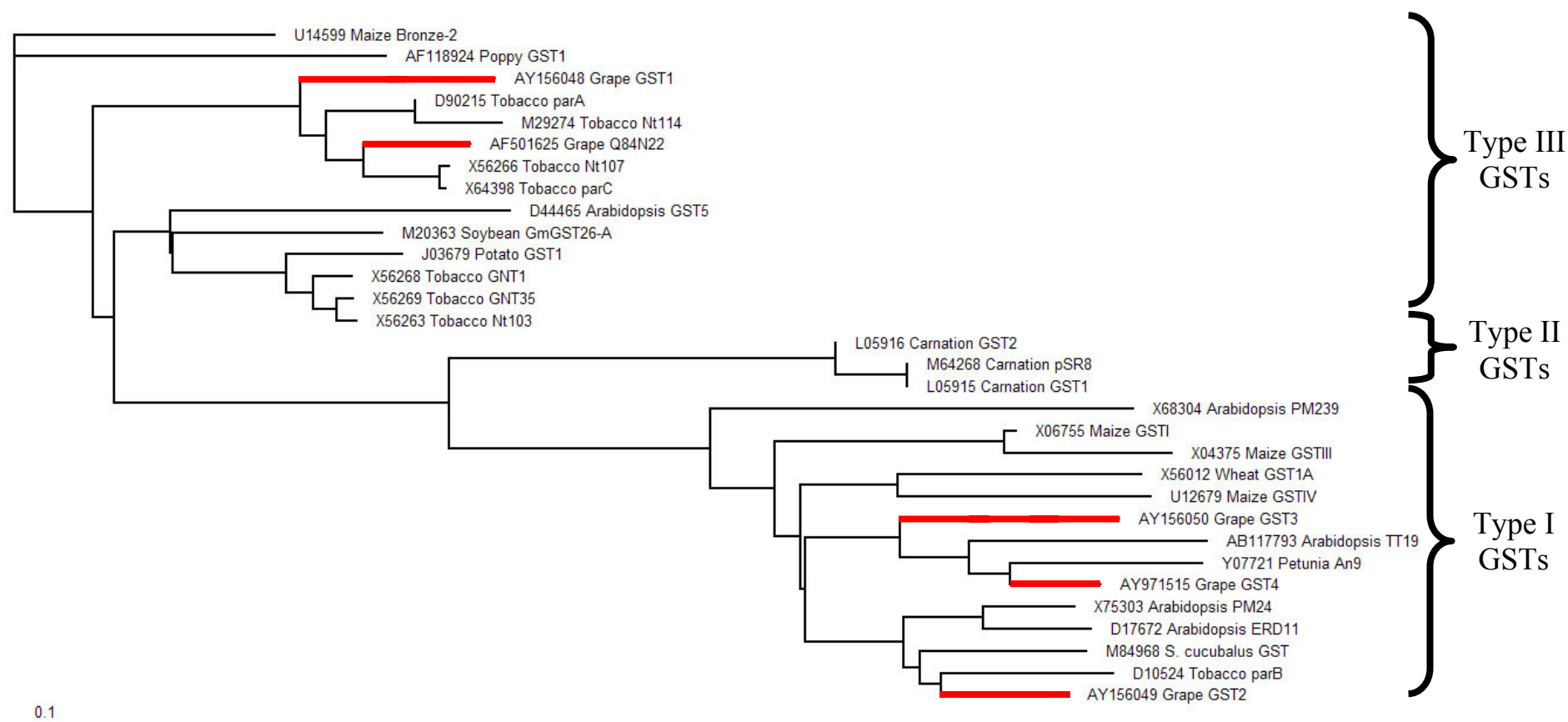


Figure 4.12: Phylogenetic tree of plant Type I, II and III GSTs. Tree was generated using the BioEdit sequence program. Sequences aligned are listed on the right-hand side and were obtained by retrieval of protein sequences from GenBank (Accession number, common species name, GST name). Grape GST sequences indicated with red line.

4.2.4 Recombinant Protein Expression

All 5 genes cloned encoded GST-like protein sequences as determined by rpsBLAST alignments, searching for conserved domains (Marchler-Bauer and Bryant, 2004). However, recombinant expression of these sequences was necessary for confirmation as functional GSTs.

4.2.4.1 Confirming size of protein

The 5 full-length GST coding sequences were cloned into pQE9, an N-terminal HIS-fusion vector, for expression in *E. coli*. Taking into account the 6 histidine residues at the N-terminus, all GSTs were of predicted size (Table 4.3, Fig. 4.13), substantiating the frameshift mutation for the cloned Q84N22 sequence. Furthermore, the larger Q84N22 sequence did not produce any detectable protein; a result of the early in-frame stop codons mentioned in Section 4.2.3.2 (data not shown).

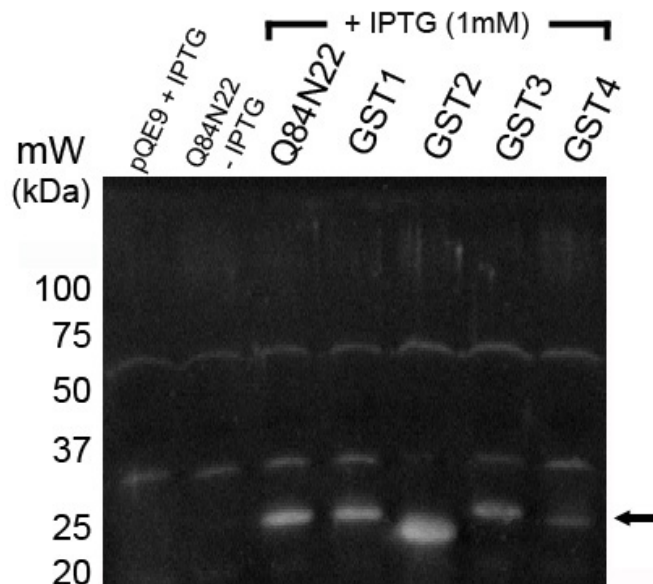


Figure 4.13: Western blot performed on crude protein extract from *E. coli* carrying vectors as indicated. pQE9: *E. coli* carrying pQE9 backbone only; Q84N22 – IPTG: *E. coli* carrying Q84N22:pQE9, not induced with IPTG. Arrow indicates HIS₆-fusion product.

4.2.4.2 GST activity of crude *E. coli* extracts

Compared to native protein from non IPTG-induced cultures carrying GST:pQE9, or IPTG-induced colonies carrying the pQE9 backbone only, GST activity was greatly enhanced in all of the clones deemed positive by Western blotting for each of the 5 GSTs (only the larger *Q84N22* product did not produce a detectable protein, or any enhanced GST activity). GST4 demonstrated the lowest activity with CDNB of all the GSTs cloned in this study. This is likely to be attributed to a reduced expression of GST4 (as can be seen in Fig. 4.13), rather than a decreased affinity to the model substrate seen with GSTs from other species (Marrs, 1996; Dixon *et al.*, 2002).

4.2.4.3 GST activity of purified protein

Highly expressing colonies of each GST were grown in larger cultures (500 ml) and 6-HIS fusion proteins purified by Ni-NTA chromatography. These were purified by stepwise imidazole gradients and the highly purified product (not purified to homogeneity; Fig. 4.14) assayed for GST activity. GST1, GST2, GST4 and *Q84N22* were found to elute at 375mM imidazole, while the majority of the GST3 protein eluted at 250mM imidazole, with some at 375mM. Results are presented here for GST1, but similar activities were seen for other GSTs, indicating GST4 did not have a decreased affinity to CDNB. All fractions were desalted and assayed for GST activity, with the 375mM imidazole fraction displaying the highest activity (Fig. 4.15). As expected, the GST activity for each purified GST was higher (80-110-fold) than for the crude IPTG-induced *E. coli* extract (Fig. 4.15).

Figure 4.14: SDS-PAGE of fractions eluted via Ni-NTA chromatography of cellular protein from IPTG-induced *E. coli* expressing GST1:pQE9. HIS₆:GS1 indicated by arrow. Imidazole conc. given in mM.

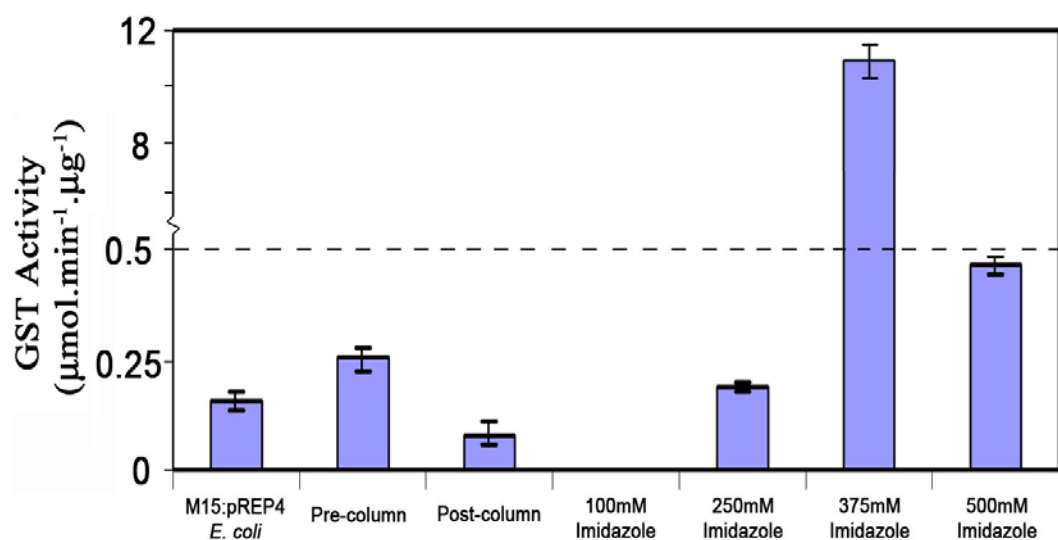
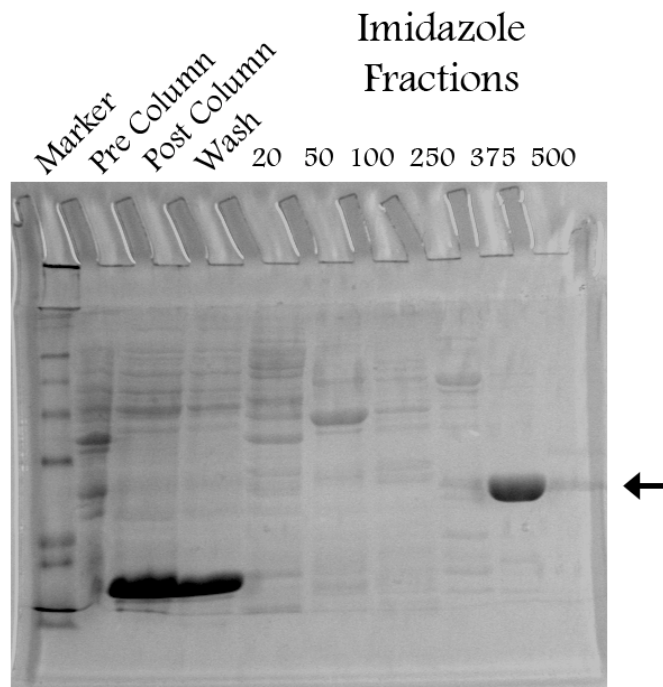


Figure 4.15: GST Activity of *E. coli* protein from HIS₆:GST1 procedure. M15:pREP4 *E. coli* refers to activity of IPTG-induced *E. coli*, carrying pQE9 backbone only.

The activity of this fraction was 3-fold higher than the combined activity for the GSTs purified from FU-01 *V. vinifera* cells (Table 4.1). While the contaminating *E. coli* proteins (<2.5% total protein by Coomassie blue staining;

Figure 4.14) may contribute to the GST activity, any contributory effect would be <2% of the total activity of the partially purified GST fraction (M15:pREP4 *E. coli* vs. 375mM imidazole; Fig. 4.15). This indicates the recombinant GST must be responsible for the majority of the detected activity.

4.3 Correlation of GST Expression with Anthocyanin

Accumulation

4.3.1 Translational Level

4.3.1.1 FU-03 (anthocyanin-deficient cell line)

GSTs were purified from non-pigmented (FU-03) cells and compared with GSTs from pigmented (FU-01) cells to determine whether a GST was deficient. Whole-cell GST activity was comparable between FU-01 and FU-03 samples, 0.083 and 0.075 Units, respectively. Total glutathione-binding proteins were separated by 2D-GE and gels were SYPRO Ruby-stained and imaged (Fig. 4.16). While there were quantitative differences in GSTs present between these cell lines, it was found that no GST was absent in non-pigmented cells compared with pigmented cells. This strategy did not implicate any particular GST in anthocyanin transport, and may be a result of the FU-03 line retaining a small amount of anthocyanin accumulation, thus requiring an active GST to be present. Therefore, another strategy was devised to correlate altered levels of GST expression with anthocyanin accumulation.

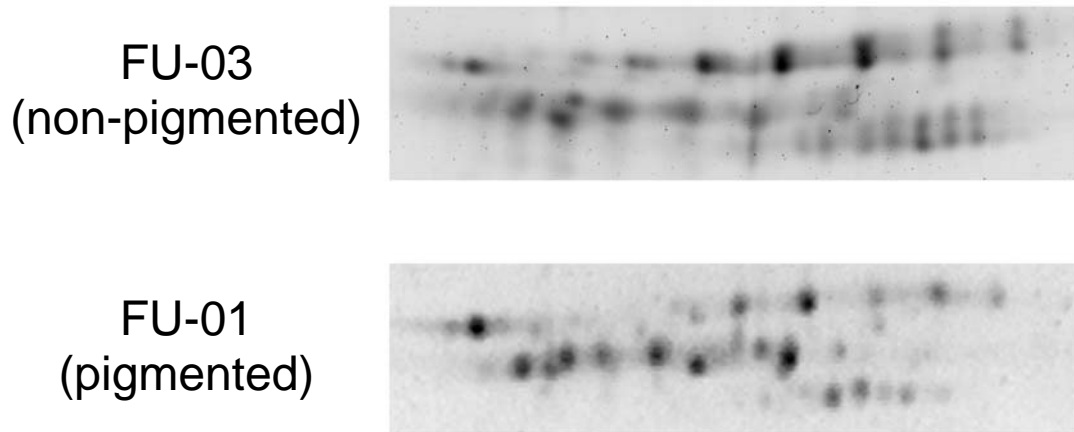


Figure 4.16: Sypro Ruby-stained 2D-gel of GSTs purified from FU-01 (lower) and FU-03 (upper) suspension cultures.

4.3.1.2 FU-01 treated with sucrose, jasmonic acid and light

Treatment of FU-01 cells with sucrose, jasmonic acid and culturing under light conditions (S+JA+L) lead to a 75% increase in total GST activity (0.145 Units) and a 110% increase in anthocyanin content at day 5.5. Total glutathione-binding proteins were purified from the same initial protein mass from matched FU-01 control and S+JA+L-elicited cells and separated by reverse-phase HPLC (Fig 4.17). Each peak on the chromatogram represents a protein and the peak area is a quantitative measure of protein concentration in the sample. A number of proteins were separated in both control and elicited cultures (Figure 4.17). Peaks were collected and separated by SDS-PAGE, with only peaks “C”, “G”, “I”, “J”, “K” corresponding to GSTs following silver-staining of SDS-PAGE separated fractions. Peak “C” showed the highest level of induction (3-fold over the respective baselines) of any of the 5 GSTs under elicitation conditions. While this does not confirm its involvement in transport, it demonstrated a link between GST inducibility and anthocyanin accumulation.

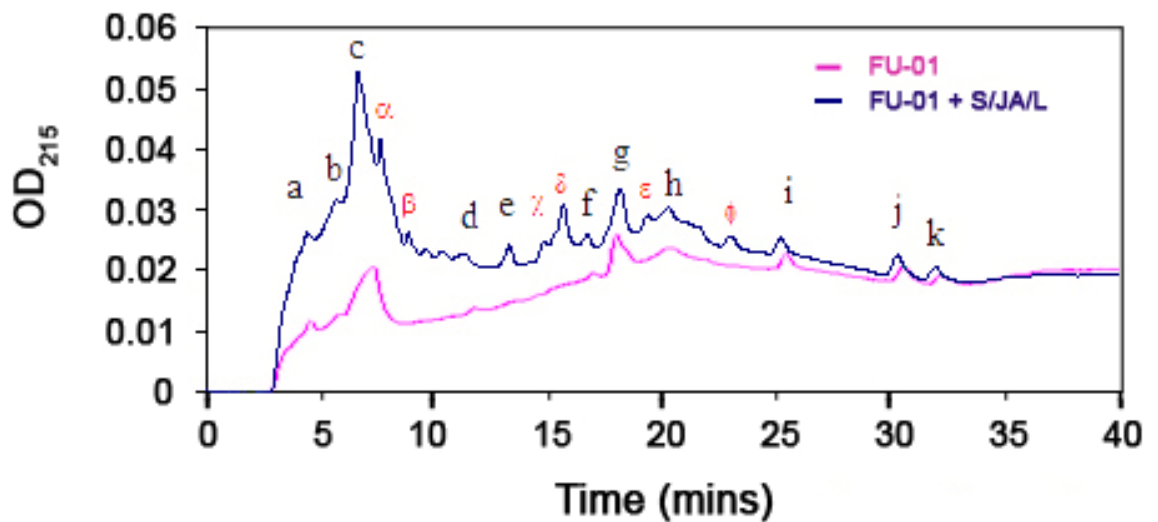


Figure 4.17: Reverse-phase HPLC of GSTs purified from untreated FU-01 cells (purple) and FU-01 cells under sucrose, jasmonic acid and light treatment (blue). Latin alphabet denotes peaks common to both conditions; Greek alphabet denotes peaks induced under elicitation.

The levels of other proteins were increased minimally and new proteins detected (annotated with Greek symbols) under elicitation conditions (Fig. 4.17). While this data was useful for the inference of GST protein induction with higher anthocyanin accumulation, further analyses (including LC/MS/MS) to identify which peak corresponds to which GST were unsuccessful.

4.3.2 Transcriptional level (QPCR)

GST expression was analysed from the control and treated FU-01 cells by QPCR. Results are presented as the mean fold-induction of transcript in the treated line over the control line at the same time-point. It was found that *GST1*

was the most highly induced GST following elicitation of FU-01 cells with S+JA+L (Fig. 4.18).

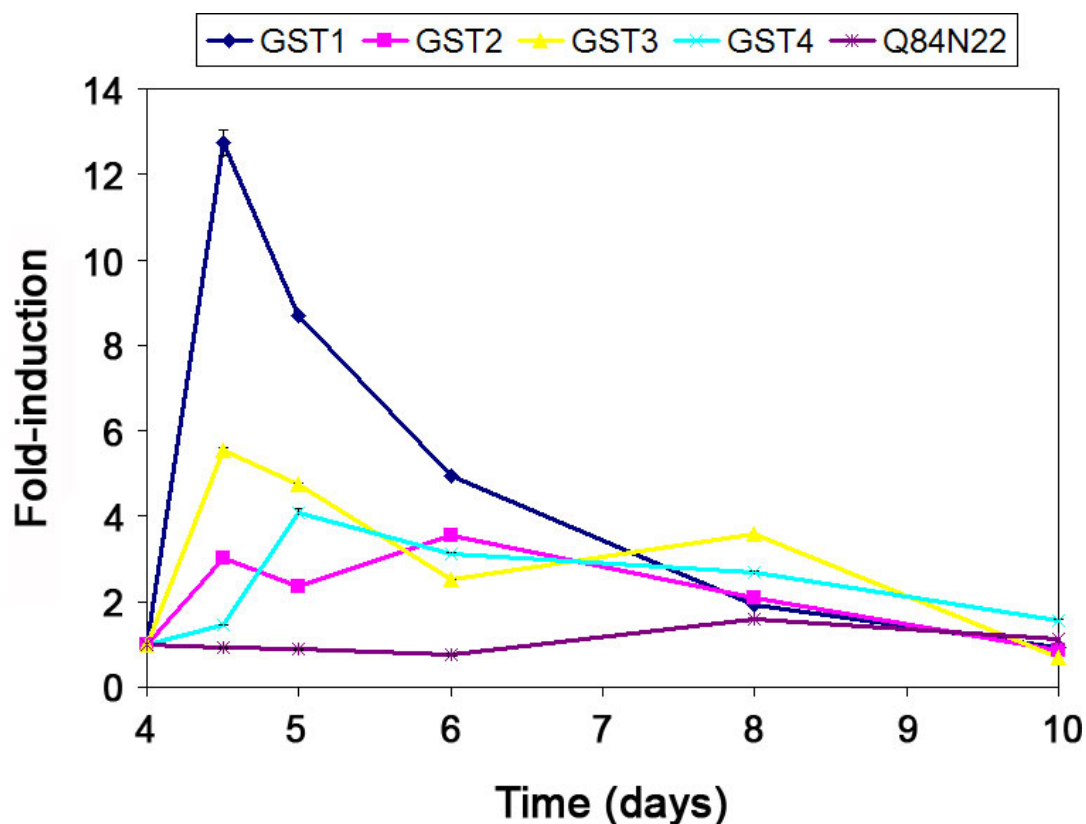


Figure 4.18: QPCR profile of GSTs following elicitation of FU-01 cells with 20 g.l⁻¹ sucrose, 10 μ M jasmonic acid and light at day 4. Results presented as fold-induction over the expression in untreated cells at the same timepoint, normalised against β -tubulin. n=3.

GST1 induction was rapid and gradually returned to the levels seen in the non-induced line by day 10. *GST3* possessed a similar rapid induction profile (5.5-fold after 12 hours), while *GST4* (4.1-fold), *GST2* (3.5-fold) and *Q84N22* (1.6-fold) reached their peak expression at day 5, 6 and 8, respectively (Fig. 4.18).

4.3.3 Effect of Individual Elicitors on GST1 Expression

The individual elicitors were also analysed for their effects on *GST1* expression (Fig. 4.19). JA and sucrose lead to a 2.9 and 3.3-fold increase in *GST1* expression compared with non-elicited cells 12 hours after elicitation. A 1.6-fold increase was detected with light elicitation after 12 hours, with maximum induction reached after an additional 12 hours. The phenomenon of minimal gene induction with light and higher induction with JA is related to the increase in anthocyanin accumulation and is also seen for the biosynthetic genes *PAL*, *CHS*, *DFR*, and *F3'5'H* (Curtin, 2005). The higher induction with sucrose treatment compared to light irradiation is not reflected in an increase in the anthocyanin content of the cells, but may reflect an osmotic response as seen for *CHS* and *DFR* (Table 3.1; Curtin, 2005).

In agreement with the GST purification from FU-03 (Fig. 4.16), all GST genes were amplifiable from FU-03 cells (data not shown). Therefore, *GST1* expression was analysed in control and S+JA+L elicited cells. A similar rapid induction of *GST1* was seen with a more rapid return to levels seen in the untreated cells as compared with FU-01 cells (Fig. 4.19).

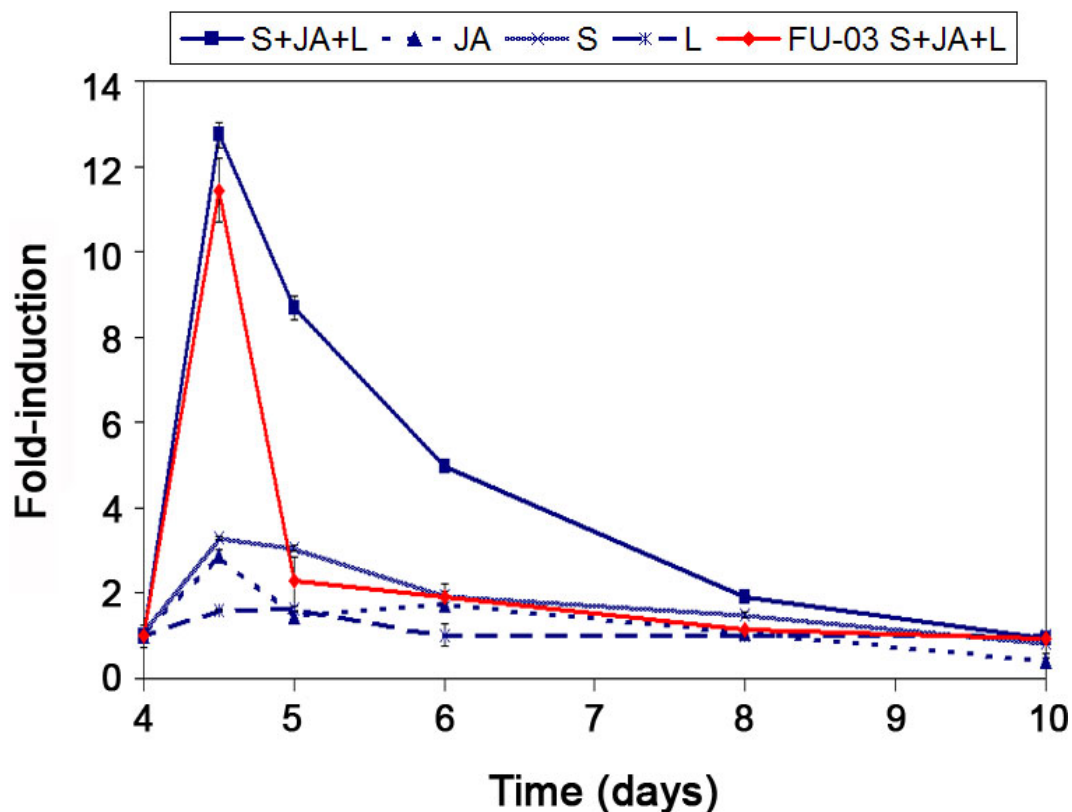


Figure 4.19: QPCR profile of GST1 in FU-01 (blue) and FU-03 (red) cells following elicitation with 20 g.l⁻¹ sucrose, 10 μ M jasmonic acid and light irradiation individually and combined at day 4. Results presented as fold-induction over the expression in untreated cells at the same timepoint, normalised against β -tubulin. n=3

4.3.4 GST Profiling in Grape Berry Skins at Veráison

Bunches of *Vitis vinifera* L. cv. Shiraz berries were obtained from the same vine at veráison from predominantly green (<10% lightly pigmented berries, which were not chosen for extraction) and fully coloured bunches (Fig. 4.20).

Figure 4.20: Green (left) and red (right) *Vitis vinifera* L. cv. Shiraz grape bunches sampled for QPCR analysis.



Veráison is defined in Shiraz berries as the accumulation of pigment and development of total soluble solid measure ($^{\circ}$ Brix) of ~ 8.0 (Kennedy *et al.*, 2000). The measure of total soluble solids for the green and red Shiraz berries was calculated as $7.6 \pm 0.3^{\circ}$ B and $14.8 \pm 1.4^{\circ}$ B, respectively. While, no anthocyanin was detected by HPLC from green berries (Appendix 6.1), the red berry skins had an anthocyanin content of 1.4 ± 0.05 mg.g-FCW $^{-1}$. These measurements justified the attribution of them as pre- and post-veráison stage berries. Expression analysis of each GST was performed on RNA from grape berry skins, normalising with ubiquitin as per Bogs *et al.* (2006). *GST4*, *GST3* and *GST2* were found to be induced with the accumulation of anthocyanin in this tissue (Table 4.5). *GST4* was the most strongly induced (~ 60 -fold) in this model, while with elicitation of suspension cells, *GST1* was the most strongly induced (~ 13 -fold). In this model, *GST1* expression was slightly down-regulated. Together, all these QPCR expression analyses suggest a strong correlation of *GST1* and *GST4* with anthocyanin accumulation, with differences arising due to possible interspecies variation, sampling point or response to specific stimuli.

Table 4.5: QPCR expression analysis of GSTs in *Vitis vinifera* L. cv. Shiraz post-veraison berry skins. Fold-induction of transcripts over pre-veraison berry skins. Mean \pm Std. Dev.

Gene	Fold-induction
GST1	0.85 \pm 0.07
GST2	1.08 \pm 0.01
GST3	2.06 \pm 0.11
GST4	60.03 \pm 3.27
Q84N22	1.13 \pm 0.17

4.4 Anthocyanin Transport Complementation Assay

4.4.1 Bombardment

Bz-2 deficient corn seeds were bombarded with GSTs in a maize expression vector for transient expression to look for revertant zones. These zones, known as complementation zones indicate the ability of the expressed gene to transport the cytoplasmic anthocyanins to the vacuole. They can be easily distinguished from the background and from necrosis resulting from the high pressure bombardment by the presence of the characteristic anthocyanin ‘halo’ (Alfenito *et al.*, 1998; Larsen *et al.*, 2003).

GST1 possessed the highest complementation effect of all the grape GSTs, with 90% of the number of complementation zones seen for the positive control (*Bronze-2*, Table 4.6). Furthermore, the average diameter of each spot was also less than that seen for *Bronze-2*, at 3.2 and 3.6 cell widths, respectively. GST4 was the only other GST tested to exhibit the complemented phenotype with 24.4% the number of spots for the positive control and a greatly reduced average diameter (2.3 cell widths, Table 4.6). All other GSTs possessed a background

level of necrosis (visible in Figure 4.21) from the bombardment, but no characteristic anthocyanin ‘halo’.

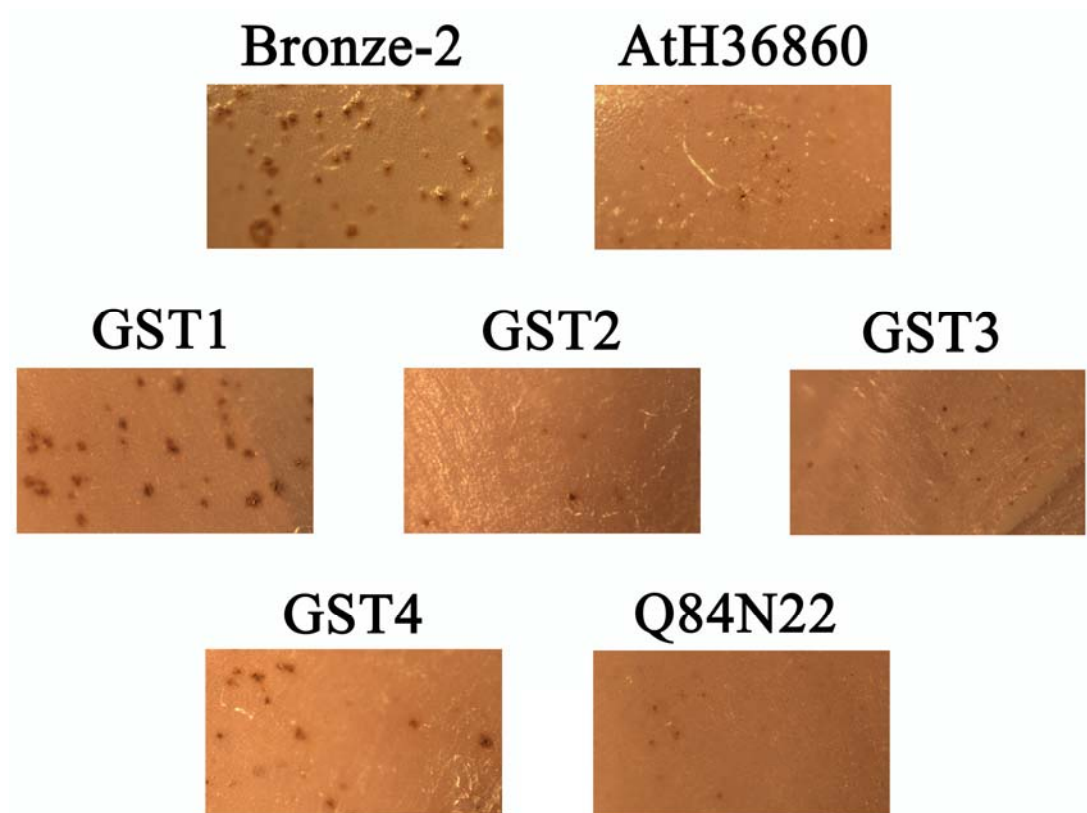


Figure 4.21: Corn kernels 48 hours after bombardment with GST constructs in pJD288 maize expression vector. 20× magnification.

Table 4.6: Protein sequence similarity between anthocyanin-transporting GSTs and sequences utilised in the complementation assay (BestFit). Counts of spots seen under a single microscopy field (a field was defined as the region falling inside the field of view using a 10× objective lens). n=2 experiments with triplicate samples.

Construct	Sectors per field (% of positive)	Complementation zones (% of each category)			Average Spot Diameter	Similarity with anthocyanin- transporting GST protein sequence (BESTFIT – GCG)		
		1-2 cell diameter	3-4 cell diameter	>5 cell diameter		Maize (Bronze-2)	Arabidopsis (TT19)	Petunia (An9)
Bronze-2	41 (100%)	22.7%	60.8%	16.5%	3.6	XXXXXX	35.5%	37.2%
pJD288 only	0	0	0	0	0	XXXXXX	XXXXXX	XXXXXX
AtH36860	0	0	0	0	0	37.1%	76.2%	64.0%
GST1	37 (90.2%)	31.9%	56.3%	11.8%	3.2	48.2%	36.9%	34.4%
GST2	0	0	0	0	0	39.6%	49.3%	48.3%
GST3	0	0	0	0	0	37.8%	59.2%	66.0%
GST4	10 (24.4%)	56.5%	43.5%	0	2.3	37.7%	68.4%	75.8%
Q84N22	0	0	0	0	0	48.3%	37.8%	41.8%

4.4.2 GST Sequence Alignments

Bestfit alignments were made between all *V. vinifera* GSTs (Fig. 4.22) and the GSTs known to complement for Bronze-2 in the maize complementation assay (Fig. 4.23; Alfenito *et al.*, 1998). It was found that GST1 possessed the second-highest similarity to Bronze-2, while the most similar sequence, Q84N22, exhibited no complementation in this assay (Table 4.6). The high similarity between Q84N22 and the other type III *V. vinifera* GST, GST1, suggests the involvement of distinct residues in achieving the anthocyanin transport (Fig. 4.22). Interestingly, the similarity with Bronze-2 was proposed as the reason for the slightly higher complementation phenotype of ZmGSTIII as opposed to An9 (Alfenito *et al.*, 1998). GST4 was the most similar of all GSTs used in this assay to An9 and the most similar *V. vinifera* GST to TT19 (Fig. 4.12 and Table 4.6). GST4 also gave a similar level of complementation in the maize bombardment assay (Alfenito *et al.*, 1998).

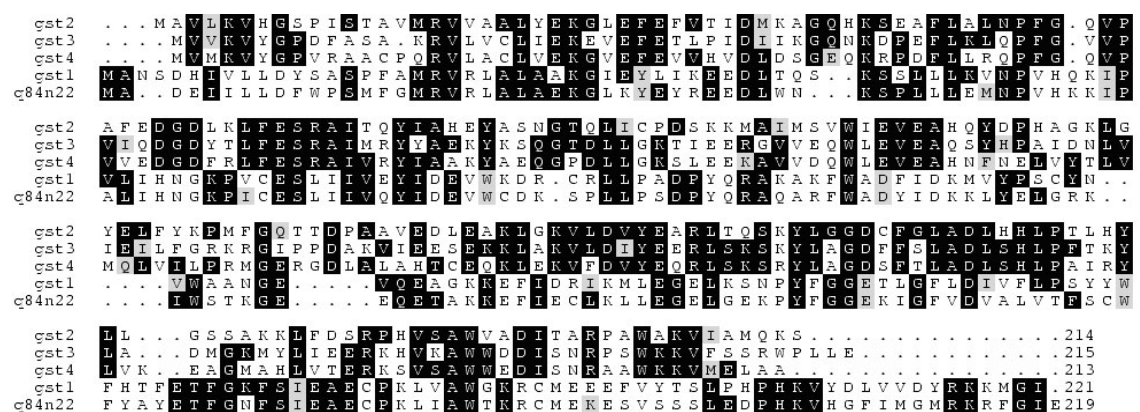


Figure 4.22: Alignment of *V. vinifera* GST protein sequences. Images generated using prettybox. Black box indicates identity, grey box indicates similar residue.

This suggested that protein sequence was influential in governing anthocyanin-transport in this model. It was theorised that homologous regions may be present in all anthocyanin-transporting GSTs in order to recognise the anthocyanin nucleus. Both GST1 and GST4 sequences were aligned with Bz2, TT19, ZmGSTIII and An9 to identify conserved residues (Fig. 4.23). Single or double amino acid residues were conserved across a number of these GSTs (deficient in other *V. vinifera* GSTs). However, as noted by Alfenito *et al.* (1998), this did not yield any clear regions of similarity distinct from non anthocyanin-transporting GSTs in this 2-dimensional analysis. As a result, the GSTs were modelled in a 3-dimensional format to reveal the location of these residues with respect to binding sites.

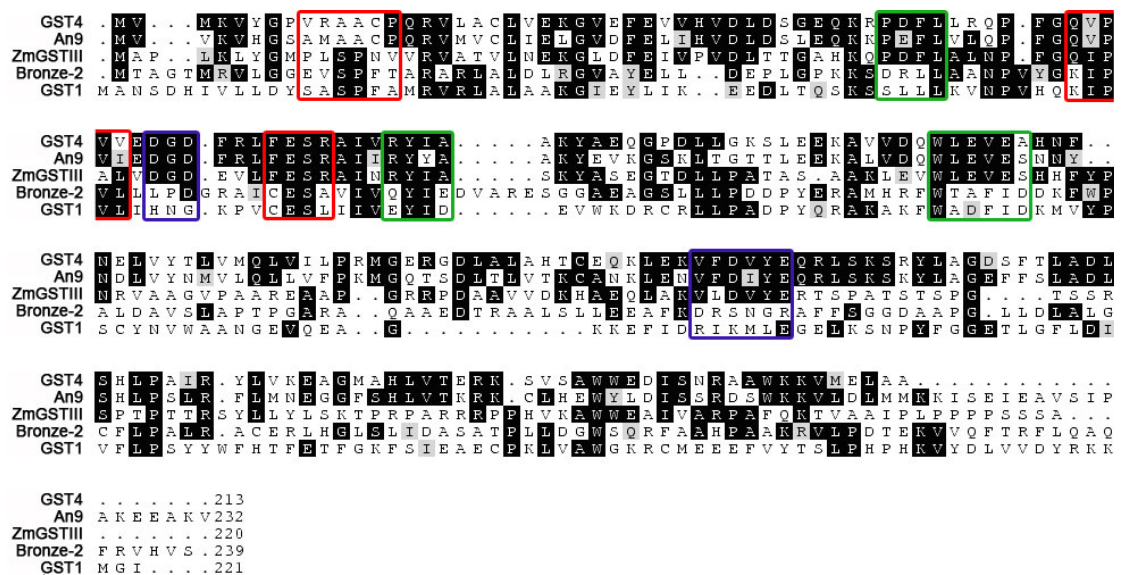


Figure 4.23: Alignment of *Bz2*-complementing protein sequences. Images generated using ClustalW and prettybox. Black shading indicates identity, grey shading indicates similar residue. Red box highlights key residues in GSH-binding (G-sites), green boxes represent dimerisation regions, blue boxes represent similar regions between type I GSTs (GST4, An9, ZmGSTIII).

The 3D model(s) used for this alignment were the *E. coli* GST Chain A, complexed with glutathionesulfonic acid (Nishida *et al.*, 1998), maize GSTI complexed with lactoylglutathione (Neuefeind *et al.*, 1997a) and maize GSTIII (Neuefeind *et al.*, 1997b). Of the known crystal structures, the *E. coli* sequence was most similar to GST1 (23% identity and 43% similarity) and with sites interacting with GSA indicated in Figure 4.24. Similar binding regions were seen for the plant GSTs and their substrates, however 3D images were not available. Some ligandin-binding sites have been shown to overlap with the H- and G-sites, thus these were the focus of the conservation of functional regions 13SASPFA, 55KIPVL, 68CESL (red boxes in Figs. 4.23 and in Fig. 4.24). There is a strong conservation in the core of these regions between GST1 and Bronze-2, while there are residues that differ with other anthocyanin-transporting GSTs. Also, residue differences between the highly similar Q84N22 and GST1 sequences fall in these regions (Fig. 4.22).

GST4, An9 and, to a lesser extent, ZmGSTIII (all type I GSTs) exhibit a similar response in the complementation assay (Alfenito *et al.*, 1998). As well as high overall similarity, these GSTs possess strong homology in miniregions that differ from the GST1/Bz2 miniregions. This includes high similarity within the aforementioned G-sites and other regions found throughout the length of the protein on the surface of each monomer (blue boxes; Fig. 4.23) and in dimerisation regions (green boxes; Fig. 4.23).

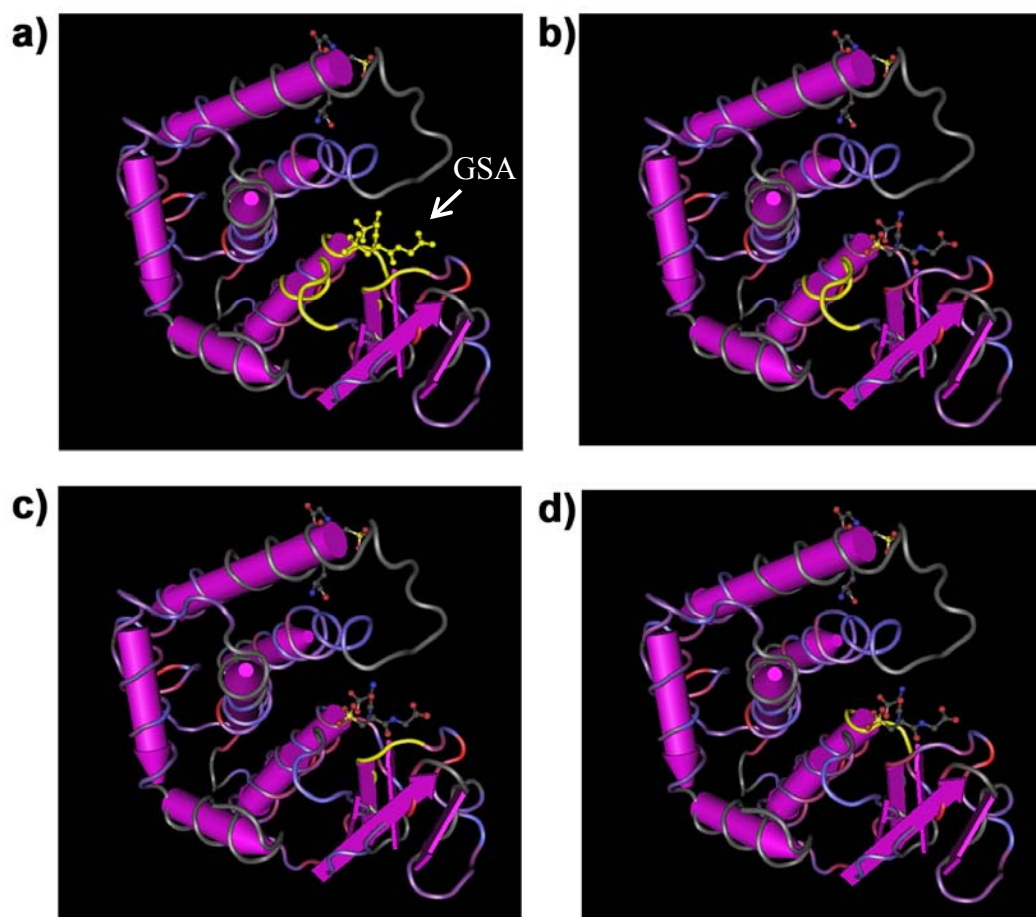


Figure 4.24: 3D domain image of *E. coli* GST Chain A (Accession No. 4389382) complexed with GSA. a) All residues within 3Å of the GSA molecule shown in yellow. Highlighted residues b) 13SASPFA; c) 55KIPVL; and d) 68CESL.

4.5 Discussion

4.5.1 *Vitis vinifera* GSTs

GSTs have been shown to be involved in anthocyanin transport in maize and petunia (Marrs *et al.*, 1995; Alfenito *et al.*, 1998; Mueller *et al.*, 2000). It was hypothesised that if GSTs were involved in anthocyanin transport in *Vitis vinifera*, they would be present during anthocyanin synthesis. Five GSTs were purified and the gene sequence cloned from pigmented *V. vinifera* suspension cell cultures and were characterised for their ability to transport anthocyanins. This study yielded 5 GSTs, the largest number identified from any species by a single-step chromatographic procedure, with only 2 GSTs identified from oat seedlings using the same approach (Zachariah *et al.*, 2000). GSTs exhibit spatial expression patterns; therefore these 5 proteins may represent the panel, or part thereof, of GSTs with specific roles for the berry suspension cells. In maize, it has been shown that the pattern of GST expression differs between roots, shoots and leaves and that they are under unique induction mechanisms (Sari-Gorla *et al.*, 1993; Rossini *et al.*, 1998). Pairoba and Walbot (2003) demonstrated that the 26kDa *Bronze-2* protein is accumulated only in anthocyanin accumulating tissues. This infers that expression of specific GSTs is tailored to the needs of the cell. There may be additional GSTs in *Vitis vinifera*, which are either poorly expressed in berry suspension cells or under a spatiotemporal pattern of expression and so would not be detected via this approach targeting anthocyanin-transporting GSTs.

4.5.2 GST Sequences

In support of the findings in this study, Terrier *et al.* (2005) identified 5 GSTs in *V. vinifera* by tBLASTX and BLASTN analysis of commercially

available ESTs in the NCBI and TIGR databases. Terrier *et al.* (2005) only published one of these sequences in their report. This EST corresponded to the GST4 sequence that was cloned in this study (AY971515). Of the five GST sequences cloned in this study from pigmented suspension cells, there were 3 Type I GSTs (*GST2*, *GST3*, and *GST4*) and 2 Type III GSTs (*GST1*, and *Q84N22*) based on intron structure and protein sequence alignments. This is the first report of the cloning of the full-length sequence for GST2, GST3 and GST4. Each recombinant protein possessed GST activity against CDNB and was subsequently cloned into the maize expression vector, pJD288 for assaying anthocyanin transport. The activity of the partially purified GSTs were between 1.3-2-fold higher than other recombinant GSTs cloned from poppy (Yu and Facchini, 2000) and petunia (Alfenito *et al.*, 1998).

The degenerate cloning procedure generated a single Type III GST product, Q84N22. While Q84N22 possessed two non-complementary nucleotides in the 5' region of the forward primer (protein WPSMFG), the reverse primer was completely homologous, yielding a single product. GST1 possessed higher non-complementarity at the 5' and 3' annealing regions of the forward (SASPFA) and reverse (AKFWAD) regions.

Interestingly, all GST proteins and transcripts were also detected in non-pigmented (FU-03) cells. The presence of the anthocyanin transporting GST in non-pigmented grape suspension cells is not surprising as the FU-03 line was isolated from pigmented cell suspension material by micro-callus selection and retains a minimal amount of pigmentation and all anthocyanin biosynthetic genes (Curtin, 2005). Furthermore, while non-functional anthocyanin biosynthetic and regulatory genes have been isolated in maize, no commercial variety has been

identified to be deficient in *Bz2* in all pigmented seed and over 100 landraces and 20 inbred lines with colourless or beige seed (V. Walbot, unpublished data). Furthermore, the *Bz2* knockout – a 2cM deletion generated by exposure to atomic bomb radiation – lead to a reduction in anthocyanin accumulation to 10% the level of expression indicating a biosynthetic inhibition (Goodman *et al.*, 2004). Together, this indicates that the GST is indispensable for anthocyanin accumulation and may possess an, as yet, unidentified role against endogenous/exogenous substrates.

Pairoba and Walbot (2003) showed that *Bz2* transcripts, but not the protein were detectable, albeit reduced 4-fold, in tissues lacking one or both of the C1/R anthocyanin transcription factors. Furthermore, both the spliced and unspliced forms of *Bz2* - found to be induced by cadmium and other stresses by Marrs and Walbot (1997) - were seen in a 1:1 ratio in all tissues studied. The expected truncated protein from the unspliced poly(A)+ mRNA was not found in any tissue, even using an N-terminal myc:*Bz2*-fusion. This indicates that the translation or *Bz2* transcript half-life may be regulated in non-anthocyanic tissue. No unspliced transcript was detected in any tissue by PCR using primers designed to span the single intron of GST1 in this study (data not shown).

4.5.3 Profile of GSTs Following Elicitation

GSTs, like anthocyanins, are induced in plants in response to many external cues, including xenobiotics, oxidative stress, nutrient limitation and pathogenesis (Marrs *et al.*, 1995; Aharoni *et al.*, 2002; Dean *et al.*, 2005). One of the mechanisms underlying this induction has been partially attributed to the activation of the promoter region, more specifically the panel of associated

enhancer elements, by specific substrates (indole acetic acid, chemical safeners, herbicides), metabolites (nitrogen) or pathway signals. As indicated in Chapter 3, jasmonic acid and light treatment does not influence global protein expression in *V. vinifera* cell cultures (<10% of protein spots effected), thus any changes in expression gives specific information on regulation.

It was found that *GST1* was the most highly induced GST under sucrose, jasmonic acid and light elicitation to increase anthocyanin synthesis in *V. vinifera* suspension cells. All 3 elicitors were capable of inducing *GST1* expression individually, with synergistic, not additive, effects as determined by QPCR. As mentioned in Section 4.2.2.1, a significant increase in anthocyanin accumulation is detected 24 hours post-elicitation with jasmonic acid alone, and continues to increase for a further 7 days. On the other hand, induction of *GST1* was rapid, reaching its peak 12 hours post-elicitation, and returning to the level of the untreated cells after 6 days. Curtin (2005) demonstrated early anthocyanin biosynthetic genes possessed a similar induction profile in response to sucrose, jasmonic acid and light – the condition yielding the greatest increase in anthocyanins. All other GSTs, except for Q84N22 ($P > 0.22$), were significantly induced over the control culture to a lesser degree than *GST1* with a variety of profiles. In FU-03 a similar fold-induction for *GST1* was seen with sucrose, jasmonic acid and light treatment, yet this returned to the level of expression in the untreated line within 12 hours. As the amount of anthocyanins is much less in FU-03 than FU-01 cells, the similar induction of *GST1* may indicate a specific response to elicitation, rather than a specific need to transport the same amount of anthocyanins. This inability to sustain higher expression levels may also be due to lack of additive elements, or transcription factors present in the FU-01 line. As all

but Q84N22 was induced in response to this treatment, expression of the genes in berry skins, pre- and post-veraison was investigated to achieve a more specific correlation of GST genes with anthocyanin accumulation.

The analysis of GST expression in pre- and post-veraison berry skins demonstrated that GST4 (and to a lesser extent GST3), but not GST1, was strongly induced along with anthocyanin accumulation. This induction of GST4 alone was also noted with the oligo array and real-time analyses by Terrier *et al.* (2005) on ripening Shiraz berries. As the single sampling point chosen for post-veraison berries was after large amounts of anthocyanin accumulation, the induction of GST1 may have been missed as seen with the return of transcript levels to normal levels in the suspension culture model. It would still be expected that transport activity would be high during this point and so comparison of protein abundance for GST1 and GST4 in these tissues may assist in resolving this matter. Together, these results indicate the correlation of GST expression, more specifically GST4 and GST1, with anthocyanin accumulation. However, enhanced gene expression does not indicate an increase in the level and activity of the protein.

Treatment of FU-01 cells with sucrose, jasmonic acid and light increased GST activity with the appearance of unique glutathione-binding proteins compared with untreated FU-01 cells by reverse-phase HPLC. A similar response was witnessed when ground nut seedlings were exposed to the herbicide, glyphosate (Jain and Bhalla-Sarin, 2001). In this study, attempts were made to identify these new peaks by SDS-PAGE and LC/MS, but were unsuccessful. GSTs are induced under conditions that give rise to increases in anthocyanin accumulation, including oxidative damage, pathogen attack and other stresses

(Marrs, 1996) and it is likely that these may represent additional GSTs not cloned in this study. In agreement with the QPCR results, one GST was seen to be enhanced more significantly under S+JA+L elicitation than the other 5 GSTs by reverse-phase HPLC of purified GSTs. A 3-fold induction of a GST protein was seen in S+JA+L treated FU-01 cells, while *GST1* gene expression was induced ~13-fold by QPCR. Therefore, translational repression affects *V. vinifera* GSTs, with the logical conclusion that the highest induced protein was GST1. However, it may represent one of the other GSTs that were induced to around the 3-fold level by QPCR, including GST2, GST3 and GST4. Unique peaks were observed under S+JA+L elicitation, a common phenomenon for GSTs when cells are under stress conditions (Daniel, 1993; Rushmore and Pickett, 1993; Arakawa *et al.*, 2002). However, these proteins cannot be solely responsible for anthocyanin transport as non-elicited FU-01 cells still accumulate anthocyanin without detectable levels of these proteins.

Tissue-specific expression can be overridden by treatment with various chemicals (Ulmasov *et al.*, 1995). Specific upregulation of GSTs can be achieved by co-incubation with herbicides (Dixon *et al.*, 1997; Jain and Bhalla-Sarin, 2001), and safeners (herbicide antidotes; Rossini *et al.*, (1998). In barley, safener treatment of plants resulted in a concomitant increase in not only the herbicide detoxifying enzyme, but also the vacuolar transporter for this compound (Gaillard *et al.*, 1994). Cadmium, arsenite and ABA induced Bz2 expression without concomitant increases in other anthocyanin biosynthetic genes (Marrs and Walbot, 1997).

Jasmonic acid (JA), or its methylated ester derivative (MeJa) is upregulated after wounding soybean (*Glycine max* L.; Creelman *et al.*, 1992) and

challenging of the plant by pathogens (Gundlach *et al.*, 1992; Mueller *et al.*, 1993). Furthermore, this plant signal has been shown to initiate *de novo* transcription of many genes associated with the plant defence response and all anthocyanin biosynthetic genes (Curtin, 2005). It is thought that this results from the induction of specific transcription factors that bind to upstream regulatory elements and induce the downstream gene(s) (Memelink *et al.*, 2001). GSTs were induced at both the transcriptional and translational level using jasmonic acid in this study, as has been noted previously using MeJa (Marrs, 1996).

One element identified in Arabidopsis, referred to as the Jasmonate and Elicitor Responsive Element (JERE) has been found in the promoter regions of genes induced during pathogenic attack (Miller *et al.*, 2002). Using JERE as bait in a yeast one-hybrid screen, octadecanoid-responsive *Catharanthus* AP2 domain proteins (ORCAs) were isolated as putative transcription factors (review Memelink *et al.*, 2001). Furthermore, these were rapidly induced by MeJa treatment and have been shown to transactivate genes in a JERE-dependent manner (Memelink *et al.*, 2001). This element has been noted in the promoter of a type II GST gene from carnation in addition to other common stress-responsive elements (Itzhaki and Maxon, 1994).

Increases in anthocyanin synthesis achieved by elicitation with sugars are thought to occur by both osmotic stress (Do and Cormier, 1991a) and metabolism of sugars (Larronde *et al.*, 1998). Hexose phosphorylation and calcium-calmodulin in sugar sensing/signalling were implicated in metabolisable sugar-responsive anthocyanin gene induction by grape cell cultures (Vitrac *et al.*, 2000; Gollop *et al.*, 2001; 2002). More recently, a sucrose-specific induction was noted for all anthocyanin biosynthetic genes in Arabidopsis (Solfanelli *et al.*, 2006).

Light treatment is known to induce anthocyanin accumulation, with the precise mechanism still unknown.

Furthermore, conditions which enhance anthocyanin accumulation, in particular, heavy metal stress, also increased the transcription of *Bz2* (Marrs and Walbot, 1997). Uniquely, cadmium stress which induced the highest level of *Bz2* expression in the study was shown to activate an alternate mRNA start site and lead to a 50-fold increase in the unspliced transcript. However, it was shown that although the transcription was increased, there was no concomitant increase in *Bz2* GST activity as determined by co-transfecting maize protoplasts with a *Bz2* expression plasmid and assaying total GST activity against the untransformed control (Marrs and Walbot, 1997).

The structure and regulation of the maize *Bronze-2* promoter is similar to that of many anthocyanin biosynthetic enzymes. A luciferase reporter gene under the control of the *Bz2* promoter required the presence of both *C1* and *R* transactivator gene products in order to be expressed in transient expression studies (Bodeau and Walbot, 1992). It was shown that a 242bp segment of the promoter, containing the putative C1- and R-motifs, was sufficient for complete C1/R regulation (Bodeau and Walbot, 1996).

Short upstream regions (< 100bp) of each *V. vinifera* GST were analysed for conserved promoter motifs. While certain elements were common (TATA, ARR1AT), only GST1 was found to possess conserved myb- and bHLH-binding regions, corresponding to the C1 and R-binding consensus motifs, necessary for anthocyanin transcription factor regulation (Schmitz and Theres, 1992). A conserved C1/R binding site is found in the promoter region of numerous anthocyanin pathway genes, including *Bronze-2*, in maize, conferring

transcriptional control (Lesnick and Chandler, 1998). While these elements were found in the 5' UTR of *GST1*, and not the promoter as with *Bronze-2*, this may still confer a transcriptional response. Bolle *et al.* (1994) demonstrated that the 5' UTR of spinach thylakoid genes is essential for quantitative transcription of these genes. Furthermore, in barley the 5' UTR was found to confer qualitative expression in an embryo-specific pattern in a GUS-fusion assay using MeJA as the elicitor (Rouster *et al.*, 1998). As grape *GST1* also responds to JA, it may be partially attributable to the identified elements in the 5' UTR.

While regulatory anthocyanin genes are highly conserved between species, there exist species-specific differences between the promoter regions of target genes (Quattrocchio *et al.*, 1998). Due to their correlation with anthocyanin development, cloning and analysis of the full *GST1* and *GST4* promoter regions would resolve the presence of JERE and anthocyanin consensus sites. Regulation inferred by JA, sucrose, light and *V. vinifera* anthocyanin transcription factors could then be determined by promoter and UTR deletion studies using a reporter plasmid as per Ulmasov *et al.* (1995).

4.5.4 Anthocyanin Transport Complementation Assay

Bz2-deficient corn seeds from the W23 inbred background line accumulate the following anthocyanins in increasing order cyanidin; cyandin-3-(3'',6''-dimalonylglucoside); cyandin-3-(6''-malonylglucoside) and cyandin-3-glucoside. Grape cells possess a large proportion of both cyanidin and cyanidin-3-glucoside, however, the anthocyanidins do not accumulate in the vacuole (Cormier and Do, 1993). Due to the presence of similar predominant

anthocyanins, it was believed this model would enable the detection of the anthocyanin transporting GST(s) isolated from *V. vinifera*.

Both GST1 and GST4 yielded positive results with this assay, with GST1 possessing the second highest similarity to *Bz2* (48.2%). Q84N22 possessed 48.3% similarity to *Bz2*, yet exhibited no transport activity. Sequence analysis for all anthocyanin transporting GSTs able to complement *Bz2* gave no consensus of functional residues or H-sites, supporting the findings of other researchers (Alfenito *et al.*, 1998; Kitamura *et al.*, 2004). However, G-sites were shown to be conserved within the GST1/*Bz2* and GST4/*An9*/*ZmGSTIII* groups, respectively. These regions were a source of dissimilarity between the highly homologous GST1 and Q84N22 and may contribute to the lack of activity of Q84N22 in the maize complementation assay. An interesting point to note is that anthocyanin-transporting GSTs are dissimilar between dicots (maize) and monocots (petunia – 37.2% similarity, Arabidopsis – 35.5% similarity). However, the strongest complementing GST in the grape dicot (GST1) is more similar to the monocot maize GST (*Bz2*), than any of the closer related dicot sequences.

This is a likely reflection of the independent evolution of GSTs with regard to the anthocyanin profile within each species. Interestingly, GST4 possessed the highest similarity of any of the grape GSTs cloned to the petunia *An9* and yielded a similar result in this assay (Alfenito *et al.*, 1998). This is as expected due to the more similar profile of anthocyanins between petunia and grape, than with either of these and maize (Spelt *et al.*, 2000). This may infer GST4 as the strongest candidate for anthocyanin transport in grape as it complemented for the *Bz2* knockout similarly to *An9*, while possessing the lowest homology with *Bz2*. In support of this, maize GSTIII (*ZmGSTIII*), but not

ZmGSTI exhibited a positive result in this complementation assay (Alfenito *et al.*, 1998). This was attributed to the sequence similarity alone between ZmGSTIII, but not ZmGSTI, with Bz2.

The fact that both GST1 and GST4 exhibited anthocyanin transport phenotypes in this assay may be a result of sequence similarities, but also matches the redundancy of the anthocyanin pathway. This redundancy is seen with numerous functional copies of biosynthetic enzymes, including CHS (Reif *et al.*, 1985; Durbin *et al.*, 2000), CHI (van Tunen *et al.*, 1988), PAL (Ozeki *et al.*, 1990a); but also the transport pumps - ZmMRP3, ZmMRP4 (Goodman *et al.*, 2004). While maize also boasts 2 GSTs with transport activity in this assay, ZmGSTIII and Bronze-2, a knockout of the latter abrogates anthocyanin vacuolar deposition (Alfenito *et al.*, 1998). This demonstrates a dependency on Bz2, yet does not eliminate the possibility of ZmGSTIII transcriptional repression in these tissues, or potential heterodimerisation with Bronze-2 for a functional ligandin. This model may also apply for GST1 and GST4 in *V. vinifera*. Analysis of gene expression for ZmGSTIII in Bz2 deficient tissues, or creation of ZmGSTIII-knockout maize would be necessary to resolve this.

The GSTs may play a role in maintaining the integrity of the transport vesicles, or pumps as indicated by the association of Bronze-2 with the insoluble, membrane fraction (Pairoba and Walbot, 2003). Other GSTs acting as ligandins, including the IAA-binding PM24 from arabidopsis, also associate with plasma membrane vesicles (Zettl *et al.*, 1994). While this report also demonstrated another IAA-binding GST that is soluble, reports exist of GSTs associating with membranes in prokaryotes and eukaryotes, as members of the MAPEG superfamily (membrane-associated proteins in eicosanoid and glutathione

metabolism; Jakobsson *et al.*, 1999). The most intensively studied MAPEG member comes from humans, where the trimeric MGST1 is theorised to be important for protecting the ER-membrane from reactive lipid intermediates (Jakobsson *et al.*, 1999; Schmidt-Krey *et al.*, 2000). MGST1 is concentrated at both the ER-surface and the mitochondrion with its G- and H-sites facing the cytosol (Andersson *et al.*, 1994; Sun and Morgenstern, 1997). Thus, the active site may benefit from the proximity to the substrates, such as for anthocyanins concentrated at the site of biosynthesis on the ER (Hrazdina *et al.*, 1987; Saslowsky and Winkel-Shirley, 2001). It would be useful to localise the *V. vinifera* GST1 and determine any interaction with biosynthetic proteins, or a membrane pump.

The diameter of the complementation zones in the maize bombardment assay is indicative of the efficiency of the transporting GST. The reason for this non-cell autonomous nature of the Bz2 knockout complementation phenotype was due to the presence of a non-cell limited factor. Revertant sectors of unstable mutants of each of the anthocyanin biosynthetic structural genes exhibit a similar phenotype, while that for the transcription factors is cell delimited. This indicates that some component produced by the intact anthocyanin pathway in the revertant sector can move to the adjacent cells, partially complementing the mutation in those cells. Goodman *et al.* (2004) identified an anthocyanin tonoplast transport protein (*ZmMRP3*), acting after Bz2 and under control of the anthocyanin transcription factors, that confers the diffusible anthocyanin to a cell-limited marker by irreversible vacuolar uptake.

4.6 Conclusions

Results presented in this study demonstrate the strong correlation between GSTs and anthocyanin accumulation in *V. vinifera*. Specifically, GST1 and GST4 are the most responsive GSTs under synthetic (elicitation) and native (veraison) conditions increasing anthocyanin accumulation, respectively. In support of this, both GST1 and GST4 possess a capacity to complement for the loss of *Bronze-2* in a maize anthocyanin transport complementation assay. Furthermore, the sequence conservation of specific residues in the GSTs contribute to their anthocyanin transporting phenotype. While no physical interaction was demonstrated between these GSTs and anthocyanins, this evidence implicates their involvement in the transport of anthocyanins.

CHAPTER 5

CHARACTERISATION OF ANTHOCYANIC VACUOLAR INCLUSIONS (AVIs) AND THEIR ROLE AS ANTHOCYANIN STORAGE SITES IN *VITIS VINIFERA* L. CELL-SUSPENSION CULTURES

5.1 Introduction

The colour of anthocyanins is a pH-dependent characteristic becoming pigmented intracellularly when localized to the highly acidic vacuole. Exceptions exist when the anthocyanins are stored in a crystalline form in the cytoplasm, or cell wall (Blank, 1946). While the profile of anthocyanin species present in a plant is the major determinant of plant colour, in *Hydrangea macrophylla* there is a range of sepal colour from blue to red, which has been correlated with a decreasing vacuolar pH and not variations in the anthocyanin profile (Yoshida *et al.*, 2003). As demonstrated in the previous chapter, transport of anthocyanins to the vacuole may be aided by GSTs in *Vitis vinifera* suspension cell cultures. Their retention within the vacuole is thought to be mediated by the pH gradient across the tonoplast, whereby anthocyanins are spontaneously ionized to their pigmented flavylium cation when imported.

This phenomenon is limited by the maximum capacity of the vacuole and when reached, would provide a uniform colour in all cells of an organism. Zhang and Wong (1996) demonstrated that efflux of glutathione conjugates via integral GS-X pumps on the plasma membrane of adenocarcinoma cells is inhibited by various plant polyphenols, including quercetin and tannic acid. A similar mechanism may explain the saturability of anthocyanins in the plant vacuole, whose movement is thought to occur via a tonoplast multidrug resistance associated protein in maize (ZmMRP3; (Goodman *et al.*, 2004). Furthermore, free anthocyanins in the vacuolar sap are more susceptible to degradative processes.

Various plant tissues, particularly flower petals, have regions of colour that vary in intensity. For example the inner petal region of lisianthus is darker than the outer lighter region. This intensification is mediated by the higher

abundance of inclusions within the vacuole of the inner petals, called anthocyanic vacuolar inclusions (AVIs), which bind and concentrate the anthocyanins above that in the vacuolar sap (Markham *et al.*, 2000). As evidence from various plant species correlates AVI abundance with anthocyanin accumulation, this enhanced storage capacity potentiates increased anthocyanin synthesis, resulting in the more intense colour.

The ability of storage structures to sequester specific anthocyanins may be of importance in controlling the profile of accumulating anthocyanins. Sequestration of specific compounds by committed storage compartments is often a protective mechanism, either by reducing their toxicity or by augmenting activity within the cell/compartment. As anthocyanins are bioactive pigments that follow spatio-temporal expression patterns and that they are concentrated in inclusions (AVIs), supports these theories.

AVIs are being investigated in *V. vinifera* L. cell suspension culture in order to qualify them as targets for augmenting anthocyanin accumulation. Fundamental studies are undertaken on the localisation and formation of AVIs, while kinetic studies correlating the abundance of AVIs with anthocyanin production can clarify whether AVIs are limiting in anthocyanin accumulation. The ability to purify these bodies enables the composition of AVIs to be determined, resolving contradictory reports of their composition. Together, this provides information that may be exploited for the future enrichment of AVIs in *V. vinifera* suspension cultures, to maximise anthocyanin production.

5.2. Localisation of AVIs in *V. vinifera* Cell Cultures

5.2.1 Light Microscopy

In this study *V. vinifera* AVIs were visualised under bright-field microscopy and believed to be intravacuolar structures. Observations were made on protoplasted suspension cells (Fig. 5.1a), microcallus (Fig. 5.1b) and protoplasted suspension cells undergoing vacuolar release (Fig. 5.1c). These AVIs moved freely around the cell by Brownian motion on unfixed samples, retarded only by the inner face of the tonoplast. Furthermore, when released into the buffer the bodies remained intact (Fig. 5.1d). Following vacuolar release AVIs still possessed Brownian motion, indicating they are not associated by non-specific adherence to the vacuolar membrane.

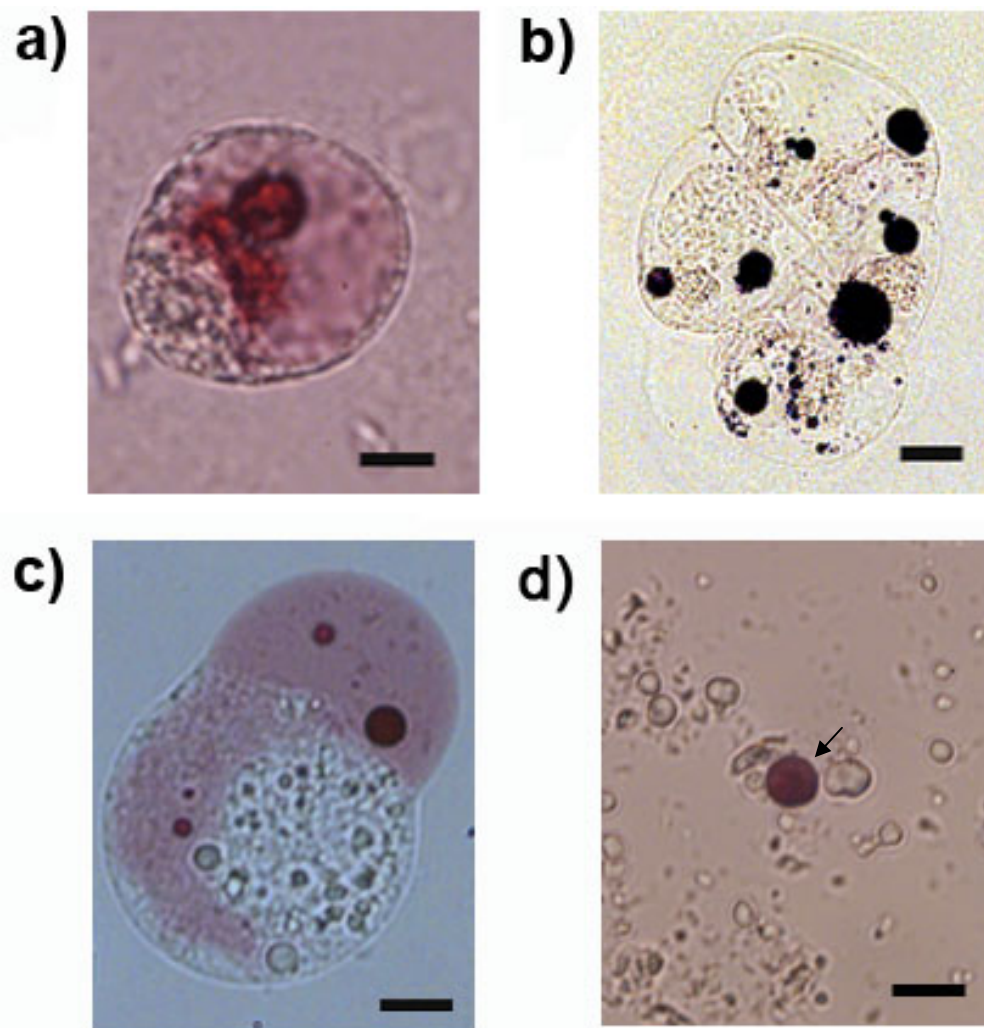


Figure 5.1: Bright-field microscope images of a) *Vitis vinifera* L. suspension cell protoplast and b) microcallus possessing AVIs. c) Intact vacuole release from protoplast and d) AVI (arrow) and cellular debris in mannitol buffer. 40× Magnification. Bar = 10µm.

5.2.2 Confocal Microscopy

Three-dimensional confocal fluorescence microscopy was utilised as a more sensitive method to determine intracellular AVI localisation. An autofluorescence in the far red region (λ_{Exc} : 647nm, λ_{Em} : 680⁺nm) was seen to be strongly associated with anthocyanic (or tannic) regions of the cell (Fig. 5.2a and b). For clarity, suspension cells were mounted in mild plasmolysis buffer (4%

sucrose in PBS, pH 5.2) to enable differentiation between vacuolar and cell membranes. Autofluorescence was detectable in the vacuole and greatly intensified in the AVIs. A minimal autofluorescence was also seen at the cell wall; however, this was at the lower limit of detection (Fig. 5.2b).

Stepwise confocal images were collected through a cell and images overlaid to create a 3-dimensional reconstruction of cellular autofluorescence, with high- and intermediate-intensity regions assigned different colours, yellow and blue, respectively (Fig. 5.2c). These thresholds consistently enabled the distinction between different cellular regions within and between callus and suspension-cell samples (refer to Appendix 6.2). This enabled the AVIs to be localised entirely within the vacuolar boundary (outermost low-intensity autofluorescent region). This observation was seen for both pigmented callus, and suspension cells irrespective of the stage of cellular growth and osmolarity of mounting buffer. This autofluorescence was not witnessed in non-pigmented suspension cells, or callus but was visible in the skins of red, but not white table grapes (Fig. 5.3). The AVIs formed large conglomerates in the vacuole, with smaller bodies present at the tonoplast boundary (Fig. 5.3a and b, green arrows).

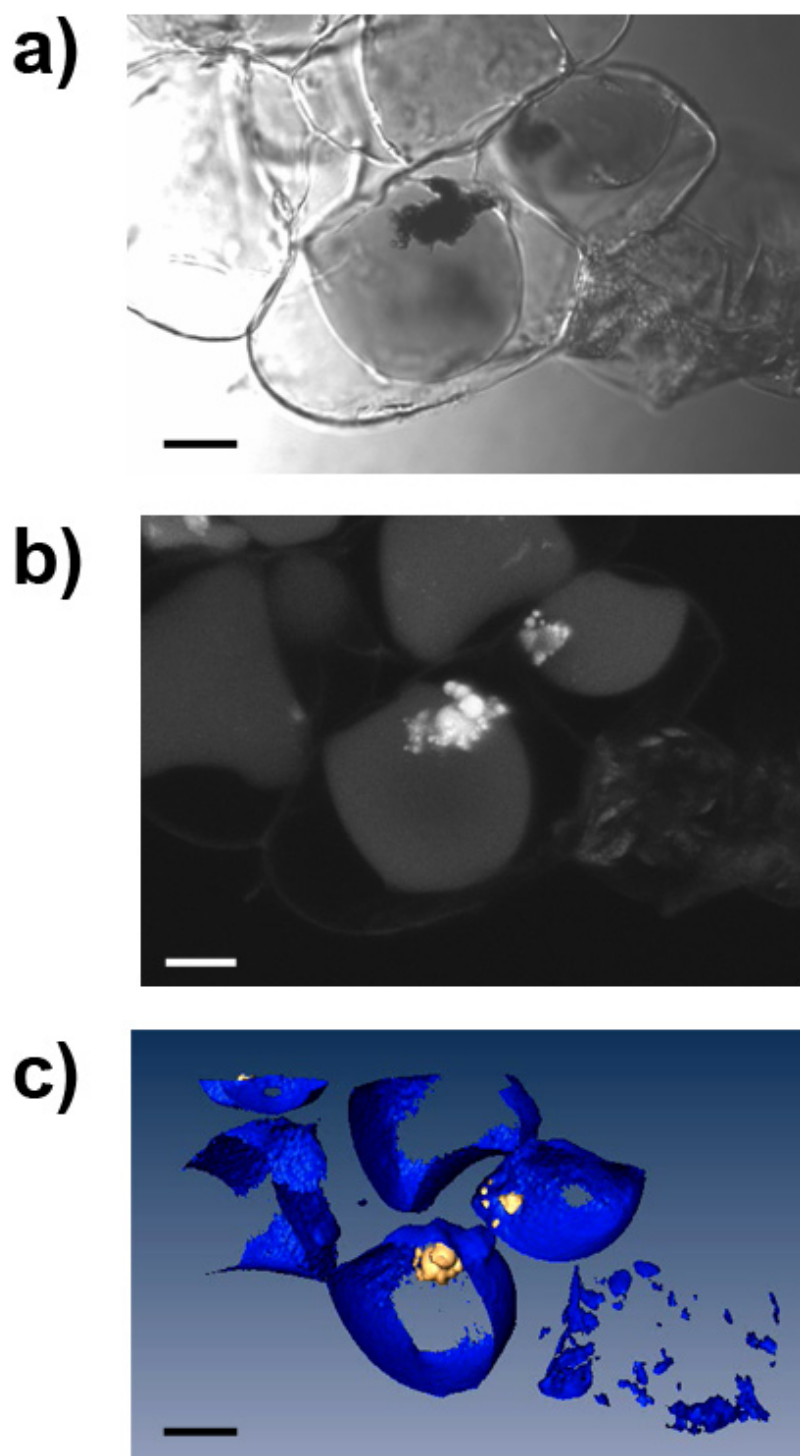


Figure 5.2: Confocal microscope images of *Vitis vinifera* L. suspension cells under a) bright-field and b) far red fluorescence modes. c) 3-dimensional reconstruction of autofluorescence for Fig. 5.2b. Maximum fluorescence (AVIs) was attributed with a yellow colour, while intermediate fluorescence (vacuoles) was given a blue boundary. 40× Magnification. Bar = 10 μ m.

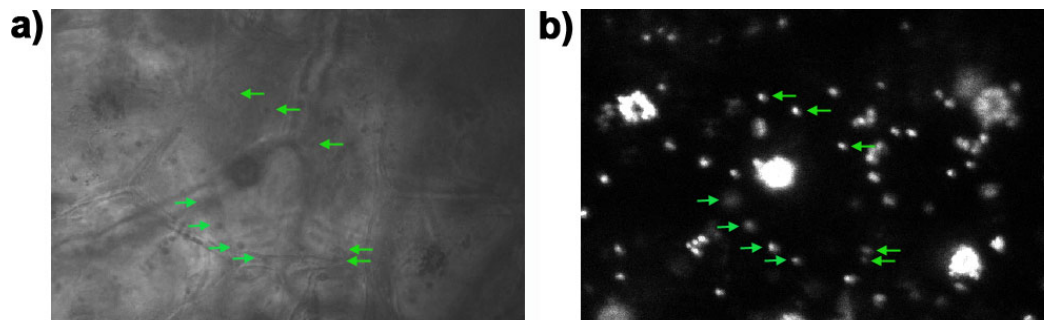


Figure 5.3: Confocal microscope images of skins from commercial red table grapes under a) bright-field and b) far red autofluorescence settings. 20× Mag. Green arrows indicate the AVIs present at the tonoplast boundary for the central cell.

Attempts were made to identify the autofluorescent compound(s) from both whole cell and AVI extracts in acidified methanol. Extracts were separated by fluorescence HPLC, yet no single compound was found to possess this autofluorescent profile (data not shown). Aqueous and acidic methanol extracts were made from whole cells and AVIs and analysed by fluorescence spectrophotometry to determine if the fluorescence resulted from the interactions of multiple compounds. Again, no far red autofluorescence was observed in these individual or combined extracts, which may indicate that the autofluorescence may be due to a fluorescence resonance energy transfer (FRET)-like, or co-pigmentation phenomenon, requiring *in vivo* conditions for the autofluorescence. Boulton (2001) and Dangles *et al.* (1993) have documented changes in the absorption spectrum of anthocyanins in non-covalent interactions with other compounds in wine and model solutions, respectively.

5.3 Formation of AVIs

5.3.1 Bombardment of Non-pigmented *V. vinifera* Cells with Anthocyanin Transcription Factors

As mentioned in Section 1.5.3.1, AVIs have previously been localised entirely to the cytoplasm in a number of species at specific stages, including grape. These observations may reflect an absolute distinction between species, or may represent the trafficking of anthocyanins by these bodies. To resolve this, a grape suspension cell bombardment assay was utilised where non-pigmented grape suspension cells were transiently transformed with *VvmybA1* (grape C1-like myb factor) and *AtEgl3* (DNA-binding bHLH factor from Arabidopsis); transcription factors capable of inducing anthocyanin accumulation in grape cells. Cells were also bombarded with eGFP, which is entirely localised to the cytosol. GFP expression was detectable after 24 hours, yet pigment only appeared between 30 and 48 hours post-bombardment (Fig. 5.4). This facilitated a study on the initial formation of these bodies, impossible with continuously subcultured pigmented cells.

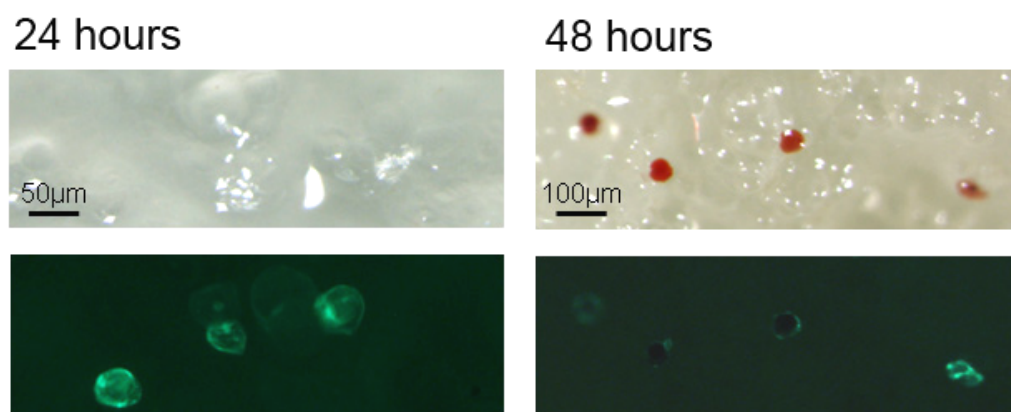


Figure 5.4: Stereo microscope images of bombarded grape cells at 24 and 48 hours post-bombardment. Bright-field images (upper), and GFP fluorescence images (lower).

5.3.2 Confocal Microscopy on AVI-containing *V. vinifera* Cells Expressing Anthocyanin Transcription Factors

At time points between 24 and 48 hours, GFP and anthocyanin positive cells were visualised by confocal fluorescence microscopy. AVIs were visible with this initial onset of pigmentation. Far red autofluorescence was diminished compared with FU-01 cells, enabling visualisation of pigmented AVIs alone, at all times up to 96 hours post-bombardment. GFP and Far Red wavelengths were simultaneously scanned with a 3-D reconstruction for an early pigmented cell, 36 hours post-bombardment (Fig. 5.5a). Figure 5.5b shows the localisation of the GFP autofluorescence as a clear cytosolic ring, with AVI complexes (Fig. 5.5c) concentrated at the cytosol/vacuole interface (Fig. 5.5d).

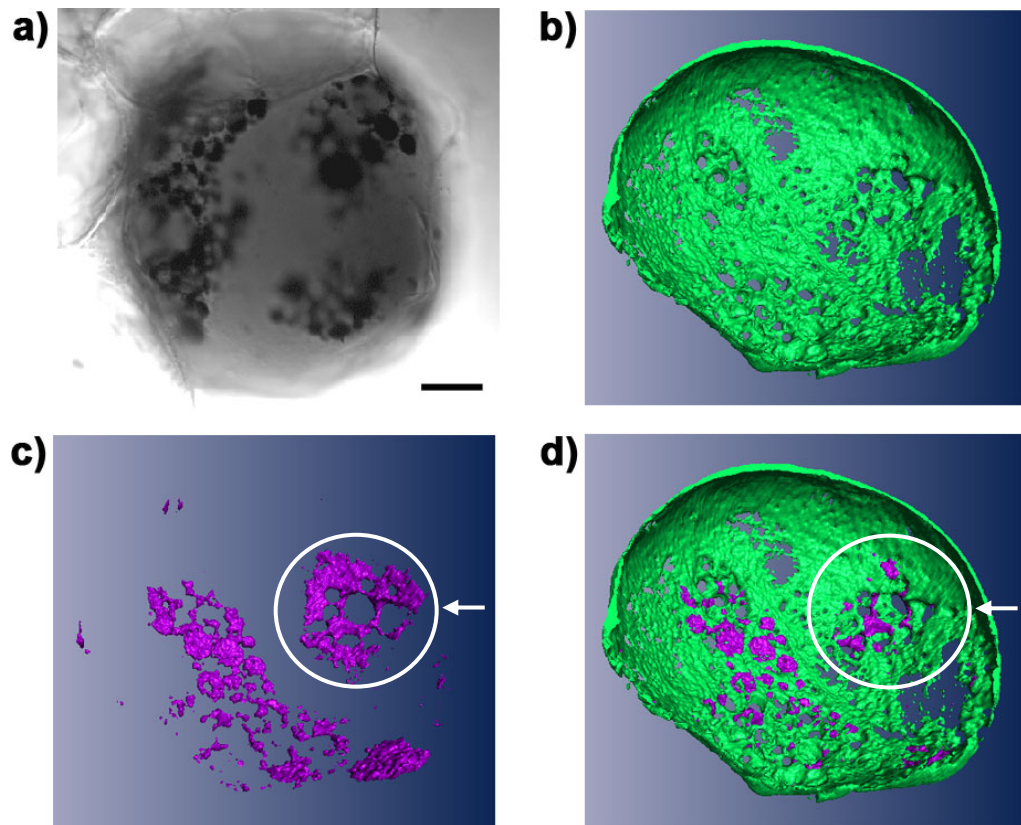


Figure 5.5: Confocal microscopy on bombarded *V. vinifera* cell at 36-hours post-bombardment. a) Bright-field image; rotated b) GFP (cytosolic) fluorescence, c) far red (AVI) fluorescence and d) merged images from above cell through vacuole. Note encircled region in Figs. c and d. Bar = 10 μ m.

All AVIs possessing this autofluorescence were also pigmented, with none visible as distinct, isolated bodies delimited by the cytosol. Much of the autofluorescent mass of bodies was contained in the cytosol (encircled regions in Fig. 5.5c and 5.5d), but were in complexes with intravacuolar bodies. Focussing on the cytosol/vacuole interface, it was evident that the AVIs traversed the cytosol and the vacuole (Fig 5.6).

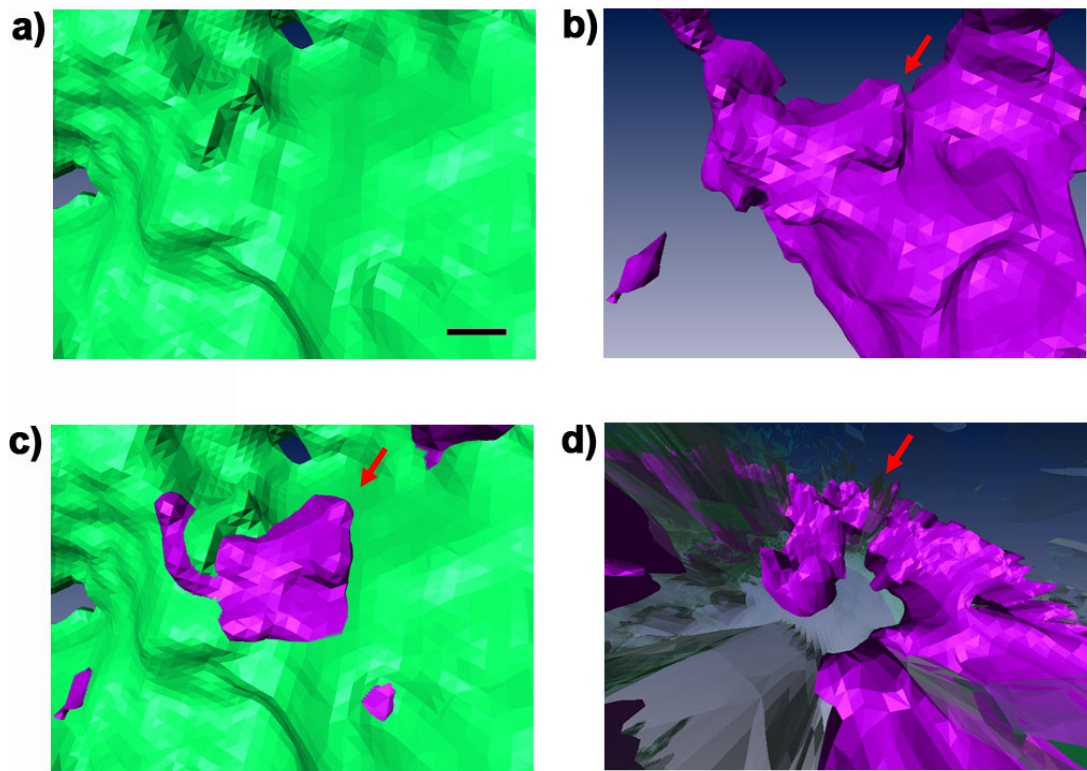


Figure 5.6: Confocal microscopy on *V. vinifera* cell at 36-hours post-bombardment. a) GFP (cytosolic) fluorescence, b) far red image, and c) merged autofluorescence (from vacuolar orientation). d) same image as a cross-section through the cytosol (vacuole beyond top-right corner). Bar = 0.5 μm . Arrow indicates same structure.

5.3.3 Intravacuolar Dynamics of AVIs

Despite using low-strength laser settings as per Di Sansebastiano *et al.* (2001) and Ruthardt *et al.* (2005) for monitoring vacuole dynamics in tobacco, this approach was detrimental to the *V. vinifera* cells and did not facilitate 4-dimensional imaging to monitor AVI shuttling, or formation. However, as with the pigmented suspension cells, AVIs were localised to the vacuole by 68 hours post-bombardment, with all of the larger ($>5\mu\text{m}$ diameter) bodies entirely localised within the vacuole (Fig. 5.2 and 5.7) Therefore, to observe the formation of larger structures from smaller bodies, the same cell was followed by

light microscopy, from 68 hrs post-bombardment (Fig. 5.7). Differently-sized bodies present at this time, were capable of moving freely around the vacuole, and forming larger complexes (Fig. 5.7; encircled region) by binding and fusing. This demonstrated that AVIs are capable of coalescing into larger structures within 1 hour.

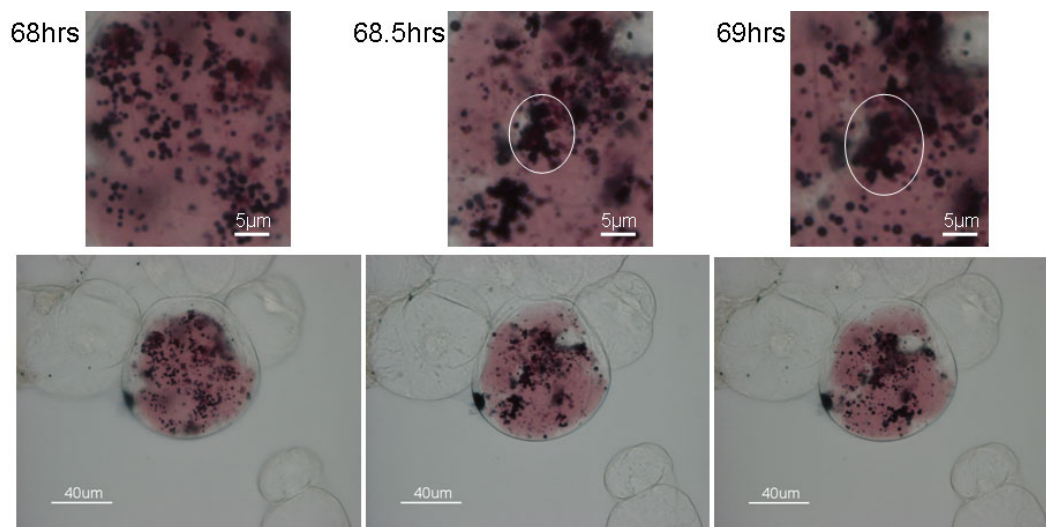


Figure 5.7: Bright-field microscopy on *V. vinifera* cell from 68-hours post-bombardment. AVI-rich region is enlarged in the upper image, with encircled region marking the same structure. 40× Mag.

In support of this observation, an increase in the average size of AVIs and a decrease in number of visible AVIs were seen over a 96-hour period in these non-pigmented grape suspension cells bombarded with anthocyanin transcription factors (Fig. 5.8). This shows that these larger AVIs arise through fusion of numerous smaller bodies. Based on this data and assuming spherical AVIs, the estimated total volume of AVIs per cell increases 7.1-fold over 48 hours. Furthermore, the increase in volume followed the increase in anthocyanin accumulation. Therefore, it would be expected that AVI volume would not

increase dramatically upon cessation of anthocyanin accumulation in these cells. However, cells did not appear viable after 120 hours, not allowing this correlation to be made.

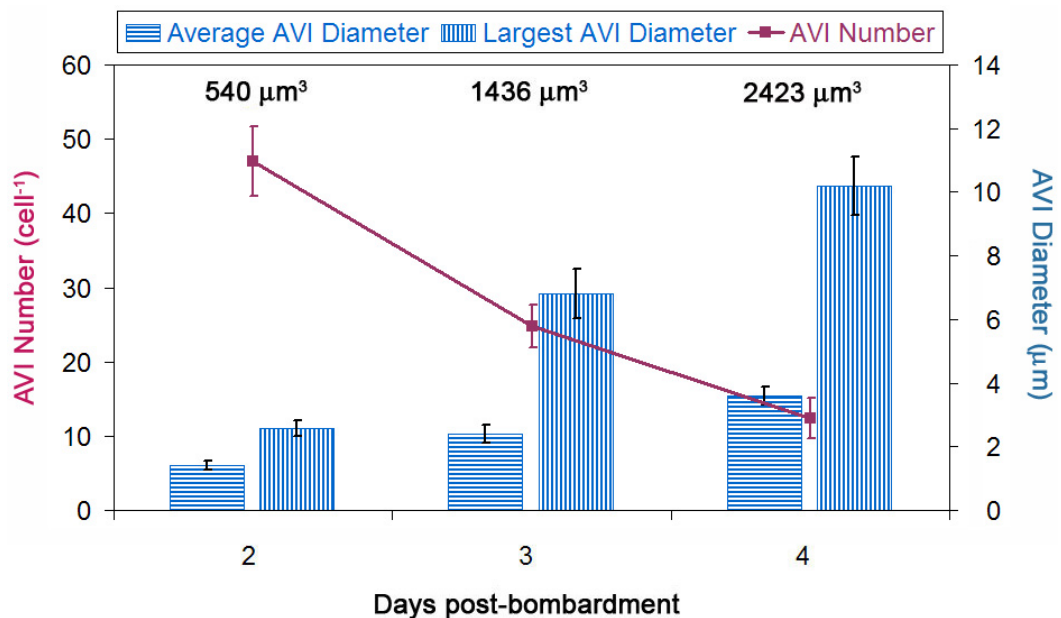


Figure 5.8: Kinetic study on bombarded *V. vinifera* cells. Average and largest AVI diameter (µm) and number of AVIs per cell. n=15 cells per time point, duplicate experiments. Estimated volume of AVIs shown for each time point (in µm³).

5.3.4 Cryogenic Scanning Electron Microscopy of AVIs

Higher magnification microscopy was important to distinguish features of the bodies, however AVIs were found to break down when cells were infiltrated with ethanol (50%-100%). These observations lead to the use of cryogenic scanning electron microscopy (cryoSEM) and freeze fracture to observe these bodies in suspension cells and callus. Numerous bodies ranging from 1-15 µm in diameter were visible in each pigmented cell (Fig. 5.9a and b), but absent in non-pigmented material. Furthermore, the proportion of AVI-containing cells within

AVI-rich callus regions and AVI-poor suspension cells counted prior to sample preparation corresponded with the prevalence of these bodies under cryoSEM, providing compelling evidence that these bodies were AVIs.

X-ray dispersive analysis (XDA) was performed on these preparations to indicate elemental composition, with larger fractured AVIs (>5 μ m diameter) utilised to avoid confounding by overlapping the 2 μ m electron beam with the background. Fig. 5.9c shows the profiles obtained for AVIs and vacuoles, with clear differences in the proportions of the dominant species – carbon, oxygen and potassium. Potassium was detected in both vacuoles and AVIs at differing levels as with the proportion of carbon:oxygen (C:O).

Fractured AVIs exposed a dense inner core, surrounded by a contrasting boundary (Fig. 5.9a). Alternate freezing and sublimation protocols were utilised to reduce the potential for this boundary to be a procedural artefact. This boundary suggested the potential for a delimiting membrane in these AVIs, as seen for radish seedlings by electron microscopy (Pecket and Small, 1982). AVIs were purified and lipid was extracted and subjected to gas chromatography (Appendix 7). AVIs were found to possess 0.029% (w/wet weight) lipid compared with the whole cell proportion of 0.044% (w/w). While the contaminating starch granules are known to have a lipid component (0.1-0.15% w/w; (Swinkels, 1985; Sreenath and Lafayette, 1992), the level of contamination in these preparations could only explain < 1.5% of the amount of lipid detected in the AVI sample (data not shown). This low lipid content indicates that AVIs are not lipid droplets, but rather suggests their membrane encasement.

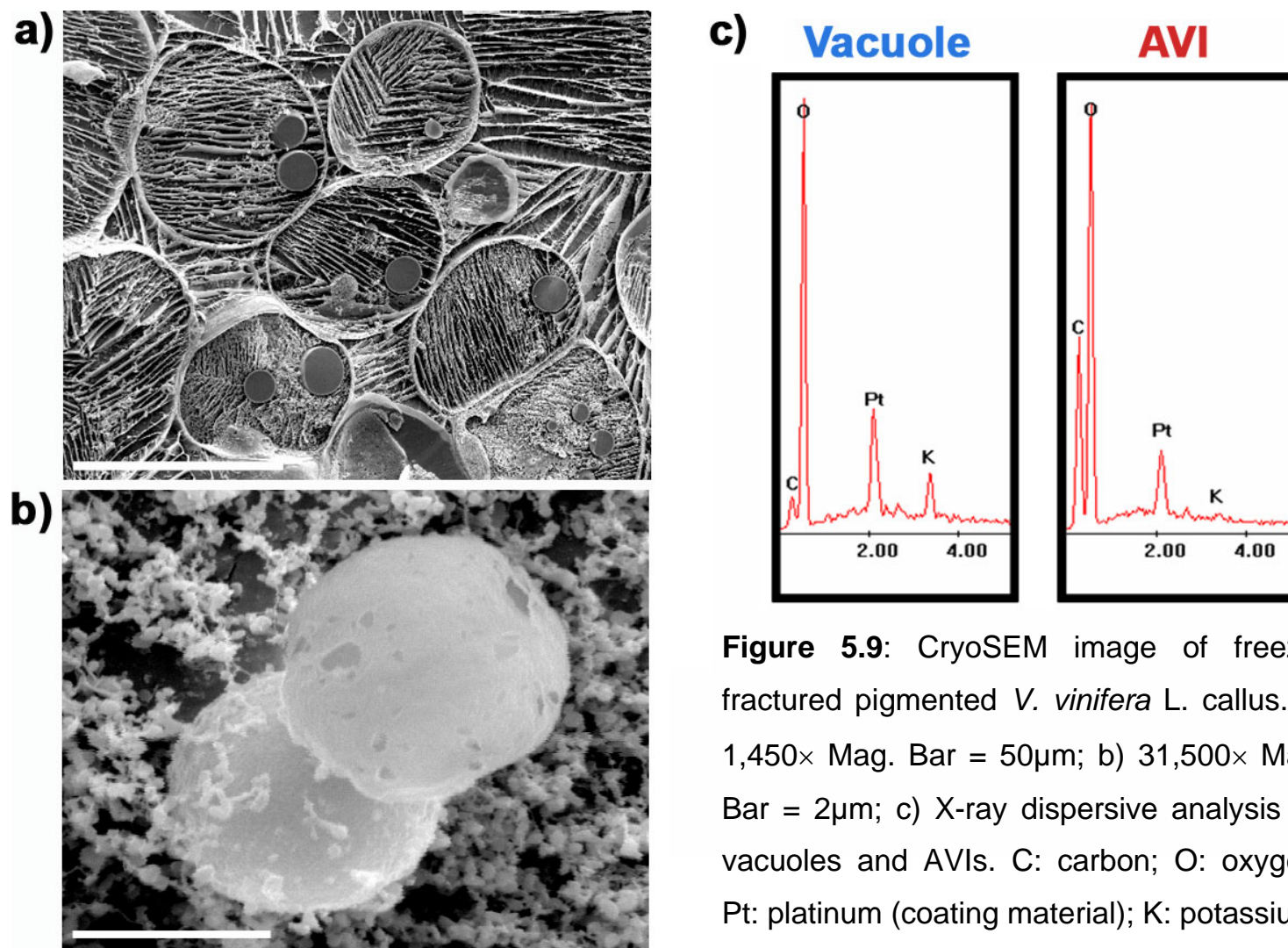


Figure 5.9: CryoSEM image of freeze-fractured pigmented *V. vinifera* L. callus. a) 1,450× Mag. Bar = 50µm; b) 31,500× Mag. Bar = 2µm; c) X-ray dispersive analysis on vacuoles and AVIs. C: carbon; O: oxygen; Pt: platinum (coating material); K: potassium.

5.4 Correlation of AVI Abundance and Anthocyanin Content in *V. vinifera*.

5.4.1 Prevalence of AVIs in *V. vinifera* Suspension Cell Lines and Callus Cultures

Grape AVIs have been observed previously in cell-suspension culture immediately following transfer from callus (Calderon *et al.*, 1993), however, they were localised to the cytoplasm. In this study, AVIs were observed only in the vacuole, and concentrated at the tonoplast interface of both continuously subcultured *V. vinifera* L. cv. Gamay Fréaux suspension cells and callus (Figure 5.1). While regions of callus used for generation of suspension cultures can have close to 90% of cells possessing AVIs, this level drops to 2-5% in routinely cultured cells (FU-01) and 7-11% in cells grown from microcallus and selected for high anthocyanin expression (FU-02), once established *in vitro* (Table 5.1). The abundance of AVIs is positively correlated with anthocyanin production, with callus possessing higher levels than suspension cells (Table 5.1). This correlation was also investigated in FU-01 suspension cells.

Table 5.1: Profile of 3-week old *Vitis vinifera* L. callus (FC) and 7-day old suspension cell lines (FU) (min. n=4 experiments. Percentage of AVI-containing cells from 1000 cells per experiment).

Description	Cell Line	AVI (%)	Anthocyanin Content (CV.g-DCW ⁻¹)
Intermediate pigmented	FC-01#	53-88%	24.1
	FU-01	2-6%	11.5
Non-pigmented	FC-02	0%	2.2
	FU-03	0%	1.0
Highly pigmented	FC-03#	75-100%	80.4
	FU-02	6-10%	40.6

Recorded in most-intense pigmented regions of each callus

5.4.2 Correlation of AVI Abundance and Anthocyanin Content in FU-01 Suspension Cells with and without Elicitation.

The AVIs in grape cells range in size from 0.5-15 μm diameter in both suspension cultures and callus, with the size and abundance appearing to be a function of anthocyanin content (Table 5.1). Anthocyanin content of FU-01 cells with and without elicitation with 10 μM jasmonic acid and light on day 4 was compared with counts of pigmented and AVI-containing cells. Figure 5.10 shows the various cells visible in FU-01 culture under light microscopy, with pigmented cells only designated if pigmentation was visible against the background.

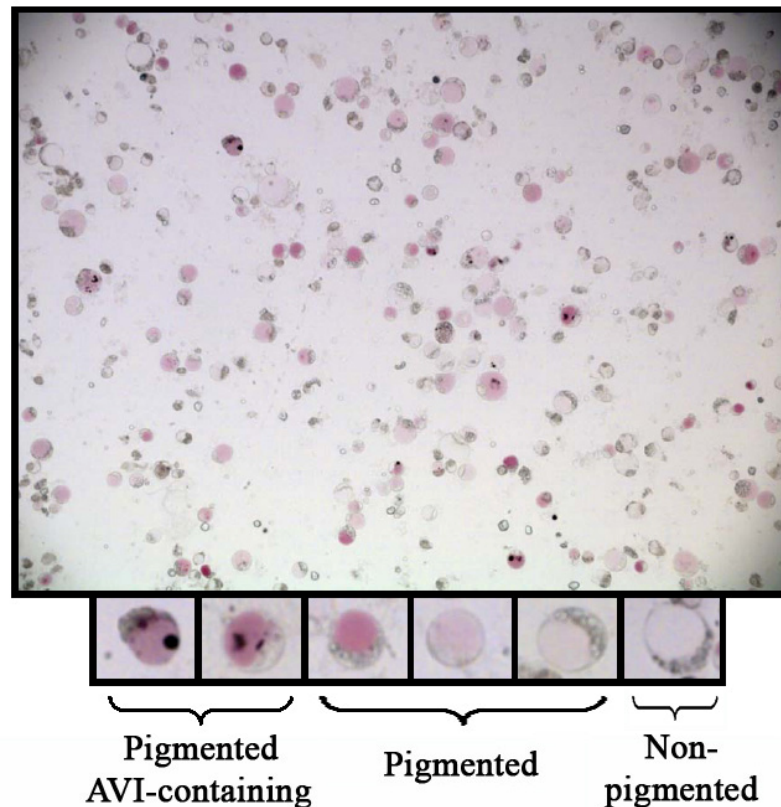


Figure 5.10: Light micrograph of FU-01 protoplasts illustrating the population heterogeneity in cellular anthocyanin content, with examples of different cell types magnified in bottom panel.

The increase in anthocyanin content was not a reflection of an increase in the number of pigmented cells (Wilson's Correlation Coefficient: $r_{FU-01}^2 = 0.15$, $r_{FU-01 + JA/L}^2 = 0.18$. Figure 5.11a), but rather was strongly correlated with an increase in the proportion of AVI-containing cells ($r_{FU-01}^2 = 0.83$, $r_{FU-01 + JA/L}^2 = 0.91$. Fig. 5.11b). A stronger correlation was seen between the size of the largest AVI per cell over the 11-day culture period ($r_{FU-01}^2 = 0.94$, $r_{FU-01 + JA/L}^2 = 0.98$. Fig. 5.11c).

These observations support those recorded in the bombarded cells (Fig. 5.8), where larger bodies increased in number over time from coalescence of smaller AVIs. Microscopically, this coalescence occurred rapidly within 1 hour (Fig. 5.7), suggesting that these bodies may be membrane-bound.

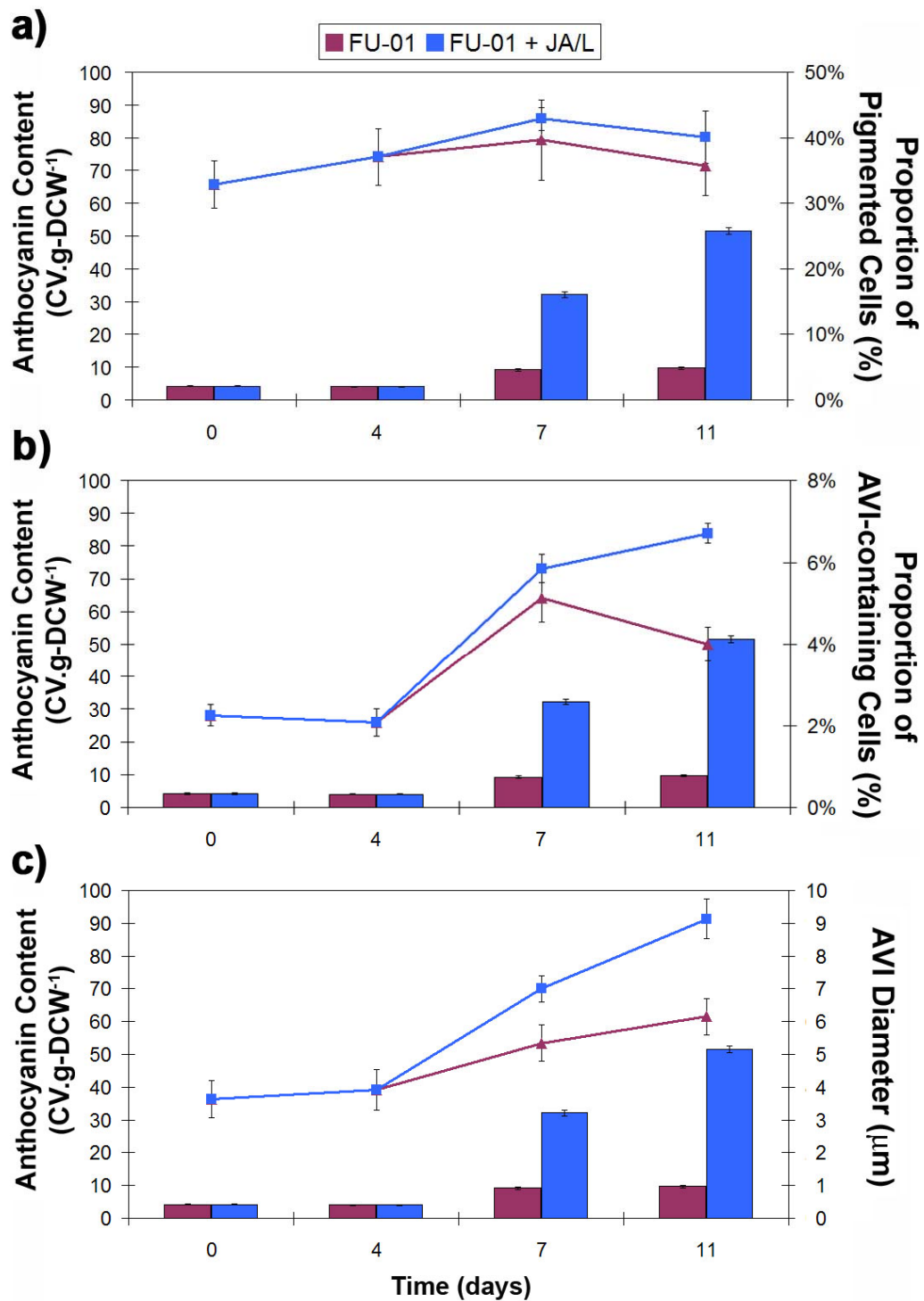


Figure 5.11: Kinetic study of FU-01 *V. vinifera* suspension cells, comparing anthocyanin content (column graphs) with a) proportion of pigmented cells (line graphs; n=10 counts of 100-120 cells, in triplicate), b) proportion of AVI-containing cells (line graphs; n=10 counts, in triplicate), and comparig c) diameter of largest AVI per cell (line graphs; n= 40 cells, minimum).

5.5 Compositional Analysis

The inability to purify AVIs from cells on a milligram scale has vitiated any detailed compositional analysis in the past. The development of an AVI purification strategy from lisianthus petals by Markham *et al.* (2000) involving protoplasting, cell lysis and density-gradient centrifugations was adapted to isolate AVIs from *V. vinifera* cell suspension cultures (Conn *et al.*, 2003).

5.5.1 Protein

Due to the insoluble nature of AVIs a number of protein solubilisation strategies were developed, including modifications from the method of Markham *et al.* (2000) for lisianthus AVIs. The type, combination and concentration of detergents used (SDS, Triton X-100, CHAPS), the pH of the solution (pH 5.5, 7.5, 9.5), the length of solubilisation, the denaturing conditions (DTT, β -ME) and the isoelectric focussing settings were all optimised to maximise the solubilisation of hydrophobic (and hydrophilic) proteins.

Protein concentration was quantified under the various solubilisation conditions, with a highly sensitive fluorescence protein estimation kit (Table 5.2).

Table 5.2: Proportion of protein extracted from AVIs (protein weight.AVI wet weight⁻¹) under various solubilisation strategies. TX-100: Triton X-100; MIX: 1% sodium deoxycholate, 0.1% SDS, 2% CHAPS.

25mM Tris, pH 7.5			7M Urea, 2M Thiourea, pH 7.5	
2% TX-100	2% SDS	MIX	2% TX-100	4% CHAPS
0.21%	0.12%	0.08%	0.23%	0.07%

All detergents tested yielded an identical profile of protein spots on a 2-D gel. However, a 2% (v/v) Triton X-100 solution in 7M Urea, 2M thiourea, 25mM DTT, 1% IPG, pH 7.5 (2%TUT) buffer solubilised the greatest amount of the insoluble pellet wet weight and yielded the largest and most reproducible number of spots on a silver-stained 2D-gel (Fig. 5.12). This strategy indicated that the AVIs were not comprised predominantly of protein as originally theorised.

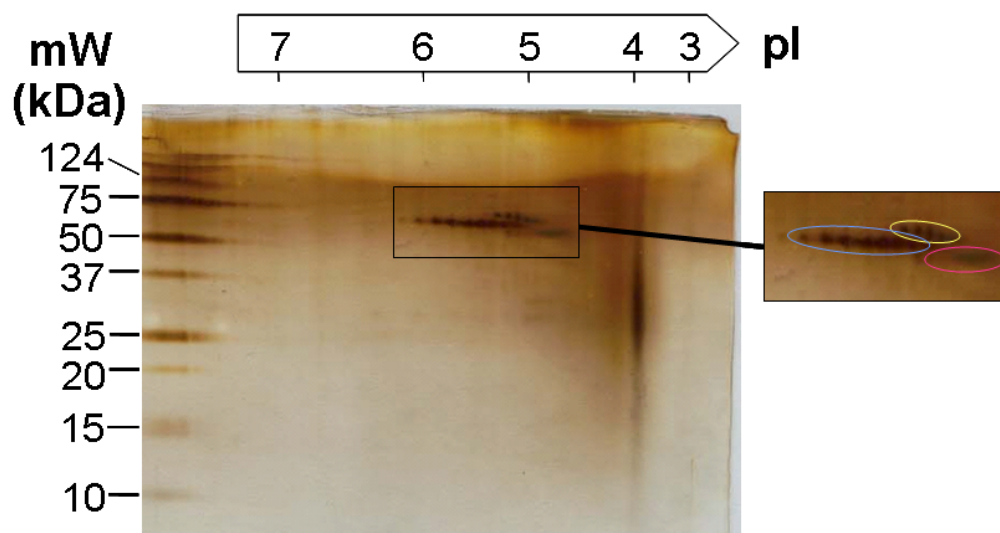


Figure 5.12: Silver-stained, 2-dimensional gel electropherogram of protein solubilised from AVIs. Enlarged region highlights 3 protein types, with encircled proteins of molecular weight 72 kDa (yellow), 68 kDa (blue) and 64 kDa (red).

Silver staining of the 2D-gels can detect proteins with a concentration less than 0.1ng, while SYPRO Ruby and Deep Purple (non-saturable, mass spectroscopy compatible stains) are less sensitive. Only three predominant bands of 64 kDa (pI~4.8), 68 kDa (pI~5-6) and 72 kDa (pI~5.1) were visualised after silver staining the solubilised protein separated by 2DGE (Fig. 5.12). These proteins were excised from a SYPRO Ruby-stained gel (Appendix 8) and

determined to be granule-bound starch synthase (GBSS) by nanoLC-MS/MS fingerprinting by their significant homology ($P < 0.0001$) to GBSS from many different species, including *Zea mays* (maize), *Z. luxurians*, *Prunus virginiana*, *Setaria italica* and *Triticum aestivum* (wheat) (Appendix 8). Estimation of starch synthase concentration on the 2D gel showed that it comprised >99.9% of total protein.

All 3 proteins analysed possessed the same protein homology, indicating they are likely to represent 3 GBSS isoenzymes. This is the first confirmation of the protein in grape, yet starch granules are clearly visible in suspension cells by light microscopy (data not shown). Their starch composition was confirmed by positive staining with iodine and plane polarised light microscopy. These granules are also very dense, possessing between 13-19% moisture content and 0.09-0.45% (w/wet weight) protein depending on source material (Swinkels, 1985; Baldwin, 2001).

Methods were undertaken to further purify the dark red AVIs from contaminating white starch grains (the source of GBSS) in order to accurately quantify the protein composition. These included additional Percoll density-gradient centrifugations and slow-speed washes with mannitol buffer. These methods yielded an AVI pellet with undetectable starch both visibly and by staining. A spectrophotometric starch assay estimated the concentration of starch at $<0.1\text{mg}\cdot\text{g}\cdot\text{WCW}^{-1}$, down from $500\text{mg}\cdot\text{g}\cdot\text{WCW}^{-1}$ before purification. This method was utilised for all compositional studies in this thesis. Once purified, the pellet was solubilised in 2%TUT and protein quantified. These results demonstrated that the protein composition did not exceed 0.0001% (w/w) – the lower limit of the protein quantification kit – in agreement with the 5000-fold

reduction in starch contamination. These results support the conclusion that the absence of protein on a 2D gel with the purified AVI pellet was not a product of the inability to uptake it into the strip or resolve it on the gel.

5.5.2 Dry mass

The purified AVI pellet was weighed (wet weight), lyophilised and the dry mass determined by microbalance measurements (0.1 μ g sensitivity). AVIs were shown to be highly dense structures, with the dry mass comprising 36.5% of the initial wet weight (66.5% water). This compares with the dry mass of the whole cell, ranging from 4.5-8.5% (w/w), increasing over the 9-day kinetic time-course. For AVIs, this proportion was constant across the kinetic period and water was deduced as the major component of this loss of mass as the proportion of volatiles would be negligible and pigment was retained, indicating anthocyanins were not lost.

5.5.3 Anthocyanin Profiles of AVIs, Vacuoles and Whole Cells

Anthocyanins were extracted from whole cells, vacuoles and purified AVIs from *V. vinifera* suspension cultured lines varying in anthocyanin content and profile. Anthocyanin was calculated to comprise $0.7 \pm 0.02\%$ (w.FCW⁻¹), and $1.85 \pm 0.05\%$ (w.DCW⁻¹) of the AVIs, regardless of cell line, elicitation strategy, or age of cells (Table 5.3). Variations were seen in FU-01 cells prior to the improved purification (M38 – 0.3% w.FCW⁻¹), while after was found to be on average 0.67% (w.FCW⁻¹) for M39, M40. This constant anthocyanin concentration (CV = 0.03%), rather than enrichment (CV = 45.4%) implies that anthocyanins composition is controlled and may be critical for AVI structure,

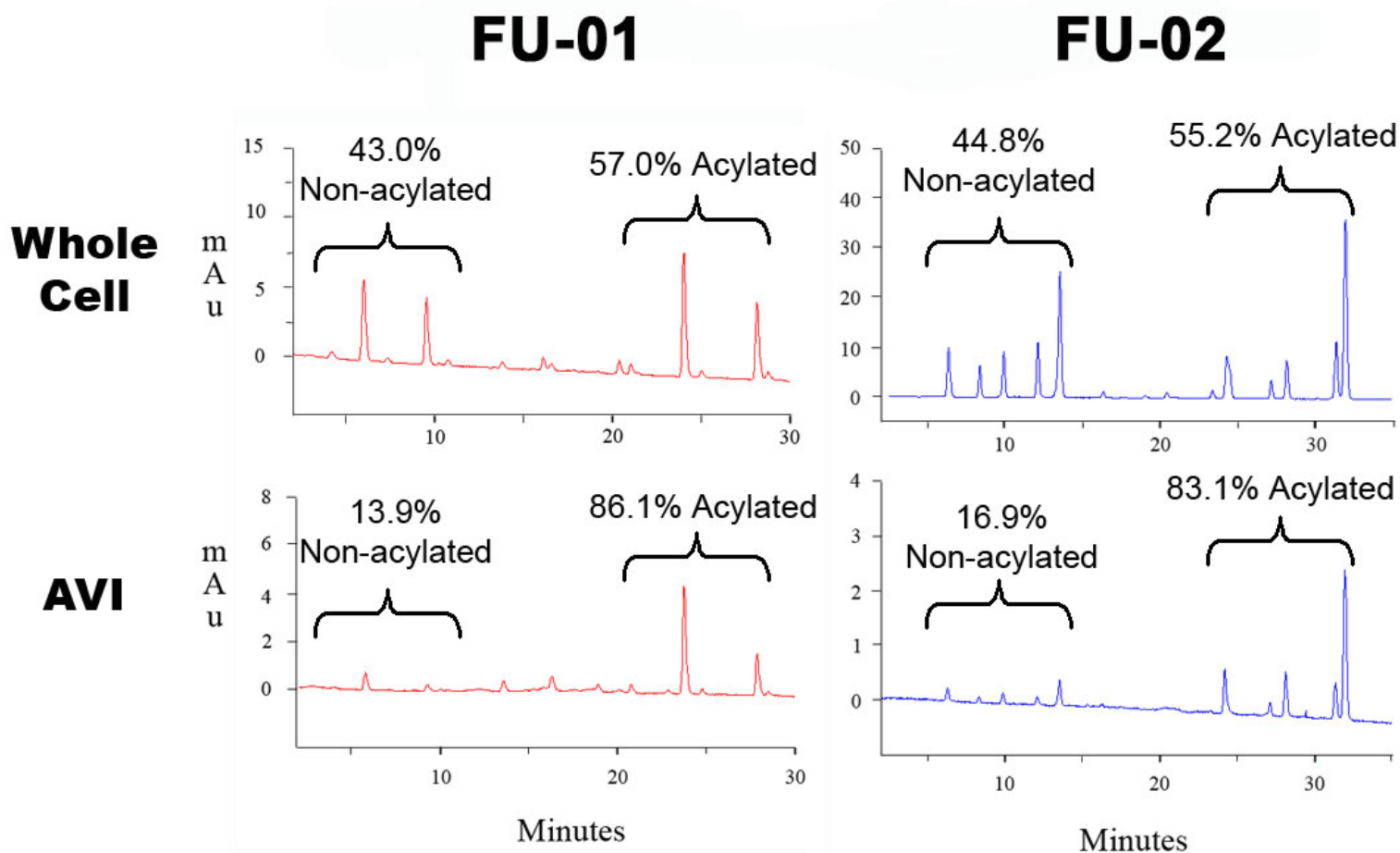
rather than being able to sequester more anthocyanin accumulating in the vacuole.

Table 5.3: Anthocyanin content of whole cells and AVIs. Enrichment of anthocyanin in AVIs calculated as the proportion of anthocyanin in AVIs compared with the whole cell profile. Values given as mean of 3 replicates and overall averages for AVI anthocyanin content ($\text{mg}\cdot 100\text{g}\text{-FCW}^{-1}$) and enrichment shown with Std. Dev.

Cell Line/ Elicitation Strategy	Age of culture (days)	Anthocyanin Content ($\text{mg}\cdot 100\text{g}\text{-FCW}^{-1}$)		Enrichment
		Whole Cell	AVI	
FU-01 (M38)	7	29.9	343	12.8
FU-01 + JA/L (M38)	7	58.9	346	5.9
FU-01 (M39)	7	25.5	689	27.2
FU-01 (M40)	7	23.2	687	30.0
FU-01 + JA/L (M40)	7	60.9	677	11.1
FU-01 (M55)	6	14.6	637	44.4
FU-01 (M63)	7	15.6	666	42.7
FU-02	6	25.3	682	27.0
FU-02	11	22.4	678	30.0
FU-02 + JA/L	7	181.4	695	4.0
AVERAGE			677 ± 18.7	29.3 ± 13.3

The anthocyanin content for high-pigmented cells (FU-02) on day 7 is over 4-fold higher than that for the intermediate-pigmented cells (FU-01; Tables 3.1 and 3.3). The major species in whole cell extracts of FU-01 are cyanidin and peonidin, while malvidin predominates in FU-02 (Fig. 5.13).

Figure 5.13: HPLC profiles of whole cell and AVI extracts of the *V. vinifera* FU-01 and FU-02 lines at 520nm. Non-acylated and acylated (*p*-coumaroylated) species are grouped and mean percentages of total peak area is shown (n=4). Peaks –
 I: C3G; II: P3G; III: M3G;
 IV: C3pCG; V: P3pCG;
 VI: M3pCG.



Comparing the anthocyanin profile from vacuoles purified as per Wagner and Seigelman (1975) with whole cell extracts showed that all intracellular anthocyanins (monoglucosides, acetylglucosides and *p*-coumaroylglucosides) were localised to the vacuole (Table 5.4). Furthermore, the ratios of the individual anthocyanin species within the non-acylated and acylated groups for both lines were maintained between whole cell, vacuolar and AVI extracts (Fig. 5.13, Table 5.4). However, the AVIs were shown to bind the acylated species (primarily *p*-coumaroylated and to a lesser extent acetylated anthocyanins) with a much higher preference than the non-acylated anthocyanins in two lines with differing profiles (Conn *et al.*, 2003).

Table 5.4: Proportions of individual anthocyanin species and combined subtypes (3-glucosides; and 3-*p*-coumaroylglucosides) in whole cell, vacuole and AVI extracts from seven day-old *V. vinifera* FU-01 and FU-02 cell lines as determined by HPLC. n=3.

Anthocyanin Species	FU-01			FU-02		
	Whole Cell	Vacuole	AVI	Whole Cell	Vacuole	AVI
Delphinidin	3.2%	2.8%	3.2%	13.8%	14.0%	14.0%
Cyanidin	46.5%	46.8%	46.3%	18.7%	18.5%	19.3%
Petunidin	1.9%	2.0%	2.0%	13.0%	13.3%	13.2%
Peonidin	46.0%	46.5%	46.3%	30.0%	29.7%	30.0%
Malvidin	2.4%	1.9%	2.2%	24.5%	24.6%	23.4%
3-Glucosides	35.2%	35.6%	13.8%	46.3%	46.0%	15.6%
<i>p</i> -coumaroylglucosides	64.8%	64.4%	86.2%	53.8%	54.0%	84.4%

Three successive extractions were performed on a single AVI pellet to validate the extraction procedure and demonstrate that no particular anthocyanins were preferentially retained after the first extraction with various solvents. While

barely distinguishable from the baseline, the anthocyanin profiles of secondary and tertiary extracts with the same or different solvents were similar to that of the primary extract and constituted <5% of the total AVI pigment in the first extract (data not shown). Furthermore, altering the acidity of the extraction solution from 5-50% acetic acid in water did not influence the profile of extracted anthocyanins.

A greater proportion of acylated (*p*-coumaroylated) anthocyanins were present in the AVI extract for the FU-01 (27.9% increase) and FU-02 (28.1% increase) lines when compared with the whole cell extract (Fig. 5.13). This resulted in a 6.2:1 ratio of acylated to non-acylated anthocyanins in the AVIs for the FU-01 line and a 4.9:1 ratio in the FU-02 line, from a 1.3:1 and 1.2:1 ratio in the whole cell (Fig. 5.13), respectively. It was prudent to determine if the AVI anthocyanin profile was dynamic with respect to changes in the whole cell profile. Therefore, kinetic analyses were undertaken on FU-01 cells with and without jasmonic acid and light elicitation.

5.5.4 Kinetic Study of Anthocyanin Profile in FU-01 Cells and AVIs

Variations were detected between the anthocyanin profiles for FU-01 (Fig. 5.14a) and FU-01 + JA/L cultures (Fig. 5.14b). Elicitation enhances the level of anthocyanin accumulation (Fig. 5.11) with an increase in the proportion of simple (non-acylated, less methylated) anthocyanins (Figs. 5.14a and b), presumably due to the increased flux through the biosynthetic pathway without a concomitant increase in anthocyanin methyltransferase and acyltransferase activity. The profile of anthocyanin species in the AVIs mimics that of the whole cell profile, but retains a clear affinity for acylated species. This was confirmed in duplicate experiments, with a representative example given in Fig. 5.14.

Despite a 16% increase in acylated anthocyanins in FU-01 cells between day 7 and 11 only a 2.8% increase is found in the AVIs (Fig. 5.14). This suggests that the level of acylated anthocyanins plateaus at around 86%, regardless of the cellular abundance. While the concentration of anthocyanin did not change significantly across the time-course (Table 5.4), the results in Fig. 5.14 suggest that the AVIs are dynamic structures, responsive to various anthocyanin types, rather than anthocyanin abundance (Table 5.4).

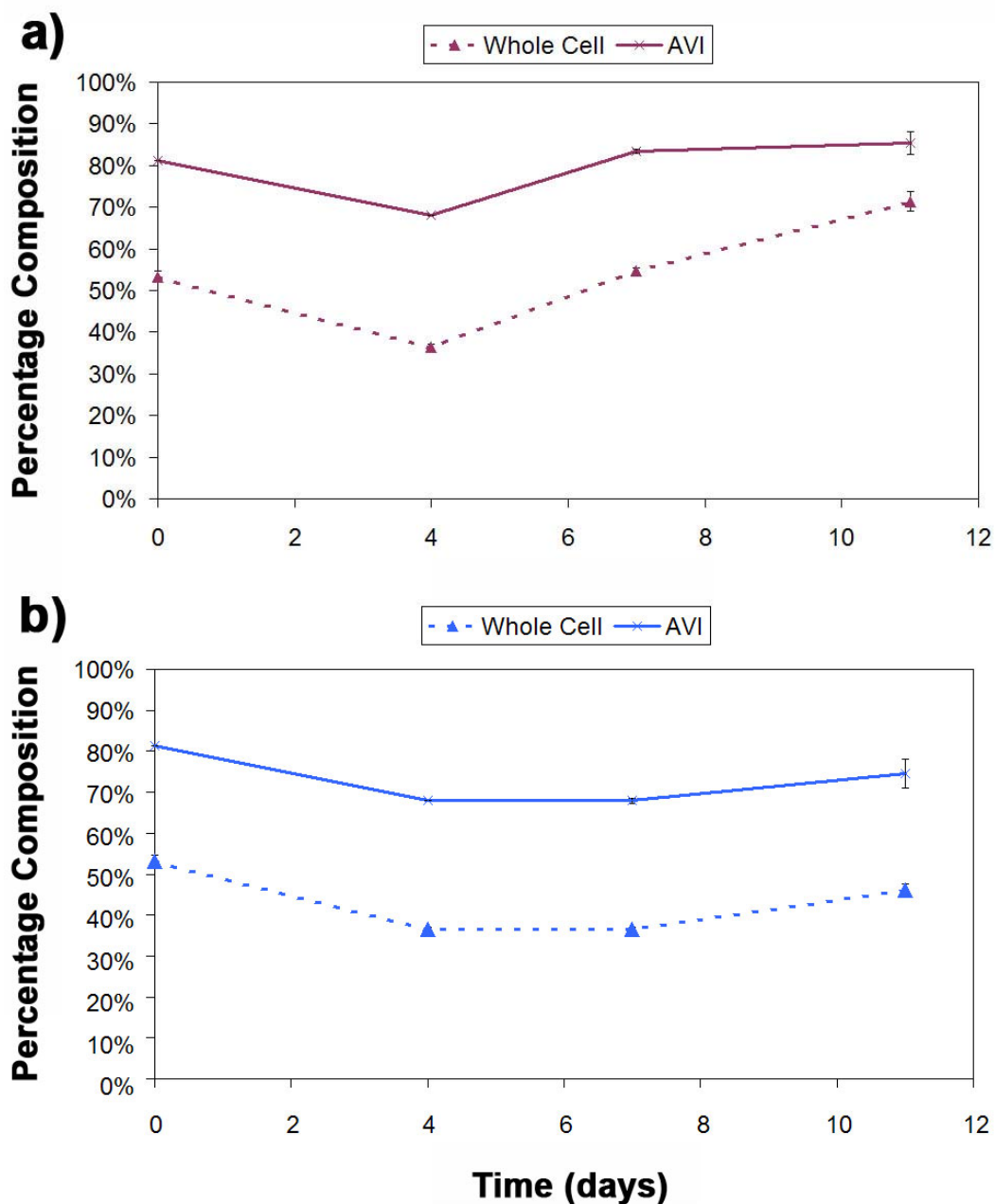


Figure 5.14: Kinetic analysis of *p*-coumaroylated anthocyanins in whole cell and AVI extracts from a) FU-01 and b) FU-01 under jasmonic acid and light treatment over an 11-day culture period (n=3).

5.5.5 Cellular Staining

A panel of stains were employed based on previous findings to identify any additional chemical substituents of the AVIs (Table 5.5). Only dilute

toluidine blue was found to stain AVIs, while starch grains were stained with iodine potassium iodide (IKI) solution and the cell wall was stained with Sudan III. Ruthenium red, a stain for pectin, did not stain the AVIs, despite reports of pectin composition in both rose and radish.

Table 5.5: Result of staining strategies on FU-01 *V. vinifera* cell cultures. Staining was performed on FU-01 suspension cells (day 4, day 7 and day 11 of culture) and FC-01 callus cultures (day 7, day 14 and day 21).

Stain	Component	AVI stained	Comments
Toluidine blue 0.005% (w/v) in PBS	Tannin	Yes	-
IKI solution 1% (w/v) KI; 1% (w/v) iodine	Starch	No	Numerous cytosolic granules stained blue/black
Ruthenium Red 0.05% (w/v)	Pectin	No	Faint colouration in cytoplasm
Sudan III 0.07% (w/v)	Lignified/suberized cell walls, Oil droplets	No	Cell wall stained

5.5.6 Tannin (proanthocyanidins)

Pigmented cells stained with dilute (0.005%) toluidine blue demonstrated a positive staining of AVIs. This was suggestive of some organic polymer, most commonly tannins, or lignin (Toriyama, 1954). A quantitative tannin analysis was undertaken on whole cells and purified AVIs by acid cleavage and phloroglucinol adduct formation according to the methods of Kennedy and Jones (2001). This technique enables stepwise cleavage of interflavan bonds with HCl, followed by formation of phloroglucinol adducts on cleaved chemicals. Terminal units (and free monomers) are not able to form adducts with phloroglucinol and so the

average chain length - given as mean degree of polymerisation (mDP) – of the tannins can be calculated by determining the number of terminal units as a proportion of the number of extension units. The amount of free monomers in the samples is subtracted from the non-adduct total by running a non-cleaved sample, giving an exact measure of terminal proanthocyanidin units.

Analysis of flavonoids was performed on cells in culture and their corresponding callus cultures. Tannins were found to accumulate in both pigmented (FU-01) and non-pigmented (FU-03) cells. However, FU-01 accumulated approximately 25% more tannin than FU-03 and elicitation with light and jasmonic acid at day 4 further enhanced the amount of tannin by ~75% in the FU-01 cells at day 7 of culture (Table 5.6). The average chain length is similar for both FU-01 and FU-03, while light and jasmonic acid elicitation leads to shorter tannin chains.

Grape seed, which accumulates 3 times the concentration of total tannins of berry skin – 4.32 and 1.39 mg-berry⁻¹, respectively – has 5-fold shorter tannin chains than berry skin (Downey *et al.*, 2003b). This trend is seen for elicited FU-01 cells, while AVIs from this line did not concentrate tannins, yet have 3-fold longer tannin chains (Table 5.6).

HPLC of uncleaved extracts highlighted further differences between the flavonoid profiles in AVIs and whole cell extracts. Peaks corresponding to unknown compounds were seen in chromatograms at 280 nm for both whole cell (~5.8; 8.9 mins) and AVI extracts (~17.4 mins; Appendix 6.3). While both peaks present in the whole cell chromatogram were found in the AVI extract, the 17.4 min peak was unique to the AVIs. Attempts to identify these compounds by LC/MS were unsuccessful and will need to be completed in the future.

Table 5.6: Extractable tannins in *V. vinifera* cells at 7 days growth (duplicate experiments), showing total extension and terminal subunits and free monomers (mg.g-FCW⁻¹). Total tannin presented as mean \pm Std. Dev. n=3. FC: callus; FU: suspension cells.

Extractable tannins as	FC-01	FU-01	FU-01 + JA/L	FU-01 AVI	FC-02	FU-03
Extension Subunits	1.136	1.492	2.578	1.248	0.866	1.193
Terminal Subunits	0.083	0.142	0.592	0.041	0.181	0.113
Free Monomers	0.032	0.000	0.331	0.000	0.000	0.061
Total Tannin (mg.g-FCW ⁻¹)	1.250 \pm 0.04	1.634 \pm 0.14	3.501 \pm 0.08	1.289 \pm 0.05	1.047 \pm 0.02	1.368 \pm 0.04
Average Chain Length (mDP)	13.760	10.525	4.355	31.49	4.790	10.53

5.6 Discussion

Lack of sufficient storage sites - either external or innate - is one possible limiting factor in anthocyanin bioprocess optimisation for suspension cell cultures. The use of artificial storage resins with suspension cultures can greatly enhance the production of specific flavonoids, in particular resveratrol (Morales *et al.*, 1998; Guiso *et al.*, 2002) and prenylated flavanones (Yamamoto *et al.*, 1996; 2001). Despite the use of artificial storage resins as a means of anthocyanin purification from plant material (Spangna and Pifferi, 1992; Di Mauro *et al.*, 2002; Scordino *et al.*, 2004), anthocyanin production in suspension cells has not been enhanced using external resins. Due to the vacuolar localisation, permeabilisation of cells was required to achieve any adsorption of anthocyanins, but this was at the expense of a reduction in cell viability (Cormier *et al.*, 1992). Therefore, enhancement of innate storage sites known to bind anthocyanins would maximise intracellular accumulation, without any known detriment to cell viability.

Various reports have analysed the prevalence and dynamics of AVIs in a variety of plant species – including grape, rose, radish, red cabbage, mung bean, *Matthiola incana*, Prunus and Japanese knotweed. Prior to this report, only in sweet potato and lisianthus have these investigations extended to biochemical and molecular characterisations, due to the inability to purify AVIs on a large-scale (Nozue *et al.*, 1995, 1997; Markham *et al.*, 2000; Xu *et al.*, 2000). Reports in grape have shown that larger AVIs develop along with an increase in anthocyanin accumulation in post-veraison berries (Kim *et al.*, 1997; Okamoto *et al.*, 2003). Furthermore, higher anthocyanic berries, including the tetraploid black ‘Kyoho’ and ‘Pione’ (*V. vinifera* x *V. labrusca*) grapes possess larger AVIs than the

anthocyanin-poor 'Beniizu' red grapes (Nakamura, 1989; Kim *et al.*, 1997; Okamoto *et al.*, 2003).

Similarly, it was found in this study that the abundance and size of the AVIs, rather than the proportion of pigmented cells was linked to the amount of anthocyanin accumulated by FU-01 *V. vinifera* L. suspension cells. This correlation along with the increase in size and volume of AVIs and decrease in number demonstrated that numerous, small AVIs must coalesce over time and that this is enhanced by anthocyanin stimulating elicitation strategies. The coalescence was observed using bombarded grape cells over a one hour time-period. A similar phenomenon was observed for AVIs in radish hypocotyls with fusion of bodies over 120 minutes (Yasuda *et al.*, 1989), while fusion of individual AVIs occurred within 5 minutes in 'Kyoho' grapes (Nakamura, 1993).

These observations on the relationship of increasing AVI size and abundance with more anthocyanin have been noted by Nakamura (1994) in grape berry skin and Yasuda and Shinoda (1985) in red radish hypocotyls. In addition, treatment of FU-01 cells with light and jasmonic acid further increased the proportion of AVI-containing cells and the diameter of the largest AVI with anthocyanin levels. The light-dependency of anthocyanin accumulation in AVIs was shown by Yasuda and Tsujino (1988) in radish seedlings. Radish AVIs grown in the light were intensely pigmented, while removal of light either pre-, or post-germination lead to the loss of pigment. The Gamay Fréaux grape suspension cells used in this study are capable of accumulating anthocyanins in the dark, and while light is not critical for AVI development, it may increase the number and total mass of these bodies per cell. As with jasmonic acid, treatment of 'Kyoho' berries with abscisic acid lead to an increase in amount of anthocyanin

accumulated and a significant increase in the diameter of the largest AVI per cell (Kim *et al.*, 1997). Growth of 'Pione' grapevines (tetraploid hybrid of Kyoho x 4x-Muscat of Alexandria) under increasing levels of nitrogenous fertiliser lead to a reduction in proportion of AVI-containing cells and anthocyanin accumulation (Okamoto *et al.*, 2003). AVI numbers and anthocyanin increased in red cabbage under nitrogen starvation and tended to decrease under phosphorous and potassium deficiencies (Hodges and Nozzolillo, 1996). This inverse relationship between growth and secondary metabolite production is well established and may be linked to an *in vivo* protective role for anthocyanins (Collin, 1987; Guardiola *et al.*, 1995; Collin, 2001).

The proportion of AVI-containing cells in FU-01 was shown to be positively correlated with cell age and anthocyanin accumulation over an 11-day culture period. Furthermore, treating cells with JA and light to enhance anthocyanin synthesis in *V. vinifera* suspension cells saw an increase in the proportion of AVI-containing cells. This results from an increase in anthocyanin synthesis per cell, not an increase in pigmented cell number. This indicates that the AVIs may occur in cells with anthocyanin accumulation above a threshold, with JA and light elicitation increasing the number of these cells in the population. Alternatively, presence of more AVIs may facilitate an higher amount of anthocyanin accumulation

This evidence suggests that targeting AVIs, or its constituents, in a rational metabolic engineering approach may facilitate enhancement of anthocyanin accumulation. An understanding of the formation and basal composition of AVIs in grape was deemed necessary to provide avenues for developing an enhancement strategy.

5.6.1 AVI Localisation and Formation

AVIs in grape suspension cells and callus were clearly localised to the vacuole, or cytosol/vacuole interface exploiting an unidentified autofluorescence strongly linked with anthocyanin localisation. In agreement with our observations, Jasik and Vancova (1992) demonstrated that osmiophilic bodies, concluded to be AVIs, were localised to the inner face of the tonoplast and not the cytoplasm, by electron microscopy on semi-thin sections of grapevine callus culture. In contrast, as mentioned in Section 1.5.3.1.6, Calderon *et al.*, (1993) found AVIs in grape to be localised to the cytosol by the inability to find them in clean vacuolar preparations. García-Florenciano *et al.* (1992) witnessed the apparent vacuolar deposition of anthocyanins by the fusion of cytoplasmically localised bodies with the tonoplast in grapevine cell culture. Therefore, the findings of Calderón *et al.* (1993) may represent the transport of these structures to the vacuole.

Furthermore, vacuolar preparations in this study did not result in a large number of AVI-containing vacuoles, which may indicate an inability to efficiently purify AVI-containing vacuoles. Autofluorescent, pigmented AVIs in our Gamay Fréaux cell line were never wholly localised to the cytosol. This was also shown in this study for Chardonnay cells immediately following bombardment with anthocyanin transcription factors to initiate anthocyanin production. This may not preclude the presence of AVIs in the cytosol, but that far red autofluorescence was not present until in contact with specific vacuolar contents. Anthocyanins have not been shown to possess this autofluorescent profile either individually, or in combination. The only known compounds with this autofluorescent profile are the phycobiliproteins (phycocyanin, phycoerythrin), common compounds in algae (Rao *et al.*, 1996). While chlorophyll b has a minor absorption peak at 647nm,

studies utilising chlorophyll autofluorescence have not detected emission under the conditions for the AVI autofluorescence (Agati *et al.*, 2005).

Presence of potassium in vacuoles by XDA on cryoSEM samples is indicative of cell viability and the integrity of the surrounding membrane in the roots and shoots of *Arabidopsis* and other plants (McCully *et al.*, 2000). The detected potassium in AVIs is also strongly suggestive of the widespread, readily precipitating salts in *Vitis* sp., potassium malate and potassium bitartrate/hydrogen tartrate (Hale, 1977; Moskowitz and Hrazdina, 1981; Possner and Kliewer, 1985; Storey, 1987). The C:O ratio in vacuoles was 1:10, while for AVIs was closer to 1:2, inferring a highly organic (carbohydrate-rich) composition for the AVIs. The presence of lipid in purified AVIs and the contrasting boundary seen under cryoSEM for the AVIs makes a compelling argument for encasement of bodies within membranes. This lipophilicity has been suggested in red cabbage and grape AVIs which possessed a strong osmiophilic reaction under electron microscopy. These bodies may be lipophilic droplets, which are common in higher plants and fungi (Matile *et al.*, 1970; Losecke *et al.*, 1980). However, the proportion of lipid in AVIs (0.5% dry mass) is low for a lipid droplet and is more supportive for a membrane encasement (Tzen *et al.*, 1993; Huang, 1996; Millichip *et al.*, 1996; Hsieh and Huang, 2004). Furthermore, when released into mannitol buffer, the AVIs do not float, as with lipid droplets (Slack *et al.*, 1980; Tzen *et al.*, 1993; Huang, 1996; Millichip *et al.*, 1996; Hsieh and Huang, 2004). Small and Pecket (1982) found a 10nm diameter membrane, similar to that of other organelle membranes, encasing vacuolar AVIs from red cabbage. It has been demonstrated that crude anthocyanins from grape skins can be solubilised in hexane (apolar) buffer by the addition of a lipophilic surfactant, through their sequestration into

reverse micelles (Kim *et al.*, 2003). There was a concomitant 4-fold intensification of colour and enhanced stability of anthocyanins in these micelles compared with acidic buffer, similar to the situation with AVIs and vacuoles in *V. vinifera*.

This study documented AVIs as globular structures traversing the tonoplast, thus the membrane may arise from the ER prior to vacuolar entry, as with bodies witnessed by Jasik and Vancova (1992) and/or through invagination of the tonoplast. As mentioned in Chapter 1, there exists much support for ER-derived vesicular trafficking of phytochemicals, including anthocyanins (Parham and Kaustinen, 1977; Hrazdina and Wagner, 1985; Grotewold, 2001). The formation of AVIs could represent the remnants of this trafficking as AVIs were seen as osmiophilic bodies in pigmented grape callus in the central vacuole, concentrated at the inner face of the tonoplast (Jasik and Vancova, 1992). However, as some cells with visible anthocyanin do not have AVIs, these may arise only under specific conditions. Also, an increase in the abundance and size of AVIs is documented with an increase in anthocyanin accumulation. Numerous, small osmiophilic globuli were seen in the cytosol of pigmented cells only, encircled by a membrane (Jasik and Vancova, 1992). Upon fusion of these vesicles with the vacuole, they were released into it, similar to the mode of transport postulated for tannins (Parham and Kaustinen, 1977). As long-chain tannin was also found as a component of *V. vinifera* AVIs this may contribute to the vesicular contents precipitating, forming the AVIs. In addition to being bound to proteins and the cell wall polysaccharides, tannin has been found as inclusions in grape berry skins as so-called 'tannin-bodies' (Amrani Jouteau *et al.*, 1994). The cause of the long-chain tannin composition of AVIs is unknown, but may be

a result of the age of the AVIs, or enzymatic conversion in the vacuole. It is also possible that leaching of shorter tannins units from the AVIs give rise to this, as with the retention of the larger acylated anthocyanins.

In addition to the composition of the AVIs, the vacuolar environment - low pH and presence of appropriate conditions (ie. salt, nutrient) - may give rise to the far red autofluorescence, unseen in the cytosol alone. Resolving this would require a combination of electron microscopic studies focusing on ER and tonoplast membranes and use of tracker dyes (either lipid, tannin or anthocyanin) with confocal microscopy.

5.6.2 AVI Composition

In vacuolar uptake experiments in *Daucus carota*, only acylated anthocyanins were taken up by intact vacuoles extracted from the same species (Hopp and Seitz 1987). However, all non-acylated anthocyanins, using vacuoles isolated from other plant species, or the absence of Mg-ATP, were excluded from the vacuole (Hopp and Seitz 1987). As all anthocyanins were found in the vacuole of *V. vinifera* cell suspension cultures, the presence of 3-monoglucosidic anthocyanins in the purified AVI extract implies that this observation is unlikely to be due to contaminating cellular material.

It was evident that the profile of the 5 specific anthocyanin species were maintained between whole cell, vacuolar and AVI extracts across an 11-day kinetic time-course. The only variation between profiles was the consistently higher acylated content of AVIs, which plateaued after reaching its maximum level. As the level of acylated anthocyanins decreased in AVI extracts following the whole cell trend and assuming no leaching of acylated anthocyanins from

AVIs, this demonstrates the involvement of new AVIs with a higher proportion of non-acylated anthocyanins. As mentioned, the inoculation of AVI-rich callus into suspension coincides with a large reduction in cells possessing AVIs. Despite this, the anthocyanin profile did not alter over the same period, but there was a large reduction in the amount of anthocyanins (Curtin, 2005). This indicates that, even with the significant selective binding of acylated anthocyanin species in AVIs, the anthocyanin contribution from the AVIs does not largely influence the overall profile. However, further study is required to determine the basis for the selectivity.

It is possible that AVIs, or its compositional units (tannin, lipid, salt) contribute to the reduction in yield of acylated anthocyanins following grape crushing prior to fermentation (Romero-Cascales *et al.*, 2005). However, there is insufficient AVI mass to account for all acylated anthocyanins in *V. vinifera*. Therefore, assuming ER-derived vesicular trafficking of all anthocyanin species, it is likely that non-acylated anthocyanins are released into the vacuole and acylated anthocyanins are preferentially retained by the AVIs. This differs from the results reported for AVIs from *Lisianthus* sp., where the primary selectivity is for diglucosidic anthocyanins (regardless of acylation status) with a preference for cyanidin (10-fold increase compared with whole cell) over delphinidin (3-fold increase; Markham *et al.* 2000).

However, both examples supported the hypothesis that an AVI protein is an ancestral enzyme, perhaps with an enzymatic activity such as a modified glucosyl-, methyl-, or acyltransferase, resulting in a higher proportion of specific anthocyanins. This hypothesis is validated by the high similarity of the sweet potato VP24 protein to the zinc metalloprotease family (Xu *et al.*, 2001) and the

fact that these enzymes possess sequence homology and similar enzymatic activity to acyltransferases (Steffens, 2000).

It was hypothesised that anthocyanin-related proteins, including acyltransferases, or integral membrane transporters may be associated with grape AVIs to cause this selectivity for acylated anthocyanins. However, only three predominant proteins, identified as GBSS isoenzymes, were found as contaminants from the AVI purification process. GBSS are a family of hydrophobic proteins which catalyse the polymerisation of sugars into starch. They associate with insoluble starch granules and can include up to 10 isozymes in the one species (Baldwin, 2001). As protein was not a major component of the AVIs, the basis of the increased acylated anthocyanin affinity may be due to a structural association/interaction with specific components of the AVIs.

AVIs have been noted in many plant species (Small and Pecket, 1980). Furthermore, research has demonstrated that they are not alike in all species in basal composition, shape, location and prevalence. In both pansy and sweet potato, the AVIs are readily soluble once liberated from vacuoles (Konczak-Islam, Pers. Comm.; Winefield, Pers. Comm.). However, AVIs in lisianthus and grape are insoluble even under strongly denaturing conditions (Markham *et al.*, 2000; Conn *et al.*, 2003). A further indication of a particular anthocyanin composition in AVIs was demonstrated by Merlin *et al.* (1985). Using resonance Raman microspectrophotometry, they were able to show that AVI-associated anthocyanins are in a neutral quinodal base form, while anthocyanins in vacuoles lacking AVIs are in the flavylium cationic form. Furthermore, the carotenoids prevalent in the vacuolar sap in the 'Pinot noir' line used were absent in the AVIs. The authors concluded that anthocyanins in AVIs are not freely in solution, but

interacting with other compounds, tannin, lipid, or salts (Merlin *et al.*, 1985). Furthermore, due to the predominant anthocyanin base form, the pH of the AVIs was concluded to be close to neutrality. While this has not been repeated in other AVI-containing species a similar result would be expected due to the AVIs insoluble structure *in situ*.

These results highlight further differences of AVIs between species. If the AVIs do result from fusion of ER-derived vesicles with the tonoplast, as proposed here, the structural differences may result directly from the composition of the vesicles. Both lisianthus and grape AVIs are insoluble once isolated from the cell, and both of these plants have a higher level of readily precipitating salts, including calcium oxalate and potassium bitartrate, than sweet potato and pansy with readily soluble AVIs upon release (Franceschi and Nakata, 2005). While VP24 expression was correlated with anthocyanin accumulation, it is not clear whether this is the cause, or result of enhanced anthocyanin accumulation. Monitoring anthocyanin accumulation in transgenic sweet potato lines overexpressing VP24 and investigating specific interactions between VP24 and various anthocyanins may resolve this.

CHAPTER 6

MAJOR PROJECT FINDINGS

Anthocyanin transport and storage were investigated as a means of optimising anthocyanin accumulation in *V. vinifera* L. suspension cell culture. Along with the cloning and characterisation of putative anthocyanin-transporting GSTs, GST1 and GST4, a clear correlation with anthocyanin accumulation was documented. This strong correlation suggests that GST-mediated anthocyanin transport may be a limiting factor in anthocyanin accumulation and a potential rational target for enhanced production. Cloning of the GST promoters may enable the rational screening of elicitors to enhance expression, thereby maximising product removal from biosynthetic complex and potential flux through the biosynthetic pathway.

The model proposed from this report has the GST protein escorting the anthocyanin and tannin compounds from the final biosynthetic reaction on the rough endoplasmic reticulum (rER) by ER-derived vesicles (Fig. 6.1). The rER is theorised to possess the integral membrane pump, and can concentrate the anthocyanin (and tannin) in budding vesicles. These vesicles (possibly via the Golgi apparatus) fuse with the central vacuole, achieving their characteristic red colour and autofluorescence. Along with this fusion, the vesicle contents, including anthocyanin and long-chain tannin either release their contents, or precipitate, with the bodies retaining a high proportion of the more hydrophobic acylated anthocyanins. While fusion of the vesicle with the vacuole removes its lipid membrane to allow the contents to enter the vacuole, a membrane boundary appears to be retained by the AVIs within the vacuole. This may be through a reverse micellar process where the AVI contents immediately precipitate upon docking with the vacuole and detaching a portion of the tonoplast. A less likely scenario given the lack of detectable protein involves the invagination of the

anthocyanin-containing vesicles by the tonoplast, thereby retaining its membrane boundary.

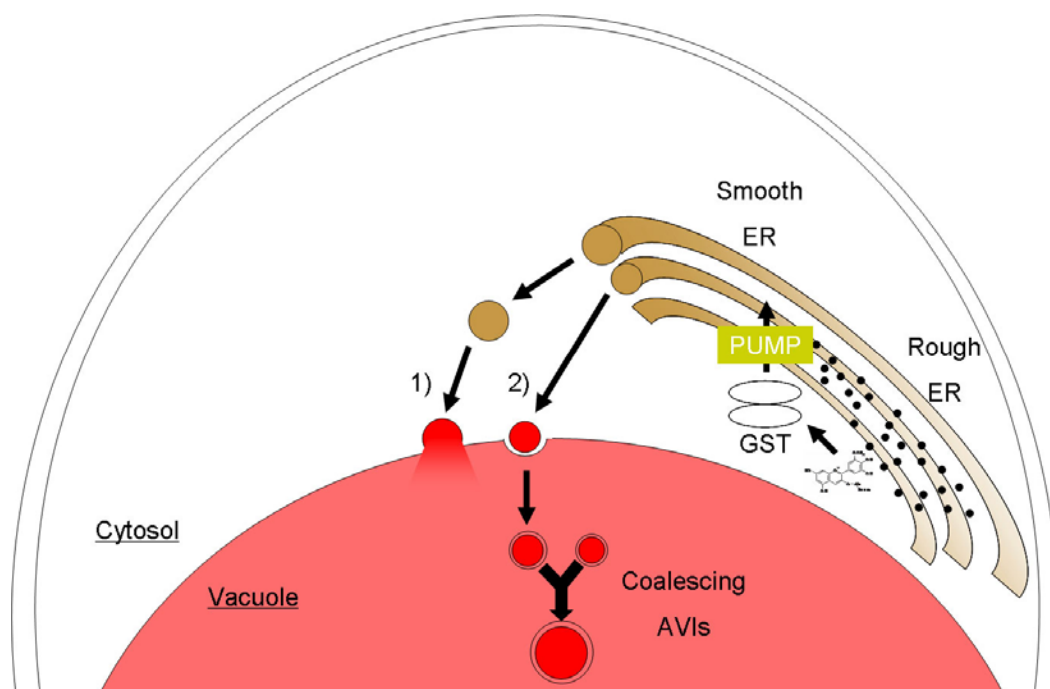


Figure 6.1: Proposed model for incorporation of AVIs and GSTs in anthocyanin transport and storage in *Vitis vinifera* L. cells. Gradient of anthocyanins in non-acidic environment in the ER represented as brown colour. Versions of anthocyanin uptake into the vacuole 1) where anthocyanins are released into the vacuole from ER-derived vesicular fusion and 2) spontaneous precipitation and formation of AVIs upon fusion with the vacuole.

As a result, the size and abundance of these bodies (AVIs) are thus correlated with anthocyanin accumulation. However, as they may be a remnant of anthocyanin transport, it may not be possible to specifically increase the amount of grape AVIs as a rational enhancement strategy. The identification of an integral protein may have facilitated a strategy to increase its expression and providing an anthocyanin storage reservoir. This may be modified to the development of

strategies to increase the prevalence of compositional units of the AVIs, or selection of an AVI-enriched population. As the concentration of anthocyanin in the AVIs is uniform, this would not only facilitate an increase in total anthocyanin, but also an enrichment of acylated anthocyanins, favoured in commercial preparations.

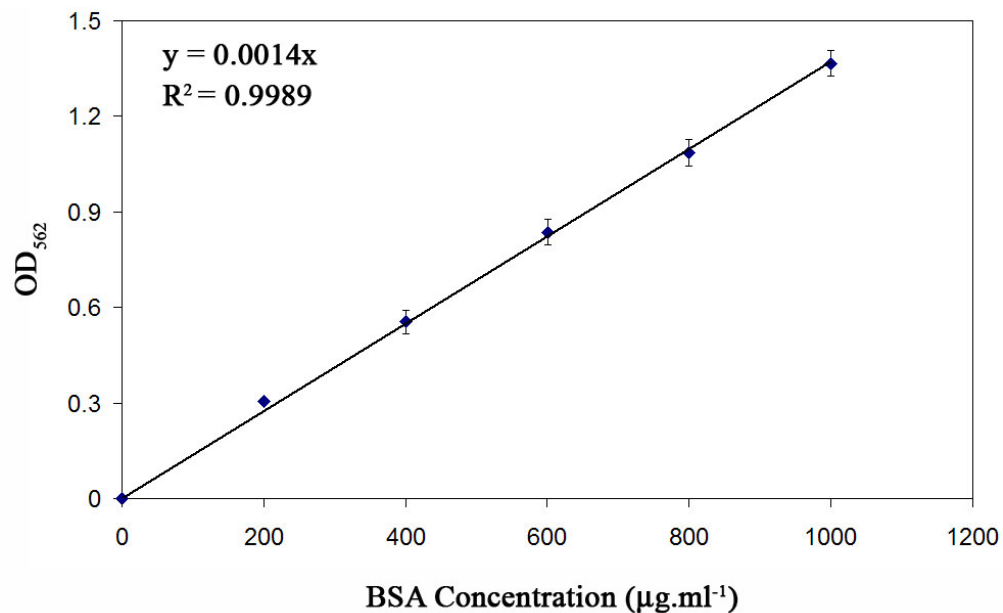
V. vinifera L. cell suspension cultures provide a useful model to study anthocyanin accumulation and a promising candidate system for their industrialised production. Integrated enhancement of both biosynthetic and post-biosynthetic pathways provide the best model for the ectopic accumulation of anthocyanins in suspension cell systems. This may provide a commercially viable cell culture strategy for anthocyanin production using *V. vinifera* L. cell suspension cultures.

Appendix 1 - B5 medium composition

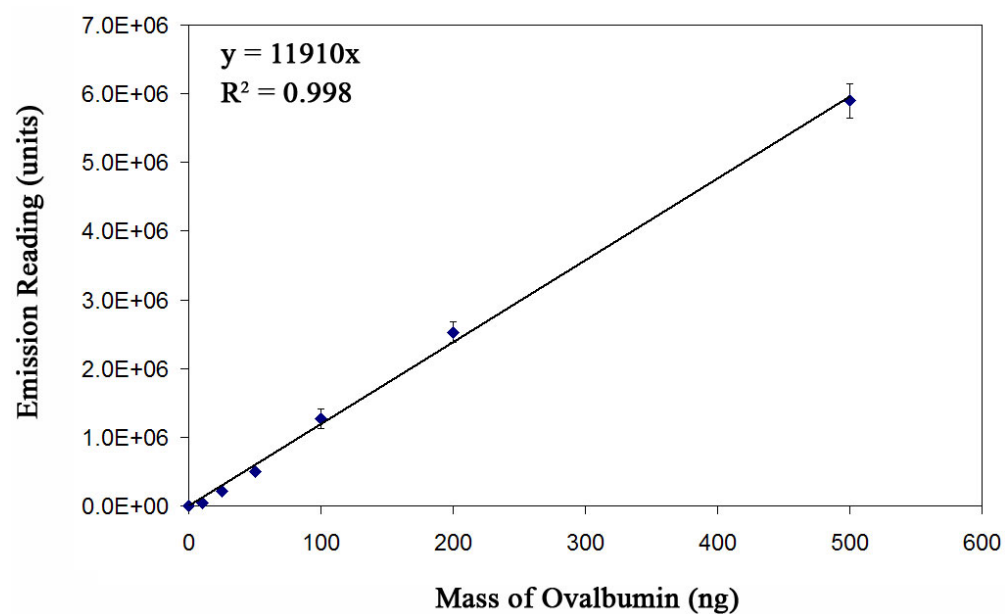
Chemical	Concentration (mg.l ⁻¹)
H ₃ BO ₃	3
MnSO ₄ .4H ₂ O	13.2
ZnSO ₄ .7H ₂ O	2
NaMoO ₄ .2H ₂ O	0.25
CoCl ₂ .6H ₂ O	0.025
CuSO ₄ .5H ₂ O	0.025
Myo-Inositol	100
Thiamine	10
Nicotinic acid	1
Pyridoxine	1
CaCl ₂ .2H ₂ O	150
KI	0.75
KNO ₃	25
MgSO ₄ .7H ₂ O	2.5
Na ₂ EDTA	0.373
FeSO ₄ .7H ₂ O	0.278
NaH ₂ PO ₄ .2H ₂ O	1.7
(NH ₄) ₂ SO ₄	1.34

Appendix 2 – Protein Standard Curves

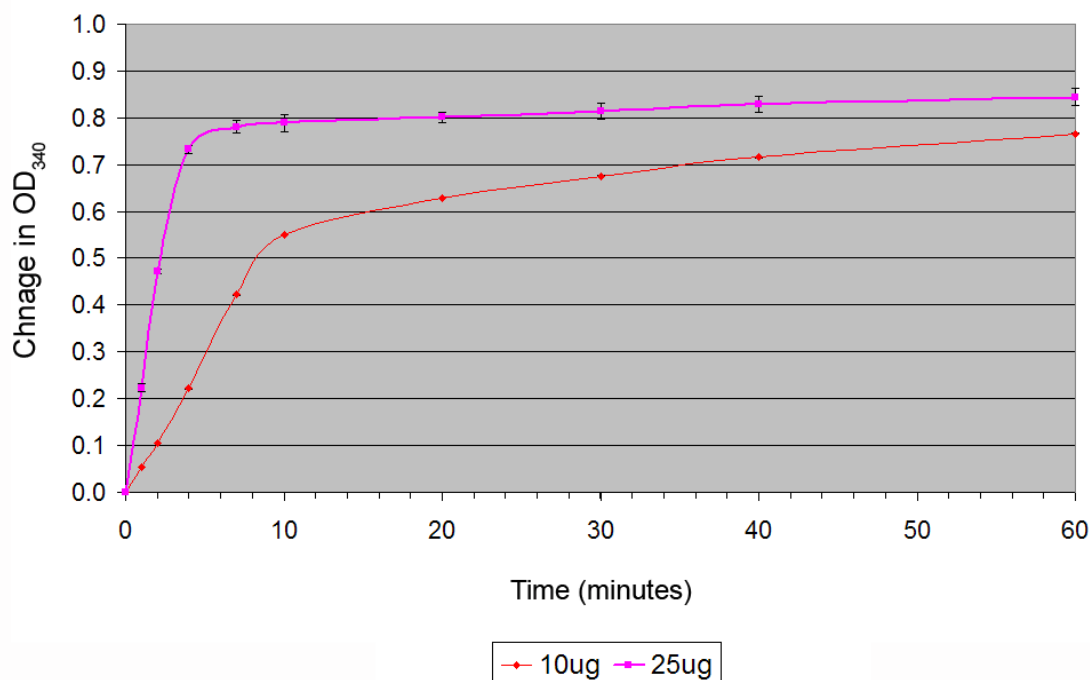
2.1 Bicinchoninic Acid Protein Quantification Assay Kit



2.2 EZQ Protein Quantification Kit



2.3 Glutathione S-transferase Assay

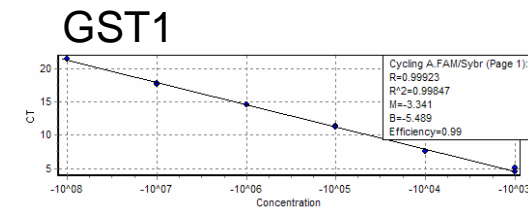


GST assay performed using FU-01 whole cell protein. Assays were performed in triplicate over 60 mins and plotted against change in OD_{340nm} against no protein control, with 10 µg and 25 µg protein added. The time-point chosen for all subsequent assays was 2 mins, ensuring change in OD₃₄₀.min⁻¹ did not exceed 0.35 for linear assay up to 25 µg protein.

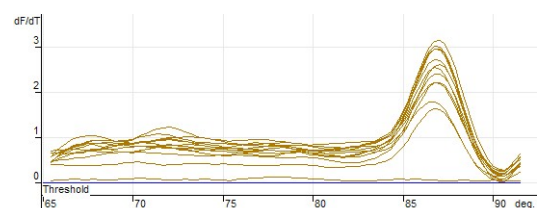
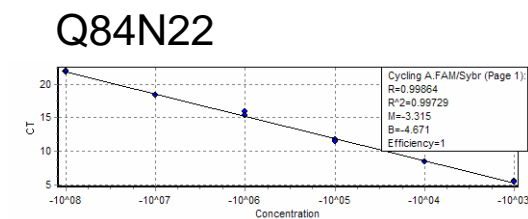
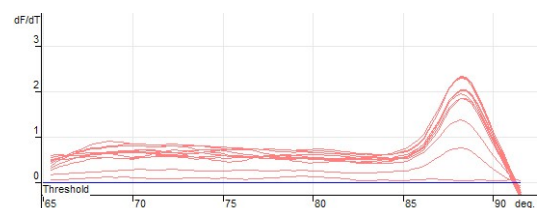
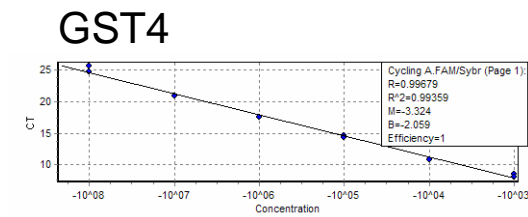
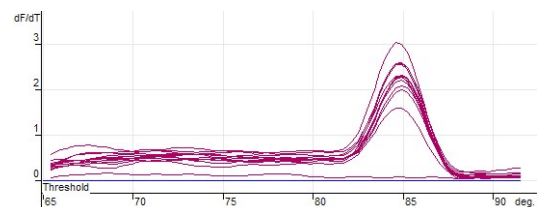
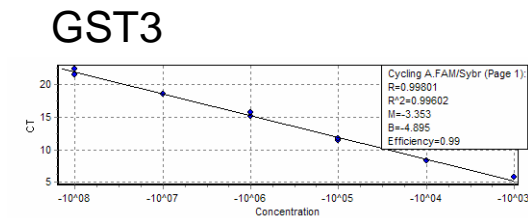
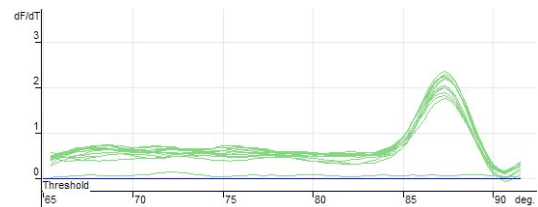
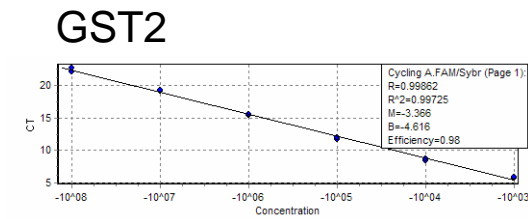
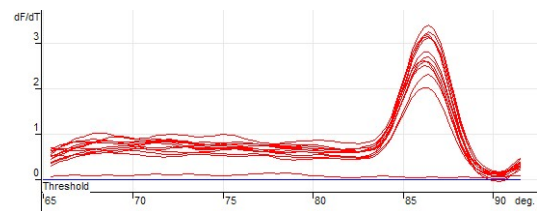
Appendix 3 – QPCR Primer Data

3.1 QPCR standard curves and melt curves for *V. vinifera* L. GSTs. PCR products were diluted (across 6 orders of magnitude) and used as templates.

Standard Curve



Melt Curve



3.2 Table summarizing variation within (Intra-assay) and between (Inter-assay) PCRs for each GST using 10⁵-fold diluted PCR product (similar results were obtained for all other dilutions).

Sequence	Intra-assay CV (%) ¹	Inter-assay CV (%) ²	Efficiency ³
GST1	1.20	2.10	2.00
GST2	1.86	1.97	1.98
GST3	2.07	2.51	1.99
GST4	1.34	1.93	2.00
Q84N22	1.50	1.79	2.00
Ubiquitin	1.34	2.01	2.00
β-Tubulin	1.37	1.94	1.89

¹ Based on Ct values for duplicate PCRs of standard dilution series (6-orders of magnitude), with CV averaged over 3 experiments.

² Derived from a minimum of 3 separate PCR runs, based on Ct values for duplicate PCRs of standard dilution series (6-orders of magnitude)

³ Derived from dilution series data using Rotorgene 6.0 software and averaged across a minimum of 3 separate runs. CV of mean efficiency was < 1% for all assays.

Appendix 4 – Mass Spectrometry Analysis of GSTs

4.1 Group 1

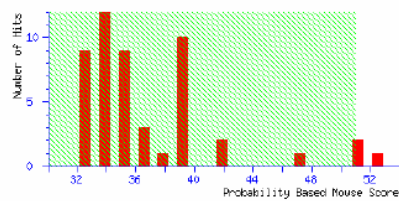
4.1.1 MASCOT Report

MASCOT Mascot Search Results

Significant hits: [TRPGTR](#) trypsin (EC 3.4.21.4) precursor - pig (tentative sequence)
[Q9FQE5](#) Glutathione S-transferase GST 13 (EC 2.5.1.18) - Glycine max (Soybean).
[Q9SXZ1](#) Dcarg-1 protein - Daucus carota (Carrot).

Probability Based Mowse Score

Score is $-10 \cdot \log(P)$, where P is the probability that the observed match is a random event.
 Individual ion scores > 51 indicate identity or extensive homology ($p < 0.05$).



Peptide Summary Report

1. [TRPGTR](#) Mass: 24394 Total score: 52 Peptides matched: 2
 trypsin (EC 3.4.21.4) precursor - pig (tentative sequence)
 Check to include this hit in error tolerant search

Query	Observed	Mr (expt)	Mr (calc)	Delta	Miss Score	Rank	Peptide
<input checked="" type="checkbox"/> 13	421.76	841.51	841.50	0.01	0 (36)	1	VATVSLPR
<input checked="" type="checkbox"/> 14	421.76	841.52	841.50	0.01	0	52	VATVSLPR

Proteins matching the same set of peptides:


[IAKSA](#) Mass: 13264 Total score: 52 Peptides matched: 2
 alpha trypsin (EC 3.4.21.4), chain A - pig
[IANIE](#) Mass: 23457 Total score: 52 Peptides matched: 2
 trypsin inhibitor, chain E - medicinal leech (fragments)
[IAVWA](#) Mass: 23460 Total score: 52 Peptides matched: 2
 trypsin (EC 3.4.21.4), chain A - pig
[IDGQA](#) Mass: 23458 Total score: 52 Peptides matched: 2
 trypsin (EC 3.4.21.4), chain A - pig
[IEPTE](#) Mass: 8814 Total score: 52 Peptides matched: 2
 Porcine e-trypsin (EC 3.4.21.4), chain B - pig

2. [Q9FQE5](#) Mass: 25182 Total score: 51 Peptides matched: 1
 Glutathione S-transferase GST 13 (EC 2.5.1.18) - Glycine max (Soybean).
 Check to include this hit in error tolerant search

Query	Observed	Mr (expt)	Mr (calc)	Delta	Miss Score	Rank	Peptide
<input checked="" type="checkbox"/> 31	691.90	1381.78	1383.75	-1.97	1	51	SADLLKYNPVHK

4.1.2 BLASTp Alignment

BLASTP2 Result

 [Bork Group's Advanced BLAST2 Search Service](#) at [EMBL](#)
[back to BLAST2](#)

Color Key: red = positive hit; green = borderline hit; black = negative result

Summary:

Sequences producing High-scoring Segment Pairs:	High Score	Total Score
sptrembl Q9FQD9 Q9FQD9 Glutathione S-transferase GST 19...	65	247
sptrembl Q9FQES Q9FQES Glutathione S-transferase GST 13...	66	207
swiss P32110 GTX6_SOYBN Probable glutathione S-transfer...	62	204
sptrembl Q9FQB1 Q9FQB1 Glutathione S-transferase GST 28...	62	185
sptrembl Q9FT21 Q9FT21 Putative glutathione S-transfera...	67	183
sptrembl Q9ZW24 Q9ZW24 Putative glutathione S-transfera...	72	182
sptrembl Q8RZB3 Q8RZB3 Putative glutathione S-transfera...	57	180
sptrembl Q9FQE7 Q9FQE7 Glutathione S-transferase GST 11...	57	147
sptrembl Q8RZB0 Q8RZB0 Putative glutathione S-transfera...	59	145
sptrembl Q9FQA3 Q9FQA3 Glutathione S-transferase GST 36...	59	143
sptrembl Q8RZB1 Q8RZB1 Putative glutathione S-transfera...	60	120
sptrembl Q8RZB2 Q8RZB2 Putative glutathione S-transfera...	56	112
swissnew P23736 T259_STAAN Type II restriction enzyme S...	55	110
sptrembl Q8S1H9 Q8S1H9 Putative glutathione transferase...	60	108
sptremblnew EAA09152 EAA09152 ENSANGP00000017280 (Fragm...	64	107
sptrembl Q9FQBS Q9FQBS Glutathione S-transferase GST 24...	54	106
sptrembl Q8S719 Q8S719 Putative glutathione S-transfera...	53	105
sptrembl Q84T17 Q84T17 Glutathione S-transferase.//:tre...	62	105
sptrembl Q9FQA0 Q9FQA0 Glutathione S-transferase GST 39...	54	104

Alignments:

^ = [sptrembl|Q9FQD9|Q9FQD9](#) Glutathione S-transferase GST 19 (EC 2.5.1.18).//:tr...
 2.5.1.18).//:tr... product: "glutathione S-transferase GST 19"; Glycine max glutathione S-transferase GST 19 mRNA, complete cds. //:gp|AF243374|11385453 glutathione S-transferase GST 19 [Glycine max]
 Length = 225

Total Score: 247

	0	50	100	150	200	225
sptrembl Q9FQD9 Q9FQD9						
Local hits (RSPs)						

Score = 65 (35.0 bits)
 Identities = 11/15 (73%), Positives = 12/15 (80%)

Query: 889 [KGVEYETLFEELSNK](#) 903
 +GVEYE L EDL NK
 Sbjct: 25 [KGVEYETLFEELSNK](#) 39

Score = 52 (28.3 bits)
 Identities = 7/13 (53%), Positives = 11/13 (84%)

Query: 2431 [BDDPLLPEEPYDR](#) 2443
 +BLLP +PY+R
 Sbjct: 78 [KKNLLPLDPYER](#) 90

Score = 49 (26.8 bits)
 Identities = 7/8 (87%), Positives = 7/8 (87%)

Query: 1228 [LEELGAME](#) 1235
 LEELG ME
 Sbjct: 165 [LEELGEME](#) 172

Score = 45 (24.8 bits)
 Identities = 6/9 (66%), Positives = 8/9 (88%)

Query: 3497 [LVNPFVHK](#) 3505
 L+ NPFVHK
 Sbjct: 44 [LVNPFVHK](#) 52

Score = 36 (20.2 bits)
 Identities = 4/6 (66%), Positives = 6/6 (100%)

Query: 4787 [BFFGGE](#) 4792
 ++FGGE
 Sbjct: 141 [KYFGGE](#) 146

4.2 Group 2

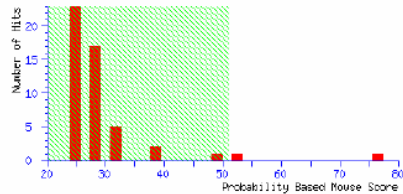
4.2.1 MASCOT Report

(MATRIX) Mascot Search Results

Significant hits: [Q84N22](#) Glutathione-S-transferase - Vitis vinifera (Grape).
[H86307](#) probable glutathione transferase [imported] - Arabidopsis thaliana

Probability Based Mowse Score

Score is $-10 \cdot \log(P)$, where P is the probability that the observed match is a random event.
 Individual ions scores > 51 indicate identity or extensive homology ($p < 0.05$).



Peptide Summary Report

1. [Q84N22](#) Mass: 15644 Total score: 77 Peptides matched: 3
 Glutathione-S-transferase - Vitis vinifera (Grape).

Check to include this hit in error tolerant search

Query	Observed	Mr(expt)	Mr(calc)	Delta	Miss Score	Rank	Peptide
2	375.71	749.41	749.41	-0.00	0	23	LYELGR
<input checked="" type="checkbox"/> 16	697.39	1392.76	1392.74	0.02	0	53	SPILLEMNPVHK + Oxidation (M)
<input checked="" type="checkbox"/> 17	465.27	1392.78	1392.74	0.04	0	(35)	1 SPILLEMNPVHK + Oxidation (M)

2. [H86307](#) Mass: 25574 Total score: 53 Peptides matched: 2
 probable glutathione transferase [imported] - Arabidopsis thaliana

Check to include this hit in error tolerant search

Query	Observed	Mr(expt)	Mr(calc)	Delta	Miss Score	Rank	Peptide
16	697.39	1392.76	1392.74	0.02	0	53	1 SPILLEMNPVHK + Oxidation (M)
17	465.27	1392.78	1392.74	0.04	0	(35)	1 SPILLEMNPVHK + Oxidation (M)

3. [Q8H9E7](#) Mass: 24956 Total score: 50 Peptides matched: 2
 Glutathione S-transferase - Cucurbita maxima (Pumpkin) (Winter squash).

Check to include this hit in error tolerant search

Query	Observed	Mr(expt)	Mr(calc)	Delta	Miss Score	Rank	Peptide
16	697.39	1392.76	1391.76	1.00	0	20	5 SPILLQMNPFVHK + Oxidation (M)
<input checked="" type="checkbox"/> 18	546.00	1634.96	1633.90	1.07	1	30	1 NKSPLLQMNPFVHK + Oxidation (M)

Proteins matching the same set of peptides:

[Q9FQE9](#) Mass: 25562 Total score: 50 Peptides matched: 2
 Glutathione S-transferase GST 10 (EC 2.5.1.18) - Glycine max (Soybean).
[Q84NH2](#) Mass: 25218 Total score: 50 Peptides matched: 2
 Glutathione S-transferase U1 - Malva pusilla.
[T06239](#) Mass: 25588 Total score: 50 Peptides matched: 2
 probable glutathione transferase (EC 2.5.1.18), 2,4-D inducible - soybean
[T09781](#) Mass: 25358 Total score: 50 Peptides matched: 2
 glutathione transferase (EC 2.5.1.18) - papaya

4.2.2 BLASTp Alignment

BLASTP2 Result



of [NORX](#) [Bork Group's](#) Advanced BLAST2 Search Service at [EMBL](#).
[back to BLAST2](#)

Color Key: red = positive hit; green = borderline hit; black = negative result

Summary:		Get the selected sequences	Reset
Sequences producing High-scoring Segment Pairs:		High Score	Total Score
sptrembl Q9FQA3 Q9FQA3	Glutathione S-transferase GST 3...	72	110
sptrembl Q9M9F4 Q9M9F4	F3F9.11.//:trembl AC013430 AC01...	66	108
sptrembl Q93WY5 Q93WY5	Putative glutathione S-transfer...	66	103
sptrembl Q9FQA7 Q9FQA7	Glutathione S-transferase GST 3...	66	101
sptrembl Q9FT22 Q9FT22	Putative glutathione S-transfer...	65	100
sptrembl Q9FQD9 Q9FQD9	Glutathione S-transferase GST 1...	84	84
sptrembl Q9FQD8 Q9FQD8	Glutathione S-transferase GST 2...	78	78
sptrembl Q9FT20 Q9FT20	Putative glutathione S-transfer...	78	78
sptrembl Q9FQE1 Q9FQE1	Glutathione S-transferase GST 1...	73	73
sptrembl Q30073 Q30073	Ferredoxin-nitrite reductase (N...	71	71
sptrembl Q9FQE4 Q9FQE4	Glutathione S-transferase GST 1...	71	71
sptrembl Q9FQE8 Q9FQE8	Glutathione S-transferase GST 1...	69	69
sptrembl Q88710 Q88710	Putative glutathione S-transfer...	69	69
sptrembl Q945X0 Q945X0	Putative glutathione S-transfer...	69	69
sptrembl Q9FQE9 Q9FQE9	Glutathione S-transferase GST 9...	68	68
sptrembl Q88560 Q88560	T12J13.14 protein (Hypothetical...	66	66
sptrembl Q945W9 Q945W9	Putative glutathione S-transfer...	66	66
sptrembl Q88718 Q88718	Putative glutathione S-transfer...	66	66
sptrembl Q9M557 Q9M557	Glutathione S-transferase (Frag...	65	65
sptrembl Q92W29 Q92W29	Putative glutathione S-transfer...	65	65
sptrembl Q92W26 Q92W26	Putative glutathione S-transfer...	65	65
sptrembl Q92W30 Q92W30	Putative glutathione S-transfer...	65	65

Alignments:

^ = [sptrembl|Q9FQA3|Q9FQA3](#) Glutathione S-transferase GST 36 (EC 2.5.1.18).//:trembl|AF244701|AF244701_1 product: "glutathione S-transferase GST 36"; Zea mays glutathione S-transferase GST 36 mRNA, complete cds.//:gp|AF244701|11386523 glutathione S-transferase GST 36 [Zea mays]
 Length = 222

Total Score: 110

	0	50	100	150	200	
sptrembl Q9FQA3 Q9FQA3						222
Local hits (HSPs)		—	—			

Score = 72 (37.9 bits)
 Identities = 9/12 (75%), Positives = 10/12 (83%)

Query: 991 [BQVEVEVLZEDL](#) 1002
 +GVEVEY EDL
 Sbjct: 27 [KQVEVEYVDEDL](#) 38

Score = 38 (20.8 bits)
 Identities = 5/9 (55%), Positives = 6/9 (66%)

Query: 1800 [TTFVEYLZE](#) 1808
 T VEY+ E
 Sbjct: 69 [TIIVEYIDE](#) 77

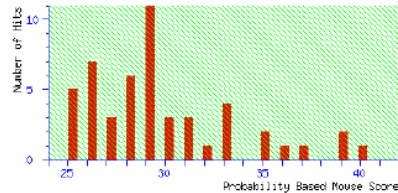
4.3 Group 3

4.3.1 MASCOT Report

(MATRIX) Mascot Search Results

Probability Based Mowse Score

Score is $-10 \cdot \log(P)$, where P is the probability that the observed match is a random event.
Individual ions scores > 51 indicate identity or extensive homology ($p < 0.05$).



Peptide Summary Report

1. [TRPGTR](#) Mass: 24354 Total score: 40 Peptides matched: 2
trypsin (EC 3.4.21.4) precursor - pig (tentative sequence)

Check to include this hit in error tolerant search

Query	Observed	Mr (expt)	Mr (calc)	Delta	Miss Score	Rank	Peptide
<input checked="" type="checkbox"/> 4	421.76	841.51	841.50	0.01	0	40	1 VATVSLPR
<input checked="" type="checkbox"/> 5	421.77	841.52	841.50	0.02	0	(38)	1 VATVSLPR

Proteins matching the same set of peptides:

[1AKSA](#) Mass: 13284 Total score: 40 Peptides matched: 2
alpha trypsin (EC 3.4.21.4), chain A - pig
[1AN1E](#) Mass: 23457 Total score: 40 Peptides matched: 2
trypsin inhibitor, chain E - medicinal leech (fragments)
[1AVWA](#) Mass: 23460 Total score: 40 Peptides matched: 2
trypsin (EC 3.4.21.4), chain A - pig
[1D3OA](#) Mass: 23458 Total score: 40 Peptides matched: 2
trypsin (EC 3.4.21.4), chain A - pig
[1EPTB](#) Mass: 8814 Total score: 40 Peptides matched: 2
Porcine e-trypsin (EC 3.4.21.4), chain B - pig

2. [GTH_SILCU](#) Mass: 24453 Total score: 40 Peptides matched: 2
Glutathione S-transferase (EC 2.5.1.18) (GST class-phi).- Silene cucubalus (Alpen leimkraut).

Check to include this hit in error tolerant search

Query	Observed	Mr (expt)	Mr (calc)	Delta	Miss Score	Rank	Peptide
<input checked="" type="checkbox"/> 8	482.77	963.52	963.50	0.02	0	40	1 VLDVYEAR
<input checked="" type="checkbox"/> 9	482.77	963.52	963.50	0.02	0	(38)	1 VLDVYEAR

Proteins matching the same set of peptides:

[1BXSA](#) Mass: 23912 Total score: 40 Peptides matched: 2
glutathione s-transferase, chain A - mouse-ear cress
[GTH4_ARATH](#) Mass: 23983 Total score: 40 Peptides matched: 2
Glutathione S-transferase FM24 (EC 2.5.1.18) (24 kDa auxin-binding protein) (GST class-phi).- Arabidopsis thaliana (Mou
[Q9LQ43](#) Mass: 24036 Total score: 40 Peptides matched: 2
Atpm24.1 glutathione S transferase.- Arabidopsis thaliana (Mouse-ear cress).
[Q9SBE3](#) Mass: 11019 Total score: 40 Peptides matched: 2
Tl4P8.11 protein (Fragment).- Arabidopsis thaliana (Mouse-ear cress).
[Q94BT5](#) Mass: 19729 Total score: 40 Peptides matched: 2
At2g47730/F17A22.12.- Arabidopsis thaliana (Mouse-ear cress).
[AAA33930](#) Mass: 24584 Total score: 40 Peptides matched: 2
SIPGTSTF NID: - Silene vulgaris
[S35269](#) Mass: 24114 Total score: 40 Peptides matched: 2
glutathione transferase (EC 2.5.1.18) gst2 - Arabidopsis thaliana
[Q42913](#) Mass: 11746 Total score: 40 Peptides matched: 2
Glutathione-S-transferase (Fragment).- Arabidopsis thaliana (Mouse-ear cress).
[AAC63629](#) Mass: 24062 Total score: 40 Peptides matched: 2
AC009309 NID: - Arabidopsis thaliana
[CAA64613](#) Mass: 23689 Total score: 40 Peptides matched: 2
ATGST6 NID: - Arabidopsis thaliana
[D84442](#) Mass: 24106 Total score: 40 Peptides matched: 2
probable glutathione S-transferase [imported] - Arabidopsis thaliana
[H84918](#) Mass: 29213 Total score: 40 Peptides matched: 2
glutathione S-transferase (GST6) [imported] - Arabidopsis thaliana


3. [T48065](#) Mass: 24637 Total score: 39 Peptides matched: 2
Glutathione transferase III-like protein - Arabidopsis thaliana

Check to include this hit in error tolerant search

Query	Observed	Mr (expt)	Mr (calc)	Delta	Miss Score	Rank	Peptide
<input checked="" type="checkbox"/> 10	490.28	978.55	978.54	0.01	0	39	1 AITAYIAEK
<input checked="" type="checkbox"/> 11	490.29	978.57	978.54	0.03	0	(26)	1 AITAYIAEK

4.3.2 BLASTp Alignment

BLASTP2 Result

 of [Bork Group](#)'s Advanced BLAST2 Search Service at [EMBL](#)
[back to BLAST2](#)

Color Key: red = positive hit; green = borderline hit; black = negative result

Summary:

Sequences producing High-scoring Segment Pairs:	High Score	Total Score
tr Emb1 AF288176 AF288176.1 gene: "GST6"; product: "glut..."	64	160
sptrembl Q9LZI9 Q9LZI9 Glutathione transferase III-like...	65	116
sptrembl Q9FQD7 Q9FQD7 Glutathione S-transferase GST 21...	60	111
sptrembl Q9LC43 Q9LC43 Atgpm24.1 glutathione S transfera...	64	104
sptremblnew AAP583395 AAP583395 Glutathione S-transferase...	64	104
sptremblnew AAP583394 AAP583394 Glutathione S-transferase...	64	104
sptremblnew AAP583393 AAP583393 Glutathione S-transferase...	64	104
swiss Q9SLM6 GTIC_ARATH Glutathione S-transferase 16 (E...	64	104

Alignments:

^ = [tr Emb1|AF288176|AF288176.1](#) gene: "GST6"; product: "glutathione S-transferase"; Arabidopsis thaliana glutathione S-transferase (GST6) mRNA, complete cds. //:pironly|H84918|H84918 glutathione S-transferase (GST6) [imported] - Arabidopsis thaliana//:gp|AF288176|11128454 glutathione S-transferase [Arabidopsis thaliana]
 Length = 263

Total Score: 160

	0	60	120	180	240	263
tr Emb1 AF288176 AF288176.1						
Local hits (HSPs)						

Score = 64 (34.4 bits)
 Identities = 8/9 (88%), Positives = 9/9 (100%)

Query: 2772 [BVLDVVEAR](#) 2780
 +VLDVVEAR
 Sbjct: 192 [KVLDVVEAR](#) 200

Score = 48 (26.2 bits)
 Identities = 6/9 (66%), Positives = 8/9 (88%)

Query: 1264 [BALTAYLAE](#) 1272
 +A+I YLAE
 Sbjct: 117 [RAITQYLAE](#) 125

Score = 48 (26.2 bits)
 Identities = 7/10 (70%), Positives = 9/10 (90%)

Query: 879 [PAAVDELEAK](#) 888
 PAAV++LE K
 Sbjct: 180 [PAAVQLEGGK](#) 189

^ = [sptrembl|Q9LZI9|Q9LZI9](#) Glutathione transferase III-like protein.//:tr Emb1|AL162651|ATF26K9_19 gene: "F26K9_190"; product: "Glutathione transferase III-like protein"; Arabidopsis thaliana DNA chromosome 3, BAC clone F26K9 //:pironly|T48065|T48065 Glutathione transferase III-like protein - Arabidopsis thaliana//:gp|AL162651|7362756 Glutathione transferase III-like protein [Arabidopsis thaliana]
 Length = 219

Total Score: 116

	0	50	100	150	200	219
sptrembl Q9LZI9 Q9LZI9						
Local hits (HSPs)						

Score = 65 (34.9 bits)
 Identities = 7/10 (70%), Positives = 10/10 (100%)

Query: 1264 [BALTAVLAEK](#) 1273
 +A+TAV+AEK
 Sbjct: 68 [RAITAVIAEK](#) 77

Score = 51 (27.8 bits)
 Identities = 6/9 (66%), Positives = 8/9 (88%)

Query: 2772 [BVLDVVEAR](#) 2780
 ++LDVVE R
 Sbjct: 143 [KILDVVEER](#) 151

```

^ = sptrembl|Q9FQD7|Q9FQD7 Glutathione S-transferase GST 21 (EC 2.5.1.18)
(Fragment) //:trmbl|AF243376|AF243376.1 product: "glutathione
S-transferase GST 21"; Glycine max glutathione S-transferase GST
21 mRNA, partial cds. //:gp|AF243376|11385457 glutathione
S-transferase GST 21 [Glycine max]
Length = 206

Total Score: 111

          0          50          100          150          200          | 206
sptrembl|Q9FQD7|Q9FQD7 |-----|
Local hits (HSPs)      |-----|

Score = 60 (32.4 bits)
Identities = 7/10 (70%), Positives = 9/10 (90%)

Query: 1264 BALTAVLAEK 1273
      +A+TAY AEK
Sbjct: 56 RAITAVVAEK 65

Score = 51 (27.8 bits)
Identities = 7/7 (100%), Positives = 7/7 (100%)

Query: 2773 VLDVYEA 2779
      VLDVYEA
Sbjct: 132 VLDVYEA 138

^ = sptrembl|Q8LC43|Q8LC43 Atpm24.1 glutathione S
transferase //:trmbl|AY086805|AY086805.1 product: "Atpm24.1
glutathione S transferase"; Arabidopsis thaliana clone 27915 mRNA,
complete sequence. //:gp|AY086805|21555418 Atpm24.1 glutathione S
transferase [Arabidopsis thaliana] //:gpnew|AY086805|21555418
Atpm24.1 glutathione S transferase [Arabidopsis thaliana]
Length = 212

Total Score: 104

          0          50          100          150          200          | 212
sptrembl|Q8LC43|Q8LC43 |-----|
Local hits (HSPs)      |-----|

Score = 64 (34.4 bits)
Identities = 8/9 (88%), Positives = 9/9 (100%)

Query: 2772 BVLDVYEA 2780
      +VLDVYEA
Sbjct: 146 KVLDVYEA 154

Score = 40 (22.2 bits)
Identities = 4/8 (50%), Positives = 7/8 (87%)

Query: 1264 BALTAVLA 1271
      +A+T Y+A
Sbjct: 69 RAITQVIA 76

```

4.4 Group 4

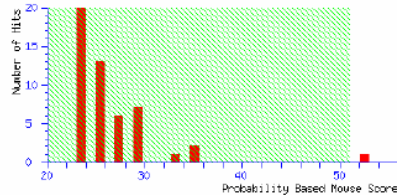
4.4.1 MASCOT Report

MASCOT Mascot Search Results

Significant hits: [TRPGTR](#) trypsin (EC 3.4.21.4) precursor - pig (tentative sequence)

Probability Based Mowse Score

Score is $-10 \cdot \log(P)$, where P is the probability that the observed match is a random event.
Individual ions scores > 51 indicate identity or extensive homology ($p < 0.05$).



Peptide Summary Report

1. [TRPGTR](#) Mass: 24394 Total score: 52 Peptides matched: 2
trypsin (EC 3.4.21.4) precursor - pig (tentative sequence)

Check to include this hit in error tolerant search

Query	Observed	Mr (expt)	Mr (calc)	Delta	Miss Score	Rank	Peptide
<input checked="" type="checkbox"/> 3	421.76	841.51	841.50	0.01	0	52	1 VATVSLPR
<input checked="" type="checkbox"/> 4	421.76	841.51	841.50	0.01	0	(30)	2 VATVSLPR

Proteins matching the same set of peptides:

[LAKSA](#) Mass: 13284 Total score: 52 Peptides matched: 2
alpha trypsin (EC 3.4.21.4), chain A - pig

[IANLE](#) Mass: 23457 Total score: 52 Peptides matched: 2
trypsin inhibitor, chain E - medicinal leech (fragments)

[IAVWA](#) Mass: 23460 Total score: 52 Peptides matched: 2
trypsin (EC 3.4.21.4), chain A - pig

[LDSCA](#) Mass: 23458 Total score: 52 Peptides matched: 2
trypsin (EC 3.4.21.4), chain A - pig

[LEPTB](#) Mass: 8814 Total score: 52 Peptides matched: 2
Porcine e-trypsin (EC 3.4.21.4), chain B - pig

2. [F72423](#) Mass: 40834 Total score: 35 Peptides matched: 1
hypothetical protein TM0053 - Thermotoga maritima (strain MSB8)

Check to include this hit in error tolerant search

Query	Observed	Mr (expt)	Mr (calc)	Delta	Miss Score	Rank	Peptide
<input checked="" type="checkbox"/> 3	489.76	977.50	977.48	0.02	0	35	1 VFEBIGER


3. [E984713](#) Mass: 1845 Total score: 34 Peptides matched: 2
H.SAPIENS JALPHA 07 PEPTIDE.- Homo sapiens (Human).

Check to include this hit in error tolerant search

Query	Observed	Mr (expt)	Mr (calc)	Delta	Miss Score	Rank	Peptide
<input checked="" type="checkbox"/> 3	421.76	841.51	841.50	0.01	0	34	2 GITLSVRP
<input checked="" type="checkbox"/> 4	421.76	841.51	841.50	0.01	0	(24)	4 GITLSVRP

4.4.2 BLASTp Alignment

BLASTP2 Result

 of [Bork Group](#)'s Advanced BLAST2 Search Service at [EMBL](#)
back to BLAST2

Color Key: red = positive hit; green = borderline hit; black = negative result

Summary: [Get the selected sequences](#) [Reset](#)

Sequences producing High-scoring Segment Pairs:	High Score	Total Score
sptrembl Q945X0 Q945X0 Putative glutathione S-transferase...	66	136
sptrembl Q9FUE4 Q9FUE4 Putative glutathione S-transferase...	66	100
sptrembl Q9FQA4 Q9FQA4 Glutathione S-transferase GST 35...	66	66
sptrembl Q92S19 Q92S19 Glutathione transferase (EC 2.5....	66	66
pdb 1GWC 1GWC-A THE STRUCTURE OF A TAU CLASS GLUTATHIO...	66	66
sptrembl Q9SB98 Q9SB98 Glutathione transferase (EC 2.5....	66	66
sptrembl Q9FQE3 Q9FQE3 Glutathione S-transferase GST 15...	66	66
sptrembl Q9FQ97 Q9FQ97 Glutathione S-transferase GST 42...	66	66

Alignments:

```

^ = sptrembl|Q945X0|Q945X0 Putative glutathione S-transferase
OsGSTU8.//:sptremblnew|AAP54756|AAP54756 Putative glutathione
S-transferase.//:tremlnew|AC091680|AC091680_10 gene:
"OSJNBa0034L04.4"; product: "putative glutathione S-transferase";
Oryza sativa chromosome 10 BAC OSJNBa0034L04 genomic sequence,
complete sequence. //:tremlnew|AE017114|AE017114_49 product:
"putative glutathione S-transferase"; Oryza sativa (japonica
cultivar-group) chromosome 10, section 68 of 77 of the complete
sequence. //:tremlnew|AC113948|AC113948_26 gene:
"OSJNBb0038A07.6"; product: "putative glutathione S-transferase";
Oryza sativa chromosome 10 BAC OSJNBb0038A07 genomic sequence,
complete sequence. //:treml|AC091680|AC091680_10 gene:
"OSJNBa0034L04.4"; product: "putative glutathione S-transferase";
Oryza sativa chromosome 10 BAC OSJNBa0034L04 genomic sequence,
complete sequence. //:treml|AC113948|AC113948_26 gene:
"OSJNBb0038A07.6"; product: "putative glutathione S-transferase";
Oryza sativa chromosome 10 BAC OSJNBb0038A07 genomic sequence,
complete sequence. //:treml|AF402798|AF402798_1 product: "putative
glutathione S-transferase OsGSTU8"; Oryza sativa subsp. japonica
putative glutathione S-transferase OsGSTU8 mRNA, complete cds.
//:gp|AF402798|15430713 putative glutathione S-transferase OsGSTU8
[Oryza sativa subsp. japonica] [Oryza sativa (japonica
cultivar-group)]//:gp|AC113948|22213181 putative glutathione
S-transferase [Oryza sativa (japonica
cultivar-group)]//:gp|AE017114|31433214 putative glutathione
S-transferase [Oryza sativa (japonica
cultivar-group)]//:gp|AC091680|20143543 putative glutathione
S-transferase [Oryza sativa (japonica
cultivar-group)]//:gpnew|AC091680|20143543 putative glutathione
S-transferase [Oryza sativa (japonica cultivar-group)]
Length = 234

```

Total Score: 136

```

          0          50          100          150          200          234
sptrembl|Q945X0|Q945X0 |-----|
Local hits (HSPs)    |-----|

```

Score = 66 (35.4 bits)
Identities = 8/9 (88%), Positives = 9/9 (100%)

Query: 1380 [LLPADPYER](#) 1388
+LLPADPYER
Sbjct: 87 ILPADPYER 95

Score = 36 (20.1 bits)
Identities = 5/5 (100%), Positives = 5/5 (100%)

Query: 945 [GHDEL](#) 949
GHDEL
Sbjct: 3 GHDEL 7

Score = 34 (19.1 bits)
Identities = 4/4 (100%), Positives = 4/4 (100%)

Query: 2211 [WLER](#) 2214
WLER
Sbjct: 196 WLER 199

4.5 Group 5

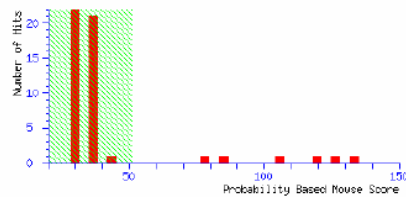
4.5.1 MASCOT Report

MATRIX Mascot Search Results

Significant hits: [T06239](#) probable glutathione transferase (EC 2.5.1.18), 2,4-D inducible - soybean
[Q84N22](#) Glutathione-S-transferase.- Vitis vinifera (Grape).
[Q9FQB8](#) Glutathione S-transferase GST 10 (EC 2.5.1.18).- Glycine max (Soybean).
[H86307](#) probable glutathione transferase [imported] - Arabidopsis thaliana
[Q8CYM1](#) GST7 like protein (Putative glutathione transferase).- Arabidopsis thaliana (Mouse-
[TRPGTR](#) trypsin (EC 3.4.21.4) precursor - pig (tentative sequence)

Probability Based Mowse Score

Score is $-10 \cdot \log(P)$, where P is the probability that the observed match is a random event.
 Individual ions scores > 51 indicate identity or extensive homology ($p < 0.05$).



Peptide Summary Report

1. [T06239](#) Mass: 25588 Total score: 133 Peptides matched: 7
 probable glutathione transferase (EC 2.5.1.18), 2,4-D inducible - soybean
 Check to include this hit in error tolerant search


Query	Observed	Mr (expt)	Mr (calc)	Delta	Miss	Score	Rank	Peptide
<input checked="" type="checkbox"/> 23	415.55	1243.62	1243.57	0.05	1	43	1	YBYKEDLR
<input checked="" type="checkbox"/> 28	697.40	1392.78	1391.76	1.02	0	28	4	SPLLLQMNPFVHK + Oxidation (M)
<input checked="" type="checkbox"/> 29	465.28	1392.80	1391.76	1.04	0	(26)	3	SPLLLQMNPFVHK + Oxidation (M)
<input checked="" type="checkbox"/> 36	507.97	1520.90	1519.85	1.05	1	(24)	6	SPLLLQMNPFVHK + Oxidation (M)
<input checked="" type="checkbox"/> 37	381.23	1520.91	1519.85	1.05	1	28	2	SPLLLQMNPFVHK + Oxidation (M)
<input checked="" type="checkbox"/> 40	545.99	1634.95	1633.90	1.06	1	(27)	1	NKSPLLLQMNPFVHK + Oxidation (M)
<input checked="" type="checkbox"/> 41	409.75	1634.97	1633.90	1.07	1	35	2	NKSPLLLQMNPFVHK + Oxidation (M)

2. [Q84N22](#) Mass: 15644 Total score: 126 Peptides matched: 6
 Glutathione-S-transferase.- Vitis vinifera (Grape).
 Check to include this hit in error tolerant search

Query	Observed	Mr (expt)	Mr (calc)	Delta	Miss	Score	Rank	Peptide
<input checked="" type="checkbox"/> 5	375.70	749.39	749.41	-0.01	0	22	3	LYELGR
<input checked="" type="checkbox"/> 28	697.40	1392.78	1392.74	0.04	0	75	1	SPLLLEMNPFVHK + Oxidation (M)
<input checked="" type="checkbox"/> 29	465.28	1392.80	1392.74	0.06	0	(35)	1	SPLLLEMNPFVHK + Oxidation (M)
<input checked="" type="checkbox"/> 30	465.28	1392.81	1392.74	0.06	0	(35)	1	SPLLLEMNPFVHK + Oxidation (M)
<input checked="" type="checkbox"/> 36	507.97	1520.90	1520.84	0.06	1	29	1	SPLLLEMNPFVHK + Oxidation (M)
<input checked="" type="checkbox"/> 37	381.23	1520.91	1520.84	0.07	1	(27)	3	SPLLLEMNPFVHK + Oxidation (M)

4.5.2 BLASTp Alignment

BLASTP2 Result

 of [Bork Group's Advanced BLAST2 Search Service](#) at [EMBL](#)
back to [BLAST2](#)

Color Key: red = positive hit; green = borderline hit; black = negative result

Summary:

Sequences producing High-scoring Segment Pairs:	High Score	Total Score
sptrembl Q9M9F4 Q9M9F4	F3F9.11.//:treml AC013430 AC01...	79 435
sptrembl Q49821 Q49821	Glutathione transferase (EC 2.5...	78 254
sptrembl P93132 P93132	Auxin-induced protein.//:treml...	70 213
sptrembl Q49235 Q49235	2,4-D inducible glutathione S-t...	70 211
sptrembl Q8H9E6 Q8H9E6	Glutathione S-transferase.//:tre...	71 207
sptrembl Q84N22 Q84N22	Glutathione-S-transferase.//:tr...	77 186
sptrembl Q9SHH7 Q9SHH7	Putative glutathione transferas...	77 180
sptrembl Q84VH2 Q84VH2	Glutathione S-transferase U1.//...	70 178
sptrembl Q9AW96 Q9AW96	Glutathione S-transferase.//:tr...	60 174
sptrembl Q81602 Q81602	Glutathione S-transferase.//:tr...	71 173
sptrembl Q9FQE3 Q9FQE3	Glutathione S-transferase GST 1...	70 170
sptrembl Q40480 Q40480	C-7 protein.//:treml X64399 NT...	82 149
swiss P25317 GTMA_TOBAC	Probable glutathione S-transfer...	77 145
sptrembl Q9AYN3 Q9AYN3	Glutathione S-transferase.//:tr...	67 142
swiss Q96324 GTH7_ARATH	Glutathione S-transferase (EC 2...	60 142
sptrembl O04426 O04426	Glutathione-S-transferase (Frag...	66 139
sptrembl Q9SHH6 Q9SHH6	Putative glutathione transferas...	67 137
sptrembl Q8H9E7 Q8H9E7	Glutathione S-transferase.//:tr...	70 136
sptrembl Q9SHH8 Q9SHH8	Putative glutathione transferas...	66 131
sptrembl Q9ZW29 Q9ZW29	Putative glutathione S-transfer...	66 129
sptrembl Q9FT21 Q9FT21	Putative glutathione S-transfer...	84 117
swiss P50471 GTX1_NICPL	Probable glutathione S-transfer...	77 112
sptrembl Q8H9E5 Q8H9E5	Glutathione S-transferase.//:tr...	78 111
sptrembl Q8LBS3 Q8LBS3	2,4-D inducible glutathione S-t...	78 110
sptrembl Q9M9F2 Q9M9F2	F3F9.13.//:treml AC013430 AC01...	74 107
sptrembl Q9SR36 Q9SR36	Putative glutathione transferas...	69 69
sptrembl Q9FT22 Q9FT22	Putative glutathione S-transfer...	68 68
sptrembl O04874 O04874	Glutathione transferase (EC 2.5...	65 65
sptrembl Q9M9F1 Q9M9F1	F3F9.14 (Glutathione transferas...	65 65
sptrembl Q8GVD1 Q8GVD1	Glutathione S-transferase-like ...	65 65
sptrembl Q9ZW30 Q9ZW30	Putative glutathione S-transfer...	65 65
sptrembl Q9FVI9 Q9FVI9	Hypothetical 25.2 kDa protein (...	64 64
sptrembl Q9SE87 Q9SE87	Glutathione-S-transferase.//:tr...	63 63
swiss P32110 GTX6_SOYBN	Probable glutathione S-transfer...	63 63
sptrembl Q9FQE6 Q9FQE6	Glutathione S-transferase GST 1...	63 63
swiss P32111 GTX1_SOLTU	Probable glutathione S-transfer...	63 63
sptrembl Q8RW02 Q8RW02	Glutathione transferase (EC 2.5...	63 63

Alignments:

^ = [sptrembl|Q9M9F4|Q9M9F4](#) F3F9.11.//:treml|AC013430|AC013430_11 product: "F3F9.11"; Genomic sequence for Arabidopsis thaliana BAC F3F9 from chromosome I, complete sequence. //:gp|AC013430|8052534 F3F9.11 [Arabidopsis thaliana] Length = 665

Total Score: 435

	0	140	280	420	560	665
sptrembl Q9M9F4 Q9M9F4						
Local hits (HSPs)						

Score = 79 (42.1 bits)
Identities = 10/12 (83%), Positives = 12/12 (100%)

Query: 213 [ELGE2PVEGGEK](#) 224
ELGE+PVFGG+K
Sbjct: 584 [ELGEKPVFGGDK](#) 595

Score = 75 (40.0 bits)
Identities = 9/16 (56%), Positives = 14/16 (87%)

```

Query: 208 BLLADELGEZPVFGGE 223
      +L ELG++PVFGG+
Sbjct: 367 KILESELGDKVPVFGGD 382

Score = 72 (38.5 bits)
Identities = 10/13 (76%), Positives = 12/13 (92%)

Query: 942 BSPILLEFNPVHK 954
      +SPILLE NP+HK
Sbjct: 465 KSPILLENNPIHK 477

Score = 63 (33.9 bits)
Identities = 9/13 (69%), Positives = 12/13 (92%)

Query: 672 BSPILLEFNPVHK 684
      +SPILL+ NP+HK
Sbjct: 274 KSPILLQSNPIHK 286

Score = 41 (22.7 bits)
Identities = 5/6 (83%), Positives = 5/6 (83%)

Query: 2303 EYZEED 2308
      EY EED
Sbjct: 455 EYREED 460

Score = 35 (19.6 bits)
Identities = 3/5 (60%), Positives = 5/5 (100%)

Query: 1118 BEFLE 1122
      +EF+E
Sbjct: 572 KEFIE 576

Score = 35 (19.6 bits)
Identities = 4/7 (57%), Positives = 6/7 (85%)

Query: 3209 BLLAWK 3215
      +L+AW K
Sbjct: 627 KLLAWGK 633

Score = 35 (19.6 bits)
Identities = 4/6 (66%), Positives = 6/6 (100%)

Query: 378 PILLEY 383
      P+LL+Y
Sbjct: 239 PILLDY 244

^ = sptrembl|Q84N22|Q84N22
      Glutathione-S-transferase.//:trembl|AF501625|AF501625_1 product:
      "glutathione-S-transferase"; Vitis vinifera
      glutathione-S-transferase mRNA, complete cds.
      //:gp|AF501625|30315017 glutathione-S-transferase [Vitis vinifera]
      Length = 132

Total Score: 186

              0      30      60      90      120
sptrembl|Q84N22|Q84N2 | _____|_____
Local hits (HSPs)    |
Score = 77 (41.1 bits)
Identities = 11/13 (84%), Positives = 12/13 (92%)

Query: 942 BSPILLEFNPVHK 954
      +SPILLE NPVHK
Sbjct: 40 KSPILLENNPVHK 52

Score = 62 (33.4 bits)
Identities = 9/11 (81%), Positives = 10/11 (90%)

Query: 1510 LLEFNPVHK 1520
      LLE NPVH+K
Sbjct: 43 LLENNPVHKK 53

Score = 47 (25.8 bits)
Identities = 6/7 (85%), Positives = 7/7 (100%)

Query: 3658 BLVELGR 3664
      +LVELGR
Sbjct: 105 KLVELGR 111

```

4.6 Negative Control Spot

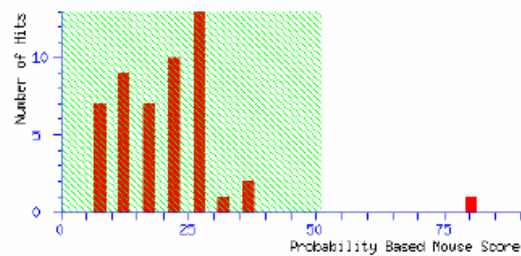
4.6.1 MASCOT Report:

{MATRIX} Mascot Search Results

User : Mark
 Email : m.raftery@unsw.edu.au
 Search title : D:\Datashare\SC#control.wiff : SC#control
 MS data file : C:\TEMP\masCD.tmp
 Database : MSDB 20030730 (1204609 sequences; 382188751 residues)
 Timestamp : 22 Sep 2003 at 22:45:30 GMT
 Significant hits: [TRPGTR](#) trypsin (EC 3.4.21.4) precursor - pig (tentative sequence)

Probability Based Mowse Score

Score is $-10 \cdot \log(P)$, where P is the probability that the observed match is a random event. Individual ion scores > 51 indicate identity or extensive homology ($p < 0.05$).



Peptide Summary Report

1. [TRPGTR](#) Mass: 24394 Total score: 80 Peptides matched: 3
 trypsin (EC 3.4.21.4) precursor - pig (tentative sequence)

Check to include this hit in error tolerant search



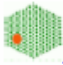
Query	Observed	Mr(expt)	Mr(calc)	Delta	Miss Score	Rank	Peptide
<input checked="" type="checkbox"/> 2	421.76	841.50	841.50	-0.00	0 (50)	1	VATVSLPR
<input checked="" type="checkbox"/> 3	421.76	841.50	841.50	0.00	0 53	1	VATVSLPR
<input checked="" type="checkbox"/> 5	523.29	1044.57	1044.56	0.02	0 28	1	LSSPATLNSR

Proteins matching the same set of peptides:

[1AKSA](#) Mass: 13284 Total score: 80 Peptides matched: 3
 alpha trypsin (EC 3.4.21.4), chain A - pig
[1AVWA](#) Mass: 23460 Total score: 80 Peptides matched: 3
 trypsin (EC 3.4.21.4), chain A - pig
[1D30A](#) Mass: 23458 Total score: 80 Peptides matched: 3
 trypsin (EC 3.4.21.4), chain A - pig
[1EPTB](#) Mass: 8814 Total score: 80 Peptides matched: 3
 Porcine e-trypsin (EC 3.4.21.4), chain B - pig

4.6.2 BLASTp Alignment:

BLASTP2 Result

 of  Bork Group's Advanced BLAST2 Search Service at  [EMBL](#)
[back to BLAST2](#)

BLASTP 2.0MP-WashU [16-Dec-1999] [irix6-rl0k-L64 23:35:48 16-Dec-1999]

Copyright (C) 1996-1999 Washington University, Saint Louis, Missouri USA.
 All Rights Reserved.

Reference: 1. Gish, W. (1996-1999) <http://blast.wustl.edu>

2. Shevchenko A, Sunyaev S, Loboda A, Shevchenko A, Bork P, Ens W, Standing KG. (2001), Anal Chem 73(9),1917-26:
 Charting the proteomes of organisms with unsequenced genomes
 by MALDI-quadrupole time-of-flight mass spectrometry and
 BLAST homology searching
[Abstract](#)

Query= query_sequence
 (601 letters)

Database: nrdb-95%
 842,893 sequences; 279,048,703 total letters.
 Searching.....10.....20.....30.....40.....50.....60.....70.....80.....90.....100% done

Color Key: red = positive hit; green = borderline hit; black = negative result

Summary:

Sequences producing High-scoring Segment Pairs:

	High Score	Total Score
^ = swissnew P00761 TRYP_PIG Trypsin precursor (EC 3.4.21.4). 3.4.21.4.//:swiss P00761 TRYP_PIG Trypsin precursor (EC 3.4.21.4). Length = 231		

Total Score: 59

	0	50	100	150	200	231
swissnew P00761 TRYP_						
Local hits (HSPs)		-----				

Score = 59 (31.8 bits)
 Identities = 8/9 (88%), Positives = 9/9 (100%)

Query: 562 [BVATVSLPR](#) 570
 +VATVSLPR
 Sbjct: 107 [RVATVSLPR](#) 115

Appendix 5 – *V. vinifera* cv. Gamay Fréaux Glutathione S-Transferases Summary Table

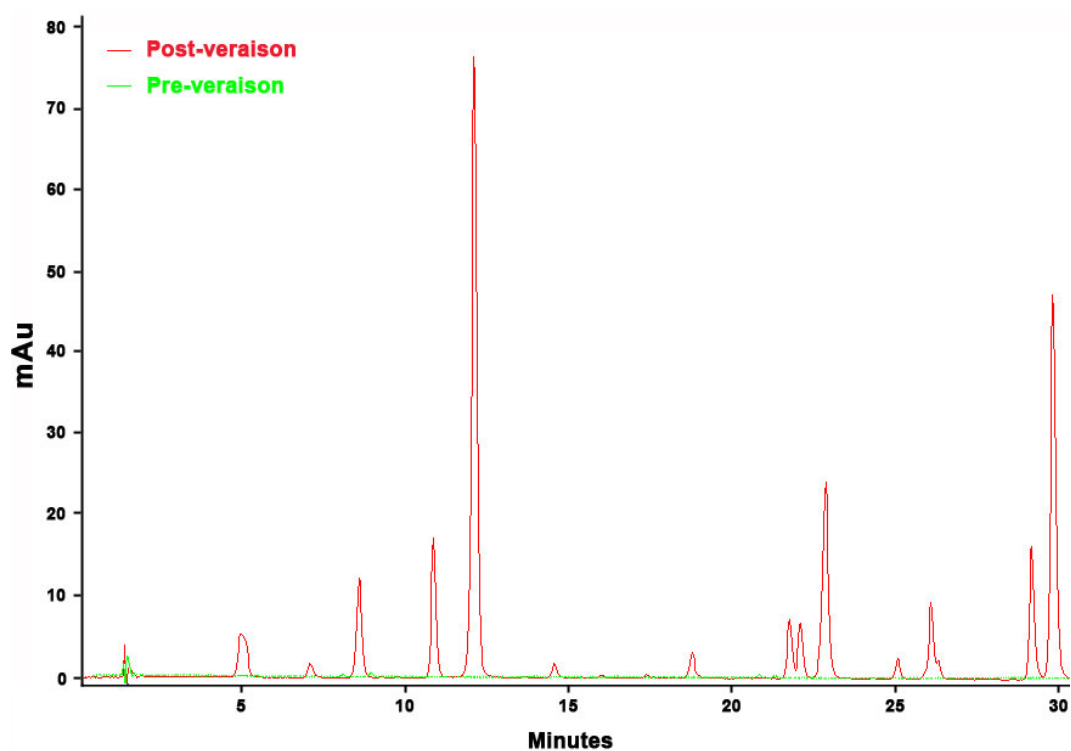
Numbering as per cDNA sequence. Base changes from published sequence.

Gene	Nucleic Acid Position	Base Change	Amino Acid Substitution
GST1 (666bp)	78	T→A	Conservative
	84	A→G	Conservative
	345	T→C	Conservative
	476	G→T	#159: G→V
	530	A→G	#177: N→S
	543	A→G	Conservative
GST2 (645bp)	31	T→A	#11: F→I
	66	T→C	Conservative
GST3 (648bp)	46	C→G	#16: L→V
	88	G→C	#30: V→L
	126	C→A	Conservative
	135	C→G	Conservative
	141	A→G	Conservative
	183	C→T	Conservative
	381	G→A	Conservative
GST4 (642bp)	192	T→G	Conservative
Q84N22 (660bp)	296	T→C	#99: V→A
	349	Removal of A	Frame Shift
	592	T→C	Conservative
	605	Removal of T	Frame Shift

Appendix 6 –

6.1 – Anthocyanin HPLC of *V. vinifera* L. cv. Shiraz grape berries.

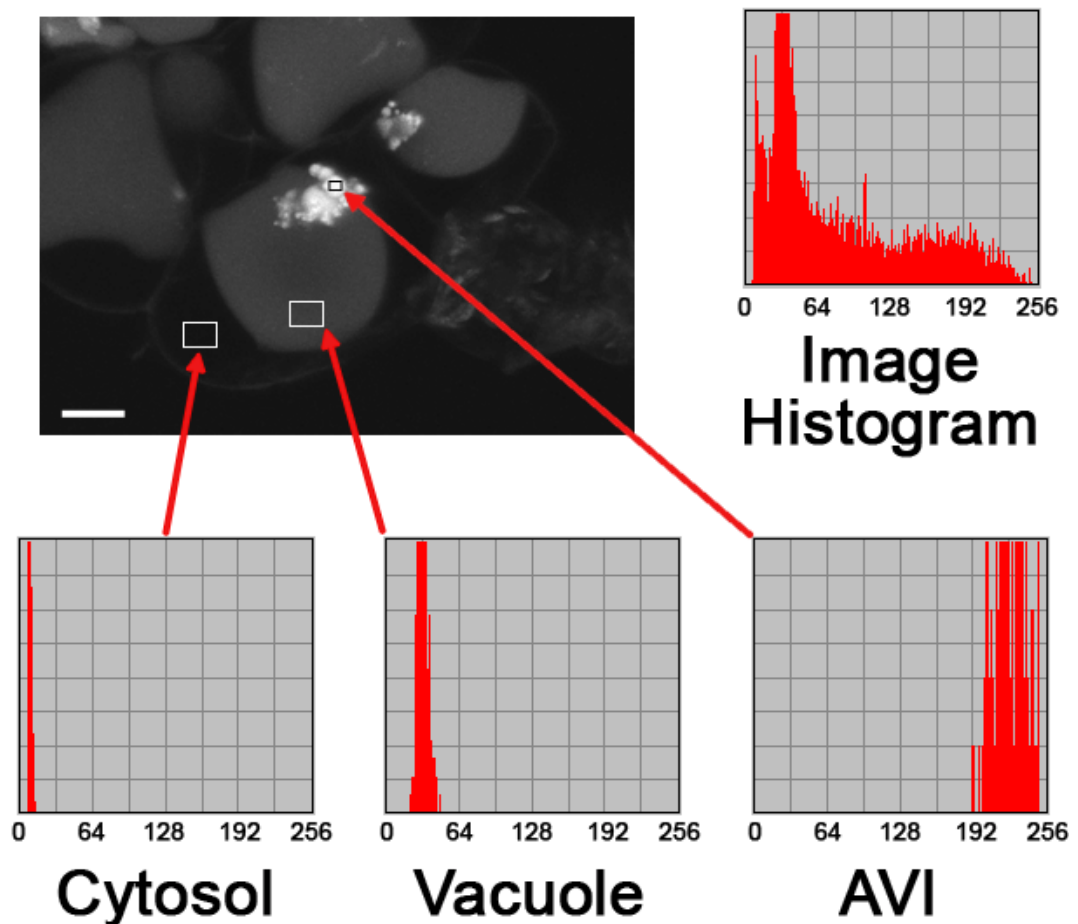
Overlaid anthocyanin (525nm) chromatograms of pre-veraison (green) and post-veraison (red) grape berry skins. Refer to Table 2.1 (Section 2.4.2.3.3) for anthocyanin identity.



6.2 - Image Histogram of Autofluorescent Confocal

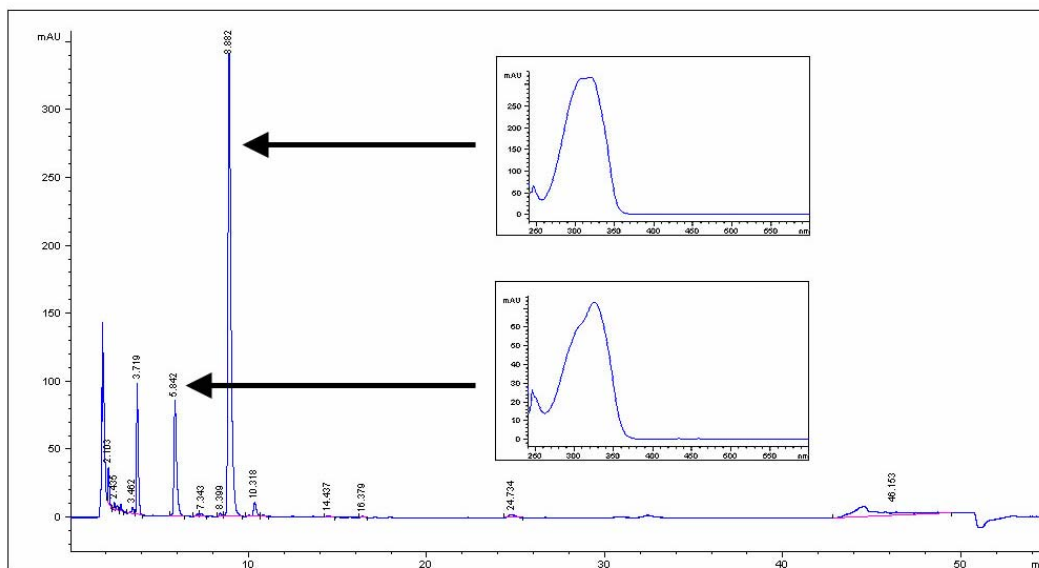
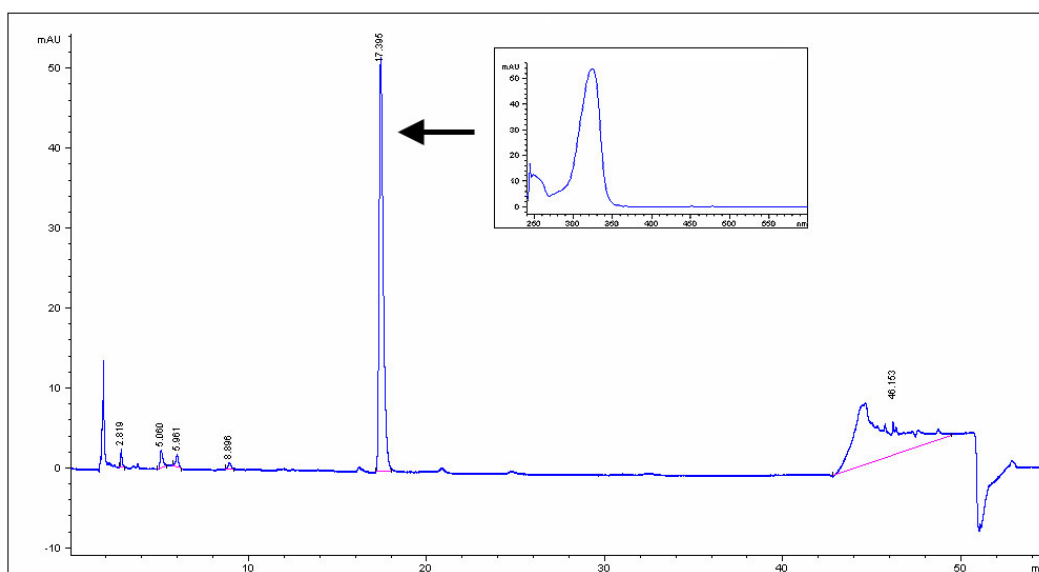
Microscopy on *V. vinifera* L. suspension cells

Confocal Microscopy Autofluorescence Histogram of seven day-old *V. vinifera* suspension cells under far red excitation wavelength. Whiteness histogram (0 = zero white pixels (black); 256 = 256 white pixels (white)) shown for the complete image, and the distinctive boxed cellular regions corresponding to the cytosol (7-13 pixels), vacuole (23-47 pixels) and AVIs (192-256 pixels). These thresholds were utilised for all image analysis. Bar = 10 μ m.



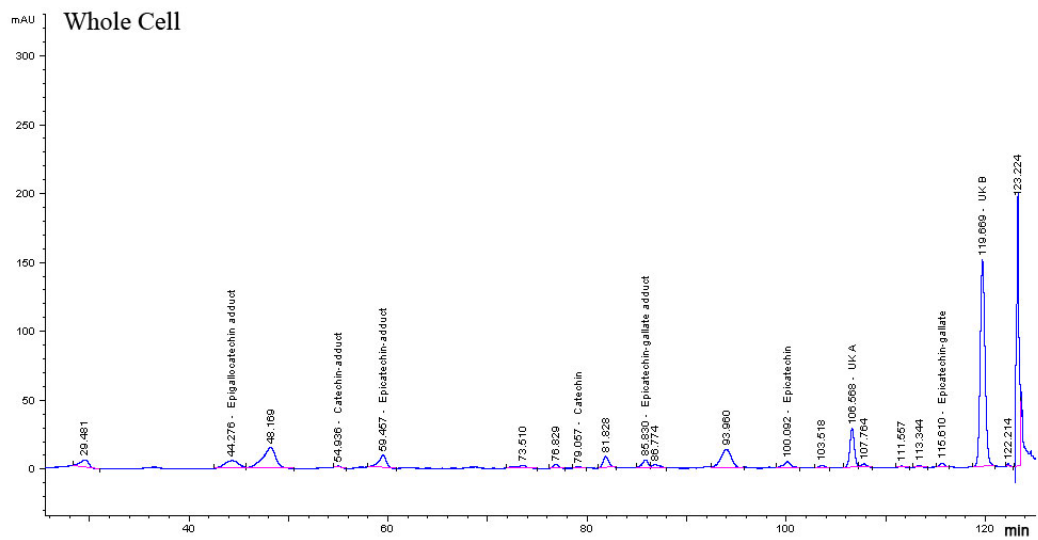
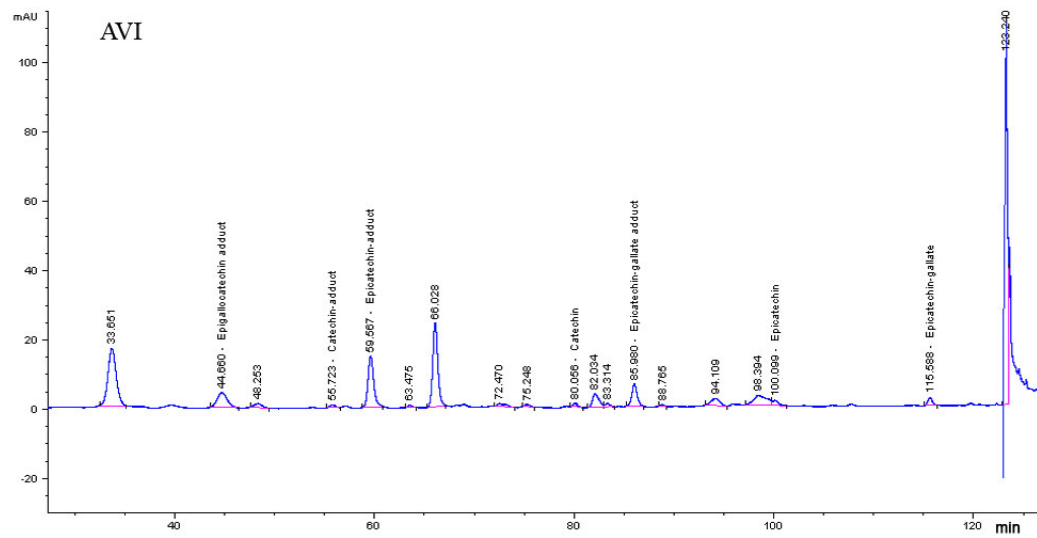
6.3 - Uncleaved Tannin Chromatogram Highlighting Unidentified Compounds

HPLC chromatographs (280nm) of acidified methanol extracts from AVIs (upper) and whole cells (lower). Peaks corresponding to unknown compounds are shown with their absorption spectrum. Separation profile as per Section 2.13.3.1.



Appendix 7 – Lipid Gas Chromatograms

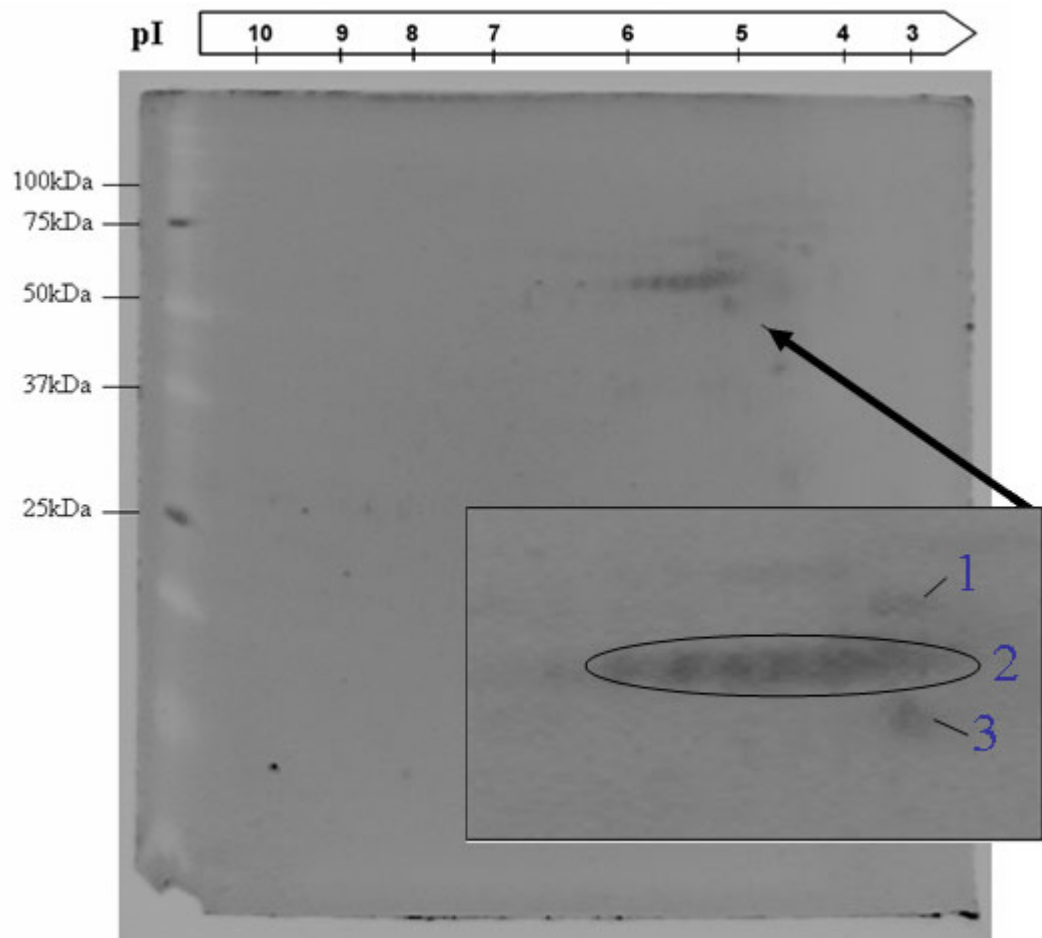
Chromatograms from *V. vinifera* AVIs and whole cell extracts having undergone acid-catalysis and phloroglucinol adduct formation.



Appendix 8 - Analysis of Protein from AVI Pellet

8.1 2-D Gel Separation of Protein Extracted from AVIs

SYPRO Ruby-stained, 2-D gel electrophoresis of protein solubilised from AVIs. Numbers indicate spots picked for mass spectroscopy.



8.2 Mass Spectrometry Analysis of AVI Protein

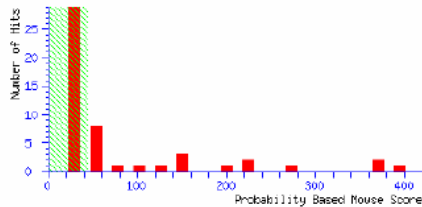
All spots showed same peptide summary. Spot 2 shown below.

(MATRIX) Mascot Search Results

User : Mascot Daemon
 Email : m.raftery@unsw.edu.au
 Search title : Submitted from QSTAR by Mascot Daemon on EMSF-QSTAR2 (SC_sample)
 MS data file : D:\mas\SC_sample.wiff
 Database : Tr embl 9_3_04 (1070786 sequences; 335820809 residues)
 Timestamp : 13 Mar 2004 at 00:37:43 GMT
 Significant hits: [Q94FE8](#) (Q94FE8) Granule-bound starch synthase (Fragment)
[Q93V80](#) (Q93V80) Granule-bound starch synthase (Fragment)
[Q8L699](#) (Q8L699) Granule bound starch synthase precursor
[Q8LLD5](#) (Q8LLD5) Granule-bound starch synthase
[Q81549](#) (Q81549) Granule-bound starch synthase (Fragment)
[Q81591](#) (Q81591) Granule-bound starch synthase (Fragment)
[Q81537](#) (Q81537) Granule-bound starch synthase (Fragment)
[Q8S4L9](#) (Q8S4L9) Granule-bound starch synthase I (Fragment)
[Q8S5D6](#) (Q8S5D6) Granule-bound starch synthase

Probability Based Mowse Score

Ions score is $-10 \cdot \log(P)$, where P is the probability that the observed match is a random event. Individual ions scores > 44 indicate identity or extensive homology ($p < 0.05$). Protein scores are derived from ions scores as a non-probabilistic basis for ranking protein hits.



Peptide Summary Report

1. [Q94FE8](#) Mass: 29168 Score: 394 Peptides matched: 14
 (Q94FE8) Granule-bound starch synthase (Fragment)

Check to include this hit in error tolerant search or archive report

Query	Observed	Mr (expt)	Mr (calc)	Delta	Miss	Score	Expect	Rank	Peptide
<input checked="" type="checkbox"/> 10	541.77	1081.52	1081.53	-0.01	0	48	0.024	1	YDVSTAVEAK
<input checked="" type="checkbox"/> 11	550.32	1098.63	1098.65	-0.02	0 (34)	0.63	1	NIPLVAFIQR	
<input checked="" type="checkbox"/> 12	550.33	1098.64	1098.65	-0.02	0	48	0.025	1	NIPLVAFIQR
<input checked="" type="checkbox"/> 13	550.33	1098.64	1098.65	-0.02	0 (24)	5.5	3	NIPLVAFIQR	
<input checked="" type="checkbox"/> 26	675.82	1349.62	1349.66	-0.04	0	42	0.083	1	VVGTPEYERIVR
<input checked="" type="checkbox"/> 27	683.82	1365.63	1365.66	-0.03	0 (29)	1.5	1	VVGTPEYERIVR + Oxidation (M)	
<input checked="" type="checkbox"/> 28	683.83	1365.65	1365.66	-0.01	0 (22)	8.6	1	VVGTPEYERIVR + Oxidation (M)	
<input checked="" type="checkbox"/> 27	698.86	1395.70	1395.74	-0.03	0	79	1.7e-005	1	EALQAEVGLPVDR
<input checked="" type="checkbox"/> 38	467.22	1398.62	1398.65	-0.03	1 (42)	0.092	1	MLMSAEERKPFQK + 2 Oxidation (M)	
<input checked="" type="checkbox"/> 38	467.22	1398.64	1398.65	-0.02	1	45	0.041	1	MLMSAEERKPFQK + 2 Oxidation (M)
<input checked="" type="checkbox"/> 53	780.87	1559.72	1559.73	-0.01	0	20	13	XSVDGNVVEPADVX	
<input checked="" type="checkbox"/> 73	608.33	1821.97	1821.99	-0.02	1	60	0.001	1	ALNKEALQAEVGLPVDR
<input checked="" type="checkbox"/> 100	727.70	2180.08	2180.12	-0.03	0	52	0.0063	1	FNAALAHHIMAGADVLAIVTSR + Oxidation (M)
<input checked="" type="checkbox"/> 101	546.03	2180.10	2180.12	-0.02	0 (50)	0.0097	1	FNAALAHHIMAGADVLAIVTSR + Oxidation (M)	

2. [Q93V80](#) Mass: 29128 Score: 364 Peptides matched: 11
 (Q93V80) Granule-bound starch synthase (Fragment)

Check to include this hit in error tolerant search or archive report

Query	Observed	Mr (expt)	Mr (calc)	Delta	Miss	Score	Expect	Rank	Peptide
<input checked="" type="checkbox"/> 10	541.77	1081.52	1081.53	-0.01	0	48	0.024	1	YDVSTAVEAK
<input checked="" type="checkbox"/> 11	550.32	1098.63	1098.65	-0.02	0 (34)	0.63	1	NIPLVAFIQR	
<input checked="" type="checkbox"/> 12	550.33	1098.64	1098.65	-0.02	0	48	0.025	1	NIPLVAFIQR
<input checked="" type="checkbox"/> 13	550.33	1098.64	1098.65	-0.02	0 (24)	5.5	3	NIPLVAFIQR	
<input checked="" type="checkbox"/> 26	697.85	1393.68	1393.69	-0.01	0	32	0.82	1	VVGTPEYERIVR + Oxidation (M)
<input checked="" type="checkbox"/> 27	698.86	1395.70	1395.74	-0.03	0	79	1.7e-005	1	EALQAEVGLPVDR
<input checked="" type="checkbox"/> 28	467.22	1398.62	1398.65	-0.03	1 (42)	0.092	1	MLMSAEERKPFQK + 2 Oxidation (M)	
<input checked="" type="checkbox"/> 28	467.22	1398.64	1398.65	-0.02	1	45	0.041	1	MLMSAEERKPFQK + 2 Oxidation (M)
<input checked="" type="checkbox"/> 73	608.33	1821.97	1821.99	-0.02	1	60	0.001	1	ALNKEALQAEVGLPVDR
<input checked="" type="checkbox"/> 100	727.70	2180.08	2180.12	-0.03	0	52	0.0063	1	FNAALAHHIMAGADVLAIVTSR + Oxidation (M)
<input checked="" type="checkbox"/> 101	546.03	2180.10	2180.12	-0.02	0 (50)	0.0097	1	FNAALAHHIMAGADVLAIVTSR + Oxidation (M)	

Proteins matching the same set of peptides:

[Q93VG4](#) Mass: 29112 Score: 364 Peptides matched: 11
 (Q93VG4) Granule-bound starch synthase (Fragment)

[Q94FE8](#) Mass: 27837 Score: 364 Peptides matched: 11
 (Q94FE8) Granule-bound starch synthase (Fragment)

References

- Agati, G., Pinelli, P., Cortes Ebner, S., Romani, A., Cartelat, A., and Cerovic, Z.G.** (2005). Nondestructive evaluation of anthocyanins in olive (*Olea europaea*) fruits by *in situ* chlorophyll fluorescence spectroscopy. *Journal of Agricultural Food Chemistry* **53**, 1354-1363.
- Aharoni, A., Keizer, L.C., van den Broeck, H.C., Blanco-Portales, R., Munoz-Blanco, J., Bois, G., Smit, P., de Vos, R.C., and O'Connell, A.P.** (2002). Novel insight into vascular, stress, and auxin-dependent and -independent gene expression programs in strawberry, a non-climacteric fruit. *Plant Physiol.* **129**, 1019-1031.
- Ahmed, M.S., Ainley, K., Parish, J.H., and Hadi, S.M.** (1994). Free radical-induced fragmentation of proteins by quercetin. *Carcinogenesis* **15**, 1627-1630.
- Akgul, B., and Tu, C.P.** (2004). Pentobarbital-mediated regulation of alternative polyadenylation in *Drosophila* glutathione S-transferase D21 mRNAs. *J. Biol. Chem.* **279**, 4027-4033.
- Alfenito, M.R., Souer, E., Goodman, C.D., Buell, R., Mol, J.N.M., Koes, R., and Walbot, V.** (1998). Functional complementation of anthocyanin sequestration in the vacuole by widely divergent glutathione s-transferases. *The Plant Cell* **10**, 1135-1149.
- Altschul, S.F., Gish, W., Miller, W., Myers, E.W., and Lipman, D.J.** (1990). Basic local alignment search tool. *J. Mol. Biol.* **215**, 403-410.
- Altschul, S.F., Madden, T.L., Schäffer, A.A., Zhang, J., Zhang, Z., Miller, W., and Lipman, D.J.** (1997). Gapped BLAST and PSI-BLAST: a new generation of protein database search programs. *Nucleic Acids Res.* **25**, 3389-3402.
- Amrani Jouteau, K., Glories, Y., and Mercier, M.** (1994). Localization of tannins in grape berry skins. *Vitis* **33**, 133-138.
- Anderson, R.G.W., and Orci, L.** (1988). A View of Acidic Intracellular Compartments. *The Journal of Cell Biology* **106**, 539-543.
- Andersson, C., Weinander, R., Lundqvist, G., DePierre, J.W., and Morgenstern, R.** (1994). Functional and structural membrane topology of rat liver microsomal glutathione transferase. *Biochim. Biophys. Acta* **1204**, 298-304.
- Andrews, C.J., Jepson, I., Skipsey, M., Townson, J.K., and Edwards, R.** (1997). Nucleotide Sequence of a Glutathione Transferase from Soybean with Activity Towards Herbicides. *Plant Physiol.* **113**, 1005-1005.
- Arakawa, Y., Masaoka, Y., Sakai, J., Higo, H., and Higo, K.** (2002). An alfalfa gene similar to glutathione S-transferase is induced in root by iron deficiency. *Soil Sci. Plant Nutr.* **48**, 111-116.
- Asen, S., Stewart, R.N., and Norris, K.H.** (1975). Anthocyanin, flavonol copigments, and pH responsible for larkspur flower colour. *Phytochemistry* **14**, 2677-2682.
- Bailly, C., Cormier, F., and Do, C.B.** (1997). Characterization and activities of S-adenosyl-L-methionine: cyanidin 3-glucoside 3'-O-methyltransferase in relation to anthocyanin accumulation in *Vitis vinifera* cell suspension cultures. *Plant Science* **122**, 81-89.
- Baker, D.C., Dougall, D.K., Glaessgen, W.E., Johnson, S.C., Metzger, J.W., Rose, A., and Seitz, H.U.** (1994). Effects of supplied cinnamic acids and

- biosynthetic intermediates on the anthocyanins accumulated by wild carrot suspension cultures. *Plant Cell Tissue and Organ Culture* **39**, 79-91.
- Baldwin, P.M.** (2001). Starch-granule associated proteins and polypeptides: A review. *Starch/Starke* **53**, 475-503.
- Bell, J.R.C., Donovan, J.L., Wong, R., Waterhouse, A.L., German, B., Walzem, R.L., and Kasim-Karakas, S.E.** (2000). (+)-Catechin in human plasma after ingestion of a single serving of reconstituted red wine. *Am. J. Clin. Nutr.* **71**, 103-108.
- Bilang, J., and Sturm, A.** (1995). Cloning and characterization of a glutathione S-transferase that can be photolabelled with 5-azido-indole-3-acetic acid. *Plant Physiol.* **109**, 253-260.
- Blank, C., Neumann, M.A., Makindes, M., and Gibson, P.A.** (2002). Optimizing DHA levels in piglets by lowering the linoleic acid to alpha-linoleic acid ratio. *Journal of Lipid Research* **43**, 1537-1543.
- Blank, F.** (1946). The anthocyanin pigments of plants. *Bot. Rev.* **13**, 241-317.
- Blount, J.W., Korth, K.L., Masoud, S.A., Rasmussen, S., Lamb, C., and Dixon, R.A.** (2000). Altering expression of cinnamic acid 4-hydroxylase in transgenic plants provides evidence for a feedback loop at the entry point into the phenylpropanoid pathway. *Plant Physiology* **122**, 107-116.
- Bock, A., Wanner, G., and Zenk, M.H.** (2002). Immunocytological localization of two enzymes involved in berberine biosynthesis. *Planta* **216**, 57-63.
- Bodeau, J.P., and Walbot, V.** (1992). Regulated transcription of the maize Bronze-2 promoter in electroporated protoplasts requires the C1 and R gene products. *Molecular & General Genetics* **233**, 379-387.
- Bodeau, J.P., and Walbot, V.** (1996). Structure and regulation of the maize Bronze2 promoter. *Plant Molecular Biology* **32**, 599-609.
- Bogs, J., Ebadi, A., McDavid, D., and Robinson, S.P.** (2006). Identification of the Flavonoid Hydroxylases from Grapevine and Their Regulation during Fruit Development. *Plant Physiol.* **140**, 279-291.
- Bolle, C., Sopory, S., Lubberstedt, T., Herrmann, R.G., and Oelmüller, R.** (1994). Segments encoding 5'-untranslated leaders of genes for thylakoid proteins contain *cis*-elements essential for transcription. *Plant J.* **6**, 513-523.
- Borevitz, J.O., Xia, Y., Blount, J., Dixon, R.A., and Lamb, C.** (2000). Activation tagging identifies a conserved *MYB* regulator of phenylpropanoid biosynthesis. *Plant Cell* **12**, 2383-2393.
- Boss, P.K., Davies, C., and Robinson, S.P.** (1996a). Analysis of the expression of anthocyanin pathway genes in developing *Vitis vinifera* L. cv Shiraz grape berries and the implications for pathway regulation. *Plant Physiology* **111**, 1059-1066.
- Boss, P.K., Davies, C., and Robinson, S.P.** (1996b). Expression of anthocyanin biosynthesis pathway genes in red and white grapes. *Plant Molecular Biology* **32**, 565-569.
- Boulton, A.** (2001). The copigmentation of anthocyanins and its role in the color of red wine: a critical review. *Am. J. Enol. Vitic.* **52**, 67-87.
- Bridle, P.A., and Timberlake, C.F.** (1997). Anthocyanins as natural food colours-selected aspects. *Food Chemistry* **58**, 103-109.
- Bruce, W., Folkerts, O., Garnaat, C., Crasta, O., Roth, B., and Bowen, B.** (2000). Expression profiling of the maize flavonoid pathway genes

- controlled by estradiol-inducible transcription factors CRC and P. *Plant Cell* **12**, 65-80.
- Bub, A., Watzl, B., Heeb, D., Rechkemmer, G., and Briviba, K.a.** (2001). Malvidin-3-glucoside bioavailability in humans after ingestion of red wine, dealcoholized red wine and red grape juice. *European Journal of Nutrition*. **40**, 113-120.
- Burbulis, I.E., and Winkel-Shirley, B.** (1999). Interactions among enzymes of the Arabidopsis flavonoid biosynthetic pathway. *Proc. Natl Acad. Sci. U.S.A.* **96**, 12929-12934.
- Calderon, A.A., Pedreno, M.A., Munoz, R., and Ros-Barcelo, A.** (1993). Evidence for non-vacuolar localization of anthocyanoplasts (anthocyanin-containing vesicles) in suspension cultured grapevine cells. *Phyton* **54**, 91-98.
- Calderon, A.A., Garcia-Florenciano, E., Pedreno, M.A., Munoz, R., and Ros-Barcelo, A.** (1992). The vacuolar localization of grapevine peroxidase isoenzymes capable of oxidizing 4-hydroxystilbenes. *Z. Naturforsch* **47c**, 215-221.
- Callebaut, A., Voets, A.M., Hendrick, X., and Motte, J.C.** (1990). Anthocyanin in Cell Cultures of *Ajuga reptans*. *Phytochemistry* **29**, 2153-2158.
- Chandler, V.L., Talbert, L.E., and Raymond, F.** (1988). Sequence, genomic distribution and DNA modification of a Mu1 element from non-mutator maize stocks. *Genetics* **119**, 951-958.
- Chang, R.Y., Chopra, S., and Peterson, P.A.** (2005). Differential excision patterns of the En-transposable element at the A2 locus in maize relate to the insertion site. *Mol. Genet. Genomics* **274**, 189-195.
- Che, P., Gingerich, D.J., Lall, S., and Howell, S.H.** (2002). Global and Hormone-Induced Gene Expression Changes during Shoot Development in Arabidopsis. *The Plant Cell* **14**, 2771-2785.
- Choi, J.W., Cho, G.H., Byun, S.Y., and Kim, D.I.** (2001). Integrated bioprocessing for plant cell cultures. *Adv. Biochem. Eng. Biotechnol.* **72**, 63-102.
- Clifford, M.N.** (2000). Anthocyanins - nature, occurrence and dietary burden. *J.Food Sci. Agric.* **80**, 1063-1072.
- Collin, H.A.** (1987). Determinants of yield of secondary products in plant tissue cultures. *Advances in Botanical Research* **13**, 145-187.
- Collin, H.A.** (2001). Secondary product formation in plant tissue cultures. *Plant Growth Regulation*. **34**, 119-134.
- Conn, S., Zhang, W., and Franco, C.** (2003). Anthocyanic vacuolar inclusions (AVIs) selectively bind acylated anthocyanins in *Vitis vinifera* L. (grapevine) suspension culture. *Biotechnology Letters* **25**, 835-839.
- Cormier, F., Crevier, H.A., and Do, C.B.** (1990). Effects of sucrose concentration on the accumulation of anthocyanins in grape (*Vitis vinifera* L.) cell suspension. *Canadian Journal of Botany* **68**, 1822-1825.
- Cormier, F., Do, C.B., and Nicolas, Y.** (1994). Anthocyanin production in selected cell lines of grape (*Vitis vinifera* L.). *In Vitro Cellular and Developmental Biology Plant*. **30P**, 171-173.
- Cormier, F., Do, C.B., Moresoli, C., Archambault, J., Chavarie, C., and Chaouki, F.** (1992). Anthocyanin release from grape (*Vitis vinifera* L.) cell suspension. *Biotechnology Letters* **14**, 1029-1034.

- Cormier, F., Brion, C., Do, C.B., Moresoli, C., DiCosmo, F., and Misawa, M.** (1996). In Development of process strategies for anthocyanin-based food colorant using *Vitis vinifera* cell cultures (New York: CRC Press), pp. 167-185.
- Creelman, R.A., and Mullet, J.E.** (1997). Oligosaccharins, brassinolides, and jasmonates: Non-traditional regulators of plant growth, development, and gene expression. *Plant Cell* **9**, 1211-1223.
- Curtin, C.** (2005). Towards molecular bioprocessing as a tool to enhance production of anthocyanins in *Vitis Vinifera* L. cell suspension culture. In Department of Medical Biotechnology (Adelaide: Flinders University).
- Curtin, C., Zhang, W., and Franco, C.** (2003). Manipulating anthocyanin composition in *Vitis vinifera* suspension cultures by elicitation with jasmonic acid and light irradiation. *Biotechnology Letters* **25**, 1131-1135.
- Dangles, O., Saito, N., and Brouillard, R.** (1993). Anthocyanin intramolecular copigment effect. *Phytochemistry* **34**, 119-124.
- Daniel, V.** (1993). Glutathione *S*-transferase: gene structure and regulation of expression. *CRC Crit. Rev. Biochem.* **25**, 173-207.
- Davies, C., and Robinson, S.P.** (2000). Differential screening indicates a dramatic change in mRNA profiles during grape berry ripening. Cloning and characterization of cDNAs encoding putative cell wall and stress response proteins. *Plant Physiol* **122**, 803-812.
- de Vetten, N., Quattrocchio, F., Mol, J., and Koes, R.** (1997). The *anthocyanin11* locus controlling flower pigmentation in petunia encodes a novel WD-repeat protein conserved in yeast, plants and animals. *Genes Dev.* **11**, 1422-1434.
- Dean, J.D., Goodwin, P.H., and Hsiang, T.** (2005). Induction of glutathione *S*-transferase genes of *Nicotiana benthamiana* following infection by *Colletotrichum destructivum* and *C. orbiculare* and involvement of one in resistance. *J. Exp. Bot.* **56**, 1525-1533.
- Debeaujon, I., Peeters, A.J., Leon-Kloosterziel, K.M., and Koornneef, M.** (2001). The transparent testa¹² gene of arabidopsis encodes a multidrug secondary transporter-like protein required for flavonoid sequestration in vacuoles of the seed coat endothelium. *Plant Cell* **13**, 853-872.
- Dedaldechamp, F., Uhel, C., and Macheix, J.J.** (1995). Enhancement of anthocyanin synthesis and dihydroflavonol reductase (DFR) activity in response to phosphate deprivation in grape cell suspensions. *Phytochemistry* **40**, 1357-1360.
- Degenhardt, A., Knapp, H., and Winterhalter, P.** (2000). Separation and purification of anthocyanins by high-speed countercurrent chromatography and screening for antioxidant activity. *Journal of Agricultural and Food Chemistry* **48**.
- Deikman, J., and Hammer, P.E.** (1995). Induction of anthocyanin accumulation by cytokinins in *Arabidopsis thaliana*. *Plant Physiology Rockville* **108**, 47-57.
- Deng, F., and Hatzios, K.K.** (2002a). Purification and Characterization of Two Glutathione *S*-Transferase Isozymes from Indica-Type Rice Involved in Herbicide Detoxification. *Pesticide Biochemistry and Physiology* **72**, 10-23.

- Deng, F., and Hatzios, K.K.** (2002b). Characterization and Safener Induction of Multiple Glutathione S-Transferases in Three Genetic Lines of Rice. *Pesticide Biochemistry and Physiology* **72**, 24-39.
- Deus-Neumann, B.** (1983). Subcellular localization of anthocyanin in red cabbage. *Biochem. Physiol. Pflanzen* **178**, 405-407.
- Deus-Neumann, B., and Zenk, M.H.** (1984). Instability of indole alkaloid production in *Catharanthus roseus* cell suspension cultures. *Planta Medica* **50**, 427-431.
- Di Mauro, A., Arena, E., Fallico, B., Passerini, A., and Maccarone, E.** (2002). Recovery of anthocyanins from pulp wash of pigmented oranges by concentration on resins. *J. Agric. Food Chem.* **50**, 5968-5974.
- Di Sansebastiano, G.P., Paris, N., Marc-Martin, S., and Neuhaus, J.M.** (2001). Regeneration of a lytic central vacuole and of neutral peripheral vacuoles can be visualized by green fluorescent proteins targeted to either type of vacuoles. *Plant Physiol.* **126**, 78-86.
- DiCosmo, F., and Misawa, M.** (1995). Plant cell and tissue culture: Alternatives for metabolite production. *Biotechnology Advances* **13**, 425-453.
- Dixon, D., Cole, D.J., and Edwards, R.** (1997). Characterisation of multiple glutathione transferases containing the GST 1 subunit with activities toward herbicide substrates in maize (*Zea mays*). *Pestic. Sci.* **50**, 72-82.
- Dixon, D.P., Laphorn, A.J., and Edwards, R.** (2002). Plant glutathione transferases. *Genome Biology* **3**, 3004:3001-3010.
- Do, C.B., and Cormier, F.** (1990). Accumulation of anthocyanins enhanced by a high osmotic potential in grape (*Vitis vinifera* L.) cell suspensions. *Plant Cell Reports* **9**, 143-146.
- Do, C.B., and Cormier, F.** (1991). Effects of high ammonium concentrations on growth and anthocyanin formation in grape (*Vitis vinifera* L.) cell suspension cultured in a production medium. *Plant Cell Tissue and Organ Culture* **27**, 169-174.
- Do, C.B., and Cormier, F.** (1991a). Effects of low nitrate and high sugar concentrations on anthocyanin content and composition of grape (*Vitis vinifera* L.) cell suspension. *Plant Cell Reports* **9**, 500-504.
- Do, C.B., and Cormier, F.** (1991b). Accumulation of peonidin 3-glucoside enhanced by osmotic stress in grape (*Vitis vinifera* L.) cell suspensions. *Plant Cell Tissue and Organ Culture* **24**, 49-54.
- Do, C.B., Cormier, F., and Nicolas, Y.** (1995). Isolation and characterization of a UDP-glucose: cyanidin 3-O-glucosyltransferase from grape cell suspension cultures (*Vitis vinifera* L.). *Plant Science* **112**, 43-51.
- Donovan, J.L., Bell, J.R., Kasim-Karakas, S., German, J.B., Walzem, R.L., Hansen, R.J., and Waterhouse, A.L.** (1999). Catechin is present as metabolites in human plasma after consumption of red wine. *J. Nutr.* **129**, 1662-1668.
- Dornenburg, H., and Knorr, D.** (1996). Generation of colors and flavors in plant cell and tissue cultures. *Critical Reviews in Plant Sciences* **15**, 141-168.
- Dougall, D.K., Baker, D.C., Gakh, E.G., Redus, M.A., and Whitemore, N.A.** (1998). Anthocyanins from wild carrot suspension cultures acylated with supplied carboxylic acids. *Carbohydrate Research* **310**, 177-189.
- Downey, M.O., and Kristic.** (In press). Development of a stable extract for anthocyanins and flavonols from grape skin. *Am. J. Enol. Vitic.* **2005**.

- Downey, M.O., Harvey, J.S., and Robinson, S.P.** (2003a). Analysis of tannins in seeds and skins of Shiraz grapes throughout berry development. *Australian Journal of Grape and Wine Research* **9**, 15-27.
- Downey, M.O., Harvey, J.S., and Robinson, S.P.** (2003b). Synthesis of flavonols and expression of flavonol synthase genes in the developing grape berries of Shiraz and Chardonnay (*Vitis vinifera* L.). *Australian Journal of Grape and Wine Research* **9**, 110-121.
- Droog, F.** (1997). Plant glutathione S-transferases, a tale of theta and tau. *J. Plant Growth Regul.* **16**, 95-107.
- Droog, F.N.J., Hooykaas, P.J.J., and Van der Zaal, B.J.** (1995). 2,4-Dichlorophenoxyacetic acid and related chlorinated compounds inhibit two auxin-regulated type III tobacco glutathione S-transferases. *Plant. Physiol.* **107**, 1139-1146.
- Duke, S.O., and Vaughn, K.C.** (1982). *Physiol. Plant* **54**, 381.
- Durbin, M.L., McCaig, B., and Clegg, M.T.** (2000). Molecular evolution of the chalcone synthase multigene family in the morning glory genome. *Plant Molecular Biology* **42**, 79-92.
- Edwards, R., Dixon, D.P., and Walbot, V.** (2000). Plant glutathione S-Transferases: enzymes with multiple functions in sickness and health. *Trends in Plant Science* **5**, 193-198.
- Elomaa, P., Mehto, M., Kotilainen, M., Helariutta, Y., Nevalainen, L., and Teeri, T.H.** (1998). A bHLH transcription factor mediates organ, region and flower type specific signals on *dihydroflavonol 4-reductase (dfr)* gene expression in the inflorescence of *Gerbera hybrida* (Asteraceae). *The Plant Journal* **16**, 93-99.
- Elomaa, P., Uimari, A., Mehto, M., Albert, V.A., Laitinen, R.A.E., and Teeri, T.H.** (2003). Activation of anthocyanin biosynthesis in *Gerbera hybrida* (Asteraceae) suggests conserved protein-protein and protein-promoter interactions between anciently diverged monocots and eudicots. *Plant Physiology* **133**, 1-12.
- Espin, J.C., Soler-Rivas, C., Wichers, H.J., and Garcia-Viguera, C.** (2000). Anthocyanin-based natural colorants: A new source of antiradical activity for foodstuff. *Journal of Agricultural and Food Chemistry* **48**, 1588-1592.
- Fang, Y., Smith, M.A.L.a., and Pepin, M.F.** (1999). Effects of exogenous methyl jasmonate in elicited anthocyanin-producing cell cultures of ohelo (*Vaccinium pahalae*). *In Vitro Cellular and Developmental Biology Plant.* **35**, 106-113.
- FDA, D.o.H.a.H.S.** (2003). Listing of Color Additives Exempt from Certification. Code of Federal Regulations **Section 73**, 169-170.
- Feild, T.S., Lee, D.W., and Holbrook, N.M.** (2001). Why leaves turn red in autumn. The role of anthocyanins in senescing leaves of red-osier dogwood. *Plant Physiol* **127**, 566-574.
- Figueiredo, P., Elhabiri, M., Toki, K., Saito, N., Dangles, O., and Brouillard, R.** (1996). New aspects of anthocyanin complexation intramolecular copigmentation as a means for colour loss? *Phytochemistry* **41**, 301-308.
- Fineran, B.A.** (1971). Ultrastructure of vacuolar inclusions in root tips. *Protoplasma* **72**, 1-18.
- Fischer, R., Emans, N., Shuster, F., Hellwig, S., and Drossard, J.** (1999). Towards molecular farming in the future: using plant-cell-suspension

- cultures as bioreactors. *Biotechnology and Applied Biochemistry* **30**, 109-112.
- Ford, C.M., Boss, P.K., and Hoj, P.B.** (1998). Cloning and characterization of *Vitis vinifera* UDP-glucose:flavonoid 3-O-glucosyltransferase, a homologue of the enzyme encoded by the maize bronze-1 locus that may primarily serve to glucosylate anthocyanidins in vivo. *Journal of Biological Chemistry* **273**, 9224-9233.
- Franceschi, V.R., and Nakata, P.A.** (2005). Calcium oxalate in plants: formation and function. *Annu. Rev. Plant Biol.* **56**, 41-71.
- Francis, F.J.** (1989). Food colorants: anthocyanins. *Crit Rev Food Sci Nutr* **28**, 273-314.
- Frank, M., Rupp, H., Prinsen, E., Motyka, V., van Onckelen, H., and Schmölling, T.** (2000). Hormone Autotrophic Growth and Differentiation Identifies Mutant Lines of *Arabidopsis* with Altered Cytokinin and Auxin Content or Signaling. *Plant Physiol.* **122**, 721-730.
- Fu, T.J.** (1998). Safety considerations for food ingredients produced by plant cell and tissue culture. *Chemtech* **28**, 40-46.
- Fujiwara, H., Tanaka, Y., Fukui, Y., Nakao, M., Ashikari, T., and Kusumi, T.** (1997). Anthocyanin 5-aromatic acyltransferase from *Gentiana triflora*. Purification, characterization and its role in anthocyanin biosynthesis. *European Journal of Biochemistry* **249**, 45-51.
- Gaillard, C., Dufaud, A., Tommassini, R., Kreuz, K., Amrhein, N., and Martinoia, E.** (1994). A herbicide antidote (safener) induces the activity of both the herbicide detoxifying enzyme and of a vacuolar transporter for the detoxified herbicide. *FEBS Letters* **352**, 219-221.
- Gamborg, O., Miller, R.A., and Ojima, K.** (1968). Nutrient requirements soybean root cells. *Experimental Cellular Research* **50**, 151-158.
- Garcia-Florenciano, E., Calderon, A.A., Munoz, R., and Barcelo, A.R.** (1992). Patterns of anthocyanin deposition in vacuoles of suspension cultured grapevine cells. *Phyton* **53**, 47-50.
- Gasteiger, E., Hoogland, C., Gattiker, A., Duvaud, S., Wilkins, M.R., and Appel, R.D.B., A.** (2005). Protein Identification and Analysis Tools on the ExPASy Server. In *The Proteomics Protocols Handbook*, J.M. Walker, ed (New York: Humana Press), pp. 571-607.
- Gish, W., and States, D.J.** (1993). Identification of protein coding regions by database similarity search. *Nature Genet.* **3**, 266-272.
- Giusti, M.M., Rodriguez-Saona, L.E., Baggett, J.R., Reed, G.L., Durst, R.W., and Wrolstad, R.E.** (1998). Anthocyanin pigment composition of red radish cultivars as potential food colorants. *J. Food Sci.* **63**, 219-224.
- Glassgen, W.E., and Seitz, H.U.** (1992). Acylation of anthocyanins with hydroxycinnamic acids via 1-O-acylglucosides by protein preparations from cell cultures of *Daucus carota* L. *Planta* **186**, 582-585.
- Glassgen, W.E., Rose, A., Madlung, J., Koch, W., Gleitz, J., and Seitz, H.U.** (1998). Regulation of enzymes involved in anthocyanin biosynthesis in carrot cell cultures in response to treatment with ultraviolet light and fungal elicitors. *Planta* **204**, 490-498.
- Gleitz, J., and Seitz, H.U.** (1989). Induction of chalcone synthase in cell suspension cultures of carrot (*Daucus carota* L. ssp. *sativus*) by ultraviolet light: evidence for two different forms of chalcone synthase. *Planta* **179**, 323-330.

- Gollop, R., Farhi, S., and Peri, A.** (2001). Regulation of leucoanthocyanidin dioxygenase gene expression in *Vitis vinifera*. *Plant Sci.* **161**, 579-588.
- Gollop, R., Even, S., Colova, T.V., and Peri, A.** (2002). Expression of the grape dihydroflavonol reductase gene and analysis of its promoter region. *Journal of Experimental Botany.* **53**, 1397-1409.
- Gonnet, J.F.** (2003). Origin of the color of Cv. Rhapsody in Blue rose and some other so-called "Blue" roses. *J. Agric. Food. Chem.* **51**, 4990-4994.
- Goodman, C.D., Casati, P., and Walbot, V.** (2004). A multidrug-resistance associated protein involved in anthocyanin transport in *Zea mays*. *The Plant Cell* **16**, 1812-1826.
- Gouka, R.J., van der Heiden, M., Swarthoff, T., and Verrips, C.T.** (2001). Cloning of a phenol oxidase gene from *Acremonium murorum* and its expression in *Aspergillus awamori*. *Appl. Environ. Microbiol.* **67**, 2610-2616.
- Gould, K.S., Markham, K.R., Smith, R.H., and Goris, J.J.** (2000). Functional role of anthocyanins in the leaves of *Quintinia serrata* A. *Cunn. J Exp Bot* **51**, 1107-1115.
- Gronwald, J.W., and Plaisance, K.L.** (1998). Isolation and characterization of glutathione S-transferase isozymes from sorghum. *Plant Physiol* **117**, 877-892.
- Gross.** (1987). Pigments in fruits, 59-85.
- Grotewold, E.** (2001). Subcellular trafficking of phytochemicals. *Recent Research Developments in Plant Physiology* **2**, 31-48.
- Grotewold, E., Drummond, B., Bowen, B., and Peterson, T.** (1994). The *Myb*-homologous *P* gene controls phlobaphene pigmentation in maize floral organs by directly activating a flavonoid biosynthetic gene subset. *Cell* **76**, 543-553.
- Grotewold, E., Chamberlin, M., Snook, M., Siame, B., Butler, L., Swenson, J., Maddock, S., St.Clair, G., and Bowen, B.** (1998). Engineering secondary metabolism in maize cells by ectopic expression of transcription factors. *The Plant Cell* **10**, 721-740.
- Guardiola, J., Iborra, J.L., and Canovas, M.** (1995). A model that links growth and secondary metabolite production in plant cell suspension cultures. *Biotechnology and Bioengineering* **46**, 291-297.
- Guillermond, A.** (1931). Sur l'existence frequente de vacuoles specialisees dans les cellules a anthocyane. *Academie des Sciences.*
- Guillermond, A.** (1932). Sur les caracteres speciaux des pigments anthocyaniques des fleurs de *Dianthus caryophyllus*. *Comp. Rend. Soc. Biol.* **111**, 973-976.
- Guiso, M., Marra, C., and Farina, A.** (2002). A new efficient resveratrol synthesis. *Tetrahedron-Letters.* **43**, 597-598.
- Gundlach, H., Mueller, M.J., Kutchan, T.M., and Zenk, M.H.** (1992). Jasmonic acid is a signal transducer in elicitor-induced plant cell cultures. *Proceedings of the National Academy of Sciences of the United States of America* **89**, 2389-2393.
- Habig, W.H., Pabst, M.J., and Jakoby, W.B.** (1974a). Glutathione S-transferases. The first enzymatic step in mercapturic acid formation. *J Biol Chem* **249**, 7130-7139.
- Hadacek, F.** (2002). Secondary metabolites as plant traits: current assessment and future perspectives. *CRC Crit. Rev. Plant Sci.* **21**, 273-322.

- Hale, C.R.** (1977). Relationship between potassium and the malate and tartrate contents of grape berries. *Vitis* **16**, 9-19.
- Hale, K.L., McGrath, S.P., Lombi, E., Stack, S.M., Terry, N., Pickering, I.J., George, G.N., and Pilon-Smits, E.A.** (2001). Molybdenum sequestration in Brassica species. A role for anthocyanins? *Plant Physiol* **126**, 1391-1402.
- Hanagata, N., Ito, A., Fukuju, Y., and Murata, K.** (1992). Red pigment formation in cultured cells of *Carthamus tinctorius* L. *Bioscience Biotechnology and Biochemistry* **56**, 44-47.
- Hanssen, M., and Marsden, J.** (1989). *The New Additive Code Breaker: Everything you should know about additives in your food.* (London: Lothian Publishing Co.).
- Hara-Nishimura, I.I., Shimada, T., Hatano, K., Takeuchi, Y., and Nishimura, M.** (1998). Transport of storage proteins to protein storage vacuoles is mediated by large precursor-accumulating vesicles. *Plant Cell* **10**, 825-836.
- Hawker, J.S., Downton, W.J.S., Wishkich, D., and Mullins, M.G.** (1973). Callus and cell culture from grape berries. *Hortscience* **8**, 398-399.
- Hemleben, V.** (1981). Anthocyanin carrying structures in specific genotypes of *Matthiola incana* R. Br. *Z. Naturforsch.* **36c**, 925-927.
- Hirasuna, T.J., Shuler, M.L., Lackney, V.K., and Spanswick, R.M.** (1991). Enhanced anthocyanin production in grape cell cultures. *Plant Science* **78**, 107-120.
- Hodges, D.M., and Nozzolillo, C.** (1996). Anthocyanin and anthocyanoplast content of cruciferous seedlings subjected to mineral nutrient deficiencies. *Journal of Plant Physiology* **147**, 749-754.
- Holton, T.A., and Cornish, E.C.** (1995). Genetics and biochemistry of anthocyanin biosynthesis. *Plant Cell* **7**, 1071-1083.
- Hong, V., and Wrolstad, R.E.** (1990). Use of HPLC separation/photodiode array detection for characterization of anthocyanins. *Journal of Agricultural and Food Chemistry* **38**, 708-715.
- Hopp, W., and Seitz, H.U.** (1987). The uptake of acylated anthocyanin into isolated vacuoles from a cell suspension culture of *Daucus carota*. *Planta* **170**, 74-85.
- Hrazdina, G., and Wagner, G.** (1985). Compartmentation of plant phenolic compounds; sites of synthesis and accumulation. *Annu. Proc. Phytochem. Soc. Europe* **25**, 120-133.
- Hrazdina, G., Wagner, G.J., and Siegelman, H.W.** (1978). Subcellular localization of enzymes of anthocyanin biosynthesis in protoplasts. *Phytochemistry* **17**, 53-56.
- Hrazdina, G., Zobel, A.M., and Hoch, H.C.** (1987). Biochemical, immunological, and immunocytochemical evidence for the association of chalcone synthase with endoplasmic reticulum membranes. *Proceedings of the National Academy of Sciences of the United States of America* **84**, 8966-8970.
- Hsieh, K., and Huang, A.H.** (2004). Endoplasmic Reticulum, Oleosins, and Oils in Seeds and Tapetum Cells. *Plant Physiol.* **136**, 3427-3434.
- Huang, A.H.** (1996). Oleosins and oil bodies in seeds and other organs. *Plant Physiol.* **110**, 1055-1061.

- Ignatowicz, E., and Baer-Dubowska, W.** (2001). Resveratrol, a natural chemopreventive agent against degenerative diseases. *Pol. J. Pharmacol.* **53**, 557-569.
- Irani, N.G., and Grotewold, E.** (2005). Light-induced morphological alteration in anthocyanin-accumulating vacuoles of maize cells. *BMC Plant Biology* **5**, 7-21.
- Ishikawa, T.** (1992). The ATP-dependent glutathione S-conjugate export pump. *Trends Biol. Sci.* **17**, 463-468.
- Itzhaki, H., and Maxon, J.M.** (1994). An ethylene-responsive enhancer element is involved in the senescence-related expression of the carnation glutathione S-transferase (GST1) gene. *Proc. Natl. Acad. Sci. USA* **91**, 8925-8929.
- Jain, M., and Bhalla-Sarin, N.** (2001). Glyphosate-Induced Increase in Glutathione S-Transferase Activity and Glutathione Content in Groundnut (*Arachis hypogaea* L.). *Pesticide Biochemistry and Physiology* **69**, 143-152.
- Jakobsson, P.-J., Morgenstern, R., Mancini, J., Ford-Hutchinson, A., and Persson, B.** (1999). Common structural features of MAPEG - a widespread superfamily of membrane associated proteins with highly divergent functions in eicosanoid and glutathione metabolism. *Protein Science* **8**, 1-4.
- Jasik, J., and Vancova, B.** (1992). Cytological study of anthocyanin production in grapevine (*Vitis vinifera* L.) callus cultures. *Acta Botanica Hungarica* **37**, 251-259.
- Jayram, S., and Konczak-Islam, I.** (2000). Investigations into the method for extraction of anthocyanins from *Vitis vinifera* cell suspensions. Food Science Australia SOP.
- JECFA.** (2000). Joint FAO/WHO Expert Committee Report 17.05 on Food Additives.
- Ji, X., von Rosenvinge, E.C., Johnson, W.W., Armstrong, R.N., and Gaillard, G.L.** (1996). Location of a potential transport binding site in a sigma class glutathione transferase by X-ray crystallography. *Proc. Natl. Acad. Sci. USA* **93**, 8208-8213.
- Jiang, L., Phillips, T.E., Hamm, C.A., Drozdowicz, Y.M., Rea, P.A., Maeshima, M., Rogers, S.W., and Rogers, J.C.** (2001). The protein storage vacuole: a unique compound organelle. *The Journal of Cell Biology* **155**, 991-1002.
- Jones, A.M.** (1994). Auxin-binding proteins. *Annu. Rev. Plant Physiol. Plant Mol. Biol.* **45**, 393-420.
- Jonsson, L.M.V., Donker-Koopman, W.E., Uitslager, P., and Schram, A.W.** (1983). Subcellular localization of anthocyanin methyltransferase in flowers of *Petunia hybrida*. *Plant Physiology* **72**, 287-290.
- Jonsson, L.M.V., Aarsman, M.E.G., Poulton, J.E., and Schram, A.W.** (1984). Properties and genetic control of four methyltransferases involved in methylation of anthocyanins in flowers of *Petunia hybrida*. *Planta* **160**, 174-179.
- Jurgens, G.** (2004). Membrane trafficking in plants. *Annu. Rev. Cell Dev. Biol.* **20**, 481-504.
- Kader, F., Haluk, J.P., Nicolas, J.P., and Metche, M.a.** (1998). Degradation of cyanidin 3-glucoside by blueberry polyphenol oxidase: Kinetic studies and

- mechanisms. *Journal-of-Agricultural-and-Food-Chemistry*. Aug., 1998; 46 (8) 3060-3065.
- Kader, F., Irmouli, M., Zitouni, N., Nicolas, J.P., and Metche, M.** (1999). Degradation of cyanidin 3-glucoside by caffeic acid o-quinone. Determination of the stoichiometry and characterization of the degradation products. *J Agric Food Chem* **47**, 4625-4630.
- Takegawa, K., Suda, J., Sugiyama, M., and Komamine, A.** (1995). Regulation of anthocyanin biosynthesis in cell suspension cultures of *Vitis* in relation to cell division. *Physiologia Plantarum* **94**, 661-666.
- Karsai, A., Mueller, S., Platz, S., and Hauser, M.T.a.** (2002). Evaluation of a home-made SYBR(R) Green I reaction mixture for real-time PCR quantification of gene expression. *BioTechniques*-. [print] **April, 2002**; **32**, 790-796.
- Kennedy, J.A., and Jones, G.P.** (2001). Analysis of proanthocyanidin cleavage products following acid-catalysis in the presence of excess phloroglucinol. *Journal of Agricultural and Food Chemistry* **49**, 1740-1746.
- Kennedy, J.A., Troup, G.J., Pilbrow, J.R., Hutton, D.R., Hewitt, D., Hunter, C.R., Ristic, R., Iland, P.G., and Jones, G.P.** (2000). Development of seed polyphenols in berries from *Vitis vinifera* L. cv. Shiraz. *Australian Journal of Grape and Wine Research* **6**, 244-254.
- Ketchum, R.E.B., Gibson, D.M., Croteau, R.B., and Shuler, M.L.** (1999). The kinetics of taxoid accumulation in cell suspension cultures of *Taxus* following elicitation with methyl jasmonate. *Biotechnology and Bioengineering* **62**, 94-105.
- Ketley, J.N., Habig, W.H., and Jakoby, W.B.** (1975). Binding of nonsubstrate ligands to the glutathione S-transferases. *J Biol Chem* **250**, 8670-8673.
- Kim, S.B., Lee, C.H., and Han, D.H.** (1997). Effect of ABA on the occurrence and development of anthocyanoplasts in 'Kyoho' grape. *J. Kor. Soc. Hort. Sci.* **38**, 55-59.
- Kim, S.H., Hur, B.K., and Byun, S.Y.** (1999). Effect of sugar concentration on camptothecin production in cell suspension cultures of *Camptotheca acuminata*. *Biotechnology and Bioprocess Engineering* **4**, 277-280.
- Kim, S.J., Cho, Y.H., Park, W., Han, D., Chai, C.H., and Imm, J.Y.** (2003). Solubilization of water soluble anthocyanins in apolar medium using reverse micelle. *J Agric Food Chem.* **51**, 7805-7809.
- Kirakosyan, A., Sirvent, T.M., Gibson, D.M., and Kaufman, P.B.** (2004). The production of hypericins and hyperforin by in vitro cultures of St. John's wort (*Hypericum perforatum*). *Biotechnol. Appl. Biochem.* **39**, 71-81.
- Kitamura, S., Shikazono, N., and Tanaka, A.** (2004). TRANSPARENT TESTA 19 is involved in the accumulation of both anthocyanins and proanthocyanidins in *Arabidopsis*. *The Plant Journal* **37**, 104-114.
- Klein, M., Weissenbock, G., Dufaud, A., Gaillard, C., Kreuz, K., and Martinoia, E.** (1996). Different energization mechanisms drive the vacuolar uptake of a flavonoid glucoside and a herbicide glucoside. *J Biol Chem* **271**, 29666-29671.
- Knight, H., and Knight, M.R.** (2001). Abiotic stress signalling pathways: specificity and cross-talk. *Trends Plant Sci* **6**, 262-267.
- Ko, K.M., Choi, Y.S., and Hwang, B.a.** (1994). Production and identification of anthocyanin in hairy root cultures of ginseng. *Journal-of-Plant-Biology*. 1994; 37 (1) 85-91.

- Kobayashi, S., Ishimaru, M., Hiraoka, K., and Honda, C.** (2002). Myb-related genes of the Kyoho grape (*Vitis labruscana*) regulate anthocyanin biosynthesis. *Planta* **215**, 924-933.
- Kohler, T.** (1995). Design of suitable primers and competitor fragments for quantitative PCR. In *Quantitation of mRNA by polymerase chain reaction*, T. Kohler, D. Labner, A.K. Rost, B. Thamm, B. Pustowoit, and H. Remke, eds (Berlin: Springer-Verlag), pp. 15-26.
- Kraemer-Schafhalter, A., Fuchs, H., Strigl, A., Silhar, S., Kovac, M., and Pfannhauser, W.** (1996). Process consideration for anthocyanin extraction from Black Chokeberry (*Aronia melanocarpa* ELL). In *Proceedings of the Second International Symposium on Natural Colorants, INF/COL II*, P.C. Hereld, ed (Hamden, Ct.: S.I.C. Publishing), pp. 153-160.
- Krisa, S., Vitrac, X., Decendit, A., Larronde, F., Deffieux, G., and Merillon, J.-M.** (1999b). Obtaining *Vitis vinifera* cell cultures producing higher amounts of malvidin-3-O-glucoside. *Biotechnology Letters* **21**, 497-500.
- Kubo, H., Nozue, M., Kawasaki, K., and Yasuda, H.** (1995). Intravacuolar spherical bodies in *Polygonum cuspidatum*. *Plant Cell Physiology* **36**, 1453-1458.
- Kuhnau, J.** (1976). The flavonoids. A class of semi-essential food components: their role in human nutrition. *World Rev. Nutr. Diet* **24**, 117-191.
- Kurata, H., Achioku, T., Okuda, N., and Furusaki, S.** (1998). Intermittent light irradiation with a second-scale interval enhances the caffeine production by *Coffea arabica* cells. *Biotechnology Progress* **14**, 797-799.
- Kutchan, T.M.** (2005). A role for intra- and intercellular translocation in natural product biosynthesis. *Curr. Opin. Plant Biol.* **8**, 292-300.
- Lachance, P.A.** (2004). Nutraceutical/drug/anti-terrorism safety assurance through traceability. *Toxicol. Lett.* **150**, 25-27.
- Laemmli, U.K.** (1970). Cleavage of Structural Proteins during the Assembly of the Head of Bacteriophage T4. *Nature* **227**, 680-685.
- Larronde, F., Krisa, S., Decendit, A., Cheze, C., Deffieux, G., and Merillon, J.M.** (1998). Regulation of polyphenol production in *Vitis vinifera* cell suspension cultures by sugars. *Plant Cell Reports* **17**, 946-950.
- Larsen, E.S., Alfenito, M.R., Briggs, W.R., and Walbot, V.** (2003). A carnation anthocyanin mutant is complemented by the glutathione S-transferases encoded by maize *Bz2* and petunia *An9*. *Plant Cell Reports* **21**, 900-904.
- Lawton, M.A., Dixon, R.A., Hahlbrock, K., and Lamb, C.J.** (1983). Rapid induction of the synthesis of phenylalanine ammonia-lyase and of chalcone synthase in elicitor-treated plant cells. *Journal of Biochemistry* **129**, 593-601.
- Lesnick, M.L., and Chandler, V.L.** (1998). Activation of the maize anthocyanin gene *a2* is mediated by an element conserved in many anthocyanin promoters. *Plant Physiology* **117**, 431-445.
- Li, Z.S., Zhao, Y., and Rea, P.A.** (1995). Magnesium Adenosine 5'-Triphosphate-Energized Transport of Glutathione-S-Conjugates by Plant Vacuolar Membrane Vesicles. *Plant Physiology* **107**, 1257-1268.
- Lin, Y., Dong, X., and Grotewold, E.** (2000). Preliminary analysis of green fluorescent compounds induced by ectopic expression of the *P* gene. *Maize Genet. Coop. Newsl.* **74**, 24-26.

- Lipmaa, T.** (1926). Die anthocyanophore der Erythraea-Arten. *Beih. Bot. Centr.* **43**, 127-132.
- Listowski, I., Abramovitz, M., and Homma, H.** (1988). Intracellular binding and transport of hormones and xenobiotics by glutathione S-transferases. *Drug Metab. Rev.* **19**, 305-318.
- Litwack, G., Ketterer, B., and Arias, I.M.** (1971). Ligandin: a hepatic protein which binds steroids, bilirubin, carcinogens, and a number of exogenous organic anions. *Nature* **234**, 466-467.
- Lopez, M.F., Patton, W.F., Sawlivich, W.B., Erdjument-Bromage, H., Barry, P., Gmyrek, K., Hines, T., Tempst, P., and Skea, W.M.** (1994). A glutathione S-transferase (GST) isozyme from broccoli with significant sequence homology to the mammalian theta-class of GSTs. *Biochim. Biophys. Acta* **1205**, 29-38.
- Losecke, W., Neumann, D., Groger, D., and Schmauder, H.P.** (1980). Changes of the cytoplasmic ultrastructure during development of sclerotia in *Claviceps purpurea*. *Arch. Microbiol.* **125**, 251-257.
- Lougarre, A., Bride, J.M., and Fournier, D.** (1999). Is the insect glutathione S-transferase I gene family intronless? *Insect Molecular Biology* **8**, 141-143.
- Loyall, L., Uchida, K., Braun, S., Furuya, M., and Frohnmeyer, H.** (2000). Glutathione and a UV light-induced glutathione S-transferase are involved in signaling to chalcone synthase in cell cultures. *Plant Cell* **12**, 1939-1950.
- Lu, Y.P., Li, Z.S., and Rea, P.A.** (1997). AtMRP1 gene of Arabidopsis encodes a glutathione S-conjugate pump: isolation and functional definition of a plant ATP-binding cassette transporter gene. *Proc Natl Acad Sci U S A* **94**, 8243-8248.
- Lu, Y.P., Li, Z.S., Drozdowicz, Y.M., Hortensteiner, S., Martinoia, E., and Rea, P.A.** (1998). AtMRP2, an Arabidopsis ATP binding cassette transporter able to transport glutathione S-conjugates and chlorophyll catabolites: functional comparisons with Atmrp1. *Plant Cell* **10**, 267-282.
- Ludwig, S.R., Habera, L.F., Dellaporta, S.L., and Wessler, S.R.** (1989). Lc, a member of the maize R gene family responsible for tissue-specific anthocyanin production, encodes a protein similar to transcriptional activators and contains the myc-homology region. *Proc. Natl Acad. Sci. USA* **86**, 7092-7096.
- Manach, C., Scalbert, A., Morand, C., Remesy, C., and Jimenez, L.** (2004). Polyphenols: food sources and bioavailability. *Am. J. Clin. Nutr.* **79**, 727-747.
- Mannervik, B., and Danielson, U.H.** (1988). Glutathione transferases: structure and catalytic activity. *CRC Crit. Rev. Biochem.* **23**, 283-337.
- Marchler-Bauer, A., and Bryant, S.H.** (2004). CD-Search: protein domain annotations on the fly. *Nucleic Acids Res.* **32**, W327-W331.
- Markham, K., Gould, K., and Ryan, K.** (2001). Cytoplasmic accumulation of flavonoids in flower petals and its relevance to yellow flower colouration. *Phytochemistry* **58**, 403-413.
- Markham, K.R., and Ofman, D.J.** (1993). Lisianthus flavonoid pigments and factors influencing their expression in flower colour. *Phytochemistry* **34**, 679-685.

- Markham, K.R., Gould, K.S., Winefield, C.S., Mitchell, K.A., Bloor, S.J., and Boase, M.R.** (2000). Anthocyanic vacuolar inclusions: Their nature and significance in flower colouration. *Phytochemistry* **55**, 327-336.
- Marrs, K.A.** (1996). The functions and regulation of glutathione S-transferases in plants. *Annual Reviews in Plant Physiology and Plant Molecular Biology* **47**, 127-158.
- Marrs, K.A., and Walbot, V.** (1997). Expression and RNA splicing of the maize glutathione s-transferase Bronze2 gene is regulated by cadmium and other stresses. *Plant Physiology* **113**, 93-102.
- Marrs, K.A., Alfenito, M.R., Lloyd, A.M., and Walbot, V.** (1995). A glutathione S-transferase involved in vacuolar transfer encoded by the maize gene Bronze-2. *Nature* **375**, 397-400.
- Martinoia, E., Grill, E., Tommasini, R., Kreuz, K., and Amrhein, N.** (1993). ATP-dependent glutathione S-conjugate 'export' pump in the vacuolar membrane of plants. *Nature* **364**, 247-249.
- Marty, F.** (1999). Plant vacuoles. *Plant Cell* **11**, 587-599.
- Mathews, H., Clendennen, S.K., Caldwell, C.G., Liu, X.L., Connors, K., Matheis, N., Schuster, D.K., Menasco, D.J., Wagoner, W., Lightner, J., and Wagner, D.R.** (2003). Activation tagging in tomato identifies a transcriptional regulator of anthocyanin biosynthesis, modification, and transport. *The Plant Cell* **15**, 1689-1703.
- Matile, P.** (1978). Biochemistry and function of vacuoles. *Annual Reviews in Plant Physiology* **29**, 193-213.
- Matile, P., Wiemken, A., and Moor, H.** (1970). Vacuolar dynamics in synchronous yeast. *Arch. Microbiol.* **70**, 89-103.
- Mauch, F., and Dudler, R.** (1993). Differential induction of distinct glutathione S-transferases of wheat by xenobiotics and by pathogen attack. *Plant Physiology* **102**, 1193-1201.
- Mazza, G.** (1995). Anthocyanins in grapes and grape products. *Critical Reviews in Food Science and Nutrition* **35**, 341-371.
- Mazza, G., and Maniati, E.** (1993). Anthocyanins in fruits, vegetables, and grains. (Boca Raton: CRC Press).
- McCarthy, J., Hopwood, F., Oxley, D., Laver, M., Castagna, A., Righetti, P.G., Williams, K., and Herbert, B.** (2003). Carbamylation of proteins in 2-D electrophoresis-myth or reality? *J. Proteome Res.* **2**, 239-242.
- McClure, J.W., Harborne, J.B., Mabry, T.J., and Mabry, H.** (1975). In *Physiology and functions of flavonoids* (New York: Academic Press), pp. 970-1055.
- McCully, M.E., Shane, M.W., Baker, A.N., Huang, C.X., Lings, L.E.C., and Canny, M.J.** (2000). The reliability of cryoSEM for the observation and quantification of xylem embolisms and quantitative analysis of xylem sap *in situ*. *Journal of Microscopy* **198**, 24-33.
- McLaughlin, M., and Walbot, V.** (1987). Cloning of a mutable bz2 allele of maize by transposon tagging and differential hybridization. *Genetics* **117**, 771-776.
- McTigue, M.A., Williams, D.R., and Trainer, J.A.** (1995). Crystal structures of a schistosomal drug and vaccine target: glutathione S-transferase from *Schistosoma japonica* and its complex with the leading antischistosomal drug praziquantel. *J. Mol. Biol.* **21-27**, 21-27.

- Melchior, F., and Kindl, H.** (1991). Coordinate- and elicitor-dependent expression of stilbene synthase and phenylalanine ammonia-lyase genes in *Vitis* cv. Optima. *Archives of Biochemistry & Biophysics* **288**, 552-557.
- Memelink, J., Verpoorte, R., and Kijne, J.W.** (2001). ORCAnization of jasmonate-responsive gene expression in alkaloid metabolism. *Trends Plant Sci* **6**, 212-219.
- Mendel, G.** (1865). Versuche über Pflanzen-Hybriden. *Verhandlungen des Naturforschenden Vereins in Brünn* **IV**, 3-47.
- Merlin, J.C., Statoua, A., and Brouillard, R.** (1985). Investigation of the *in vivo* organization of anthocyanins using resonance raman microspectrometry. *Phytochemistry* **24**, 1575-1581.
- Metzlaff, M., O'Dell, M., Cluster, P.D., and Flavell, R.B.** (1997). RNA-mediated RNA degradation and chalcone synthase A silencing in petunia. *Cell* **88**, 845-854.
- Meyer, H.J., and Van Staden, J.** (1995). The *in vitro* production of an anthocyanin from callus cultures of *Oxalis linearis*. *Plant Cell Tissue and Organ Culture* **40**, 55-58.
- Miller, K., Strommer, J., and Taylor, L.** (2002). Conservation in divergent solanaceous species of the unique gene structure and enzyme activity of a gametophytically-expressed flavonol 3-O-galactosyltransferase. *Plant Molecular Biology* **48**, 233-242.
- Millichip, M., Tatham, A.S., Jackson, F., Griffiths, G., Shewry, P.R., and Stobart, A.K.** (1996). Purification and characterization of oil-bodies (oleosomes) and oil-body boundary proteins (oleosins) from the developing cotyledons of sunflower (*Helianthus annuus* L.). *Biochem J.* **314**, 333-337.
- Mol, J., Grotewold, E., and Koes, R.** (1998). How genes paint flowers and seeds. *TRENDS IN PLANT SCIENCE* **3**, 212-217.
- Moller, S.G., and Chua, N.-H.** (1999). Interactions and intersections of plant signaling pathways. *Journal of Molecular Biology* **293**, 219-234.
- Morales, M., Bru, R., Carcia-Carmona, F., Ros-Barcelo, A., and Pedreno, M.A.** (1998). Effect of dimethyl-beta-cyclodextrins on resveratrol metabolism in Gamay grapevine cell cultures before and after inoculum with *Xylophilus ampelinus*. *Plant Cell, Tissue and Organ Culture* **53**, 179-187.
- Mori, T., Sakurai, M., Shigeta, J.-I., Yoshida, K., and Kondo, T.** (1993). Formation of anthocyanins from cells cultured from different parts of strawberry plants. *Journal of Food Science* **58**, 788-792.
- Moskowitz, A.H., and Hrazdina, G.** (1981). Vacuolar contents of fruit subepidermal cells of *Vitis* species. *Plant Physiol.* **68**, 686-692.
- Mozer, T.J., Tiemeier, D.C., and Jaworski, E.G.** (1983). Purification and characterization of corn glutathione S-transferase. *Biochemistry* **22**, 1068-1072.
- Mueller, L.A., and Walbot, V.** (2001). Models for vacuolar sequestration of anthocyanins. *Recent Adv. Phytochem.* **35**, 291-312.
- Mueller, L.A., Goodman, C.D., Silady, R.A., and Walbot, V.** (2000). AN9, a petunia glutathione S-transferase required for anthocyanin sequestration, is a flavonoid-binding protein. *Plant Physiol* **123**, 1561-1570.
- Mueller, M.J., Brodschelm, W., Spannagl, E., and Zenk, M.H.** (1993). Signaling in the elicitation process is mediated through the octadecanoid

- pathway leading to jasmonic acid. Proceedings of the National Academy of Sciences of the United States of America **90**, 7490-7494.
- Nair, H.K., Rao, K.V., Aalinkeel, R., Mahajan, S., Chawda, R., and Schwartz, S.A.** (2004). Inhibition of Prostate Cancer Cell Colony Formation by the Flavonoid Quercetin Correlates with Modulation of Specific Regulatory Genes. Clin Diagn Lab Immunol. **11**, 63-69.
- Nakamura, K., and Matsuoka, K.** (1993). Protein targeting to the vacuole in plant cells. Plant Physiol **101**, 1-5.
- Nakamura, M.** (1989). Development of anthocyanoplasts in relation to coloration of 'Kyoho' grapes. J. Japan Soc. Hort. Sci. **58**, 537-543.
- Nakamura, M.** (1993). Anthocyanoplasts in 'Kyoho' grapes. J. Japan Soc. Hort. Sci. **62**, 353-358.
- Nakamura, M.** (1994). Distribution and formation of anthocyanoplasts in the skin of 'Kyoho' grapes. J. Japan Soc. Hort. Sci. **62**, 717-723.
- Neuefeind, T., Huber, R., Reinemer, P., Knablein, J., Prade, L., Mann, K., and Bieseler, B.** (1997b). Cloning, sequencing, crystallization and X-ray structure of glutathione S-transferase-III from *Zea mays* var. mutin: a leading enzyme in detoxification of maize herbicides. J Mol Biol **274**, 577-587.
- Neuhaus, J.M., and Rogers, J.C.** (1998). Sorting of proteins to vacuoles in plant cells. Plant Mol Biol **38**, 127-144.
- Nishida, M., Harada, S., Noguchi, S., Satow, Y., Inoue, H., and Takahashi, K.** (1998). Three-dimensional structure of *Escherichia coli* glutathione S-transferase complexed with glutathione sulfonate: catalytic roles of Cys10 and His106. J. Mol. Biol. **281**, 135-147.
- Nissim-Levi, A., Kagan, S., Ovadia, R., and Oren-Shamir, M.** (2003). Effects of temperature, UV-light and magnesium on anthocyanin pigmentation in cocoplum leaves. J. Hort. Sci. Biotechnol. **78**, 61-64.
- Noh, B., and Spalding, E.P.** (1998). Anion channels and the stimulation of anthocyanin accumulation by blue light in arabidopsis seedlings. Plant Physiology **116**, 503-509.
- Nozue, M., and Yasuda, H.** (1985). Occurrence of anthocyanoplasts in cell suspension cultures of sweet potato. Plant Cell Reports **4**, 252-255.
- Nozue, M., Kubo, H., Nishimura, M., and Yasuda, H.** (1995). Detection and characterization of a vacuolar protein (VP24) in anthocyanin-producing cells of sweet potato in suspension culture. Plant and Cell Physiology **36**, 883-889.
- Nozue, M., Yamada, K., Nakamura, T., Kubo, H., Kondo, M., and Nishimura, M.** (1997). Expression of a vacuolar protein (VP24) in anthocyanin-producing cells of sweet potato in suspension culture. Plant Physiology **115**, 1065-1072.
- Nozue, M., Kubo, H., Nishimura, M., Katou, A., Hattori, C., Usuda, N., Nagata, T., and Yasuda, H.** (1993). Characterization of intravacuolar pigmented structures in anthocyanin-containing cells of sweet potato suspension cultures. Plant and Cell Physiology **34**, 803-808.
- Nozzolillo, C.** (1972). The site and chemical nature of red pigmentation in seedlings. Canadian Journal of Botany **50**, 29-34.
- Nozzolillo, C.** (1994). Anthocyanoplasts: organelles or inclusions? Polyphenols Actualités **11**, 16-18.

- Nozzolillo, C., and Ishikura, N.** (1988). An investigation of the intracellular site of anthocyanoplasts using protoplasts and vacuoles. *Plant Cell Reports* **7**, 389-392.
- O'Brien, T.P., Feder, N., and McCully, M.E.** (1964). Polychromatic staining of plant cell walls with toluidine blue O. *Protoplasma* **59**, 367-373.
- Oakley, A.J., Bello, M.L., Nuccetelli, M., Mazzetti, A.P., and Parker, M.W.** (1999). The ligandin (non-substrate) binding site of human Pi class glutathione transferase is located in the electrophile binding site (H-site). *J Mol Biol* **291**, 913-926.
- Okamoto, G., Onishi, H., and Hirano, K.** (2003). The effect of different fertilizer application levels on anthocyanoplast development in berry skin of Pione grapevines (*V. vinifera* x *V. labrusca*). *Vitis* **42**, 117-122.
- Oren-Shamir, M., and Levi-Nissim, A.** (1997a). Temperature effects on the leaf pigmentation of *Cotinus coggygria* 'Royal Purple'. *J. Hort. Sci.* **72**, 425-432.
- Oren-Shamir, M., and Levi-Nissim, A.** (1997b). UV-light effect on the leaf pigmentation of *Cotinus coggygria* 'Royal Purple'. *Sci Hortic.* **71**, 59-66.
- Oren-Shamir, M., Shaked-Sachray, L., Nissim-Levi, A., and Ecker, R.** (1999). Anthocyanin pigmentation of lisianthus flower petals. *Plant Sci.* **140**, 99-106.
- Ovecka, M., Lang, I., Baluska, F., Ismail, A., Illes, P., and Lichtscheidl, I.K.** (2005). Endocytosis and vesicle trafficking during tip growth of root hairs. *Protoplasma* **226**, 39-54.
- Ozeki, Y., and Komamine, A.** (1981). Induction of anthocyanin synthesis in relation to embryogenesis in a carrot suspension culture: correlation of metabolic differentiation with morphological differentiation. *Physiol. Plant* **53**, 570-577.
- Ozeki, Y., Matsui, K., Sakuta, M.-a., Matsuoka, M., Ohashi, Y., Kano-Murakami, Y., Yamamoto, N., and Tanaka, Y.** (1990a). Differential regulation of phenylalanine ammonia-lyase genes during anthocyanin synthesis and by transfer effect in carrot cell suspension cultures. *Physiologia Plantarum* **80**, 379-387.
- Pairoba, C.F., and Walbot, V.** (2003). Post-transcriptional regulation of expression of the *Bronze-2* gene of *Zea mays* L. *Plant Mol Biol* **53**, 75-86.
- Parham, R.A., and Kaustinen, H.M.** (1977). On the site of tannin synthesis in plant cells. *Botanical Gazette* **138**, 465-467.
- Paz-Ares, J., Wienand, U., Peterson, P.A., and Saedler, H.** (1986). Molecular cloning of the C locus of *Zea mays*: a locus regulating the anthocyanin pathway. *EMBO J.* **5**, 829-833.
- Paz-Ares, J., Ghosal, D., Wienand, U., Peterson, P.A., and Saedler, H.** (1987). The regulatory *CI* locus of *Zea mays* encodes a protein with homology to MYB proto-oncogene products with structural similarities to transcriptional activators. *EMBO Journal* **6**, 3553-3558.
- Pearse, A.G.E.** (1985). *Histochemistry, theoretical and applied: analytical technology.* (Edinburgh: Churchill Livingstone).
- Pecket, R.C., and Small, C.J.** (1980). Occurrence, location and development of anthocyanoplasts. *Phytochemistry* **19**, 2571-2576.
- Pfaffl, M.W.** (2001). A new mathematical model for relative quantification in real-time RT-PCR. *Nucleic Acids Research* **29**, 2002-2007.

- Pickett, C.B., and Lu, A.Y.H.** (1989). Glutathione *S*-transferases: gene structure, regulation, and biological function. *Annu. Rev. Biochem.* **58**, 743-764.
- Piffaut, B., Kader, F., Girardin, M., and Metche, M.** (1994). Comparative degradation pathways of malvidin 3,5-diglucoside after enzymatic and thermal treatments. *Food Chemistry* **50**, 115-120.
- Politis, J.** (1911). Sopra speciali corpi cellulari che formano Anthocianine. Nota preliminare. *Atti d.Acad.d.lineei Rendie* **21**, 828-834.
- Politis, J.** (1914). Sopra speciali corpi cellulari che formano Anthocianine. *Atti. 1st Bot. Pavia* **14**, 363-366.
- Politis, J.** (1959). Cytological observations on the production of anthocyanin in certain Solanaceae. *Bulletin of the Torrey Botanical Club* **86**, 387-393.
- Possner, D.R.E., and Kliever, W.M.** (1985). The localisation of acids, sugars and potassium in developing grape berries. *Vitis* **24**, 229-240.
- Prade, L., Huber, R., and Bieseler, B.** (1998). Structures of herbicides in complex with their detoxifying enzyme glutathione *S*-transferase - explanations for the selectivity of the enzyme in plants. *Structure* **6**, 1445-1452.
- Quattrocchio, F., Wing, J.F., Leppen, H.T.C., Mol, J.N.M., and Koes, R.E.** (1993). Regulatory genes controlling anthocyanin pigmentation are functionally conserved among plant species and have distinct sets of target genes. *The Plant Cell* **5**, 1497-1512.
- Quattrocchio, F., Wing, J.F., van der Woude, K., Mol, J.N., and Koes, R.** (1998). Analysis of bHLH and MYB domain proteins: species-specific regulatory differences are caused by divergent evolution of target anthocyanin genes. *Plant J* **13**, 475-488.
- Rajendran, L., Suvarnalatha, G., Ravishankar, G.A., and Venkataraman, L.V.** (1994). Enhancement of anthocyanin production in callus cultures of *Daucus carota* L. under the influence of fungal elicitors. *Applied Microbiology and Biotechnology* **42**, 227-231.
- Rao, S.R., and Ravishankar, G.A.** (2002). Plant cell cultures: Chemical factories of secondary metabolites. *Biotechnology Advances* **20**, 101-153.
- Rao, S.R., Sarada, R., and Ravishankar, G.A.** (1996). Phycocyanin, a new elicitor for capsaicin and anthocyanin accumulation in plant cell cultures. *Appl Microbiol Biotechnol* **46**, 619-621.
- Rea, P.A., Li, Z.-S., Lu, Y.-P., Drozdowicz, Y.M., and Martinoia, E.** (1998). From vacuolar GS-X pumps to multispecific ABC transporters. *Annual Reviews in Plant Physiology and Plant Molecular Biology* **49**, 727-760.
- Reddy, G.M., and Coe Jr, E.H.** (1962). Inter-tissue complementation: A simple technique for direct analysis of gene-action sequence. *Science* **138**, 149-150.
- Reif, H.J., Niesbach, U., Deumling, B., and Saedler, H.** (1985). Cloning and analysis of two genes for chalcone synthase from *Petunia hybrida*. *Molecular & General Genetics* **199**, 208-215.
- Robertson, D.S.** (1978). Characterization of a mutator system in maize. *Mutation Research* **51**, 21-28.
- Robinson, D.G., Hinz, G., and Holstein, S.E.** (1998). The molecular characterization of transport vesicles. *Plant Mol. Biol.* **38**, 49-76.
- Romero-Cascales, I., Ortega-Regules, A., López-Roca, J.M., Fernández-Fernández, J.I., and Gómez-Plaza, E.** (2005). Differences in

- Anthocyanin Extractability from Grapes to Wines According to Variety. *Am. J. Enol. Vitic.* **56**, 212-219.
- Romero, C., and Bakker, J.** (2000). Effect of storage temperature and pyruvate on kinetics of anthocyanin degradation, vitisin A derivative formation, and color characteristics of model solutions. *Journal of Agriculture and Food Chemistry* **48**, 2135-2141.
- Rose, A., Glaessgen, W.E., Hopp, W., and Seitz, H.U.** (1996). Purification and characterization of glycosyltransferases involved in anthocyanin biosynthesis in cell-suspension cultures of *Daucus carota* L. *Planta* **198**, 397-403.
- Rossini, L., Frova, C., Pe, M.E., Mizzi, L., and Gorla, M.S.** (1998). Alachlor regulation of maize glutathione S-transferase genes. *Pesticide Biochemistry and Physiology* **60**, 205-211.
- Roubelakis-Angelakis, K.A., and Kliewer, W.M.** (1986). Effects of exogenous factors on phenylalanine ammonia-lyase activity and accumulation of anthocyanins and total phenolics in grape berries. *Am. J. Enol. Vitic.* **37**, 275-280.
- Rouster, J., van Mechelen, J., and Cameron-Mills, V.** (1998). The untranslated leader sequence of the barley *lipoxygenase 1 (Lox1)* gene confers embryo-specific expression. *The Plant Journal* **15**, 435-440.
- Rushmore, T.H., and Pickett, C.B.** (1993). Glutathione S-transferases, structure, regulation, and therapeutic implications. *J. Biol. Chem.* **268**, 11475-11478.
- Ruthardt, N., Gulde, N., Spiegel, H., Fischer, R., and Emans, N.** (2005). Four-dimensional imaging of transvacuolar strand dynamics in tobacco BY-2 cells. *Protoplasma* **225**, 205-215.
- Ruzin, S.E.** (1999). *Plant microtechnique and microscopy*. (New York: Oxford University Press).
- Sainz, M.B., Grotewold, E., and Chandler, V.L.** (1997). Evidence for direct activation of an anthocyanin promoter by the maize C1 protein and comparison of DNA binding by related Myb domain proteins. *Plant Cell* **9**, 611-625.
- Saito, K., and Yamazaki, M.** (2002). Biochemistry and molecular biology of the late-stage of biosynthesis of anthocyanin: lessons from *Perilla frutescens* as a model plant. *New Phytologist* **155**, 9-23.
- Sakuta, M., Hirano, H., Kakegawa, K., Suda, J., Hirose, M., Joy, R.W.I.V., Sugiyama, M., and Komamine, A.** (1994). Regulatory mechanisms of biosynthesis of betacyanin and anthocyanin in relation to cell division activity in suspension cultures. *Plant Cell Tissue and Organ Culture* **38**, 167-169.
- Sambrook, J.F., and Maniatis, T.** (1989). *Molecular cloning: a laboratory manual*, 2nd Edn.
- Sanford, J.C., Smith, F.D., and Russell, J.A.** (1993). Optimizing the biolistic process for different biological applications. *Methods Enzymol.* **217**, 483-509.
- Sari-Gorla, M., Ferrario, S., Rossini, L., Frova, C., and Villa, M.** (1993). Developmental expression of glutathione S-transferase in maize and its possible connection with herbicide tolerance. *Euphytica* **67**, 221-230.
- Sarma, A.D., Sreelakshmi, Y., and Sharma, R.** (1997). Antioxidant ability of anthocyanins against ascorbic acid oxidation. *Phytochemistry* **45**, 671-674.

- Saslowsky, D., and Winkel-Shirley, B.** (2001). Localization of flavonoid enzymes in arabidopsis roots. *The Plant Journal* **27**, 37-48.
- Satue-Gracia, M.T., Heinonen, M., and Frankel, E.** (1997). Anthocyanins as antioxidants on human low-density lipoprotein and lecithin-liposome systems. *J. Agric. Food Chem.*, 3362-3367.
- Schmidt-Krey, I., Mitsuoka, K., Hirai, T., Murata, K., Cheng, Y., Fujiyoshi, Y., Morgenstern, R., and Hebert, H.** (2000). The three-dimensional map of microsomal glutathione transferase 1 at 6Å resolution. *EMBO J.* **19**, 6311-6316.
- Schmitz, G., and Theres, K.** (1992). Structural and functional analysis of the *Bz2* locus of *Zea mays*: characterization of overlapping transcripts. *Mol. Gen. Genet.* **233**, 269-277.
- Scordino, M., Di Mauro, A., Passerini, A., and Maccarone, E.** (2004). Adsorption of flavonoids on resins: Cyanidin 3-glucoside. *Journal of Agricultural and Food Chemistry* **52**, 1965-1972.
- Seitz, H.U., and Hinderer, W.** (1988). Anthocyanins. In *Cell culture and somatic cell genetics of plants*, I.K. Vasil, ed (New York: Academic Press), pp. 49-76.
- Shaked-Sachray, L., Weiss, D., Moshe, R., Nissim-Levi, A., and Oren-Shamir, M.** (2002). Increased anthocyanin accumulation in aster flowers at elevated temperatures due to magnesium treatment. *Physiol. Plant* **114**, 559-565.
- Shvarts, M., Borochoy, A., and Weiss, D.** (1997). Low temperature enhances petunia flower pigmentation and induces chalcone synthase gene expression. *Physiologia Plantarum* **99**, 67-72.
- Singh, M., Silva, E., Schulze, S., Sinclair, D.A., Fitzpatrick, K.A., and Honda, B.M.** (2000). Cloning and characterization of a new theta-class glutathione-S-transferase (GST) gene, *gst-3*, from *Drosophila melanogaster*. *Gene* **247**, 167-173.
- Slack, C.R., Bertaud, W.S., Shaw, B.D., Holland, R., Browse, J., and Wright, H.** (1980). Some studies on the composition and surface properties of oil bodies from the seed cotyledons of safflower (*Carthamus tinctorius*) and linseed (*Linum usitatissimum*). *Biochem J.* **190**, 551-561.
- Small, C., and Pecket, R.** (1982). The ultrastructure of anthocyanoplasts in red-cabbage. *Planta* **154**, 97-99.
- Snyder, B.A., and Nicholson, R.L.** (1990). Synthesis of phytoalexins in sorghum as a site-specific response to fungal ingress. *Science* **248**, 1637-1638.
- Solfanelli, C., Poggi, A., Loreti, E., Alpi, A., and Perata, P.** (2006). Sucrose-specific induction of anthocyanin biosynthetic pathway in Arabidopsis. *Plant Physiol.* **140**, 637-646.
- Spangna, G., and Pifferi, P.G.** (1992). Purification and separation of oenocyanin anthocyanins on sulphonyethylcellulose. *Food Chemistry* **44**, 185-188.
- Sparvoli, F., Martin, C., Scienza, A., Gavazzi, G., and Tonelli, C.** (1994). Cloning and molecular analysis of structural genes involved in flavonoid and stilbene biosynthesis in grape (*Vitis vinifera* L.). *Plant Molecular Biology* **24**, 743-755.
- Spelt, C., Quattrocchio, F., Mol, J.N., and Koes, R.** (2000). *anthocyanin1* of petunia encodes a basic helix-loop-helix protein that directly activates transcription of structural anthocyanin genes. *Plant Cell* **12**, 1619-1632.

- Sreenath, H.K., and Lafayette, W.** (1992). Studies on starch granules digestion by [alpha]-amylase. *Starch* **44**, 61-63.
- Srinivasan, V., Ciddi, V., Bringi, V., and Shuler, M.L.** (1996). Metabolic inhibitors, elicitors, and precursors as tools for probing yield limitation in taxane production by *Taxus chinensis* cell cultures. *Biotechnology Progress* **12**, 457-465.
- Stafford, H.A.** (1994). Anthocyanins and betalains: evolution of the mutually exclusive pathways. *Plant Science* **101**, 91-98.
- Steffens, J.C.** (2000). Acyltransferases in protease's clothing. *Plant Cell* **12**, 1253-1256.
- Storey, R.** (1987). Potassium localization in grape berry pericarp by energy-dispersive X-ray microanalysis. *Am. J. Enol. Vitic.* **38**, 301-309.
- Sun, T.-H., and Morgenstern, R.** (1997). Binding of glutathione and an inhibitor to microsomal glutathione transferase. *Biochem J.* **326**, 193-196.
- Suzuki, H., Nakayama, T., and Nishino, T.** (2003a). Proposed Mechanism and Functional Amino Acid Residues of Malonyl-CoA:Anthocyanin 5-O-Glucoside-6"-O-Malonyltransferase from Flowers of *Salvia splendens*, a Member of the Versatile Plant Acyltransferase Family. *Biochemistry* **42**, 1764-1771.
- Suzuki, M.** (1995). Enhancement of anthocyanin accumulation by high osmotic stress and low pH in grape cells (*Vitis* hybrids). *Journal of Plant Physiology* **147**, 152-155.
- Suzuki, M., Ketterling, M.G., Li, Q.B., and McCarty, D.R.** (2003b). *Viviparous1* alters global gene expression patterns through regulation of abscisic acid signaling. *Plant Physiology* **132**, 1664-1677.
- Swinkels, J.J.M.** (1985). Composition and properties of commercially native starches. *Starch/Starke* **37**, 1-5.
- Tabata, H.** (2004). Paclitaxel production by plant-cell-culture technology. *Adv. Biochem. Eng. Biotechnol.* **87**, 1-23.
- Takeda, J., Abe, S., Hirose, Y., and Ozeki, Y.** (1993). Effect of light and 2,4-dichlorophenoxyacetic acid on the level of mRNAs for *phenylalanine ammonia-lyase* and *chalcone synthase* in carrot cells cultured in suspension. *Physiologia Plantarum* **89**, 4-10.
- Tamura, H., Kumaoka, Y., and Sugisawa, H.** (1989). Identification and quantitative variation of anthocyanins produced by cultured callus tissue of *Vitis* sp. *Agric. Biol. Chem.* **53**, 1969-1970.
- Taylor, L.P., and Grotewald, E.** (2005). Flavonoids as developmental regulators. *Curr. Opin. Plant Biol.* **8**, 317-323.
- Terrier, N., Glissant, D., Grimplet, J., Barrieu, F., Abbal, P., Couture, C., Ageorges, A., Atanassova, R., Leon, C., Renaudin, J.P., Dedaldechamp, F., Romieu, C., Delrot, S., and Hamdi, S.** (2005). Isogene specific oligo arrays reveal multifaceted changes in gene expression during grape berry (*Vitis vinifera* L.) development. *Planta*, 1-16.
- Thompson, J.D., Higgins, D.G., and Gibson, T.J.** (1994). CLUSTAL W: improving the sensitivity of progressive multiple sequence alignment through sequence weighting, position specific gap penalties and weight matrix choice. *Nucleic Acids Research*.
- Timberlake, C.F.** (1988). The biological properties of anthocyanin compounds. *NATCOL Quarterly Bulletin* **1**, 4-15.

- Toriyama, H.** (1954). Observational and experimental studies of sensitive plant, II. On the changes in motor cells of diurnal and nocturnal condition. *Cytologia* **19**, 29-40.
- Tzen, J., Cao, Y., Laurent, P., Ratnayake, C., and Huang, A.** (1993). Lipids, Proteins, and Structure of Seed Oil Bodies from Diverse Species. *Plant Physiol.* **101**, 267-276.
- Ulmasov, T., Ohmiya, A., Hagen, G., and Guilfoyle, T.** (1995). The soybean GH214 gene that encodes a glutathione *S*-transferase has a promoter that is activated by a wide range of chemical agents. *Plant Physiol.* **108**, 919-927.
- Vaknin, H., Bar-Akiva, A., Ovadia, R., Nissim-Levi, A., Forer, I., Weiss, D., and Oren-Shamir, M.** (2005). Active anthocyanin degradation in *Brunfelsia calycina* (yesterday-today-tomorrow) flowers. *Planta*.
- van Tunen, A.J., Koes, R.E., Spelt, C.E., van der Krol, A.R., Stuitje, A.R., and Mol, J.N.** (1988). Cloning of the two chalcone flavanone isomerase genes from *Petunia hybrida*: coordinate, light-regulated and differential expression of flavonoid genes. *EMBO J* **7**, 1257-1263.
- Verpoorte, R., van der Heijden, R., ten Hoopen, H.J.G., and Memelink, J.** (1999). Metabolic engineering of plant secondary metabolite pathways for the production of fine chemicals. *Biotechnology Letters* **21**, 467-479.
- Vitrac, X., Larronde, F., Krisa, S., Decendit, A., Deffieux, G., and Merillon, J.M.** (2000). Sugar sensing and Ca²⁺-calmodulin requirement in *Vitis vinifera* cells producing anthocyanins. *Phytochemistry* **53**, 659-665.
- Wagner, G.J., and Seigelman, H.W.** (1975). Large-scale isolation of intact vacuoles and isolation of chloroplasts from protoplasts of mature plant tissues. *Science* **190**, 1298-1299.
- Walker, A.** (unpublished results).
- Walker, A.R., Davison, P.A., Bolognesi-Winfield, A.C., James, C.M., Srinivasan, N., Blundell, T.L., Esch, J.J., Marks, M.D., and Gray, J.C.** (1999a). The *TRANSPARENT TESTA GLABRA1* locus, which regulates trichome differentiation and anthocyanin biosynthesis in *Arabidopsis*, encodes a WD40 repeat protein. *Plant Cell* **11**, 1337-1350.
- Wang, C., Zien, C.A., Afithile, M., Welti, R., Hildebrand, D.F., and Wang, X.** (2000). Involvement of Phospholipase D in Wound-Induced Accumulation of Jasmonic Acid in *Arabidopsis*. *Plant Cell* **12**, 2237-2246.
- Wang, H., Cao, G., and Prior, R.** (1997). Oxygen radical absorbing capacity of anthocyanins. *J. Agric. Food Chem.*, 304-309.
- Wang, S.Y., and Lin, H.S.** (2000). Antioxidant activity in fruits and leaves of blackberry, raspberry, and strawberry varies with cultivar and developmental stage. *J Agric Food Chem* **48**, 140-146.
- Wang, W., and Ballatori, N.** (1998). Endogenous glutathione conjugates: occurrence and biological functions. *Pharmacological Reviews* **50**, 335-355.
- Waterhouse, A.L.** (1995). Wine and heart disease. *Chem. Ind.*, 338-341.
- Weiss, M.R.** (1995). Floral color change - a widespread functional convergence. *Am. J. Bot.* **82**, 167-185.
- Wellmann, E., Hrazdina, G., and Grisebach, H.** (1976). Induction of anthocyanin formation and of enzymes related to its biosynthesis by UV light in cell cultures of *Haplopappus gracilis*. *Phytochemistry* **15**, 913-915.
- Wilkins, M.R., Lindskog, I., Gasteiger, E., Bairoch, A., Sanchez, J.-C., Hochstrasser, D.F., and Appel, R.D.** (1997). Detailed peptide

- characterisation using PEPTIDEMASS - a World-Wide Web accessible tool. *Electrophoresis* **18**, 403-408.
- Winicur, Z.M., Zhang, G.F., and Staehelin, L.A.** (1998). Auxin deprivation induces synchronous golgi differentiation in suspension-cultured tobacco BY-2 cells. *Plant Physiol.* **117**, 501-513.
- Winkel-Shirley, B.** (1999). Evidence for enzyme complexes in the phenylpropanoid and flavonoid pathways. *Physiologia Plantarum* **107**, 142-149.
- Winkel-Shirley, B.** (2001a). It takes a garden. How work on diverse plant species has contributed to an understanding of flavonoid metabolism. *Plant Physiology* **127**, 1399-1403.
- Winkel-Shirley, B.** (2001b). Flavonoid biosynthesis. A colorful model for genetics, biochemistry, cell biology, and biotechnology. *Plant Physiol* **126**, 485-493.
- Wolkoff, A.W., Weisiger, R.A., and Jakoby, W.B.** (1979). The multiple roles of the glutathione transferases (ligandins). *Prog Liver Dis* **6**, 213-224.
- Wulf, L.W., and Nagel, C.W.** (1978). High-pressure liquid chromatographic separation of anthocyanins of *Vitis vinifera*. *Am. J. Enol. Vitic.* **29**, 42-49.
- Wysokinska, H., and Nguyen, T.X.G.** (1990). Selection of penstamide and serrulatolose producing clones in *Penstemon serrulatus* by small-aggregate cloning. *Plant Cell Reports* **9**, 378-381.
- Xu, W., Shioiri, H., Kojima, M., and Nozue, M.** (2001). Primary structure and expression of a 24-kd vacuolar protein (vp24) precursor in anthocyanin-producing cells of sweet potato in suspension culture. *Plant Physiol* **125**, 447-455.
- Xu, W., Moriya, K., Yamada, K., Nishimura, M., Shioiri, H., Kojima, M., and Nozue, M.** (2000). Detection and characterization of a 36-kDa peptide in C-terminal region of a 24-kDa vacuolar protein (VP24) precursor in anthocyanin-producing sweet potato cells in suspension culture. *Plant Science* **160**, 121-128.
- Yamakawa, T., Kato, S., Ishida, K., Kodama, T., and Minoda, Y.** (1983b). Production of anthocyanins in *Vitis* cells in suspension culture. *Agric. Biol. Chem* **47**, 2185-2191.
- Yamamoto, H., Yamaguchi, M., and Inoue, K.** (1996). Adsorption and increase in the production of prenylated flavanones in *Sophora flavescens* cell suspension cultures by cork pieces. *Phytochemistry (Oxford)* **43**, 603-608.
- Yamamoto, H., Yato, A., Yazaki, K., Hayashi, H., Taguchi, G., and Inoue, K.** (2001). Increases of secondary metabolite production in various plant cell cultures by co-cultivation with cork. *Biosci. Biotechnol. Biochem.* **65**, 853-860.
- Yamamoto, Y., Nishimura, M., Hara-Nishimura, I., and Noguchi, T.** (2003). Behavior of vacuoles during microspore and pollen development in *Arabidopsis thaliana*. *Plant Cell Physiol.* **44**, 1192-1201.
- Yamazaki, M., Gong, Z., Fukuchi-Mizutani, M., Fukui, Y., Tanaka, Y., Kusumi, T., and Saito, K.** (1999). Molecular cloning and biochemical characterization of a novel anthocyanin 5-O-glucosyltransferase by mRNA differential display for plant forms regarding anthocyanin. *Journal of Biological Chemistry* **274**, 7405-7411.
- Yamazaki, M., Yamagishi, E., Gong, Z., Fukuchi-Mizutani, M., Fukui, Y., Tanaka, T., Yamaguchi, M., and Saito, K.** (2002). Two flavonoid

- glucosyltransferases from *Petunia hybrida*: molecular cloning, biochemical properties and developmentally regulated expression. *Plant Molecular Biology* **48**, 401-411.
- Yarnell, J.W.G., and Evans, A.E.** (2000). The Mediterranean diet revisited - towards resolving the (French) paradox. *QJM* **93**, 783-785.
- Yasuda, H.** (1970). Studies on "bluing effect" in the petals of red rose, I. Some cytochemical observations on epidermal cells having a bluish tinge. *Bot. Mag. Tokyo* **83**, 233-236.
- Yasuda, H.** (1973). Studies on the "bluing" effect in the petals of red rose. III. The histochemical detection of iron in the bluing petals of rose. *Jour. Fac. Sci. Shinshu. Univ.* **8**, 91-94.
- Yasuda, H.** (1974a). Studies on the insoluble states of anthocyanin in rose petals, I. The insoluble state of anthocyanin and its relationship to petal colour, together with a new instance of this relationship. *J. Fac. Sci. Shinshu Univ.* **9**, 63-69.
- Yasuda, H.** (1974b). Studies on "bluing effect" in the petals of red rose II. Observation on the development of the tannin body in the upper epidermal cells of bluing petals. *Cytologia* **39**, 107-112.
- Yasuda, H.** (1976). Studies on the insoluble states of anthocyanin in rose petals. II: histochemical observation on its basal substance. *Cytologia* **41**, 487-492.
- Yasuda, H.** (1979). Studies on the insoluble states of anthocyanin in rose petals, III. The observation on the developmental process of the massive structure. *Cytologia* **44**, 687-692.
- Yasuda, H., and Kikuchi, M.** (1978). Studies on "bluing effect" in the petals of red rose, V. A survey of the various bluing types. *J. Fac. Sci. Shinshu Univ.* **13**, 79-86.
- Yasuda, H., and Kumagai, T.** (1984). Electron microscopic observations on the anthocyanoplasts in the radish seedlings. *Proc. Ann. Meet. 24th Symp. Jap. Soc. Plant Physiol.*, 206.
- Yasuda, H., and Shinoda, H.** (1985). The studies on the spherical bodies containing anthocyanins in plant cell. I: Cytological and cytochemical observations on the bodies appearing in the seedling hypocotyls of radish plants. *Cytologia* **50**, 397-403.
- Yasuda, H., and Tsujino, Y.** (1988). The studies on the spherical bodies containing anthocyanins in plant cells, II. The effects of light on the pigmentation of spherical bodies in the seedling hypocotyls of the radish plant. *J. Fac. Sci. Shinshu University* **23**, 1-6.
- Yasuda, H., Mitsui, T., and Onishi, M.** (1989). Studies on the spherical bodies containing anthocyanins in plant cells. III: Observations on the developments of anthocyanoplasts in the radish hypocotyls. *Cytologia* **54**, 673-678.
- Yazaki, K.** (2005). Transporters of secondary metabolites. *Current Opinion in Plant Biology* **8**, 301-307.
- Yeoman, M.M., and Yeoman, C.L.** (1996). Manipulating secondary metabolism in cultured plant cells. *New Phytologist* **134**, 553-569.
- Yoshida, K., Toyama-Kato, Y., Kameda, K., and Kondo, T.** (2003). Sepal colour variation of *Hydrangea macrophylla* and vacuolar pH measured with a proton-selective microelectrode. *Plant Cell Physiol* **44**, 262-268.

- Yoshida, K., Kawachi, M., Mori, M., Maeshima, M., Kondo, M., Nishimura, M., and Kondo, T.** (2005). The Involvement of Tonoplast Proton Pumps and Na⁺(K⁺)/H⁺ Exchangers in the Change of Petal Color During Flower Opening of Morning Glory, *Ipomoea tricolor* cv. Heavenly Blue. *Plant and Cell Physiology* **46**, 407-415.
- Yoshimoto, M., Okuno, S., Kumagai, T., Yoshinaga, M., and Yamakawa, O.** (1999b). Distribution of antimutagenic components in colored sweetpotatoes. *JARQ* **33**, 143-148.
- Yoshinaga, M., Yamakawa, O., and Nakatani, M.** (1999). Genotypic diversity of anthocyanin content and composition in purple-fleshed sweet potato (*Ipomoea batatas* (L.) Lam). *Breeding Science* **49**, 43-47.
- Yu, M., and Facchini, P.J.** (2000). Molecular cloning and characterization of a type III glutathione S-transferase from cell suspension cultures of opium poppy treated with a fungal elicitor. *Physiologia Plantarum* **108**, 101-109.
- Zachariah, V.T., Walsh-Sayles, N., and Singh, B.R.** (2000). Isolation, purification, and characterization of glutathione S-transferase from oat (*Avena sativa*) seedlings. *Journal of Protein Chemistry* **19**, 425-430.
- Zeng, Q.-Y., and Wang, X.-R.** (2005). Catalytic properties of glutathione-binding residues in a (tau) class glutathione transferase (PtGSTU1) from *Pinus tabulaeformis*. *FEBS Lett* **579**, 2657-2662.
- Zettl, R., Schell, J., and Palme, K.** (1994). Photoaffinity labeling of *Arabidopsis thaliana* plasma membrane vesicles by 5-azido-[7-³H]indole-3-acetic acid: Identification of a glutathione S-transferase. *Proc. Natl. Acad. Sci. U.S.A.* **91**, 689-693.
- Zhang, K., and Wong, K.P.** (1996). Inhibition of the efflux of glutathione S-conjugates by plant polyphenols. *Biochem. Pharmacol.* **52**, 1631-1638.
- Zhang, W., and Furusaki, S.** (1999). Production of anthocyanins by plant cell cultures. *Biotechnology and Bioprocess Engineering* **4**, 231-252.
- Zhang, W., Curtin, C., and Franco, C.** (2002b). Towards manipulation of post-biosynthetic events in secondary metabolism of plant cell cultures. *Enzyme and Microbial Technology* **30**, 688-696.
- Zhang, W., Curtin, C., Kikuchi, M., and Franco, C.** (2002a). Integration of jasmonic acid and light irradiation for enhancement of anthocyanin biosynthesis in *Vitis vinifera* suspension cultures. *Plant Science* **162**, 459-468.
- Zhang, W., Franco, C., Curtin, C., and Conn, S.** (2004). To stretch the boundary of secondary metabolite production in plant cell-based bioprocessing: Anthocyanin as a case study. *Journal of Biomedicine and Biotechnology* **5**, 264-271.
- Zhao, Z., Raftery, M.J., Niu, X.M., Daja, M.M., and Russell, P.J.** (2004). Application of in-gel protease assay in a biological sample: characterization and identification of urokinase-type plasminogen activator (uPA) in secreted proteins from a prostate cancer cell line PC-3. *Electrophoresis* **25**, 1142-1148.
- Zhong, J.-J., Seki, T., Kinoshita, S.I., and Yoshida, T.** (1991). Effect of light irradiation on anthocyanin production by suspended culture of *Perilla frutescens*. *Biotechnology and Bioengineering* **38**, 653-658.
- Zobel, A.M., and Hrazdina, G.** (1995). Chalcone synthase localization in early stages of plant development: I. immunohistochemical use of plasmolysis

for localizing the enzyme in epidermal cell cytoplasm of illuminated buckwheat hypocotyls. *Biotechnic and Histochemistry* **70**, 1-6.